

INFORMATION TO USERS

This manuscript has been reproduced from the microfilm master. UMI films the text directly from the original or copy submitted. Thus, some thesis and dissertation copies are in typewriter face, while others may be from any type of computer printer.

The quality of this reproduction is dependent upon the quality of the copy submitted. Broken or indistinct print, colored or poor quality illustrations and photographs, print bleedthrough, substandard margins, and improper alignment can adversely affect reproduction.

In the unlikely event that the author did not send UMI a complete manuscript and there are missing pages, these will be noted. Also, if unauthorized copyright material had to be removed, a note will indicate the deletion.

Oversize materials (e.g., maps, drawings, charts) are reproduced by sectioning the original, beginning at the upper left-hand corner and continuing from left to right in equal sections with small overlaps.

ProQuest Information and Learning
300 North Zeeb Road, Ann Arbor, MI 48106-1346 USA
800-521-0600

UMI[®]

University of Alberta

A Novel Variable Group Hybrid Interference Cancellation for CDMA Systems

by

Kay Wee Ang ©

**A thesis submitted to the Faculty of Graduate Studies and Research in partial fulfillment
of the requirements for the degree of Doctor of Philosophy**

Department of Electrical and Computer Engineering

**Edmonton, Alberta, Canada
Spring 2005**



Library and
Archives Canada

Bibliothèque et
Archives Canada

Published Heritage
Branch

Direction du
Patrimoine de l'édition

0-494-08203-8

395 Wellington Street
Ottawa ON K1A 0N4
Canada

395, rue Wellington
Ottawa ON K1A 0N4
Canada

Your file *Votre référence*

ISBN:

Our file *Notre référence*

ISBN:

NOTICE:

The author has granted a non-exclusive license allowing Library and Archives Canada to reproduce, publish, archive, preserve, conserve, communicate to the public by telecommunication or on the Internet, loan, distribute and sell theses worldwide, for commercial or non-commercial purposes, in microform, paper, electronic and/or any other formats.

The author retains copyright ownership and moral rights in this thesis. Neither the thesis nor substantial extracts from it may be printed or otherwise reproduced without the author's permission.

AVIS:

L'auteur a accordé une licence non exclusive permettant à la Bibliothèque et Archives Canada de reproduire, publier, archiver, sauvegarder, conserver, transmettre au public par télécommunication ou par l'Internet, prêter, distribuer et vendre des thèses partout dans le monde, à des fins commerciales ou autres, sur support microforme, papier, électronique et/ou autres formats.

L'auteur conserve la propriété du droit d'auteur et des droits moraux qui protègent cette thèse. Ni la thèse ni des extraits substantiels de celle-ci ne doivent être imprimés ou autrement reproduits sans son autorisation.

In compliance with the Canadian Privacy Act some supporting forms may have been removed from this thesis.

Conformément à la loi canadienne sur la protection de la vie privée, quelques formulaires secondaires ont été enlevés de cette thèse.

While these forms may be included in the document page count, their removal does not represent any loss of content from the thesis.

Bien que ces formulaires aient inclus dans la pagination, il n'y aura aucun contenu manquant.


Canada

ABSTRACT

The CDMA system is multiple access interference (MAI) limited. The conventional matched filter (MF) receiver is non optimal as the MAI is treated as useless noise. This leads to the proposal of the optimal multiuser receiver which has very good performance but is too complex to be practical. Sub-optimal detectors such as interference cancellation (IC) receivers seem promising due to their structural simplicity and good performance. The variable group hybrid interference cancellation (VGHIC) receiver proposed in this thesis combines the advantages of the parallel IC (PIC) and successive IC (SIC) in a novel way. In the VGHIC, users are grouped such that those with similar powers are selected into the same group. The PIC is used within the members of each group while the SIC is applied between groups of different powers. Theoretical analysis as well as simulations show that the VGHIC has an overall performance advantage over other IC receivers. Improvements have also been proposed to further enhance the performance of the VGHIC. They include the ranking of users, use of the averaged correlation samples, partial combining of correlation samples and partial cancellation. These techniques are found to be effective. Due to the adaptive nature of the VGHIC structure, it exhibits different processing delay profiles depending on the power spread of received signals. A simple method of limiting the processing delay has been proposed. It can reduce the processing delay by 40% at the expense of 4.5% reduction in user capacity. When phase and timing estimation errors are introduced, the VGHIC has better performance than other IC schemes even with high estimation errors. The VGHIC with RAKE receiver is investigated using realistic channel conditions and the results verify that it outperforms the conventional RAKE receiver. The major advantage of the VGHIC over other IC schemes is the ability to adapt its structure according to changing power profile of the received signals. Hence, the VGHIC is able to perform consistently in different environments. Moreover, its structure can be easily changed by modifying the design parameter. All these features make the VGHIC a viable option for increasing the capacity of CDMA systems.

ACKNOWLEDGEMENTS

I would like to thank Dr. Witold Krzymień for his guidance, invaluable advices, generosity and support. I am also grateful to the staff and fellow students of *TRLabs* for making my stay pleasant and memorable. I appreciate the help and support from the friendly staff of the former Centre of Wireless Communications (CWC). Last but not least, I would like to thank the former National Science and Technology board (NSTB) of Singapore and *TRLabs* for their support and funding.

TABLE OF CONTENT

1:	Introduction	1
1.1	Multiple access interference in CDMA systems and its mitigation	1
1.2	Contributions	3
1.3	Thesis outline	4
2:	Multi-user detection and interference cancellation	6
2.1	Basic principles	6
2.1.1	Spread spectrum communication systems	6
2.1.2	Code division multiple access (CDMA)	10
2.1.3	Conventional matched filter (MF) receiver	14
2.2	Multisuser detectors	15
2.2.1	The optimal detector	16
2.2.2	Linear multisuser detectors	19
2.3	Interference cancellation	21
2.3.1	Parallel interference cancellation (PIC)	22
2.3.2	Successive interference cancellation (SIC)	27
2.3.3	Hybrid interference cancellation (HIC)	32
2.4	Summary	35
3:	The Variable Group Hybrid Interference Cancellation scheme (VGHIC)	38
3.1	System model	38
3.2	Receiver structure	40
3.3	System assumptions and simplifications for the analysis	47
3.4	AWGN performance	49
3.4.1	Matched filter	49
3.4.2	Parallel interference cancellation (PIC)	51
3.4.3	Successive interference cancellation (SIC)	54
3.4.4	Variable group hybrid interference cancellation (VGHIC)	57

3.5	Performance in Rayleigh fading	65
3.5.1	Matched filter	66
3.5.2	Parallel interference cancellation (PIC)	68
3.5.3	Successive interference cancellation (SIC)	70
3.5.4	Variable group hybrid interference cancellation (VGHIC)	72
3.6	Performance comparison	76
3.6.1	Additive white Gaussian noise (AWGN) channel	76
3.6.2	Rayleigh fading	80
3.7	Summary	82
4:	Improvements to the basic VGHIC structure	84
4.1	Methods of ordering users	84
4.1.1	Effect in AWGN channel	87
4.1.2	Effect in fading channel	88
4.2	Averaging correlation samples	92
4.2.1	Effect in AWGN channel	93
4.2.2	Effect in fading channel	94
4.3	The multi-stage structure	101
4.4	Partial combination of correlations samples and partial cancellation ..	105
4.4.1	Partial combination of correlation samples	106
4.4.2	Partial cancellation	107
4.4.3	Effects in AWGN channel	108
4.4.4	Effects in Rayleigh fading channel	111
4.5	Processing delay	113
4.5.1	Statistics of the delay	114
4.5.2	A method of limiting the delay	116
4.5.3	Effect on performance	117
4.6	Summary	122

5:	Performance of the VGHIC with non-ideal channel conditions	124
5.1	Robustness against imperfect channel parameter estimates	125
5.1.1	BER improvement over the single stage VGHIC with errors ..	125
5.1.2	BER degradation on the multi-stage structures	129
5.1.3	Capacity comparison	134
5.2	RAKE receiver implementations	137
5.2.1	Various configurations	138
5.2.2	The simulation system	141
5.2.3	Performance comparison	142
5.3	Summary	149
6:	Conclusions	150
6.1	Summary and concluding remarks	150
6.2	Future work	153
Appendix A:	Property of the Cross-Correlation and Time Delay	154
A.1	The Cross-Correlation between users	154
A.2	Probability density function (pdf) of $\Delta\tau_{ij}$	157
Appendix B:	Mean and variance of the correlation sample for SIC	161
Appendix C:	The CDF and PDF of the sum of Rayleigh and Gaussian random variables.	164
Appendix D:	The Simulation System	167
D.1	Parameters used	167
D.2	Receiver structures used	168
References	169

LIST OF FIGURES

Figure 2.1:	A general spread spectrum system.	7
Figure 2.2:	Spectrum of the original and spread signal.	8
Figure 2.3:	Different multiple access scheme.	10
Figure 2.4:	The spreading process.	11
Figure 2.5:	The despreading process.	12
Figure 2.6:	Shift register circuit for generating the m-sequence based on the primitive polynomial $x^4 + x + 1$	12
Figure 2.7:	Auto-correlation of a m-sequence.	13
Figure 2.8:	The 1-stage parallel interference cancellation.	22
Figure 2.9:	The structure of the interference cancellation unit for step i of stage s , $ICU(i, s)$ of the SIC.	28
Figure 2.10:	Structure of the M -stage SIC.	30
Figure 2.11:	Structure of the HIC.	33
Figure 2.12:	Structure of the AHSPIC.	34
Figure 3.1:	The working principle behind the variable group hybrid interference cancellation scheme.	41
Figure 3.2:	Structure of the group cancellation unit for the j^{th} subtractive step of the VGHC scheme, $GCU(j)$	42
Figure 3.3:	Structure of the parallel cancellation block in the $GCU(j)$	46
Figure 3.4:	Asynchronous system with time delays limited to within one T_c	48
Figure 3.5:	Structure of 1 stage of the PIC scheme.	52
Figure 3.6:	Structure of the i^{th} subtractive step of the SIC scheme.	54
Figure 3.7:	The simplified variable group interference cancellation (VGHC).	57
Figure 3.8:	Comparison of the derived BER (3.86) and (3.87) from Proakis [29] for the case where $D = 1$ and $D = 3$	68
Figure 3.9:	The comparison of the analytical BER performance versus the SNR in AWGN channel.	79
Figure 3.10:	The comparison of the analytical BER performance versus the number of users in AWGN channel.	80
Figure 3.11:	The comparison of the analytical BER performance versus the SNR in Rayleigh fading channel.	81
Figure 3.12:	The comparison of the analytical BER performance versus the number of users in the Rayleigh fading channel.	82
Figure 4.1:	Ordering methods for the VGHC or SIC.	86
Figure 4.2:	Comparison of the BER performance for the VGHC($\delta = 0.8$) in AWGN channel between the ordering methods.	89

Figure 4.3:	Comparison of the BER performance for the VGHIC($\delta=0.4$) in the AWGN channel between the ordering methods.	89
Figure 4.4:	Comparison of the BER performance for the SIC in the AWGN channel between the ordering methods	90
Figure 4.5:	Comparison of the BER performance for the VGHIC($\delta=0.8$) in the Rayleigh fading channel between the ordering methods.	90
Figure 4.6:	Comparison of the BER performance for the VGHIC($\delta=0.4$) in the Rayleigh fading channel between the ordering methods.	91
Figure 4.7:	Comparison of the BER performance for the SIC in the Rayleigh fading channel between the ordering methods.	91
Figure 4.8:	Effect of the number of averaging bits on the BER performance of the PIC in AWGN channel.	96
Figure 4.9:	Effect of the number of averaging bits on the BER performance of the SIC in AWGN channel.	96
Figure 4.10:	Effect of the number of averaging bits on the BER performance of the VGHIC($\delta=0.4$) in AWGN channel.	97
Figure 4.11:	Effect of the number of averaging bits on the BER performance of the VGHIC($\delta=0.8$) in AWGN channel.	97
Figure 4.12:	Effect of the number of averaging bits on the BER performance of the PIC and SIC (with ordering method M1 and M2) in Rayleigh fading channel with maximum Doppler shift of 100 Hz.	98
Figure 4.13:	Effect of the number of averaging bits on the BER performance of the VGHIC($\delta=0.4$) (with ordering method M1 and M2) in Rayleigh fading channel with maximum Doppler shift of 100 Hz.	98
Figure 4.14:	Effect of the number of averaging bits on the BER performance of the VGHIC($\delta=0.8$) (with ordering method M1 and M2) in Rayleigh fading channel with maximum Doppler shift of 100 Hz.	99
Figure 4.15:	Effect of the number of averaging bits on the BER performance of the PIC and SIC (with ordering method M1 and M2) in Rayleigh fading channel with maximum Doppler shift of 300 Hz.	99
Figure 4.16:	Effect of the number of averaging bits on the BER performance of the VGHIC($\delta=0.4$) (with ordering method M1 and M2) in Rayleigh fading channel with maximum Doppler shift of 300 Hz.	100
Figure 4.17:	Effect of the number of averaging bits on the BER performance of the VGHIC($\delta=0.8$) (with ordering method M1 and M2) in Rayleigh fading channel with maximum Doppler shift of 300 Hz.	100
Figure 4.18:	Structure of the group cancellation unit (GCU) for the j^{th} subtractive step of the s^{th} cancellation stage for a M -stage VGHIC scheme	102
Figure 4.19:	Structure of the M -stage VGHIC scheme	105

Figure 4.20:	BER of the one-stage VGHIC scheme with the partial combining of correlation samples (PCC) and partial cancellation (PC) in a single-cell asynchronous system with perfect fast and slow power control. Cancellations were done for 30-bit blocks and the average correlation sample value over 30 bits was used.	109
Figure 4.21:	Performance comparison between the multistage VGHIC and I-VGHIC schemes in AWGN channel with different SNRs (a single-cell asynchronous system)	110
Figure 4.22:	BER comparison between the I-VGHIC scheme and other subtractive cancellation schemes in flat Rayleigh fading channel with no AWGN (an asynchronous single-cell system)	112
Figure 4.23:	Performance comparison between the I-VGHIC scheme and other subtractive cancellation schemes in AWGN channel at SNR = 10 dB (asynchronous single-cell system)	113
Figure 4.24:	The number of subtractive steps for one stage of the I-VGHIC with $\delta = 0.6, 0.7$ and 0.8 , in the AWGN (SNR = 10 dB) and flat Rayleigh fading channels with different numbers of users (asynchronous single-cell system). \square : AWGN channel; \blacksquare : Flat Rayleigh fading channel.	115
Figure 4.25:	Cumulative distribution of the number of subtractive step for each full I-VGHIC interference cancellation stage of an asynchronous single-cell system. Processing gain = 63.	116
Figure 4.26:	Performance comparison between the standard I-VGHIC and the I-VGHIC(m,n) (both with $\delta = 0.7$) for different values of m and n in flat Rayleigh fading channel with 60 simultaneously transmitting users. (Asynchronous single-cell BPSK/CDMA system with maximum Doppler shift = 100 Hz and processing gain = 32).	118
Figure 4.27:	Comparison of the BER performance of the multi-stage I-VGHIC and I-VGHIC(m,n) with $\delta = 0.7$ in flat Rayleigh fading channel.	119
Figure 4.28:	Delay profile showing the processing delays of one stage of the SIC, I-VGHIC and I-VGHIC(m,n) (with $\delta = 0.7$ and 0.8) in AWGN and flat Rayleigh fading channels.	121
Figure 5.1:	BER improvement versus phase estimation error for various receivers in an AWGN channel.	127
Figure 5.2:	BER improvement versus delay timing estimation error for various receivers in AWGN channel.	127
Figure 5.3:	BER improvement versus phase estimation error for various receivers in a flat Rayleigh fading channel.	128
Figure 5.4:	BER improvement versus delay timing estimation error for various receivers in flat Rayleigh fading channel.	128

Figure 5.5:	BER degradation versus phase and timing estimation errors for the multi-stage VGHIC in AWGN channel.	131
Figure 5.6:	BER degradation versus phase and timing estimation errors for the multi-stage VGHIC in flat Rayleigh fading channel.	131
Figure 5.7:	BER degradation versus phase and timing estimation errors for the multi-stage SIC in AWGN channel.	132
Figure 5.8:	BER degradation versus phase and timing estimation errors for the multi-stage SIC in flat Rayleigh fading channel.	132
Figure 5.9:	BER degradation versus phase and timing estimation errors for the multi-stage PIC in AWGN channel.	133
Figure 5.10:	BER degradation versus phase and timing estimation errors for the multi-stage PIC in flat Rayleigh fading channel.	133
Figure 5.11:	User capacity of the multi-stage PIC, SIC and VGHIC with the timing error in AWGN channel.	135
Figure 5.12:	User capacity of the multi-stage PIC, SIC and VGHIC with the phase error in AWGN channel.	135
Figure 5.13:	User capacity of the multi-stage PIC, SIC and VGHIC with the timing error in Rayleigh fading channel.	136
Figure 5.14:	User capacity of the multi-stage PIC, SIC and VGHIC with the phase error in Rayleigh fading channel.	136
Figure 5.15:	A H -finger RAKE receiver	137
Figure 5.16:	Modified parallel interference cancellation (PIC) with RAKE receivers	139
Figure 5.17:	Structure of the multistage I-VGHIC-M3	140
Figure 5.18:	Pedestrian (3 km/h) - Channel A: 1-stage I-VGHIC	145
Figure 5.19:	Pedestrian (3 km/h) - Channel B: 1-stage I-VGHIC	145
Figure 5.20:	Vehicular (120 km/h) - Channel A: 1-stage I-VGHIC	146
Figure 5.21:	Vehicular (120 km/h) - Channel B: 1-stage I-VGHIC	146
Figure 5.22:	Pedestrian (3 km/h) - Channel A: 2-stage I-VGHIC	147
Figure 5.23:	Pedestrian (3 km/h) - Channel B: 2-stage I-VGHIC	147
Figure 5.24:	Vehicular (120 km/h) - Channel A: 2-stage I-VGHIC	148
Figure 5.25:	Vehicular (120 km/h) - Channel B: 2-stage I-VGHIC	148
Figure A.1:	Delay between user i and j	155
Figure C.1:	Graphical representation of the region of Z	165

LIST OF SYMBOLS

C	-	capacity in bits per second
W	-	bandwidth
SNR	-	signal-to-noise ratio
$c(t)$	-	spreading waveform
$p_{T_c}(t)$	-	pulse with the chip period, T_c
$C^{(n)}$	-	spreading chip sequence with index n
$p_{T_h}(t)$	-	pulse with the duration or hop time T_h
$F^{(n)}$	-	pseudo-noise frequency shift sequence with index n
N_f	-	number of positions within the interval period of T_d
$p_{T_d}(t)$	-	pulse with the duration, T_d / N_f
$T^{(n)}$	-	pseudo-noise position sequence with integer values between zero and $(N_f - 1)$, and index n
ρ	-	processing or spreading gain
BW_{spread}	-	is the bandwidth of the spread spectrum system
$BW_{information}$	-	the minimum bandwidth required to transmit the information
T_{pulse}	-	period of the spread spectrum pulse
$T_{information}$	-	period of the information bit
$s(t)$	-	direct sequence spread spectrum signal
$b(t)$	-	narrowband signal corresponding to the data waveform
$i(t)$	-	interference and noise
$r(t)$	-	received signal
L_m	-	period / length of m-sequence
$\alpha(k)$	-	auto-correlation function
K	-	total number of users in a system
B_i	-	information bit corresponding to user i
E_i	-	transmitted energy of user i
$c_i(t)$	-	spreading waveform of user i
L	-	log-likelihood function
G	-	$K \times K$ matrix of the received powers
R	-	cross-correlation matrix
N	-	total number of bits in a sequence
τ_i	-	delay for user i
T	-	bit period
L_{MMSE}	-	linear transformation matrix
$S_k(t)$	-	regenerated signal of user k

\tilde{B}_k	- estimated data for user k
$r_i(t)$	- cleaned signal for user i after the interference cancellation
$R_i^{(PIC)}$	- improved tentative decision for user i after parallel interference cancellation (PIC)
$r_i^{(M)}(t)$	- cleaned signal for user i after M -stages of interference cancellation
ρ_M	- partial cancellation parameter for stage M of the PIC
$\rho_{M,k}$	- partial cancellation parameter for user k of stage M
A_k	- received amplitude for user k
A_{max}	- largest amplitude among the users
ρ_k	- cancellation selection parameter for user k
$R_i^{(SIC)}$	- improved tentative decision for user i after successive interference cancellation (SIC)
$S_k^{(s)}(t)$	- regenerated signal of user k in stage s
$r_{i,j+1}(t)$	- input of the MF for user i after the j^{th} cancellation step
$S_{i,j}(t)$	- regenerated signal of user i at cancellation step j
G_j	- number of users in a group at cancellation step j
D_j	- number of users that have yet to be detected and cancelled at subtractive step j
G_n	- number of users in group n
N_g	- last group of users to be detected
$R_{i,j}^{(MF)}(m)$	- correlation sample of bit m of the user i in the j^{th} subtractive step at the output of the MF
δ	- design parameter for the VGHIC
GCU(j)	- group cancellation unit at step j
$r^{(j)}(t)$	- signal before GCU(j)
$R_{i,j}^{(PIC)}(m)$	- correlation sample of bit m of the user i at the output of the PIC block within GCU(j)
$\gamma_{ki}(m)$	- cross-correlation factor for bit m between user k and i
$\Psi_{ki}(m)$	- continuous-time partial cross-correlation function
$\tilde{\Psi}_{ki}(m)$	- continuous-time partial cross-correlation function
τ_i	- time delay of user i
$P_e^{(MF)}$	- bit error rate (BER) of the matched filter
μ_s	- mean of the matched filter output
σ_s	- standard deviation of the matched filter output
$P_e^{(PIC)}$	- bit error rate of the parallel interference cancellation
$P_e^{(SIC)}$	- bit error rate of the successive interference cancellation

$P_e^{(VGHIC)}$	- bit error rate of the variable group hybrid interference cancellation
$\bar{R}_{(g)}^{(MF)}$	- average correlation sample value corresponding to the rank g
g_j^{ref}	- reference index for group j
α_i	- Rayleigh distributed channel gain term for user i
α^2	- is the variance of the Gaussian random variables
θ_i	- phase of user i
b^2	- normalized variance of the multi-access interference and noise term
$\bar{\gamma}_b$	- average signal-to-noise ratio
$r_f(t)$	- received signal under fading channel
$\bar{R}_{i,j}^{(MF,s)}(n)$	- average correlation sample value of the MF over n bits for user i at the j^{th} step of stage s
$\bar{R}_{i,j}^{(PIC,s)}(n)$	- average correlation sample value of the PIC over n bits for user i at the j^{th} step of stage s
$\bar{R}_{i,j}^{p(MF,s)}(n)$	- average correlation sample value of the MF over n bits for user i at the j^{th} step of stage s after partial combining
$\bar{R}_{i,j}^{p(PIC,s)}(n)$	- average correlation sample value of the PIC over n bits for user i at the j^{th} step of stage s after partial combining
$p_f(s)$	- partial combining factor to be set for stage s
$p_c(s)$	- partial cancellation factor for stage s
LPF	- low pass filter

Chapter 1: Introduction

The second generation (2G) cellular networks may be the most widespread wireless system to date with a huge subscriber base. They use digital modulations and are primarily designed for voice traffic with limited capacity for data traffic. It has been envisaged that the demand for data traffic will increase beyond the capabilities of present 2G systems. This leads to the proposal and standardization of 3G networks which have much more advanced voice and data handling capabilities. The 3G network supports both symmetric circuit switched services (speech or video) as well as asymmetric packet switched services (internet data flows). For the 3G system potential customers will be able to receive live music, conduct interactive web sessions, and have simultaneous voice and data access with multiple parties at the same time. Third generation networks are based on CDMA technologies with three main standards: wideband CDMA (W-CDMA), cdma2000 and time division-synchronous CDMA (TD-SCDMA). All these 3G standards have provisions for multiuser detection which highlights the importance of multiuser detections for high capacity CDMA systems.

1.1 Multiple access interference in CDMA systems and its mitigation

In a conventional Code Division Multiple Access (CDMA) system, mobile users are able to communicate with the base station simultaneously over a common radio channel using different pseudo random spreading codes assigned to them. In the reverse link, the signals of all the transmitting users interfere with each other as the spreading codes are not orthogonal. At the base station, the desired user is detected with a correlator or matched filter (MF) treating the multiple access interference (MAI) as useless noise. To increase the capacity of CDMA systems, multiuser detectors have been proposed to cancel the MAI. The optimum detector proposed by Verdú [1] has excellent performance but its complexity increases exponentially with the number of transmitting mobiles. Hence, sub-optimum multiuser detection schemes such as the decorrelator, minimum mean square error (MMSE)

detector and interference cancellation (IC) receivers are considered as practically viable alternatives.

Comparisons between the MF, linear multiuser detectors (decorrelator and MMSE) and the IC multiuser receivers have been done in additive white Gaussian noise (AWGN) [2], flat [3] and frequency selective [4] Rayleigh fading channels. All multiuser receivers are able to provide significant gains over the conventional MF.

For the AWGN channel, all the multiuser detectors have similar performance. For the flat Rayleigh fading channel the decorrelator and MMSE detectors have a performance advantage over the IC receivers. The situation is different in the frequency selective Rayleigh fading channel where the IC receivers are able to outperform linear detectors. With imperfect channel estimations and timing misalignment, the performance of the decorrelator and the MMSE detectors are found to degrade more rapidly than the IC receivers. Moreover, the performance of the decorrelator is extremely sensitive to the frequency of the updates for its parameters. Comparing the computational requirement, the parallel (PIC) and successive (SIC) interference cancellation are less complex. This is supported by the fact that hardware implementations of the PIC [5][6] and SIC [7][8] already exist and their performance is published. In [9], the effect of imperfect power control and imperfect channel estimation are investigated for the decorrelator, MMSE, conventional and improved version of the PIC. Results show that the PIC structures have better performance.

The IC receivers with simpler structures, coupled with comparable if not better performance than the linear detectors, make them a highly viable choice for practical implementations. However, there are still areas which one can improve on the existing IC receivers. Hence, the focus of this thesis would be on the promising IC receiver structures.

1.2 Contributions

The work in this thesis has made a few novel contributions to the field. Following the order of this thesis, the contributions are:

- Detailed survey of the current state of technologies for interference cancellation techniques.
- Proposal of a novel variable group hybrid interference cancellation (VGHIC) structure.
- Theoretical analysis of the VGHIC for additive white Gaussian noise (AWGN) and Rayleigh fading channels.
- Theoretical analysis of the parallel (PIC) and successive (SIC) interference cancellation for AWGN and Rayleigh fading channels taking into account the effect of self-cancellation due to the correlation samples in the cancellation process.
- Study of the effect of different ways of ordering users on the performance of the VGHIC and SIC.
- Proposal of the partial combination of correlation samples to enhance the performance.
- Investigation of the processing delay of the VGHIC and the proposal of a method to limit the delay.
- Investigation of the effect of timing and phase error on the performance and capacity of the multistage IC structures.
- Proposal and investigation on three different implementations of the RAKE receiver in the VGHIC under realistic multipath fading environments.

Some of the work and results have been published in [10][11][12][13][14]. At the time of writing, new developments of structures similar to that of the VGHIC have been done by other groups in [15][16].

1.3 Thesis outline

In Chapter 2, a brief overview of the spread spectrum system is given, outlining the basic concepts behind the code division multiple access (CDMA) systems and their limitations. After that, the optimal and linear multiuser detectors are presented and discussed. Then, an in-depth discussion of the IC receivers is presented with their merits and shortcomings compared and discussed.

In Chapter 3, the structure of the variable group hybrid interference cancellation (VGHIC) scheme is presented first. Then, an analysis is done on the bit error rate (BER) performance of the matched filter (MF) receiver, parallel interference cancellation (PIC), successive interference cancellation (SIC) and the variable group hybrid interference cancellation (VGHIC). Here, the self cancellation term is taken into account as the correlation samples are used in the signal generation and cancellation process.

In Chapter 4, several techniques of further improving the VGHIC are proposed. The impact of the user ordering methods on the VGHIC and SIC in the AWGN and Rayleigh fading channel is investigated. Then, the use of the averaged correlation samples in the interference cancellation process is studied. After that, the multi-stage structure for the VGHIC is presented. This is followed by the idea of partial correlation combining and partial cancellation. The processing delay of the VGHIC is then being looked into and a method for reducing its processing delay is proposed.

In Chapter 5, the performance of the VGHIC in non-ideal conditions is examined. The impact of the timing and phase estimation errors on the bit error rate (BER) performance of different schemes is studied. The effect of estimation errors on the effectiveness of the multi-stage structure is compared with that of the single stage VGHIC for the AWGN and flat Rayleigh fading channels. Then, three different RAKE receiver implementations in the VGHIC are investigated and studied. The BER performance of the VGHIC with different RAKE implementations is presented and discussed for four different frequency selective fading channels.

In Chapter 6, the observations and results of studies are summarized and concluding remarks on the VGHIC is made. The future extension of this work is also being suggested.

Chapter 2: Multi-user detection and interference cancellation

The works on improving the performance and capacity of the code division multiple access (CDMA) systems have been ongoing. A typical area is the use of multiuser detectors or interference cancellation (IC) receivers. Even though there are many types of multiuser and IC receivers, they can be classified into a few basic groups. The optimal receiver is the maximum likelihood multiuser detector. The linear and the non-linear receivers are the two main groups of sub-optimal receivers which are less complex than the optimal receiver. For the linear receivers, the main candidates are the decorrelator and minimum mean square error (MMSE) detectors. The IC receivers belong to a major and important group of non-linear receivers. These IC receivers will be the focus of discussion.

In this chapter, the reader will be given a brief overview of the spread spectrum system and the basic concepts behind the code division multiple access (CDMA) systems and its limitations in Section 2.1. After this, the optimal and the linear multiuser detectors are presented in Section 2.2. Then, an in-depth discussion on the IC receivers is provided in Section 2.3 with their merits and shortcomings compared and discussed.

2.1 Basic principles

This section provides the reader with the basics of the spread spectrum systems and brief discussions of the various transmission strategies. Then, the more in-depth discussion is done on the CDMA system which is relevant to this thesis.

2.1.1 Spread spectrum communication systems

The primary use of spread spectrum technologies in the early days was military anti-jamming communication systems [17]. Because the properties of the spread spectrum systems are

highly desirable in the present mobile communications systems, there are more and more commercial applications in recent years. The third generation (3G) mobile system is based on the spread spectrum system.

The spread spectrum system has been defined as a means of transmitting the information by a signal which occupies a bandwidth much larger than necessary. This is accomplished by the use of a spreading code which allows the information to be recovered at the receiver when synchronized. A general spread spectrum system is shown in Figure 2.1.

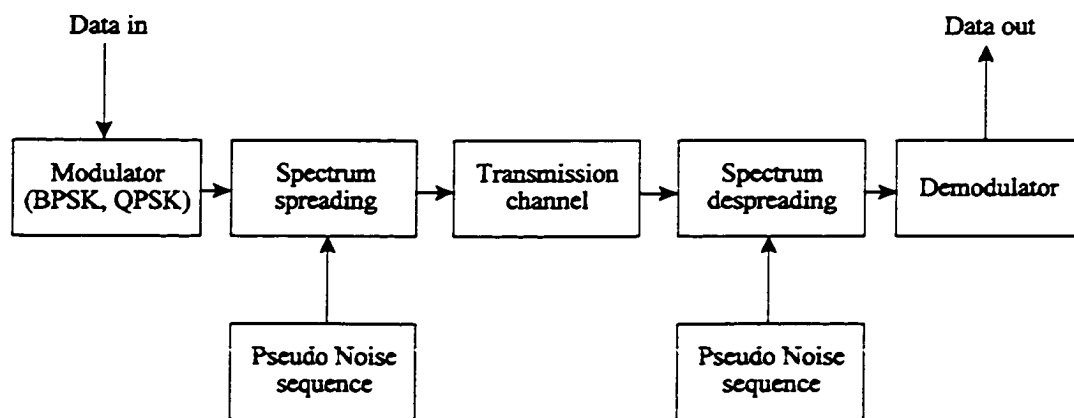


Figure 2.1: A general spread spectrum system.

The data is first modulated by a conventional narrowband modulation technique such as binary phase shift keying (BPSK). This narrowband-modulated signal is then spread using the pseudo noise (PN) sequence before transmission. The result of spreading is a wideband signal shown in Figure 2.2. At the receiver, despreading is done with the same PN sequence and this collapses the spectrum of the spread signal down to that of the narrowband signal. The narrowband signal is then demodulated in the usual way to retrieve the data. The basis for the spread spectrum technology can be derived from the Shannon's channel capacity theorem [18],

$$C = W \log_2 (1 + SNR) \quad (2.1)$$

where C is the capacity in bits per second, W is the bandwidth and SNR is the signal-to-noise ratio. From [19], (2.1) can be simplified to

$$C \approx 1.44 SNR \times W \quad (2.2)$$

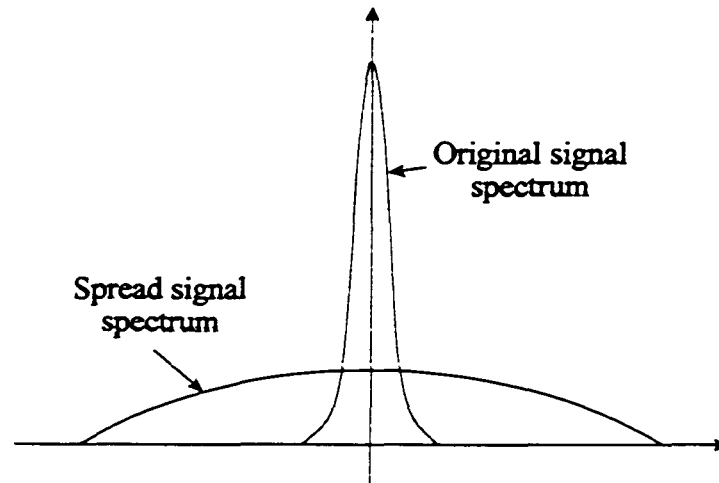


Figure 2.2: Spectrum of the original and spread signal.

From (2.2), one can see that if the bandwidth is increased, the same amount of data can be transmitted with a lower *SNR*. This way of transmission leads to several desirable properties [17], [19], [20] some of which are relevant to mobile communication systems such as:

1. Interference rejection
2. Selective addressing capability
3. Multiple access using code division
4. Multipath protection

There are a few types of spread spectrum systems around and the more commonly known ones are the direct sequence, frequency hopping and time hopping spread spectrum systems.

In direct sequence (DS) systems, the spectrum spreading is done by the waveform,

$$c(t) = \sum_n C^{(n)} p_{T_c}(t - nT_c) \quad (2.3)$$

where $p_{T_c}(t)$ is a pulse with the chip period T_c , and the $C^{(n)}$ is spreading chip sequence which is generated by a pseudo-noise (PN) generator. The term n is the index of the chip sequence.

The wideband spreading waveform is directly multiplied with the modulated narrowband signal to produce a wideband spread spectrum signal, hence the name direct sequence.

For frequency hopping (FH) systems, the spreading waveform is,

$$c(t) = \sum_n \exp[j(2\pi F^{(n)})] p_{T_h}(t - nT_h) \quad (2.4)$$

where $p_{T_h}(t)$ is a pulse with the duration or hop time T_h , $F^{(n)}$ is the pseudo-noise frequency shift sequence with index n . The effect of using this spreading waveform is the carrier frequency of the signal will change every T_h in a predestinated fashion determined by the frequency shift sequence, $F^{(n)}$. In other words, the frequency of the system hops around.

As the name suggests, in the time hopping (TH) system, the signal hops to any of the N_t positions within the predesignated interval period of T_d seconds. The spreading waveform is therefore,

$$c(t) = \sum_n p_{T_d} \left(t - \left(n + \frac{T^{(n)}}{N_t} \right) T_d \right) \quad (2.5)$$

where $p_{T_d}(t)$ is a pulse with the duration T_d / N_t , and $T^{(n)}$ is the pseudo-noise position sequence with integer values assuming anything between zero and $(N_t - 1)$.

An important term associated with the spread spectrum system is the processing or spreading gain, ρ . It is given by,

$$\begin{aligned} \rho &= \frac{BW_{spread}}{BW_{information}} \\ &= \frac{T_{information}}{T_{pulse}} \end{aligned} \quad (2.6)$$

where BW_{spread} is the bandwidth of the spread spectrum system and $BW_{information}$ is the minimum bandwidth required to transmit the information. The period of the spread spectrum pulse and the information bit are T_{pulse} and $T_{information}$, respectively.

2.1.2 Code division multiple access (CDMA)

Allowing multiple users to have access to a common transmission channel is a classical communication problem. The two most commonly used techniques are the frequency division multiple access (FDMA) and time division multiple access (TDMA). In FDMA, different users access the channel with unique carrier frequencies assigned all the time. While for TDMA, users have the same frequency but they access the channel in a different but predefined time. Then, with spread spectrum techniques, there is code division multiple access (CDMA) where the users are able to transmit all the time using the same frequency (Figure 2.3). In CDMA users are differentiated by unique spreading codes. Although CDMA can be implemented using the different spread spectrum techniques, when CDMA is referenced, it usually refers to the direct sequence version of the CDMA or DS-SS-CDMA.

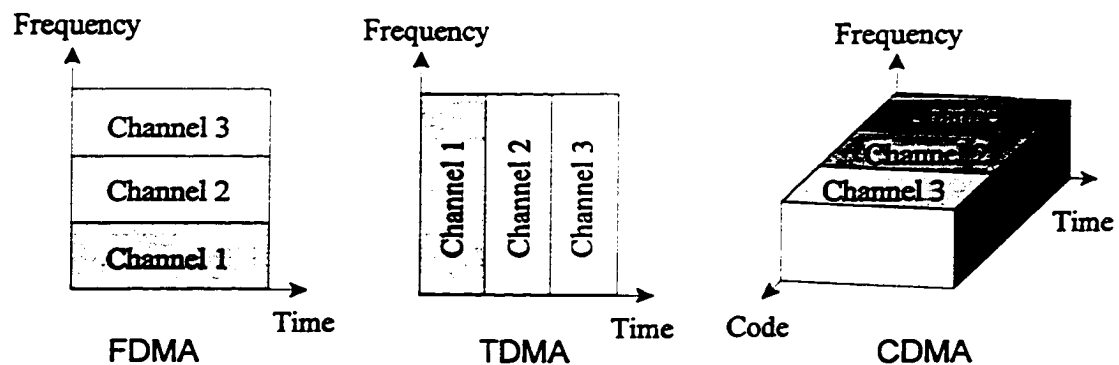


Figure 2.3: Different multiple access scheme.

In a DS spread spectrum system, spectrum spreading is accomplished by modulating the information data with a wideband pseudo-noise (PN) code to produce the DS signal, $s(t)$,

$$s(t) = c(t)b(t) \quad (2.7)$$

where $c(t)$ is the spreading waveform given in (2.3) and $b(t)$ is the narrowband signal corresponding to the data waveform. This process is illustrated in Figure 2.4 where the multiplication in the time domain corresponds to convolution in the frequency domain. That is why the resulting signal $s(t)$ is wideband.

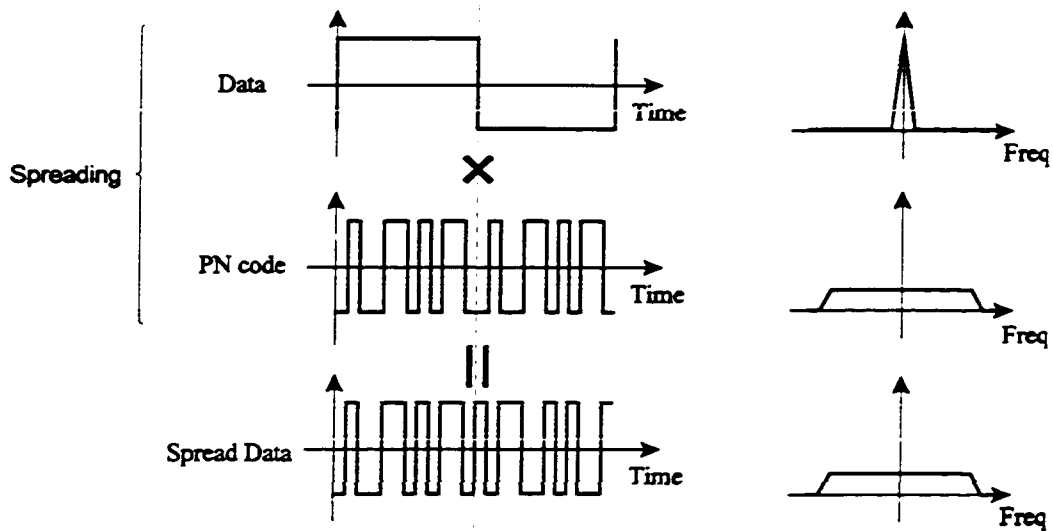


Figure 2.4: The spreading process.

The received signal, $r(t)$ is,

$$r(t) = s(t) + i(t) \quad (2.8)$$

where $i(t)$ represents the interference and noise. After despreading (Figure 2.1) one obtains,

$$\begin{aligned} z(t) &= r(t)c(t) \\ &= b(t) + c(t)i(t) \end{aligned} \quad (2.9)$$

where $c^2(t) = 1$ and the narrowband signal $b(t)$ has been recovered. The interference term remains as a wideband signal as it does not have the correct spreading code. Then, after passing through the narrowband demodulator, most of the interference would have been filtered out and the effect of the interference on the desired signal has been significantly reduced as shown in Figure 2.5.

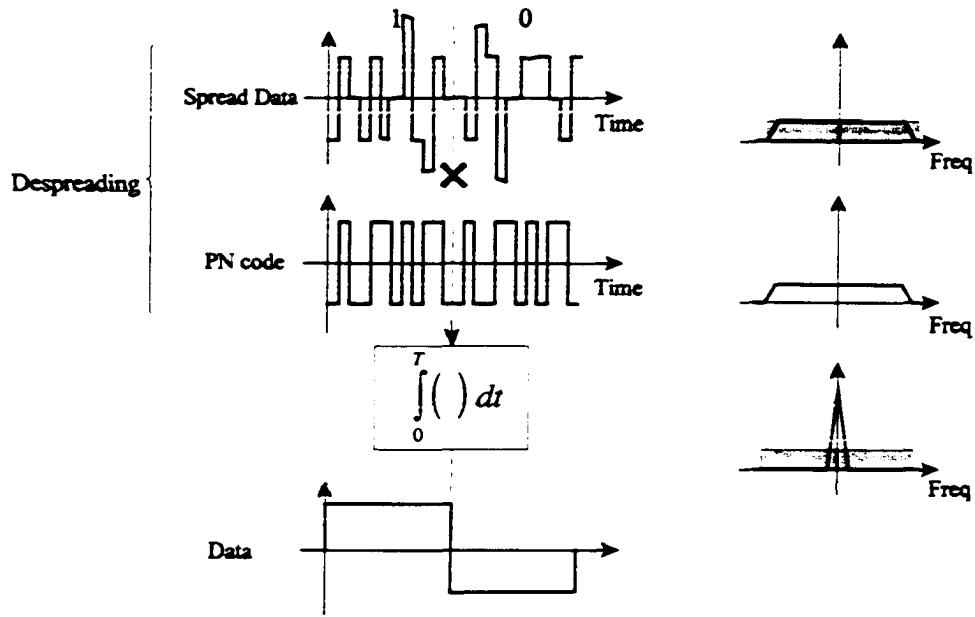


Figure 2.5: The despreading process.

The pseudo-noise (PN) spreading code is an important component of the CDMA system. A PN sequence is a coded sequence of ones and zeros with certain auto-correlation properties. Let us consider the maximum-length sequence or the m-sequence which is commonly used in CDMA systems. The m-sequences are periodic with length L_m given by,

$$L_m = 2^l - 1 \quad (2.10)$$

where l is the l -stage shift register that generates the sequence. Figure 2.6 shows the shift register circuit based on the primitive polynomial $x^4 + x + 1$ [17][21][22][23].

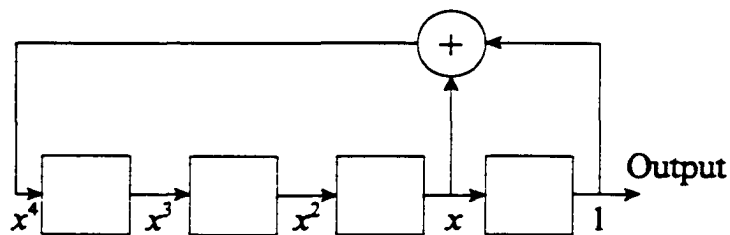


Figure 2.6: Shift register circuit for generating the m-sequence based on the primitive polynomial $x^4 + x + 1$.

The properties of the m-sequence are:

- 1 In each period of the m-sequence, the number of ones is always one more than the number of zeros. This is known as the balance property.
- 2 Among the runs of ones and zeros in each period of a m-sequence, one half of the runs of each kind is of length one, one-fourth is of length two, one-eighth is of length three, and so on. This is known as the run property. The length of the "run" means the number of consecutive identical symbols (ones or zeros) within one period of the m-sequence. The total number of runs for a m-sequence of period L_m is $(l + 1) / 2$. The term l is defined in (2.10). For the exact mathematical definitions, please refer to [17].
- 3 The auto-correlation function $\alpha(k)$ of a m-sequence is periodic and bi-valued. It is shown in Figure 2.7 and given by,

$$\alpha(k) = \begin{cases} L_m & , \text{for } k = 0, \pm L_m, \pm 2L_m, \dots \\ -1 & , \text{otherwise} \end{cases} \quad (2.11)$$

where L_m is the period of the m-sequence.

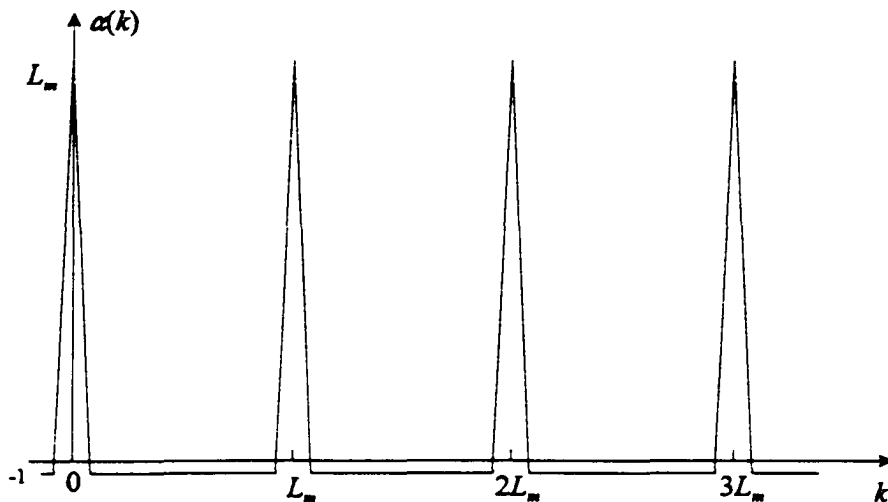


Figure 2.7: Auto-correlation of a m-sequence.

After having a brief understanding of the DS system which CDMA is based on, the limitation of the CDMA will be discussed next. For CDMA, all the users in the system access the channel at the same time using the same carrier frequency. They are only differentiated by the unique spreading codes assigned to each of them. If one can design spreading codes that are orthogonal, the signals of the users in the system would not interfere with each other. However, in practice, it is very difficult to design the spreading codes such that orthogonality is maintained under any conditions. Orthogonal codes in the multipath fading channel will lose their orthogonality. As a result, users in the system will experience interference from each other. This interference is known as the multi access interference (MAI). For every user added into the system, the level of MAI will increase. This will degrade the signal quality of the users and ultimately limit the number of users in the CDMA system. Hence, the CDMA is an interference limited system.

Another problem is the near-far effect. The received signal of the user nearer to the base station will be higher than that of the user further away. While the nearer user may experience little interference, the MAI that the further user experience may be significant enough for the transmission quality to degrade rapidly. This effect may be alleviated by the use of power control where much research has been done [24][25][26][27][28]. However, power control can only make sure that the received signal of each user experiences about the same amount of MAI. The MAI is still present in the system. In the following sections, receivers that can combat the effects of MAI are discussed and compared.

2.1.3 Conventional matched filter (MF) receiver

In a K -user synchronous system, the received signal is given by,

$$r(t) = \sum_{i=1}^K \sqrt{E_i} c_i(t) B_i + n(t) \quad (2.12)$$

where B_i is the information bit corresponding to user i . The transmitted energy and spreading waveform of user i is E_i and $c_i(t)$, respectively. The noise term is denoted by $n(t)$. At the output of the conventional matched filter (MF) receiver for user i , one obtains

$$R_i^{(MF)} = \underbrace{\sqrt{E_i} B_i}_{\text{desired term}} + \underbrace{\sum_{\substack{k=1 \\ k \neq i}}^K \sqrt{E_k} B_k \gamma_{ki}}_{\text{MAI term}} + \underbrace{\eta}_{\text{noise term}} \quad (2.13)$$

where the cross-correlation is

$$\gamma_{ki} = \int_0^T c_k(t) c_i(t) dt \quad (2.14)$$

and η is the noise term after despreading.

Looking at (2.13), increasing the number of users in the CDMA system increases the amount of MAI which reduces the signal-to-noise ratio of the desired signal. This leads to the problems highlighted in the previous subsection.

The MF receiver is the optimal receiver in additive white Gaussian noise [29]. When used in the CDMA system, it treats the MAI as unwanted and useless noise. This is clearly not optimal. The better way is to make use of the information about the MAI for better detection. The receivers that make use of this MAI knowledge for detection can be classified into two general groups: the single user receiver with MAI suppression and the multi-user receivers. The basic principle behind the single user receiver with MAI suppression is the use of adaptive or blind filters to remove the MAI. Details can be found in [30][31][32][33]. The multi-user receivers will be discussed in the next few sections.

2.2 Multiuser detectors

In this section, the optimal and the linear multiuser detectors are discussed. For the linear receivers, the basic principles of the two most popular receivers are presented.

2.2.1 The optimal detector

The main principle behind the optimal detector is to determine the most probable bit sequences sent out by all users given the received signal. This is done by generating the transmitted signal, subtracting it from the received signal and taking note of the absolute difference. The set of bit sequences for all users that results in the smallest difference between the generated and received signal is deemed the most probable set. The optimal detector for the synchronous system is considered first and will be expanded to the asynchronous case.

For the K -user synchronous system with the received signal given in (2.12), the optimal maximum-likelihood receiver will select the bits for all users $\{B_i, i = 1 \dots K\}$ such that the log-likelihood function, L

$$L = \int_0^T \left[r(t) - \sum_{i=1}^K \sqrt{E_i} c_i(t) B_i \right]^2 dt \quad (2.15)$$

is minimized [29]. Minimizing L may be simplified [34] to maximizing

$$C(\mathbf{b}) = 2\mathbf{b}^{Tr} \mathbf{G} \mathbf{y} - \mathbf{b}^{Tr} \mathbf{G} \mathbf{R} \mathbf{G} \mathbf{b} \quad (2.16)$$

where \mathbf{b}^{Tr} is the transpose of \mathbf{b} . The bits for the users are represented as the vector

$$\mathbf{b} = [B_1 \ B_2 \ \dots \ B_K]^{Tr} \quad (2.17)$$

The matched filter outputs for K users are,

$$\begin{aligned} \mathbf{y} &= [y_1 \ y_2 \ \dots \ y_K]^{Tr} \\ y_i &= \int_0^T r(t) c_i(t) dt \end{aligned} \quad (2.18)$$

The $K \times K$ matrix of the received powers is

$$\mathbf{G} = \text{diag}\{\sqrt{E_1}, \sqrt{E_2}, \dots, \sqrt{E_K}\} \quad (2.19)$$

and the cross-correlation matrix

$$\mathbf{R} = \begin{bmatrix} \gamma_{11} & \cdots & \gamma_{1K} \\ \vdots & \ddots & \vdots \\ \gamma_{K1} & \cdots & \gamma_{KK} \end{bmatrix} \quad (2.20)$$

with

$$\gamma_{ij} = \int_0^T c_i(t) c_j(t) dt \quad (2.21)$$

To arrive at the optimal solution, (2.16) needs to be computed 2^k times corresponding to the number of combinations possible for \mathbf{b} assuming B_i is binary. This complexity grows exponentially with the number of users K , present in the system.

For the asynchronous system, there are two consecutive bits (assuming binary phase shift keying or BPSK) from other users that interfere with the desired bit of the desired user. Therefore, to apply the optimal detector to the asynchronous system, one has to consider the whole transmission sequence (N bits) of each user during the detection process. Following the procedure in [34], one could view the K -user asynchronous system each transmitting N -bits as a KN -user synchronous system with,

$$B_{i+(n-1)K} = B_i^{(n)} \quad , \quad i = 1, \dots, K, \quad n = 1, \dots, N \quad (2.22)$$

where $B_i^{(n)}$ represents bit n for the interval $[\tau_i+(n-1)T, \tau_i+(n-1)T+T]$. The delay for user i and the bit period are τ_i and T , respectively. Hence,

$$y_j = \int_{-\infty}^{\infty} r(t) c'_j(t) dt \quad (2.23)$$

$$c'_{i+(n-1)K}(t) = c_i(t - (n-1)T - \tau_i)$$

Similarly, to achieve optimal detection, one needs to maximize,

$$\mathbf{C}(\mathbf{b}) = 2\mathbf{b}^T \mathbf{G} \mathbf{y} - \mathbf{b}^T \mathbf{G} \mathbf{R} \mathbf{G} \mathbf{b} \quad (2.24)$$

where now

$$\mathbf{b} = [B_1 \ B_2 \ \dots \ B_{KN}]^{Tr} \quad (2.25)$$

the matched filter outputs are,

$$\mathbf{y} = [y_1 \ y_2 \ \dots \ y_{KN}]^{Tr} \quad (2.26)$$

the $KN \times KN$ diagonal matrix of the received powers, \mathbf{G} has diagonal elements corresponding to $[i+(n-1)K]$ having the value $\sqrt{E_i}$, and the cross-correlation matrix becomes,

$$\mathbf{R} = \begin{bmatrix} \mathbf{R}[0] & \mathbf{R}^T[1] & 0 & 0 & \dots & 0 & 0 \\ \mathbf{R}[1] & \mathbf{R}[0] & \mathbf{R}^T[1] & 0 & \dots & 0 & 0 \\ 0 & \mathbf{R}[1] & \mathbf{R}[0] & & \ddots & \vdots & \vdots \\ 0 & 0 & & \ddots & & 0 & 0 \\ \vdots & \vdots & \ddots & & \mathbf{R}[0] & \mathbf{R}^T[1] & 0 \\ 0 & 0 & \dots & 0 & \mathbf{R}[1] & \mathbf{R}[0] & \mathbf{R}^T[1] \\ 0 & 0 & \dots & 0 & 0 & \mathbf{R}[1] & \mathbf{R}[0] \end{bmatrix} \quad (2.27)$$

where $\mathbf{R}[0]$ and $\mathbf{R}[1]$ are defined as having elements

$$R_{ij}[0] = \begin{cases} 1 & , \ i = j \\ \gamma_{ij} & , \ i < j \\ \gamma_{ji} & , \ i > j \end{cases} \quad (2.28)$$

$$R_{ij}[1] = \begin{cases} 0 & , \ i \geq j \\ \gamma_{ji} & , \ i < j \end{cases}$$

and where

$$\gamma_{ij} = \int_{-\infty}^{\infty} c'_i(t) c'_j(t) dt \quad (2.29)$$

Hence, the complexity in this case is 2^{KN} . However, by exploiting the structure of the matrix \mathbf{GRG} the complexity can be reduced to 2^K [34].

Although with very good performance compared with the MF, the complexity of the optimal detector is very high at 2^K . It also needs the knowledge of the user delays, phases and powers to be effective. If this information is inaccurate, its performance will degrade rapidly [35]. In view of this, sub-optimal multiuser receivers have been proposed to achieve as near its performance as possible but with a much lower computational complexity.

2.2.2 Linear multiuser detectors

In this section, the decorrelator is discussed first and then it is followed by the minimum mean square error (MMSE) detector.

2.2.2.1 Decorrelator

Recall from previous section that the outputs of the bank of MF can be expressed as,

$$\mathbf{y} = \mathbf{R}\mathbf{G}\mathbf{b} + \mathbf{n} \quad (2.30)$$

where \mathbf{R} is the correlation matrix defined in (2.20) assumed to be invertible. Then one applies the \mathbf{R}^{-1} to the matched filters outputs

$$\mathbf{R}^{-1}\mathbf{y} = \mathbf{G}\mathbf{b} + \mathbf{R}^{-1}\mathbf{n} \quad (2.31)$$

where the signals from all users are freed from multiple access interference (MAI). The receiver that uses this technique for detections is known as the decorrelator which has been analyzed in details in [36]. From the above expression, the decorrelator does not suffer from near-far effect and it has been shown that it has the same degree of near-far resistance as the optimal detector [37].

The decorrelator has a computational complexity that is far less than that of the optimal receiver. However, the cost of computing the inverse matrix \mathbf{R}^{-1} is not low. Since \mathbf{R}^{-1} is computed based on the users spreading codes, it is easy to see that there is no need for the

decorrelator to estimate the received powers of the users. The received powers of users are required for the optimal detector. Also a direct consequence of the decorrelating process, it has very good near-far resistance.

There is one major disadvantage for this detector. The noise term is being enhanced. Examining the noise covariance, one has

$$\mathbf{E}\left[\left(\mathbf{R}^{-1}\mathbf{n}\right)\left(\mathbf{R}^{-1}\mathbf{n}\right)^T\right] = \sigma^2\mathbf{R}^{-1} \quad (2.32)$$

where σ^2 is the noise power. In the channel where the background AWGN is dominant, in the case where the signal-to-noise ratio (SNR) is low, the convention MF may outperform the decorrelator. In addition, there are certain correlation matrices that cause the MF to give better a bit error rate (BER) than the decorrelator for all SNR.

In spite of the above drawback, the correlator is generally able to provide performance gain over the MF in some typical mobile radio environments. In these situations, the SNR degradation from the noise enhancement is about 1 to 2 dB [38].

2.2.2.2 Minimum mean square error (MMSE)

For the decorrelator in the previous subsection, the noise term is not taken into account in the detection process. As a result, the noise term is enhanced. Here, a detector that takes into account of noise is presented. Here, the linear transformation is done such that it minimizes the mean square error between the estimations and actual data. The mean square error is given by,

$$\mathcal{E} = \mathbf{E}\left[\left(\mathbf{b} - \mathbf{L}_{MMSE}\mathbf{y}\right)^2\right] \quad (2.33)$$

which after some derivation gives \mathbf{L}_{MMSE} as a linear transformation matrix

$$\mathbf{L}_{MMSE} = \left[\mathbf{R} + \sigma^2\mathbf{A}^{-1}\right]^{-1} \quad (2.34)$$

where σ^2 is the noise power and,

$$\sigma^2 \mathbf{A}^{-1} = \text{diag} \left\{ \frac{\sigma^2}{E_1}, \dots, \frac{\sigma^2}{E_K} \right\} \quad (2.35)$$

The resulting receiver is known as the MMSE detector. From here, it can be noted that the MMSE detector requires information about the signal-to-noise ratios (SNR) of the users in order to work, whereas this information is not necessary in the decorrelator. The implication of this would be the loss of some near-far resistance [39] in place of better performance in noisy systems as compared with the decorrelator.

2.3 Interference cancellation

Interference cancellation techniques have been one of the major research topics in multiuser detection. They have attracted much attention due to their relatively simple structure and their effectiveness in mitigating the effect of MAI. As such, it is not difficult to find the basic interference cancellation structures being implemented in hardware, and their performance investigated [40][41][42][43][44].

The principle behind the interference cancellation techniques is to subtract the generated MAI from the received signal so that the desired signal will experience less MAI in the detection process. After the initial detection usually by matched filter (MF) receivers, the tentative decisions at the output of the MF are used for the regeneration of the signals. Then these regenerated signals are used in the cancellation process to remove the MAI. This “cleaned” signal is then passed into the MF for re-detection. In a multistage structure, this process is repeated.

There are basically three main interference cancellation structures, namely the parallel interference cancellation (PIC), successive interference cancellation (SIC) and the hybrid interference cancellation (HIC). These structures will be presented and discussed in the following subsections.

2.3.1 Parallel interference cancellation (PIC)

The block diagram for the single stage PIC is shown in Figure 2.8. In the PIC, initial detections are done with a bank of matched filters (MF). The tentative decisions at the output of the MF are then used for the regeneration of the signals for corresponding users. From the regenerated signals, the MAI affecting different users are then reconstructed in parallel with the partial summer shown. After which, these estimated MAI are subtracted from the buffered received signal. The cleaned signal is then passed into the MF of the respective users for detection.

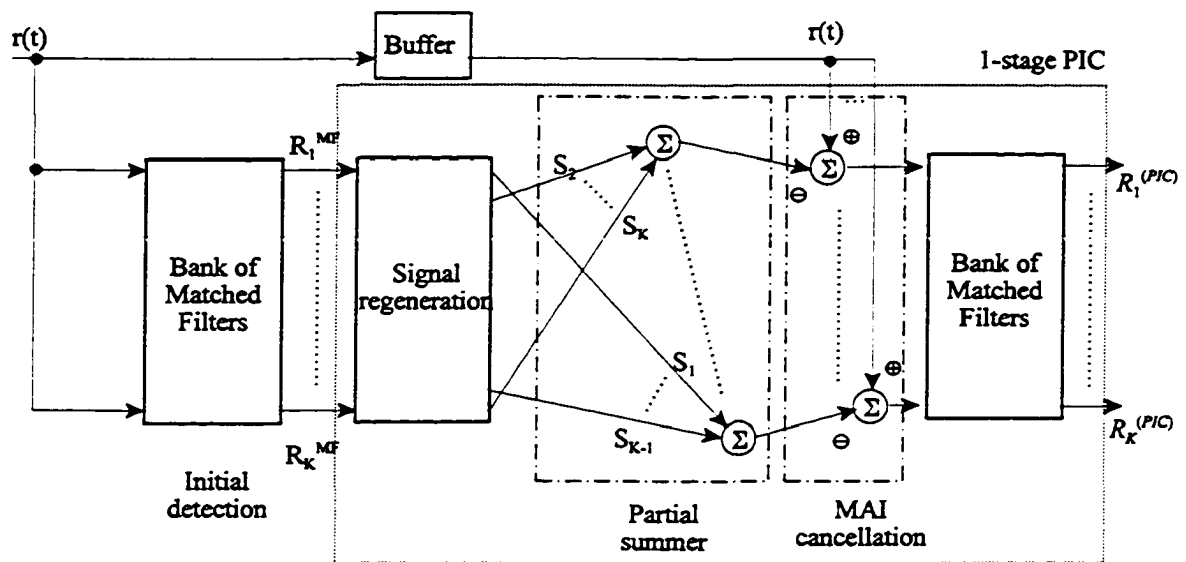


Figure 2.8: The 1-stage parallel interference cancellation.

The cleaned signal for user i after the MAI cancellation is

$$r_i(t) = r(t) - \sum_{k=1, k \neq i}^K S_k(t) \quad (2.36)$$

where $S_k(t)$ is the regenerated signal of user k . After the re-detection by the MF, one obtains the improved tentative decision for user i as

$$R_i^{(PIC)} = B_i + \sum_{k=1, k \neq i}^K (B_k - \tilde{B}_k) \gamma_{ki} \quad (2.37)$$

where B_k and \tilde{B}_k are the actual and estimated data for user k . If the estimated signal is perfect, the users will experience no MAI in the system. One of the early proposals of this PIC structure is [45]. Its main intention is to reduce the complexity of the maximum likelihood detector by splitting the users up into smaller groups and processing them in parallel. The multistage PIC can be easily constructed by cascading individual PIC stages in Figure 2.8. This way, the accuracy of the estimated MAI will improve with every stage of PIC [46].

In the paper, the tentative data estimates are based on hard estimates. The signal powers are assumed to have been estimated by other means. The performance of the hard-decision PIC is evaluated in [47]. These results show that significant performance advantage over the conventional MF, but the channel estimates should be accurate. Once the estimates are not precise, performance drops rapidly. This sensitivity to estimation errors is also studied and observed in [48]. In addition, when unknown interference is added, the performance of this PIC degrades quite significantly.

In [49], soft decision estimates have been proposed and investigated. It is found that they improve the performance. More detailed investigation on the effects of different mapping functions for the soft estimates can be found in [50]. As the number of stages increases, it is shown that the PIC with soft decision approaches the performance of the decorrelator [51].

In [52], it is shown that the single stage and multistage PIC are able to outperform the conventional MF by a significant margin under different conditions such as the power controlled environment or the Rician channel. However, more in-depth investigation on the near-far resistance of the multistage PIC suggests that the PIC is generally not near-far resistant. Despite this weakness, the PIC is still able to outperform the conventional MF. A

separate study [53] also observes this behaviour but mentions that if the power difference is moderate ($< 3\text{dB}$), the PIC is still able to handle the difference.

Under high level of the interference, the PIC exhibits the “ping-pong” effect [54]. In other words, instead of the performance converging with more PIC stages, the performance oscillates with every PIC stage added. Here, the interference cancellation process is formulated into an iterative expression. It is found that the extreme eigenvalues of the iterative matrix term in this expression will cause fluctuations in the iterative expression and lead to the ping-pong effect. By limiting these extreme eigenvalues using weighted cancellations, the ping-pong effect can be avoided.

The resulting weighted PIC in [55] has superior performance over that of the standard PIC with much better near-far resistance and it is able to approach close to the MMSE performance for as few as three stages. A similar PIC using partial cancellation has been proposed in [56], the idea is not to cancel the entire amount of MAI when the tentative decision is noisy (which leads to inaccurate MAI estimations), but do it partially. As the interference cancellation progresses into the next stage of PIC, with more accurate MAI estimations, one can then increase the amount of MAI to be cancelled. The cleaned signal for user i after M -stages of PIC, $r_i^{(M)}(t)$, is

$$r_i^{(M)}(t) = r(t) - \rho_M \sum_{k=1, k \neq i}^K S_k^{(M)}(t) \quad (2.38)$$

where $S_k^{(M)}(t)$ is the regenerated signal of user k and ρ_M is the partial cancellation parameter for stage M of the PIC. The value of ρ_M is found via simulation such that $\rho_M > \dots > \rho_2 > \rho_1$ for good performance. Results in the channel with uniform power distribution among users or additive white Gaussian noise (AWGN) channel are presented and the proposed partial PIC outperforms the regular PIC. The performance of this PIC over Rayleigh fading channel is investigated in [57] where the effect of the partial cancellation parameter and the tentative decision device function have been examined in details. It has been shown that this PIC with partial cancellation outperforms the regular PIC in the fading channel.

The improved partial PIC in [58] introduces further improvements by assigning different values of the partial cancellation parameter for different users according to their received power in addition to which PIC stage they are in. The cleaned signal for user i after M -stages of PIC, $r_i^{(M)}(t)$, is

$$r_i^{(M)}(t) = r(t) - \sum_{k=1, k \neq i}^K \rho_{M,k} S_k^{(M)}(t) \quad (2.39)$$

where $\rho_{M,k}$ is the partial cancellation parameter for user k of stage M and it is given by

$$\rho_{M,k} = \rho_M + \frac{A_k}{2A_{\max}} \quad (2.40)$$

where ρ_M is the partial cancellation parameter stage M , A_k is the received amplitude for user k , and A_{\max} is the largest amplitude among the users. The reasoning for using $\rho_{M,k}$ is that the stronger users could be detected more reliably and they are likely to cause more interference to other weaker users. Hence, a larger portion of their signal is removed during the cancellation process for other users. A similar structure is presented in [59]. For this structure, the weights or the partial cancellation parameters are determined in a groupwise manner.

With this line of reasoning, [60] proposes that the tentative decisions of the users at the output of the MF be compared with a threshold S . If the user is deemed to be reliable enough, its signal will be used in the MAI cancellation process, otherwise its signal will be omitted. The cancellation selection parameter, ρ_k is defined as,

$$\rho_k = \begin{cases} 1 & , \quad R_k^{(MF)} \geq S \\ 0 & , \quad -S < R_k^{(MF)} < S \\ -1 & , \quad \textit{otherwise} \end{cases} \quad (2.41)$$

where $R_k^{(MF)}$ is the tentative decision for user k . The cleaned signal for user i , $r_i(t)$, is therefore

$$r_i(t) = r(t) - \sum_{k=1, k \neq i}^K \rho_k S_k(t) \quad (2.42)$$

The threshold S is determined from simulations.

An adaptive type of the PIC is suggested in [61] where a RAKE filter, forward filter and feedback filter (where the recursive least squares, RLS algorithm has been used) is introduced into the PIC structure to mitigate the effects of the inter-symbol interference (ISI) and MAI. It has a superior performance over that of the conventional MF and MMSE-DFE (decision feedback equalizer) detector [62]. However, its performance hinges on the accuracy of the initial data estimates.

Another adaptive multistage PIC is proposed with the least mean square (LMS) algorithm used to adjust the cancellation weights [63]. One problem with using the LMS algorithm is its slow convergence. This is partially solved by implementing a multistage structure. This receiver shows excellent performance in the AWGN and fading channels against the MF, convention PIC, partial PIC and the RLS decorrelator. Similar to the previous adaptive scheme, its good performance depends on the accuracy of the initial estimates. A method of finding good weights using the minimization of mean residual interference power is presented in [64].

All the different PICs mentioned so far use the MF for the initial and subsequence detections of the users' signal. However, this does not have to be the case. The MF is replaced by the minimum mean square error (MMSE) detector in [65]. The performance of this hybrid PIC/MMSE receiver is better than that of the standard MMSE as it is more near-far resistant and insensitive to the cross-correlation matrix. However, by replacing the MF with MMSE, one inevitably increases the computational complexity which may be an issue in the actual implementation. The PIC has also been applied together with beamforming algorithm [66] and diversity technique [67] to increase system capacity.

2.3.2 Successive interference cancellation (SIC)

For the SIC, the interference cancellation is done in a step-by-step manner where only one user is considered and processed at a time [68][69]. This is different from the PIC where all users are dealt with at the same. The SIC algorithm is as follows:

1. Order or rank the users according to their signal strength.
2. Choose the user with the strongest signal for the current cancellation step.
3. Make a tentative decision for the user.
4. Regenerate the signal for that user based on the tentative decision.
5. Subtract the regenerated signal from the composite received signal.
6. Pass this partially clean composite received signal to the next cancellation step.
7. Repeat step 2 to 6 until all users are detected.

The reasons for implementing the SIC algorithm this way is that the user with the strongest received signals is the most reliable. Being the user with the strongest signal would also mean that it causes the most interference to other weaker users. Thus, it makes sense to have this user detected first. Then, based on the detection outcome, the signal is regenerated and removed from the received signal to produce the cleaned composite signal with the MAI from the strongest user removed. As a result, the weaker users will experience less MAI and this will make their detection more reliable. This composite signal is then used for the detection of the next strongest user where the procedure mentioned is repeated until all users are detected. The structure of the interference cancellation unit for the SIC is shown in Figure 2.9.

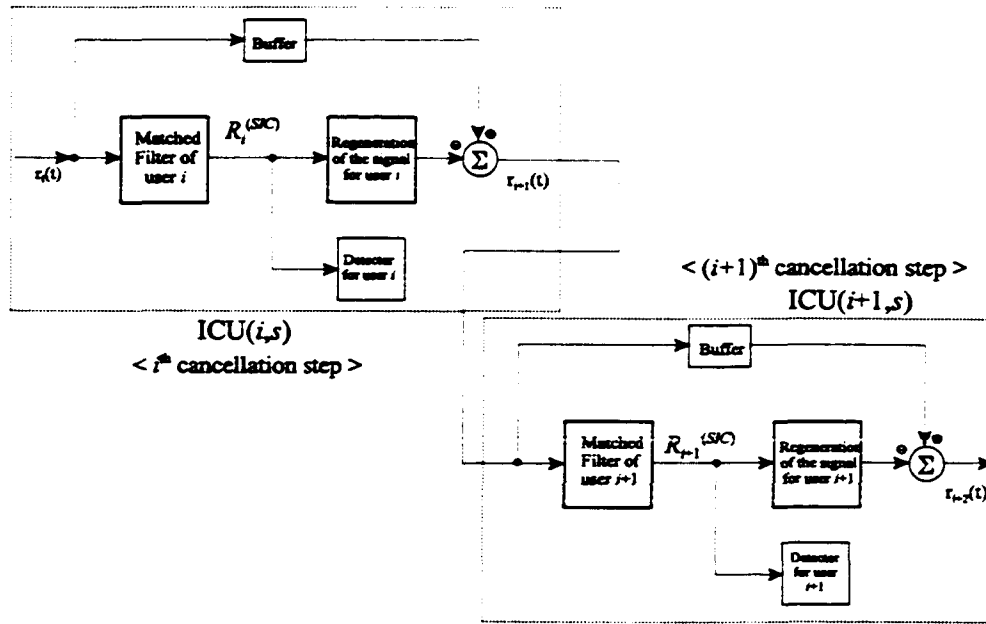


Figure 2.9: The structure of the interference cancellation unit for step i of stage s , $ICU(i, s)$ of the SIC.

The strongest user is denoted as user 1 while the weakest user as user K which is the last to be detected. Hence, the cancellation step i corresponds to user i for convenience. The composite signal at the input of the interference cancellation unit for step $(i + 1)$ of stage s $ICU(i, s)$ of the SIC, $r_{i+1}(t)$

$$\begin{aligned}
 r_{i+1}(t) &= r_i(t) - S_i(t) \\
 &= r(t) - \sum_{k=1}^i S_k(t)
 \end{aligned} \tag{2.43}$$

where $S_k(t)$ is the regenerated signal of user k . After the re-detection by the MF, one obtains the improved tentative decision for user i as

$$R_i^{(SIC)} = B_i + \underbrace{\sum_{k=i+1}^K B_k \gamma_{ki}}_{\text{uncancelled MAI}} + \underbrace{\sum_{k=1}^{i-1} (B_k - \tilde{B}_k) \gamma_{ki}}_{\text{cancellation noise}} \tag{2.44}$$

where B_k and \tilde{B}_k are the actual and estimated data for user k . If the estimated signal is perfect, there will be no cancellation noise in the system. From (2.44), one can notice that

as the stronger signals are removed, the weaker users will experience less MAI and this will help improve the reliability of their detection. However, the accuracy of the MAI estimates will determine the effectiveness of the SIC. For the SIC presented here, it is assumed that the received powers of the user signals are known and ordering or the ranking of the users is done. In [70], the users are not ranked at the beginning of the SIC stage, instead before every cancellation step, a bank of MFs is applied to the composite signal. The user with the largest correlation sample is then selected for the cancellation step. This removes the need for ordering the users according to their received powers at the beginning. However, the receiver complexity is increased with the addition of a bank of MF's in front of every cancellation step.

Analysis of the SIC can be done in a few ways. In this thesis, as well as in most papers, the correlation method is used [71]. Alternative ways of analysis using the matrix-algebraic approach and spatial cell modeling can be found in [72] and [73], respectively.

The multistage structure of the SIC can be shown in Figure 2.10 for a M -stage SIC. Alternatively, the structure can be represented as in [74].

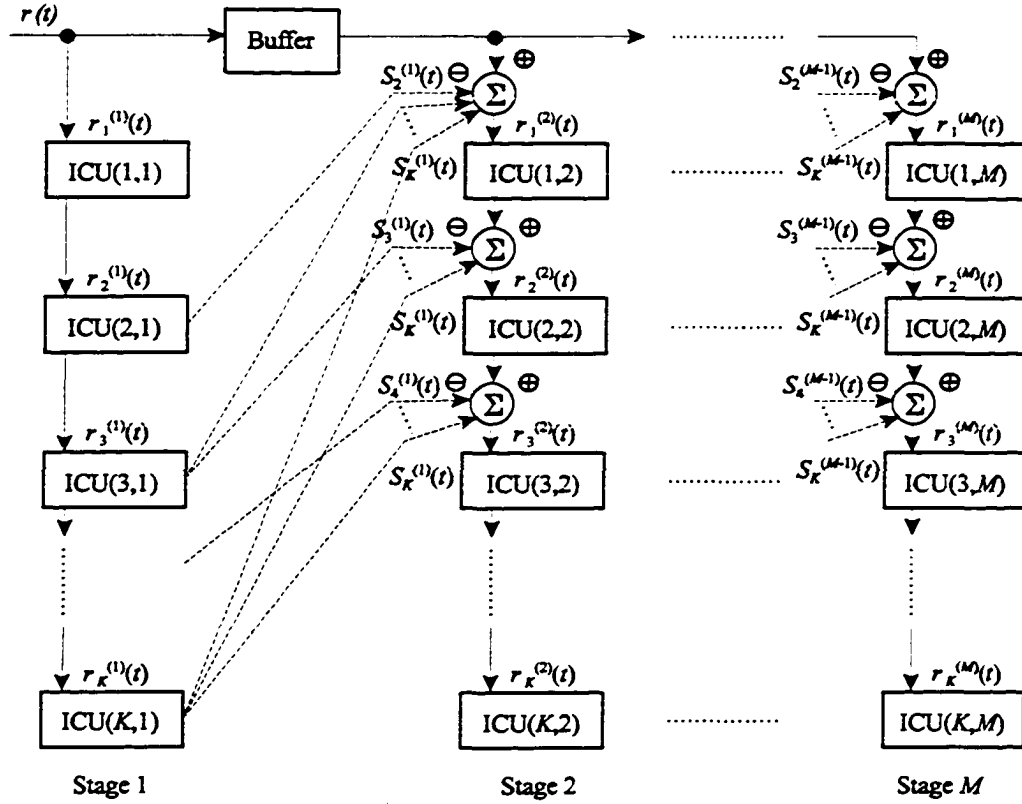


Figure 2.10: Structure of the M -stage SIC.

The composite signal at the input of the ICU(i,s), $r_i^{(s)}(t)$, is

$$\begin{aligned}
 r_{i+1}^{(s)}(t) &= r_i^{(s)}(t) - S_i^{(s)}(t) - \sum_{k=i+2}^K S_k^{(s-1)}(t) \\
 &= r(t) - \sum_{k=1}^i S_k^{(s)}(t) - \sum_{k=i+2}^K S_k^{(s-1)}(t)
 \end{aligned} \tag{2.45}$$

where $S_k^{(s)}(t)$ is the regenerated signal of user k in stage s . The performance of the multistage SIC is investigated in [75] with mapping functions [50]. It is found that the multistage clipped soft decision SIC has the best performance. It also outperforms the limited tree search detector which is a maximum likelihood detector with constrained complexity [76]. The optimum detector is a maximum likelihood detector with unconstrained complexity. The impact of delay estimation errors is studied in [77]. It is found that the soft decision multistage SIC is more robust than the hard decision SIC and the limited tree search detector.

In a multipath fading channel, the multistage SIC using soft decisions [78] also outperforms the SIC that uses hard decisions [79]. The multistage structure with differential PSK in multipath fading is compared with the multipath decorrelating detector in [80] and it was found that they performed similarly.

Due to the successive cancellation nature of the SIC, the bit error rates (BER) vary with different users. An expression is derived in [81] so that the required power profile can be obtained to provide equal BER for all users.

Although the SIC has good performance when the received powers of users are dissimilar as in the fading channel, it has relatively poor performance in the AWGN channel where the received powers are equal when compared with the PIC [82]. In [83], the conventional MF in the SIC is replaced with a simple form of joint modulation which works well when users have similar powers. The SIC can be also combined with the MMSE filters and decorrelator to produce good results [84][85], respectively. A proposed SIC structure that has very good performance is the pipelined SIC [86]. In this structure, the MAI estimates of the weaker users are fed back to the stronger users so that the stronger user can be re-detected with the MAI of the weaker user removed. For the standard SIC, the stronger users are not re-detected at all. The adaptive version of the pipelined SIC is presented in [87] and it is able to provide an even better performance than the original scheme. Another way improving the SIC performance is through the use of signal orthogonalization for the synchronized system [88]. However, more investigation should be done in the asynchronous channel with multipath fading. An iterative type of the SIC structure is proposed in [89] where the estimate-maximize (EM) algorithm is used to seek the maximum likelihood solution iteratively.

As the SIC has a simple structure, it can be readily adapted with other diversity techniques that can improve performance. The SIC receiver with multiple antennas is proposed and investigated in [90], [91] and [92] to provide good performance. The SIC has also been combined with coding schemes with excellent results. In [93], the integration of the SIC with linear block coding leads to excellent performance. This receiver outperforms the coded conventional SIC and the coded decorrelating detector. The SIC with the Viterbi decoder and

random interleaver integrated in [94] is able to provide huge performance gain over the standard SIC with Viterbi decoding and interleaving. Another SIC structure with Viterbi decoder can be found in [95], although the performance gain is not as large. The SIC is also being applied to the orthogonal frequency division multiplexing (OFDM) [96] and multi-carrier CDMA (MC-CDMA) [97] to combat the MAI and enhance system performance.

2.3.3 Hybrid interference cancellation (HIC)

In the previous two subsections the PIC and SIC have been presented. It is shown that in the AWGN channel when there are uniform received powers, the PIC has better performance than the SIC. However, when the received powers are non-uniform as in the fading channel without fast power control, the SIC is more effective. The disadvantage of using the PIC is that its performance degrades rapidly when there is a high level of interference. As for the SIC, the processing delay is linearly proportional to the number of users it has to detect which may take too long for it to be practical especially when multiple stages are to be implemented. There are many ways of improving the PIC and SIC, some of which have been discussed. However, for all the methods proposed, the basic structures of the PIC and SIC are preserved. An alternative way is to combine the structures of the PIC and SIC together into a hybrid form to either improve the performance or reduce the limitations. In this subsection, the types of hybrid interference cancellation (HIC) will be discussed.

One of the earlier HICs is the groupwise SIC (GSIC) proposed in [98]. The objective for this proposal is to reduce hardware complexity. The structure of this GSIC is the same as that of the SIC in [70] and in Figure 2.9 with the difference only in the number of users detected and cancelled per cancellation step in the ICU. For the SIC, one user is detected and the corresponding regenerated signal cancelled while for the GSIC, a N_{GSIC} number of users are detected and their signals cancelled at every cancellation step. The analysis of the GSIC is the same as that in [70] but with N_{GSIC} users instead of one. The performance of this GSIC is worse than the SIC but with the advantage of having the computational complexity and processing gain reduced.

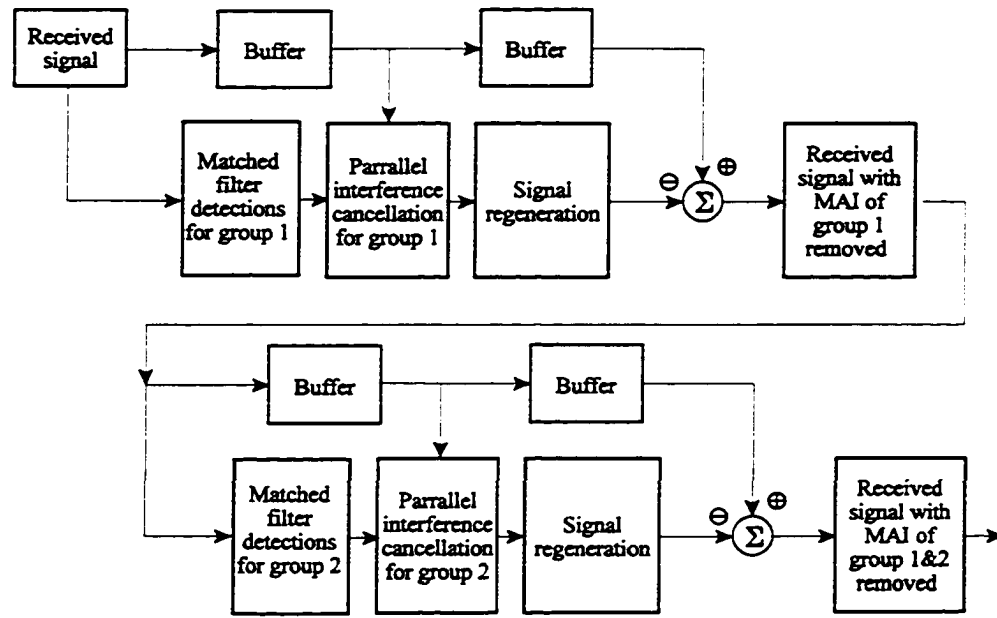


Figure 2.11: Structure of the HIC.

An improved version of the GSIC can be found in [99], where PIC is being done on the group of users to be detected in a cancellation step (Figure 2.11). For this receiver, the design parameter is the number of cancellation steps and the number of users for each cancellation step. A similar receiver named the multistage HIC (multistage is similar to that of SIC in Figure 2.10) is investigated in [100] for single and multipath AWGN and Rayleigh fading channels, and it has good performance. Then, this multistage HIC is analyzed in [101] where it is found that if there are more than four or five groups per stage, the performance of the HIC will converge to that of the decorrelating detector. Variations of this HIC are studied in [102] where the structure is called the linear groupwise SIC or LGSIC. In this paper, different receivers are being used in group detection blocks in Figure 2.11. They can be the matched filter (MF), multistage PIC, the decorrelator or the MMSE receiver. Their performance in the AWGN channel is investigated and the results show that the HIC with MF as the initial detection (Figure 2.11) gives the lowest minimum BER with increasing number of stages. However, its convergence is slower than other receivers.

An adaptive hybrid serial/parallel interference cancellation (AHSPIC) is presented in [103]. This receiver is shown in Figure 2.12.

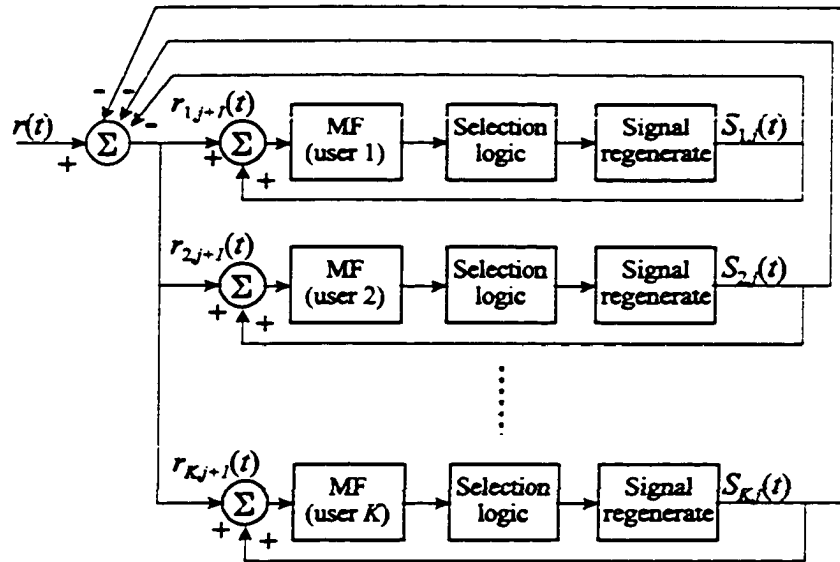


Figure 2.12: Structure of the AHSPIC.

The input of the MF for user i after the j^{th} cancellation step is

$$r_{i,j+1}(t) = r(t) - \sum_{k=1, k \neq i}^{jG_j} S_{i,j}(t) \quad (2.46)$$

where $S_{i,j}(t)$ is the regenerated signal of user i , and G_j is the number of users in a group at the cancellation step j . For this receiver, similarly, the design parameters to be set are the total number of cancellation steps (that the receiver can have) and the number of users in a group. The AHSPIC is different from the HIC receivers mentioned in the last paragraph as the composite signals of all the users in the system are constantly being updated at every cancellation step regardless of which group they are in. The HIC receivers mentioned earlier only used the information of each user once if it is a single stage structure. This way of constant updates will help improve the user signal estimates, and enhance overall performance. It is demonstrated that under the Rayleigh fading channel, the AHSPIC is able to outperform the conventional SIC. Note that if one sets the number of users in a group to be one, and the total number of cancellation steps to be equal to the number of users in the system, K , this structure becomes the pipelined SIC and a similar scheme discussed in [87] and [104], respectively.

Another HIC is given in [105]. Its structure is similar to the one in Figure 2.11. After the detection for the group, instead of using the signals of all users in that group for the MAI regeneration process, only the signals belonging to the few stronger users of the group are used. Once again, the number of users in the group, the number of groups and the number of the stronger users in each group are determined through simulations.

A simple hybrid scheme is proposed in [106] where the few stronger users are detected and cancelled using SIC. The remaining users are then detected using PIC. The objective is to reduce the complexity of the receiver without sacrificing much performance. It is shown that the complexity of this HIC is about a third that of the PIC and HIC in [105]. A similar hybrid scheme has also been proposed earlier and it is known as the multistage adaptive serial-parallel (ASPIC) scheme [107]. In the ASPIC, the main objective is to use SIC in the first stage whenever necessary in the fading channel. A threshold, K_T , on the number of users is set. For the first stage, when the processing delay of the SIC is too long due to the larger number of users present in the system, the stronger K_T users are detected with SIC. The remaining users will be detected using PIC. In the subsequent stages, PIC is used exclusively.

2.4 Summary

An overall view of the CDMA system has been presented. It has been shown that the capacity of the CDMA system is interference limited. This is due to the nature of the system where all users can access the same radio channel simultaneously being differentiated only by their unique spreading codes. The signal of every user will interfere with each other and this interference is known as the multiple access interference (MAI). An important consequence of this is the near-far effect where the signal of the weaker user will be overwhelmed by that of the stronger user. Although the matched filter (MF) receiver used is the optimal receiver in the Gaussian noise channel, its use in CDMA is not optimal in the sense that it treats the MAI as useless and unwanted noise in the detection process. Clearly, if one can make full use of the information regarding the MAI, the detection process will be much better.

Receivers that make use of the MAI information during detection are named multiuser detectors. The optimal multiuser receiver based on the maximum likelihood detection has very good performance over that of the conventional MF, however, its computational complexity is very high, and this limits its application in practice. In addition, it requires the knowledge of the user received powers. Sub-optimal receivers with less severe computational requirement have been proposed as a result. The detectors that have been discussed are the decorrelator, the minimum mean square error (MMSE) detectors and various interference cancellation (IC) receivers.

The decorrelator is found to be excellent in mitigating the MAI, and it is insensitive to the near-far effect. It also does not require the knowledge of the received user powers in the detection process. However, the noise is enhanced inherently. In certain conditions, the decorrelator will perform worse than the conventional MF. The MMSE detector does not have the problem of noise enhancement but it requires the received powers of all users to be estimated. For both of these detectors, the matrix inversion process is computationally intensive and this will pose constraints on the receiver design.

For the IC receivers, there are three main categories. They are the parallel, successive and hybrid IC receivers. The basic PIC and SIC have been successfully implemented in hardware because of their much simpler structure compared with that of the optimal and linear multiuser detectors.

The PIC processes all users at the same time, and has very short processing delay. It has a better performance than the SIC in the additive white Gaussian noise (AWGN) channel where received signal powers are equal. The performance of the multistage PIC has been shown to converge to that of the MMSE with increasing number of stages. However, when the received powers are not uniform, as in the case of the fading channel with ineffective or no power control, the PIC performance degrades rapidly. This points to the fact that the PIC suffers from the near-far effect. Improvements to the structure have been proposed, and they prove to be effective in increasing the PIC near-far resistance with varying success.

Contrary to the PIC, the SIC exhibits good performance in the fading channel where the received power profile is spread over a larger range. On the other hand, the SIC has worse performance than that of the PIC in the AWGN channel. Another disadvantage of the SIC is the associated high processing delay. This is due to the structure of the SIC which detects the user sequentially one after another. Techniques and modifications have been suggested to solve these problems and improve the performance of the SIC. They are found to be effective with varying degree, but limited success has been achieved in reducing its processing delay without affecting performance.

So far, the improvements proposed have been made with the preservation of the basic PIC and SIC structures in mind. Hence, there are limited changes to these structures. This is so not to jeopardize the existing advantages when one is resolving to mitigate the limitations. Another method would be to combine the structure of the PIC and SIC in the hope that their advantages will be combined. The result is the hybrid IC or HIC. For the HIC, SIC is applied between groups of users. Within each group, the members are detected using PIC. From all the HIC proposed, the focus is on the determination of the number of groups, and the number of users in each group. One could set the number of groups, and then assign users to each group appropriately. Or one could first determine the number of users in the group, and derive the corresponding number of groups. Any enhancements proposed are also based on the mentioned approach to determine the HIC structure. It is demonstrated that these HICs are able to provide the same if not superior performance as the PIC and SIC without much of their limitations.

The variable group HIC (VGHIC) proposed in this thesis is different from others. For the previously proposed HIC, their main intentions seem to be reducing the limitations of the PIC and SIC. For the VGHIC, the idea is to combine the advantages of the PIC and SIC. The VGHIC is presented in the next chapter.

Chapter 3: The Variable Group Hybrid Interference Cancellation scheme (VGHIC)

In this chapter the structure of the variable group hybrid interference cancellation (VGHIC) scheme is presented first. Then, the bit error rate (BER) performance of the matched filter receiver (MF), parallel interference cancellation (PIC), successive interference cancellation (SIC) and the variable group hybrid interference cancellation (VGHIC) are analysed and compared using an unified approach. The analysis here is different from those found in the literature as the self cancellation term is taken into account as a result of using the correlation samples in the signal generation and cancellation process. The receivers performance in additive white Gaussian noise (AWGN) channel are analyzed first. Then, this is followed by the analysis in the fast Rayleigh fading channel. After this, the BER performance of the receivers is compared and discussed.

The organization of this chapter is as follows. Section 3.1 describes the system model used. Section 3.2 presents the structure of the proposed VGHIC. Then, in Section 3.3, certain assumptions and simplifications for the analysis are highlighted before proceeding to Section 3.4 and Section 3.5 for the analysis of the matched filter (MF), parallel interference cancellation (PIC), successive interference cancellation (SIC) and VGHIC in AWGN and Rayleigh fading channel, respectively. A comparison of the BER of these receivers is done in Section 3.6 and Section 3.7 to sum up this chapter.

3.1 System model

This section describes the reverse link model of a simple single-cell asynchronous direct sequence CDMA system. For this system, the coherent binary phase shift keying (BPSK) modulation is used. The system contains K users that are transmitting simultaneously to the base station. The received signal at the base station is:

$$\begin{aligned}
r(t) &= \sum_{i=1}^K \sqrt{\frac{2E_i}{T}} c_i(t - \tau_i) b_i(t - \tau_i) \cos(\omega_c t + \theta_i) + n(t) \\
&= \sum_{i=1}^K A_i(t) S_i(t) + n(t)
\end{aligned} \tag{3.1}$$

where

$$A_i(t) = \sqrt{E_i} b_i(t - \tau_i) \tag{3.2}$$

and

$$S_i(t) = \sqrt{\frac{2}{T}} c_i(t - \tau_i) \cos(\omega_c t + \theta_i) \tag{3.3}$$

such that the energy of the signal from user i is

$$\int_{\tau_i}^{T+\tau_i} (A_i(t) S_i(t))^2 dt = E_i \tag{3.4}$$

The assumptions for user i are that its time delay τ_i is tracked perfectly in $[0, T)$, and phase θ_i is uniformly distributed in $[0, 2\pi)$. The information bit, $b_i(t)$, and spreading waveform, $c_i(t)$, for user i are given by

$$b_i(t) = \sum_{m=-\infty}^{\infty} B_i^{(m)} p_T(t - mT) \tag{3.5}$$

and

$$c_i(t) = \sum_{n=-\infty}^{\infty} C_i^{(n)} p_{T_c}(t - nT_c) \tag{3.6}$$

where $p_T(t)$ and $p_{T_c}(t)$ are assumed to be rectangular pulses with duration T and T_c , respectively. That is, $b_i(t) = B_i^{(m)}$ for $(m-1)T \leq t < mT$ and $c_i(t) = C_i^{(n)}$ for $(n-1)T_c \leq t < nT_c$. The terms $B_i^{(m)}$ and $C_i^{(n)}$ are the information bit sequence and the spreading chip sequence, respectively. The spreading waveform $c_i(t)$ also has the following properties:

$$\Lambda_{ij} = \frac{1}{T} \int_{\tau_i}^{T+\tau_i} c_i(t - \tau_i) c_j(t - \tau_j) dt \quad , \quad i \neq j ;$$

$$\Lambda_{ii} = 1 \quad , \quad i = 1, 2, \dots, K$$
(3.7)

The processing gain is given by

$$\rho = \frac{T}{T_c}$$
(3.8)

The term $n(t)$ is the additive white Gaussian noise (AWGN) with zero mean and power spectral density of $N_0/2$.

3.2 Receiver structure

It was shown in [82] that PIC performs better than SIC under ideal fast power control conditions where the signal powers of all users, as seen by the base station, are equal. However, in a rapidly fading channel where power control is ineffective, SIC performs better than PIC. Hence, we would expect that in a realistic situation where power control is imperfect, SIC should outperform PIC. However, the major disadvantage associated with SIC is the long processing delay that is inherent in the SIC structure. Hence, various hybrid schemes with shorter processing delay have been proposed [98][100].

Here, we propose a hybrid structure that combines the advantages of both the PIC and SIC schemes. The idea is to combine the good performance of the PIC scheme in AWGN channel, and that of the SIC scheme in fading channel into one hybrid interference cancellation scheme. The resulting hybrid scheme is the VGHIC. The main idea is presented in Figure 3.1. After the detection of all users using the matched filter receivers, the users of similar power levels are selected and grouped. The PIC scheme is then used for the detection of the current group of users. After this, the signals belonging to that group of users are regenerated and subtracted from the received signal producing a composite signal which is passed on to the next round of user grouping and detection. This process carries on until all

users are detected. Effectively, the users are adaptively selected into different ad-hoc groups of similar user power levels. Within each group the PIC scheme is used for detection, and between groups of different power levels, the SIC scheme is used between groups of different power levels, the SIC scheme is used.

This hybrid approach is very different from other groupwise hybrid structures [98][100][103][108]. In [100], the number of groups is fixed and the users are distributed evenly among the groups, whereas for [98] and [108], the number of users in each group is fixed and the difference is that no PIC is done on the users within each group in [98]. The hybrid scheme proposed in [103] has iterative loops built-in, but the number of users in each group is fixed.

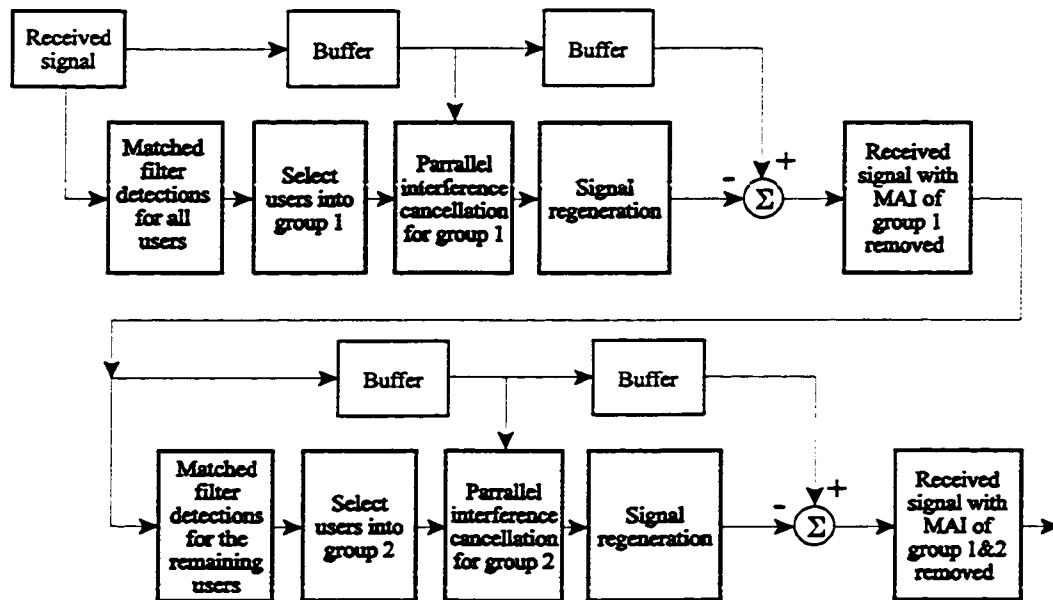


Figure 3.1: The working principle behind the variable group hybrid interference cancellation scheme.

For the VGHIC proposed here, the number of users in each group is directly related to the user signal level spread. As a result, the number in each group is not the same, and the number of groups is not fixed. When the powers between users are very different, the VGHIC effectively becomes a SIC scheme. On the other hand, when the power level of every

user are the same, the VGHC becomes a PIC scheme. In other words, we may say that the structure of the VGHC is able to adapt itself to different channel conditions.

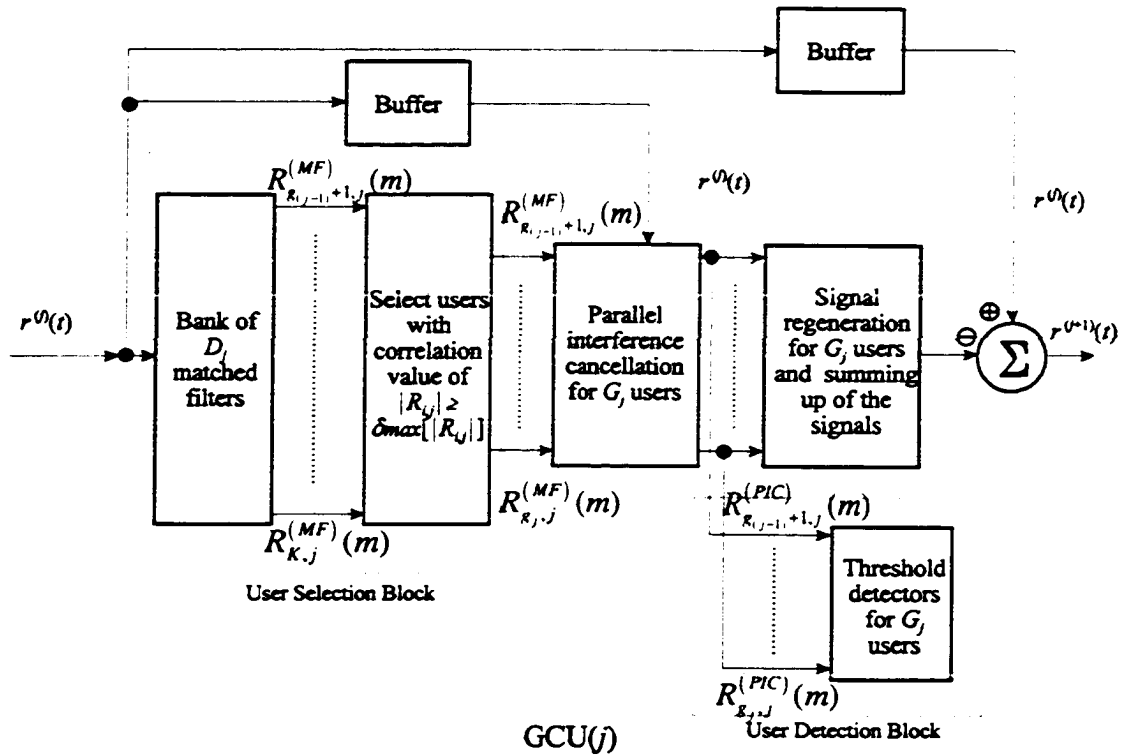


Figure 3.2: Structure of the group cancellation unit for the j^{th} subtractive step of the VGHC scheme, $\text{GCU}(j)$.

The structure of the group cancellation unit for the j^{th} subtractive step of the VGHC scheme, $\text{GCU}(j)$ is illustrated in Figure 3.2. The index j also represents the group number. The users are split into a total of N groups and hence, $j = 1, \dots, N$. D_j is the number of users that have yet to be detected and cancelled at the j^{th} subtractive step. It is given by

$$D_j = K - \sum_{n=1}^{j-1} G_n \quad (3.9)$$

where G_n is the number of users in group n and group N is the last group of users to be detected. At the first subtractive step $D_1 = K$ as the number of the users remaining is K since none of them has been detected.

After the bank of D_j matched filters, we have the term $R_{i,j}^{(MF)}(m)$ which is the correlation sample of bit m of the user i at the output of the matched filter in the j^{th} subtractive step for the period $(m-1)T + \tau_i \leq t < mT + \tau_i$. Without loss of generality and for the clarity of presentation, we may denote the user with the highest correlation sample at its matched filter output as user 1, the user with second highest correlation sample as user 2, and so on, that is, $|R_{1,j}^{(MF)}(m)| > |R_{2,j}^{(MF)}(m)| > \dots > |R_{K,j}^{(MF)}(m)|$. The selection rule for group j is defined by

$$|R_{i,j}^{(MF)}(m)| \geq \delta \max \left[|R_{i,j}^{(MF)}(m)|_{i=g_{(j-1)}+1, \dots, K} \right] \quad (3.10)$$

where the grouping parameter δ assumes the values of $0 \leq \delta \leq 1$. The function $\max[x]$ is defined as the maximum value of x and $|x|$ is the absolute value of x . In the extreme cases of $\delta = 0$ and $\delta = 1$, the structure of the VGHC approaches that of the PIC and SIC scheme, respectively. The optimal value of δ will be found using simulations.

For the VGHC scheme presented here, correlation sample values are used as measures of the user signal power levels and also for the regenerations of user signals in the cancellation process. In general, users are split into groups of different power levels based on the magnitudes of their correlation samples, $|R_{i,j}^{(MF)}(m)|$. These correlation samples are obtained at the output of the matched filter of the corresponding user.

At the first detection ($j = 1$) by the bank of $D_j = K$ matched filters, the user with the highest magnitude of correlation sample is selected as the reference. In this case, our reference is $|R_{1,1}^{(MF)}(m)|$. Then users are selected into group 1 when the magnitude of their correlation sample are such that, $|R_{i,1}^{(MF)}(m)| \geq \delta |R_{1,1}^{(MF)}(m)|$, $i = 2 \dots K$. Therefore, the users in group 1 have indices $i = 1, 2, \dots, g_{(1)}$.

The indices i of the users for the j^{th} subtractive step are such that

$$i = g_{(j-1)} + 1, \dots, g_{(j)} \quad (3.11)$$

with the initial condition $g_0 = 0$. The term $g_{(j)}$ and the number of users in group j , G_j , is determined by the selection rule (3.10). These two quantities are related by the following equations

$$G_j = g_{(j)} - g_{(j-1)} \quad (3.12)$$

and

$$g_{(j)} = \sum_{i=1}^j G_i \quad (3.13)$$

The groupings are mutually exclusive. The input to $GCU(j)$ is

$$r^{(j)}(t) = r^{(j-1)}(t) - \sum_{k=g_{(j-2)}+1}^{g_{(j-1)}} \left[R_{k,(j-1)}^{(PIC)}(m) S_k(t) \right] \quad (3.14)$$

where $R_{ij}^{(PIC)}(m)$ is the correlation sample of bit m of the i^{th} user at the output of the PIC block within $GCU(j)$ in the period $(m-1)T + \tau_i \leq t < mT + \tau_i$. The term $S_k(t)$ is defined in (3.3). For the first subtractive step, the input is the received signal (3.1),

$$r^{(0)}(t) = r(t) \quad (3.15)$$

After the bank of D_j matched filters, the correlation sample of bit m of the user i in the j^{th} subtractive step for the period $(m-1)T + \tau_i \leq t < mT + \tau_i$, $R_{ij}^{(MF)}(m)$ is given by

$$R_{i,j}^{(MF)}(m) = A_i(m) + \sum_{\substack{k=g_{(j-1)}+1 \\ k \neq i}}^K A_k(m) \gamma_{ki}(m) + \sum_{k=g_{(j-2)}+1}^{g_{(j-1)}} \Delta_k^{(j-1)} \gamma_{ki}(m) + \eta \quad (3.16)$$

where η is the noise term, and

$$A_i(m) = \sqrt{E_i} \cdot B_i^{(m)} \quad (3.17)$$

and

$$\Delta_k^{(j)} = A_k(m) - R_{k,j}^{(PIC)}(m) \quad (3.18)$$

The cross-correlation factor for bit m between user k and i ($k \neq i$) is defined by,

$$\gamma_{ki}(m) = \begin{cases} \frac{1}{T} [B_i^{(m-1)} \Psi_{ki}(m) + B_i^{(m)} \tilde{\Psi}_{ki}(m)] \cos(\theta_i - \theta_k) & ; \tau_i > \tau_k \\ \frac{1}{T} [B_i^{(m)} \Psi_{ki}(m) + B_i^{(m+1)} \tilde{\Psi}_{ki}(m)] \cos(\theta_i - \theta_k) & ; \tau_i < \tau_k \end{cases} \quad (3.19)$$

and $\gamma_{ii}(m) = 1$. $\Psi_{ki}(m)$ and $\tilde{\Psi}_{ki}(m)$ are the continuous-time partial cross-correlation functions (modified from [109]) for bit m :

$$\Psi_{ki}(m) = \begin{cases} \int_{(m-1)T+\tau_k}^{(m-1)T+\tau_k+\tau_i} c_k(t-\tau_k) c_i(t-\tau_i) dt & ; \tau_i > \tau_k \\ \int_{(m-1)T+\tau_k}^{mT+\tau_i} c_k(t-\tau_k) c_i(t-\tau_i) dt & ; \tau_i < \tau_k \end{cases} \quad (3.20)$$

$$\tilde{\Psi}_{ki}(m) = \begin{cases} \int_{(m-1)T+\tau_k+\tau_i}^{mT+\tau_k} c_k(t-\tau_k) c_i(t-\tau_i) dt & ; \tau_i > \tau_k \\ \int_{mT+\tau_k}^{mT+\tau_i} c_k(t-\tau_k) c_i(t-\tau_i) dt & ; \tau_i < \tau_k \end{cases}$$

After the determination of the users in group j , the correlation samples of only the users in group j are passed into the PIC block (Figure 3.3) for processing.

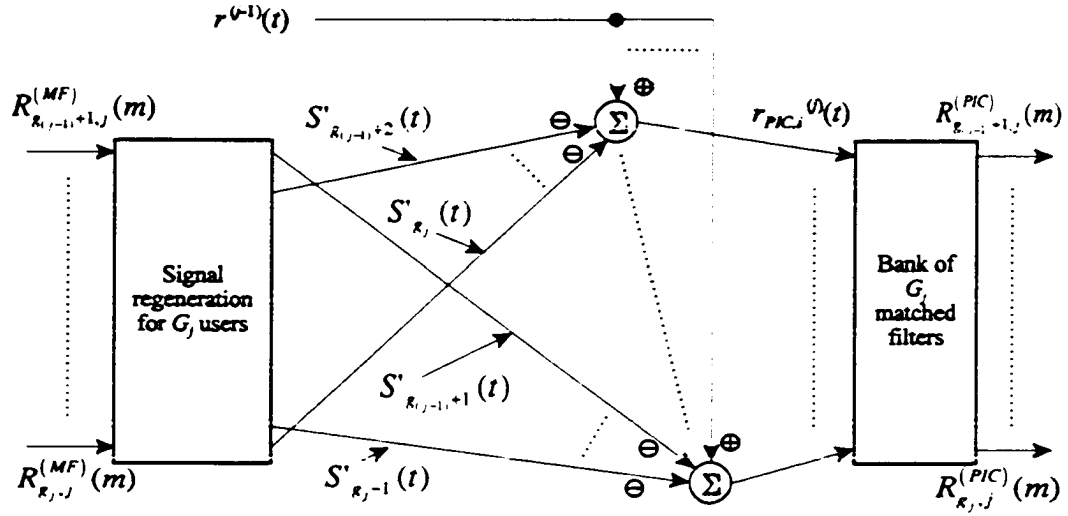


Figure 3.3: Structure of the parallel cancellation block in the GCU(j).

In the PIC block, the regenerated signal is

$$S'_n(t) = R_{n,j}^{(MF)}(m) S_n(t) \quad (3.21)$$

where $n = g_{(j-1)}+1 \dots g_j$. After PIC, we have

$$r_{PIC,i}^{(j)}(t) = r^{(j-1)}(t) - \sum_{\substack{k=g_{(j-1)}+1 \\ k \neq i}}^{g_j} R_{k,j}^{(MF)}(m) S_k(t) \quad (3.22)$$

Detecting using the matched filter receivers,

$$\begin{aligned} R_{i,j}^{(PIC)}(m) = & A_i(m) + \sum_{k=g_j+1}^K A_k(m) \gamma_{ki}(m) \\ & + \sum_{\substack{k=g_{(j-1)}+1 \\ k \neq i}}^{g_j} \Lambda_k^{(j)} \gamma_{ki}(m) + \sum_{k=g_{(j-2)}+1}^{g_{(j-1)}} \Delta_k^{(j-1)} \gamma_{ki}(m) + \eta \end{aligned} \quad (3.23)$$

where the term $S_k(t)$ is defined in (3.3), and $A_i(m) = (\sqrt{E_i})B_i^{(m)}$ for the period $(m-1)T + \tau_i \leq t < mT + \tau_i$, and

$$\Lambda_k^{(j)} = A_k(m) - R_{k,j}^{(MF)}(m) \quad (3.24)$$

The improved correlation samples at outputs of the PIC structure are then used for detection and signal regeneration. Following that, the regenerated signals are then subtracted from the delayed composite signal. This signal is represented in (3.14) with the value of the index j increased by one. The resulting composite signal is then passed forward to the $j + 1$ subtractive step for the detection of the next group of users. This carries on until all the users are detected.

3.3 System assumptions and simplifications for the analysis

Before proceeding with the analysis, various assumptions and simplifications are made so that the analysis is tractable and remains reasonably accurate. The system model and the equations in the previous sections describe a general system without any specifications on the type of information bits and spreading sequences.

The following analysis investigates the system where the information bit sequence, $B_i^{(m)}$, and the spreading chip sequence, $C_i^{(m)}$, are binary independent and identically distributed (i.i.d) random variables with 1 and -1 being equally probable. Furthermore, the time delay, τ_i , of user i is assumed to be tracked perfectly and uniformly distributed on $[0, T_c)$ instead of $[0, T)$. The explanation is as follows.

The time delay of user i can be represented as

$$\tau_i = \varepsilon\tau_i + n_i T_c \quad (3.25)$$

where

$$\varepsilon\tau_i = \text{remainder} \left[\frac{\tau_i}{T_c} \right] \quad (3.26)$$

is the remainder of the division of τ_i/T_c , and

$$n_i = \left\lfloor \frac{\tau_i}{T_c} \right\rfloor \quad (3.27)$$

The term n_i is the largest integer that is less than τ_i/T_c .

Where the analysis of BER is concerned, it is shown in Appendix A that $\varepsilon\tau$, directly affects the results of the expectation and variance of the cross-correlation term. On the other hand, n_i has no effect on these results. This means that the interval $[0, T_c)$ instead of $[0, T)$ can be used without sacrificing accuracy of the analysis. One has to be mindful that random spreading codes are assumed.

The direct consequence of limiting the time delays of users within the interval $[0, T_c)$ is that one can further simplify the system model such that the analysis can be done on one information bit (Figure 3.4) instead of consecutive information bits as in (3.19). However, to have a reasonable accuracy in the analysis, the processing gain of the users should be sufficiently large so that the effect of the first and last chip of the information bit is insignificant.

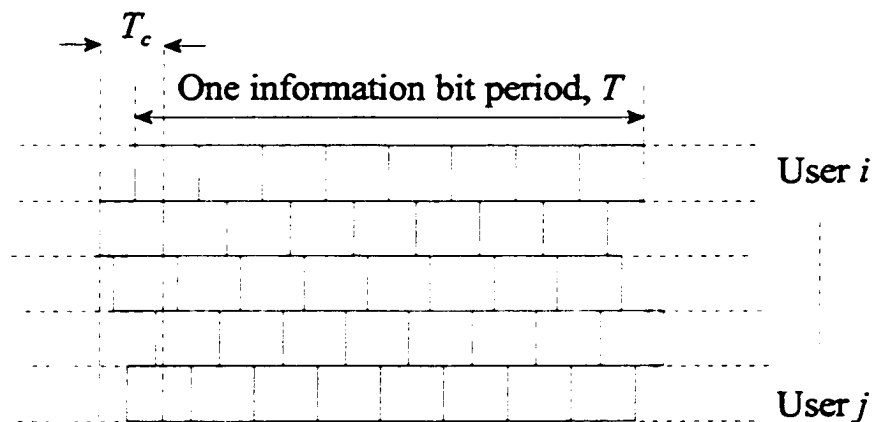


Figure 3.4: Asynchronous system with time delays limited to within one T_c .

Hence, in the following sections, the information bit of interest will be bit $m = 1$ corresponding to the interval $[0, T)$ and the indices m are dropped from the equations from the previous sections.

3.4 AWGN performance

In this section, the bit error rate (BER) performance of the matched filter, PIC, SIC and simplified VGHIC schemes in the AWGN channel are analyzed using similar approaches. Thus, this enables us to make direct comparison between the different schemes.

3.4.1 Matched filter

After despreading with the i^{th} spreading waveform and demodulating coherently, at the output of the matched filter receiver, one obtains

$$R'_i = \int_{\tau_i}^{T+\tau_i} \sqrt{\frac{2}{T}} r(t) c_i(t - \tau_i) \cos(\omega_c t + \theta_i) dt \quad (3.28)$$

Then, removing the high frequency term through low pass filtering, we obtain the correlation sample for user i as

$$R_i^{(MF)} = \sqrt{E_i} B_i + \underbrace{\sum_{\substack{k=1 \\ k \neq i}}^K \sqrt{E_k} B_k \gamma_{ki}}_{MAI \text{ term}} + \eta \quad (3.29)$$

where η is the noise term with zero mean and variance of $N/2$

$$\eta = \int_{\tau_i}^{T+\tau_i} n(t) c_i(t - \tau_i) \cos(\omega_c t + \theta_i) dt \quad (3.30)$$

and the cross-correlation in the multi-access interference (MAI) term is given as

$$\gamma_{ki} = \frac{1}{T} \int_{\tau_i}^{T+\tau_i} c_k(t - \tau_k) c_i(t - \tau_i) \cos(\theta_k - \theta_i) dt \quad (3.31)$$

This expression is much simpler than (3.19) as a result of the simplifications done in Section 3.3. It can be shown that [110][111][112]

$$E[\gamma_{ki}] = \begin{cases} 0 & , k \neq i \\ 1 & , k = i \end{cases}$$

$$Var[\gamma_{ki}] = \begin{cases} \frac{1}{D\rho} & , k \neq i \\ 0 & , k = i \end{cases} \quad (3.32)$$

with the factor D defined as follows

$$D = \begin{cases} 1 & , \text{Synchronous and random phase} \\ 1/2 & , \text{Synchronous} \\ 3 & , \text{Asynchronous and random phase} \\ 3/2 & , \text{Asynchronous} \end{cases} \quad (3.33)$$

The BER of the matched filter, $P_e^{(MF)}$, for BPSK scheme can be shown to be

$$P_e^{(MF)} = Q\left(\frac{\mu_s}{\sigma_s}\right) \quad (3.34)$$

where μ_s and σ_s are the mean and standard deviation of the output of the matched filter respectively, and $Q(x)$ is defined as

$$Q(x) = \frac{1}{\sqrt{2\pi}} \int_x^{\infty} e^{-t^2/2} dt \quad , \quad x \geq 0 \quad (3.35)$$

Modeling the interference as Gaussian using the central limit theorem, and applying (3.34) directly, the BER of user i is

$$P_e^{(MF)} = Q \left(\frac{\sqrt{E_i}}{\sqrt{\frac{1}{D\rho} \sum_{k=1, k \neq i}^K E_k + \frac{N_o}{2}}} \right) \quad (3.36)$$

It should be noted that the Gaussian approximation for MAI is only accurate when the number of users, K , is large enough. For equal power users, $E_i = E_b$, $i = 1, 2, \dots, K$, the BER expression is given by

$$P_e^{(MF)} = Q \left[\left(\frac{K-1}{D\rho} + \frac{1}{2} \left(\frac{E_b}{N_o} \right)^{-1} \right)^{-\frac{1}{2}} \right] \quad (3.37)$$

The above results do not apply to systems that use short and orthogonal spreading codes because long and random spreading codes have been assumed.

We shall now proceed to obtain the BER of the PIC, SIC and VGHIC scheme using the correlation samples, $R_i^{(MF)}$ given by (3.29), as the measures of the received power of each user.

3.4.2 Parallel interference cancellation (PIC)

For the PIC scheme, initial detection is done with a bank of matched filters. Then, the regenerated signals from other users are subtracted from the delayed version of the original received signal to form the composite signal for the desired user. After this the desired user is detected again from the composite signal. Further detail and alternative analysis of the multistage PIC structure can be found in [56][82]. The structure of the PIC scheme is shown in Figure 3.5.

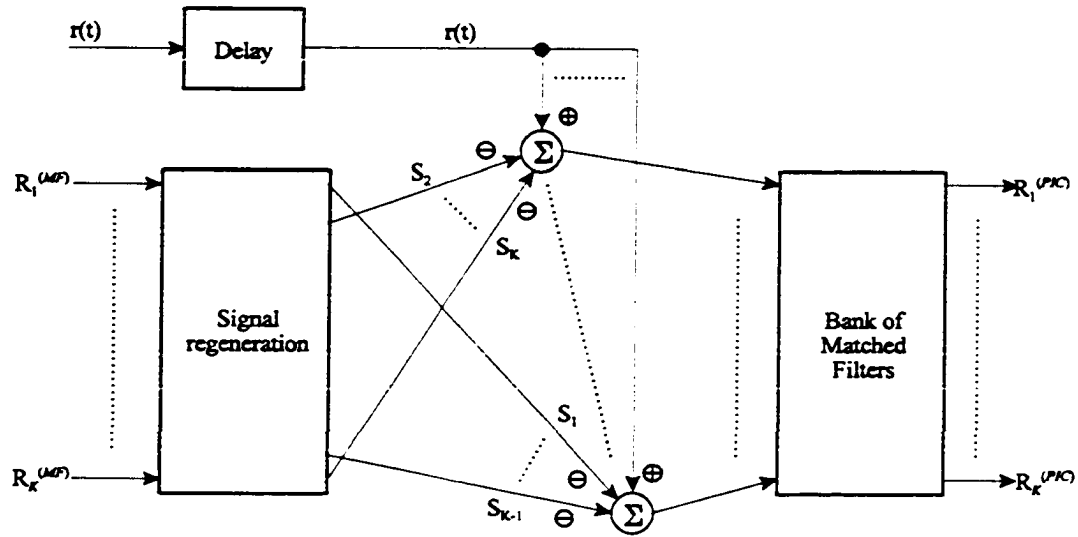


Figure 3.5: Structure of 1 stage of the PIC scheme.

After the initial detection by the bank of K matched filters, the multiple access interference (MAI) is reconstructed. The MAI is then subtracted from the delayed or buffered version of the original received signal. Thus, the received signal after PIC for user i is

$$r_i(t) = r(t) - \sum_{\substack{k=1 \\ k \neq i}}^K \sqrt{\frac{2}{T}} R_k^{(MF)} c_k(t - \tau_k) \cos(\omega_c t - \theta_k) \quad (3.38)$$

After despreading, demodulation and passing the signal through the low-pass filter, we have

$$R_i^{(PIC)} = \sqrt{E_i} B_i + \sum_{\substack{k=1 \\ k \neq i}}^K \left(\sqrt{E_k} B_k - R_k^{(MF)} \right) \gamma_{ki} + \eta \quad (3.39)$$

Substituting (3.29) into (3.39), and simplifying, we have

$$\begin{aligned}
R_i^{(PIC)} = & \sqrt{E_i} B_i \underbrace{\left(1 - \sum_{\substack{k=1 \\ k \neq i}}^K \gamma_{ik}^2 \right)}_{\text{Self Cancellation term}} \\
& - \underbrace{\sum_{\substack{k=1 \\ k \neq i}}^K \sum_{\substack{n=1 \\ n \neq k, i}}^K \sqrt{E_n} B_n \gamma_{nk} \gamma_{ki}}_{\text{Cancellation noise}} \\
& + \eta \underbrace{\left(1 - \sum_{\substack{k=1 \\ k \neq i}}^K \gamma_{ki} \right)}_{\text{AWGN term}}
\end{aligned} \tag{3.40}$$

from which, the following results are obtained using (3.32):

$$\begin{aligned}
E[R_i^{(PIC)}] &= \sqrt{E_i} \left(1 - \frac{K-1}{D\rho} \right) \\
\text{Var}[R_i^{(PIC)}] &= \left(\frac{1}{D\rho} \right)^2 \sum_{\substack{k=1, \\ k \neq i}}^K \sum_{\substack{n=1, \\ n \neq i, k}}^K E_n + \frac{N_o}{2} \left(1 - \frac{K-1}{D\rho} \right)
\end{aligned} \tag{3.41}$$

The self cancellation and the cancellation noise term in (3.40) (also (3.46) and (3.55)) is due to the fact that (3.29) is used as the estimation of the amplitude of each user for cancellation.

Hence, for equal power users and using (3.34), the bit error probability is given by

$$P_e^{(PIC)} = Q \left(\frac{1 - \frac{K-1}{D\rho}}{\sqrt{\frac{(K-1)(K-2)}{(D\rho)^2} + \frac{1}{2E_b/N_o} \left(1 + \frac{K-1}{D\rho} \right)}} \right) \tag{3.42}$$

3.4.3 Successive interference cancellation (SIC)

The basic structure of the SIC scheme is shown in Figure 3.6. The figure shows the i^{th} subtractive step of a cancellation stage. A subtractive step is defined when a particular user is being detected, and the effect of that user's interference is being cancelled from the composite signal. K individual subtractive steps form a cancellation stage for the SIC. The SIC scheme cancels each user from the composite signal successively according to the power level of each user's signal. The signal of the user with the highest power level will be detected, regenerated, and cancelled from the composite signal first, then the user with the next lower power, and so on. More information can be found in [70][113][114]. However, the analysis of the SIC here is different. It takes into account the self cancellation term due to the use of the correlation samples in the signal regeneration and cancellation process.

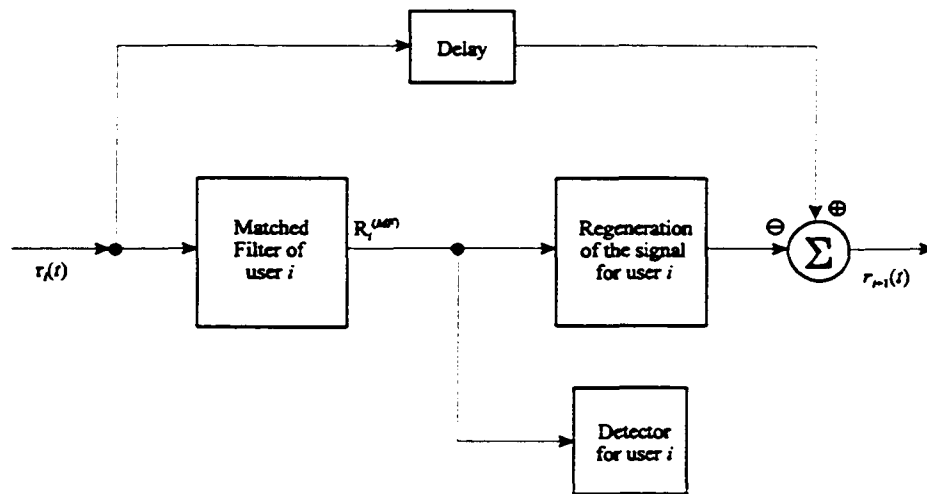


Figure 3.6: Structure of the i^{th} subtractive step of the SIC scheme.

We denote the strongest user as user 1 and hence $E_1 > E_2 > E_3 > \dots > E_K$. After despreading, demodulation, and LPF, for user 1, from (3.29)

$$R_1^{(SIC)} = \sqrt{E_1} B_1 + \sum_{k=2}^K \sqrt{E_k} B_k \gamma_{k1} + \eta \quad (3.43)$$

Then, using the correlation sample value as the estimate of the user signal power, the regenerated signal of user 1 is subtracted from the delayed version of the original received signal $r(t)$ resulting in the composite signal

$$r_2(t) = r(t) - \sqrt{\frac{2}{T}} R_1^{(SIC)} c_1(t - \tau_1) \cos(\omega_c t - \theta_1) \quad (3.44)$$

After despreading, demodulation and LPF for user 2, one obtains

$$R_2^{(SIC)} = \sqrt{E_2} B_2 + \sum_{k=3}^K \sqrt{E_k} B_k \gamma_{k2} + \left(\sqrt{E_1} B_1 - R_1^{(SIC)} \right) \gamma_{k1} + \eta \quad (3.45)$$

Substituting (3.43) into (3.45) and simplifying, one obtains

$$\begin{aligned} R_2^{SIC} = & \underbrace{\sqrt{E_2} B_2 (1 - \gamma_{21} \gamma_{12})}_{\text{Self cancellation term}} \\ & + \sum_{k=3}^K \sqrt{E_k} B_k \left(\underbrace{\gamma_{k2}}_{\text{Uncancelled MAI term}} - \underbrace{\gamma_{k1} \gamma_{12}}_{\text{Cancellation noise}} \right) + \underbrace{\eta (1 - \gamma_{12})}_{\text{AWGN term}} \end{aligned} \quad (3.46)$$

Hence,

$$\begin{aligned} E[R_2^{(SIC)}] &= \sqrt{E_2} \left(1 - \frac{1}{D\rho} \right) \\ \text{Var}[R_2^{(SIC)}] &= \left(\frac{1}{D\rho} \right) \left(1 + \frac{1}{D\rho} \right) \sum_{k=3}^K E_k + \left(1 + \frac{1}{D\rho} \right) \frac{N_o}{2} \end{aligned} \quad (3.47)$$

Similarly, for user 3 and user 4 (Appendix A),

$$\begin{aligned} E[R_3^{(SIC)}] &= \sqrt{E_3} \left(1 - 2 \left(\frac{1}{D\rho} \right) \right) \\ \text{Var}[R_3^{(SIC)}] &= \left(\frac{1}{D\rho} \right)^3 E_3 + \left(\frac{1}{D\rho} \right)^2 \left(1 + \frac{1}{D\rho} \right) E_2 \\ &+ \left(\frac{1}{D\rho} \right) \left(1 + \frac{1}{D\rho} \right)^2 \sum_{k=4}^K E_k + \left(1 + \frac{1}{D\rho} \right)^2 \frac{N_o}{2} \end{aligned} \quad (3.48)$$

and

$$\begin{aligned}
E[R_4^{(SIC)}] &= \sqrt{E_4} \left(1 - 3\left(\frac{1}{D\rho}\right)\right) \\
\text{Var}[R_4^{(SIC)}] &= \left(\frac{1}{D\rho}\right)^3 \left(1 + \frac{1}{D\rho}\right) E_4 + \left(\frac{1}{D\rho}\right)^2 \left(1 + \frac{1}{D\rho}\right) \left(2 + \frac{1}{D\rho}\right) E_3 \\
&\quad + \left(\frac{1}{D\rho}\right)^2 \left(1 + \frac{1}{D\rho}\right)^2 E_2 \\
&\quad + \left(\frac{1}{D\rho}\right) \left(1 + \frac{1}{D\rho}\right)^3 \sum_{k=5}^K E_k + \left(1 + \frac{1}{D\rho}\right)^3 \frac{N_o}{2}
\end{aligned} \tag{3.49}$$

respectively. Generalizing, for user i ,

$$\begin{aligned}
E[R_i^{(SIC)}] &= \sqrt{E_i} \left(1 - \frac{i-1}{D\rho}\right) \\
\text{Var}[R_i^{(SIC)}] &= \left(\frac{1}{D\rho}\right) \left[\left(1 + \frac{1}{D\rho}\right)^{i-1} - \left(1 + \frac{i-1}{D\rho}\right) \right] E_i \\
&\quad + \left(\frac{1}{D\rho}\right) \sum_{k=2}^{i-1} \left(1 + \frac{1}{D\rho}\right)^{i-k} \left[\left(1 + \frac{1}{D\rho}\right)^{k-1} - 1 \right] E_k \\
&\quad + \left(\frac{1}{D\rho}\right) \left(1 + \frac{1}{D\rho}\right) \sum_{k=i+1}^K E_k \\
&\quad + \left(1 + \frac{1}{D\rho}\right)^{i-1} \frac{N_o}{2}
\end{aligned} \tag{3.50}$$

The above expression is obtained if one considers the effect of the self cancellation (3.46) when the correlation sample is used in the regeneration of signals. For the case where the self cancellation effect is not accounted for, one can refer to [115]. If one does not factor in the self cancellation effect, (3.50) can be simplified to (18) of the mentioned reference. Hence, for equal power users and using (3.34), the bit error probability for user i is given by

$$P_e(i) = Q \left(\frac{E[R_i^{(SIC)}]}{\sqrt{\text{Var}[R_i^{(SIC)}]}} \right) \tag{3.51}$$

Therefore, the average probability for the whole SIC stage would be

$$P_e^{(SIC)} = \frac{1}{K} \sum_{i=1}^K P_e(i) \quad (3.52)$$

3.4.4 Variable group hybrid interference cancellation (VGHIC)

In order to get a closed form analytical result for the VGHIC scheme so that comparisons can be made with the PIC and SIC schemes with reasonable accuracy, we would need to simplify the proposed VGHIC scheme for our analysis. Instead of choosing the users for each group at the start of each subtractive step (as in Figure 3.1), users are separated into different groups after detections by the initial bank of matched filter receivers. This knowledge about the groupings is then passed to the corresponding group canceling units (GCU). For the subsequent j^{th} subtractive step, a bank of G_j matched filters replaces the users selection block found in Figure 3.2. The block diagram of the resulting simplified VGHIC is shown in Figure 3.7. The number of users in each group, G_j , has already been determined at the first subtractive step. We have also assumed that $|R_{1,j}^{MF}| > |R_{2,j}^{MF}| > \dots > |R_{K,j}^{MF}|$.

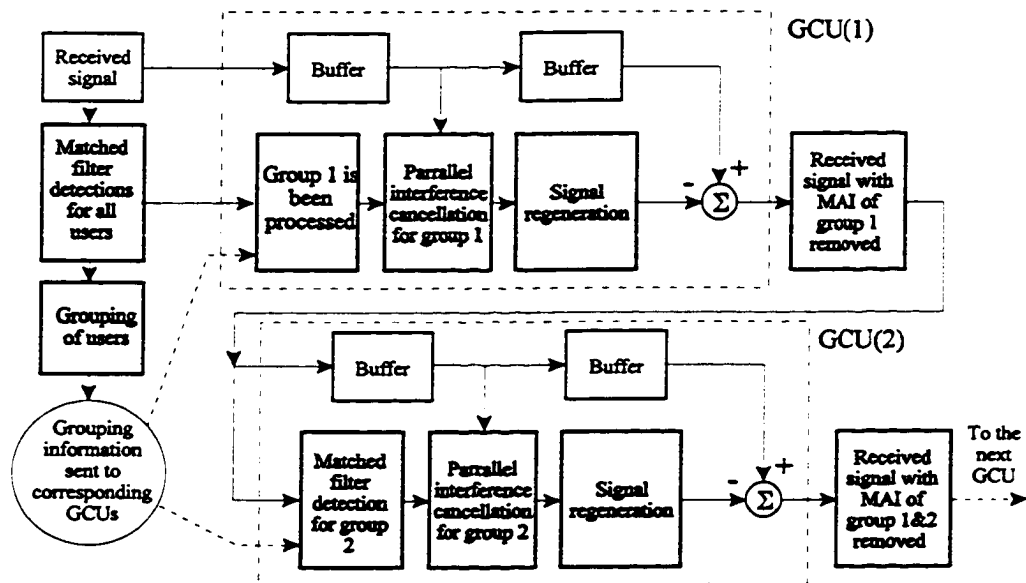


Figure 3.7: The simplified variable group interference cancellation (VGHIC).

Analysis of the simplified VGHIC receiver

At the initial bank of matched filters, the correlation sample for each user is given by (3.29). Using these samples, G_1 users are selected into group 1. Applying PIC on the group 1 users results in the following composite signal for user i ,

$$r_i^{(1,PIC)}(t) = r^{(1)}(t) - \sum_{\substack{k=1 \\ k \neq i}}^{G_1} \sqrt{\frac{2}{T}} R_{k,1}^{(MF)} c_k(t) \cos(\omega_c t + \theta_k) \quad (3.53)$$

After correlating using the i^{th} matched filter and simplifying, we have, after the PIC block in the 1st subtractive step,

$$\begin{aligned} R_{i,1}^{(PIC)} &= \sqrt{E_i} B_i + \sum_{k=g_1+1}^K \sqrt{E_k} B_k \gamma_{ki} + \sum_{\substack{k=1 \\ k \neq i}}^{G_1} \left(\sqrt{E_k} B_k - R_{k,1}^{(MF)} \right) \gamma_{ki} + \eta \\ &= \underbrace{\sqrt{E_i} B_i \left(1 - \sum_{\substack{k=1 \\ k \neq i}}^{G_1} \gamma_{ik}^2 \right)}_{\text{Self Cancellation term}} + \underbrace{\sum_{k=G_1+1}^K \sqrt{E_k} B_k \gamma_{ki}}_{\text{Uncancelled MAI}} \\ &\quad - \underbrace{\sum_{\substack{k=1 \\ k \neq i}}^{G_1} \sum_{\substack{n=1 \\ n \neq k, j}}^K \sqrt{E_n} B_n \gamma_{nk} \gamma_{ki}}_{\text{Cancellation noise}} + \underbrace{\eta \left(1 - \sum_{\substack{k=1 \\ k \neq i}}^{G_1} \gamma_{ki} \right)}_{\text{AWGN term}} \end{aligned} \quad (3.54)$$

and this $R_{i,1}^{(PIC)}$ is used as the estimate of the signal amplitude for user i in the signal regeneration process. The regenerated signal is then used in the following interference cancellation operation. After this, the regenerated signals belonging to the users in group 1 are subtracted from the delayed version of the received signal, $r^{(1)}(t)$. Using (3.46), (3.54) and simplifying, it can be shown that the matched filter output of user i in subtractive step 2 (corresponding to group 2) is

$$\begin{aligned}
R_{i,2}^{(MF)} = & \sqrt{E_i} B_i \left(1 - \sum_{k=i}^{G_1} \gamma_{ki}^2 + \sum_{k=i}^{G_1} \sum_{\substack{n=1 \\ n \neq k}}^{G_1} \gamma_{in} \gamma_{nk} \gamma_{ki} \right) & \left. \vphantom{R_{i,2}^{(MF)}} \right\} & \text{Self Cancellation term} \\
& + \sum_{\substack{k=G_1+1 \\ k \neq i}}^K \sqrt{E_k} B_k \gamma_{ki} & \left. \vphantom{R_{i,2}^{(MF)}} \right\} & \text{Uncancelled MAI} \\
& + \sum_{k=1}^{G_1} \sum_{\substack{n=1 \\ n \neq k}}^{G_1} \sqrt{E_k} B_k \gamma_{nk}^2 \gamma_{ki} & \left. \vphantom{R_{i,2}^{(MF)}} \right\} & \\
& - \sum_{k=1}^{G_1} \sum_{\substack{n=G_1+1 \\ n \neq k, i}}^K \sqrt{E_n} B_n \gamma_{nk} \gamma_{ki} & \left. \vphantom{R_{i,2}^{(MF)}} \right\} & \text{Cancellation noise} \\
& + \sum_{k=1}^{G_1} \sum_{\substack{n=1 \\ n \neq k}}^{G_1} \sum_{\substack{m=1 \\ m \neq n, k, i}}^K \sqrt{E_m} B_m \gamma_{mn} \gamma_{nk} \gamma_{ki} & \left. \vphantom{R_{i,2}^{(MF)}} \right\} & \\
& + \eta \left(1 - \sum_{\substack{k=1 \\ k \neq i}}^{G_1} \gamma_{ki} + \sum_{k=1}^{G_1} \sum_{\substack{n=1 \\ n \neq k}}^{G_1} \gamma_{nk} \gamma_{ki} \right) & \left. \vphantom{R_{i,2}^{(MF)}} \right\} & \text{AWGN term}
\end{aligned} \tag{3.55}$$

It is clear that the correlation equation becomes more and more complex as we evaluate further subtractive steps. To simplify matters, we shall consider the case when the energies of all users are the same and equal to E_b , so that the correlation sample values can be normalized by $\sqrt{E_b}$. Let

$$\begin{aligned}
E[R_{i,j}^{(k)} | B_i] &= \mu^{(k)} \\
\text{Var}[R_{i,j}^{(k)} | B_i] &= V_{(x,y)}^{(k)}
\end{aligned} \tag{3.56}$$

where k is a function of j and the type of receiver. The term k is defined in the following

$$\begin{aligned}
R_{i,1}^{(0)} &= R_{i,1}^{(MF)} \\
R_{i,1}^{(1)} &= R_{i,1}^{(PIC)} \\
R_{i,2}^{(2)} &= R_{i,2}^{(MF)} \\
R_{i,2}^{(3)} &= R_{i,2}^{(PIC)} \\
&\vdots \\
R_{i,j}^{[(j-1)\times 2]} &= R_{i,j}^{(MF)} \\
R_{i,j}^{(2j-1)} &= R_{i,j}^{(PIC)}
\end{aligned} \tag{3.57}$$

For the output of the matched filter, $R_{ij}^{(MF)}$, one uses $k = [(j-1)\times 2]$. If it is the output of the PIC, $R_{ij}^{(PIC)}$, the relation $k = (2j-1)$ should be used.

The indices x and y are needed in the recursive equation below to produce the correct expression for the variance; $x, y \in \{-1, 0\}$. Therefore, generalizing the expression for the variance of the correlation sample at the output of the matched filters for all subtractive steps, we have for $k \geq 2$,

$$\mu^{(k)} = \begin{cases} 1 - \frac{1}{D\rho} (G_{(\frac{k+1}{2})} - 1) - \frac{1}{D\rho} \sum_{j=1}^{\frac{k-1}{2}} G_j & , \quad k \text{ odd} \\ 1 - \frac{1}{D\rho} \sum_{j=1}^{\frac{k}{2}} G_j & , \quad k \text{ even} \end{cases} \tag{3.58}$$

$$V_{(x,y)}^{(k)} = \begin{cases} \frac{1}{D\rho} \left(K + x - \sum_{j=1}^{\frac{k+1}{2}} G_j \right) + \frac{1}{D\rho} (G_{(\frac{k+1}{2})} - 1) V_{(y,0)}^{(k-1)} \\ \quad + \frac{1}{D\rho} \sum_{j=1}^{\frac{k-1}{2}} G_{(2j-1)} V_{(y,0)}^{(2j-1)} + \frac{1}{2 \binom{E_b/N_o}{}} , k \text{ odd} \\ \\ \frac{1}{D\rho} \left(K - 1 + x - \sum_{j=1}^{\frac{k}{2}} G_j \right) \\ \quad + \frac{1}{D\rho} \sum_{j=1}^{\frac{k}{2}} G_{(2j-1)} V_{(y,0)}^{(2j-1)} + \frac{1}{2 \binom{E_b/N_o}{}} , k \text{ even} \end{cases} \quad (3.59)$$

with the following initial conditions

$$\begin{aligned} \mu^{(0)} &= 0 \\ \mu^{(1)} &= 1 - \frac{1}{D\rho} (G_1 - 1) \\ V_{(x,0)}^{(0)} &= V_{(x,-1)}^{(0)} = \frac{1}{D\rho} (K - 1 + x) + \frac{1}{2 \binom{E_b/N_o}{}} \\ V_{(x,y)}^{(1)} &= \frac{1}{D\rho} (K - G_1 + x) + \frac{1}{D\rho} (G_1 - 1) V_{(y,0)}^{(0)} + \frac{1}{2 \binom{E_b/N_o}{}} \end{aligned} \quad (3.60)$$

To evaluate the variance using (3.59), one needs to put $x = 0$ and $y = -1$ for the recursive expression to be valid. Treating the interference as Gaussian and using (3.34), the average BER of the VGHC, at the outputs of the PIC blocks for all the subtractive steps, in AWGN is given by

$$P_e^{(VGHC)} = \frac{1}{K} \sum_{j=1}^{N_g} G_j Q \left(\frac{\mu^{(2j-1)}}{\sqrt{V_{(0,-1)}^{(2j-1)}}} \right) \quad (3.61)$$

where N_g is the total number of groups.

Determination of user groups

In order to evaluate (3.61), the number of users in each cancellation group needs to be determined. In VGHC, users are grouped according to the magnitude of their respective correlation sample values at the matched filter outputs. As the correlation sample, $R_{ij}^{(MF)}$, is a random variable and assumed to be Gaussian, one can determine the average number of users in each group. This can be done by finding the probability of a user having a correlation sample value that satisfies the group selection rule (3.10). This in turn enables one to find the average number of users in each group and also the average number of groups.

Note that in the simplified VGHC, only the outputs of the initial bank of matched filters are used to determine the groupings of users. That is, $R_{i,1}^{(MF)}$ are used. This makes the term j in $R_{ij}^{(MF)}$ redundant as j always have the value of one. Thus, to avoid any confusion later on in this section, let

$$R_i^{(MF)} = R_{i,1}^{(MF)} \quad (3.62)$$

Now, the normalized output of the matched filter in the first subtraction step (conditioned on B_i) with the assumption that the energies of all users are the same and equal to E_b is represented by

$$R_i^{(MF)} = 1 + \sum_{\substack{k=1 \\ k \neq i}}^K B_k \gamma_{ki} + \frac{\eta}{\sqrt{E_b}} \quad (3.63)$$

The correlation sample value of (3.63) is approximately Gaussian with mean $\mu = 1$ and variance $\sigma^2 = \frac{1}{D\rho} (K - 1) + \frac{1}{2} \left(\frac{E_b}{N_s} \right)^{-1}$. The parameter D is defined in (3.33).

The users are ordered according to the values of their matched filter outputs and they are ranked in descending order of the correlation sample values, $R_i^{(MF)}$. The user with the largest $R_i^{(MF)}$ is assigned the rank index $g = 1$, the user with the next highest $R_i^{(MF)}$ will have $r = 2$ and so on. Hence, after ranking, one will have the ordered correlation samples (denoted by $R_{(g)}^{(MF)}$)

), $R_{(1)}^{(MF)} > R_{(2)}^{(MF)} > \dots > R_{(g)}^{(MF)} \dots > R_{(K)}^{(MF)}$ where g and K are the ranking of the user and the total number of users, respectively¹. It shall be pointed out that the probability density function (pdf) of $R_i^{(MF)}$ is different from that of the ordered $R_{(g)}^{(MF)}$. The $R_i^{(MF)}$ is approximately having a Gaussian distribution, whereas the pdf of the ordered correlation sample value is obtained using order statistics [116] and given by

$$f_r(x) = \frac{K!}{(r-1)!(K-r)!} F(x)^{(K-r)} [1-F(x)]^{(r-1)} f(x) \quad (3.64)$$

where $f(x)$ and $F(x)$ are the pdf and cumulative distribution function (cdf) of the original unordered correlation sample value, $R_i^{(MF)}$, respectively. These functions are

$$f(x) = \frac{1}{\sigma\sqrt{2\pi}} \exp\left(-\frac{(x-\mu)^2}{2\sigma^2}\right) \quad (3.65)$$

and

$$F(x) = 1 - \frac{1}{2} \operatorname{erfc}\left(\frac{x-\mu}{\sqrt{2}\sigma}\right) \quad (3.66)$$

From (3.64), (3.65) and (3.66), the average correlation sample value corresponding to the rank g is obtained as

$$\begin{aligned} \tilde{R}_{(g)}^{(MF)} &= \frac{1}{\sigma\sqrt{8\pi}} \frac{K!}{(g-1)!(K-g)!} \\ &\times \int_{-\infty}^{\infty} \left\{ x \left[1 - \frac{1}{2} \operatorname{erfc}\left(\frac{x-\mu}{\sqrt{2}\sigma}\right) \right]^{(K-g)} \operatorname{erfc}\left(\frac{x-\mu}{\sqrt{2}\sigma}\right)^{(g-1)} \exp\left(-\frac{(x-\mu)^2}{2\sigma^2}\right) \right\} dx \end{aligned} \quad (3.67)$$

Although (3.67) cannot be found analytically, it can easily be evaluated numerically. Then, the average correlation sample values obtained are used to find the average number of users in each group and also the average number of groups.

¹ Usually, for convenience, the indices i and g are made equal to each other (consequently, $R_i^{(MF)} = R_{(g)}^{(MF)}$). However, they are treated differently here to avoid confusions.

Let g_j^{ref} be the index of the reference used to select members of group j . Then $\tilde{R}_{(1)}^{(MF)}$ is the reference to be used in the selection rule (3.10) for the selection of group 1. The term δ is a design parameter to be set. Users are grouped together as group 1 if,

$$\tilde{R}_{(g)}^{(MF)} \geq \delta \tilde{R}_{(g_1^{ref}=1)}^{(MF)} \quad (3.68)$$

The absolute function is dropped from (3.68) as $R_i^{(MF)}$ is conditioned on B_i . Let the rank of the user with the smallest $\tilde{R}_{(g)}^{(MF)}$ that satisfies (3.68) be $g_j, j = 1$. Hence, at the end of the selection for group 1, we have

$$\begin{aligned} \tilde{R}_{(g_1)}^{(MF)} &\geq \delta \tilde{R}_{(g_1^{ref})}^{(MF)} \\ \tilde{R}_{(g_1+1)}^{(MF)} &< \delta \tilde{R}_{(g_1^{ref})}^{(MF)} \end{aligned} \quad (3.69)$$

The number of users in group 1 can be determined from

$$G_1 = g_1 - g_1^{ref} + 1 = g_1 \quad (3.70)$$

Next, $\tilde{R}_{(g_1+1)}^{(MF)}$ is chosen as the reference for the selection of the members for group 2, thus

$$g_2^{ref} = g_1 + 1 \quad (3.71)$$

The same process of grouping is repeated until all users are grouped.

Generalizing the procedure, the reference can be determined using

$$g_j^{ref} = g_{j-1} + 1 \quad , \quad g_0 = 0 \quad (3.72)$$

Here, the correlation sample values have been rearranged in descending order. Thus, $R_{(g)}^{(MF)} \geq R_{(g+1)}^{(MF)}$ is always true. Members of group j are then selected based on

$$\tilde{R}_{(g)}^{(MF)} \geq \delta \tilde{R}_{(g_j^{ref})}^{(MF)} \quad (3.73)$$

The rank index g is increased (and users are being selected into the group) until the following conditions have been reached:

$$\begin{aligned}\tilde{R}_{(g_j)}^{(MF)} &\geq \delta \tilde{R}_{(g_j^{ref})}^{(MF)} \\ \tilde{R}_{(g_{j+1})}^{(MF)} &< \delta \tilde{R}_{(g_j^{ref})}^{(MF)}\end{aligned}\quad (3.74)$$

Then, the number of users in group j , G_j , can be determined using

$$G_j = g_j - g_j^{ref} + 1 \quad (3.75)$$

From the recursive equation (3.72) and (3.75), one can deduce

$$G_j = g_j - \sum_{k=1}^{j-1} G_k \quad (3.76)$$

When the last group of users has been determined, that corresponding group number J is the average number of groups. With J and $G_j, j = 1 \dots J$ known, one can then evaluate the average BER of the VGHC using (3.61).

3.5 Performance in Rayleigh fading

This section investigates analytically the bit error rate (BER) performance of the matched filter, PIC, SIC and simplified VGHC schemes in the flat Rayleigh fading channel where there is no power control or where the power control is ineffective. The received signal differs slightly from the one for the AWGN case (3.1) and is shown here:

$$r_f(t) = \sum_{i=1}^K \alpha_i \sqrt{\frac{2E_i}{T}} c_i(t - \tau_i) b_i(t - \tau_i) \cos(\omega_c t + \theta_i) + n(t) \quad (3.77)$$

The difference is the presence of the channel gain term for user i , α_i , where α_i is a Rayleigh distributed random variable with the pdf given by

$$P_{Rayleigh}(z) = \frac{z}{a^2} e^{-\frac{z^2}{2a^2}}, \quad z \geq 0 \quad (3.78)$$

where α^2 is the variance of the Gaussian random variables that make up α_i . If Z is the Rayleigh random variable², it is defined by

$$Z = \sqrt{X^2 + Y^2} \quad (3.79)$$

where X and Y are zero-mean statistically independent Gaussian random variables with their variances equal to α^2 . In the analysis, the power of the channel gain is normalized such that $E[\alpha_i^2] = 1$ (or $\alpha^2 = 1/2$). The effect of the fading on the received phase has been lumped together with the phase of user i and is represented by θ_i , which is assumed to be tracked perfectly and uniformly distributed on the interval $[0, 2\pi)$.

3.5.1 Matched filter

Using similar procedures in the previous sections, the correlation sample at the output of the matched filter for user i can be found to be

$$R_i^{(MF)} = \alpha_i \sqrt{E_i} B_i + \underbrace{\sum_{\substack{k=1 \\ k \neq i}}^K \alpha_k \sqrt{E_k} B_k \gamma_{ki}}_{MAI \text{ term}} + \eta \quad (3.80)$$

where all terms have been defined in previous sections. Normalizing (3.80) and conditioning on α_i , one can obtain

$$E[R_i^{(MF)}] = \alpha_i \quad (3.81)$$

and

$$\text{Var}[R_i^{(MF)}] = \frac{1}{D\rho} \sum_{\substack{k=1 \\ k \neq i}}^K E[(\alpha_k)^2] \frac{E_k}{E_i} + \frac{N_o}{2E_i} \quad (3.82)$$

² A random variable is a function whose domain is the set of experimental outcomes. For a random variable Z , its distribution function is given by $P\{Z \leq z\} = F_z(z)$.

First, the interference is approximated as Gaussian using the central limit theorem. Then one can interpret (3.80) as the sum of a Rayleigh and Gaussian random variable. The Rayleigh variable is α_i , while the Gaussian variable corresponds to the multi-access interference (MAI) and the noise term. Hence, the cdf of $R_i^{(MF)}$ is found in Appendix C to be

$$F_{MF}(z) = \frac{1}{2} + \frac{1}{2} \operatorname{erf}\left(\frac{z}{\sqrt{2b^2}}\right) - \sqrt{\frac{a^2}{a^2+b^2}} e^{-\frac{1}{2}\left(\frac{1}{a^2+b^2}\right)z^2} \left[\frac{1}{2} + \frac{1}{2} \operatorname{erf}\left(\frac{az}{\sqrt{2b^2(a^2+b^2)}}\right) \right] \quad (3.83)$$

and the pdf of $R_i^{(MF)}$ is

$$p_{MF}(z) = \frac{b}{\sqrt{2\pi(a^2+b^2)}} e^{-\frac{z^2}{2b^2}} + \frac{az}{2(a^2+b^2)\sqrt{a^2+b^2}} e^{-\frac{1}{2}\left(\frac{z^2}{a^2+b^2}\right)} \left[1 + \operatorname{erf}\left(\frac{az}{\sqrt{2b^2(a^2+b^2)}}\right) \right] \quad (3.84)$$

where a^2 is defined in (3.78) for α_i , and b^2 is the normalized variance of the MAI and noise term and is given by

$$b^2 = \frac{1}{D\rho} \sum_{\substack{k=1, \\ k \neq i}}^K \frac{E_k}{E_i} + \frac{N_o}{2E_i} \quad (3.85)$$

since $E[\alpha_i^2] = 1$. Note that the mean of the MAI and noise term is zero, and the Gaussian approximation for the MAI and noise term is only accurate when the number of users, K , is sufficiently large. The BER expression for the Rayleigh fading channel when conditioned on B_i is given by

$$P_e^{(MF)} = \int_{-\infty}^0 p_{MF}(z) dz \quad (3.86)$$

In [117], an expression of the BER performance in Rayleigh fading channel for BPSK has also been derived, and it is shown below (using the original notations in the reference),

$$P_2 = \frac{1}{2} \left(1 - \sqrt{\frac{\bar{\gamma}_b}{1 + \bar{\gamma}_b}} \right) \quad (3.87)$$

where $\bar{\gamma}_b$ is the average signal-to-noise ratio, defined as

$$\bar{\gamma}_b = \frac{E_b}{N_o} E[\alpha_i^2] \quad (3.88)$$

where α_i has been defined previously. The BER expressions (3.86) and (3.87) are plotted and compared in Figure 3.8 with parameters shown. One can see that there is no noticeable difference between the two expressions and this observation verifies (3.86).

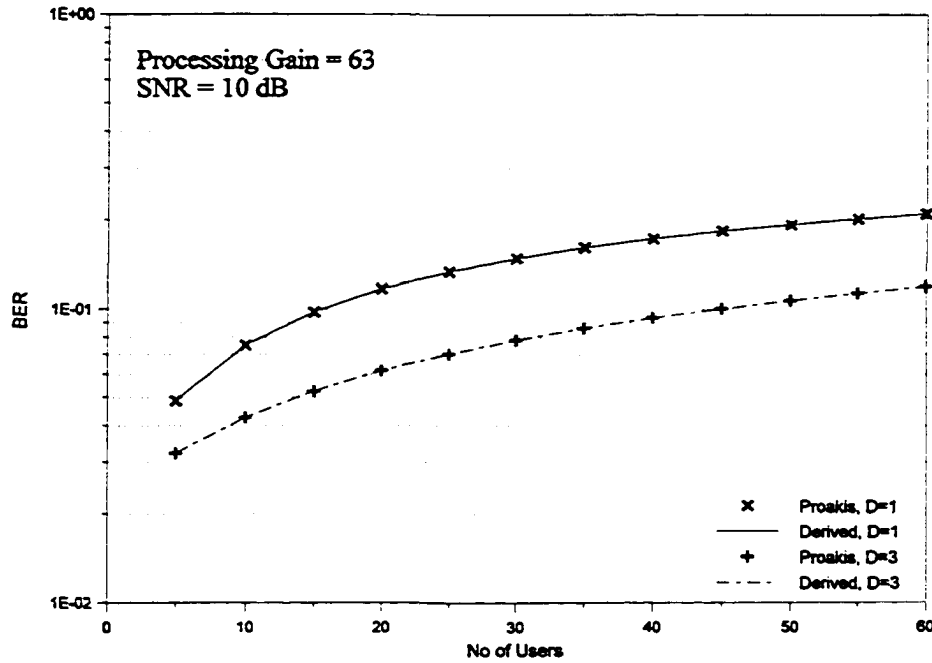


Figure 3.8: Comparison of the derived BER (3.86) and (3.87) from Proakis [29] for the case where $D = 1$ and $D = 3$.

3.5.2 Parallel interference cancellation (PIC)

With Rayleigh fading, the received signal after PIC for user i , $r_{(f,i)}(t)$ is

$$r_{(f,i)}(t) = r_f(t) - \sum_{\substack{k=1 \\ k \neq i}}^K \alpha_k \sqrt{\frac{2}{T}} R_k^{(MF)} c_k(t - \tau_k) \cos(\omega_c t - \theta_k) \quad (3.89)$$

where $r_f(t)$ is defined in (3.77). After despreading and demodulation

$$R_i^{(PIC)} = \alpha_i \sqrt{E_i} B_i + \sum_{\substack{k=1 \\ k \neq i}}^K \left(\alpha_k \sqrt{E_k} B_k - R_k^{(MF)} \right) \gamma_{ki} + \eta \quad (3.90)$$

Substituting for $R_k^{(MF)}$ using (3.80) and simplifying, one finds

$$R_i^{(PIC)} = \alpha_i \sqrt{E_i} B_i \left(\underbrace{1 - \sum_{\substack{k=1 \\ k \neq i}}^K \gamma_{ik}^2}_{\text{Self Cancellation term}} \right) - \underbrace{\sum_{\substack{k=1 \\ k \neq i}}^K \sum_{\substack{n=1 \\ n \neq k, i}}^K \alpha_n \sqrt{E_n} B_n \gamma_{nk} \gamma_{ki}}_{\text{Cancellation noise}} + \eta \left(\underbrace{1 - \sum_{\substack{k=1 \\ k \neq i}}^K \gamma_{ki}}_{\text{AWGN term}} \right) \quad (3.91)$$

Using (3.91) and conditioning on (α_i, B_i) , the following results are obtained:

$$E[R_i^{(PIC)}] = \alpha_i \sqrt{E_i} \left(1 - \frac{K-1}{D\rho}\right) \quad (3.92)$$

$$\text{Var}[R_i^{(PIC)}] = \left(\frac{1}{D\rho}\right)^2 \sum_{\substack{k=1 \\ k \neq i}}^K \sum_{\substack{n=1 \\ n \neq i, k}}^K E_n + \frac{N_o}{2} \left(1 + \frac{K-1}{D\rho}\right) \quad (3.93)$$

since $E[\alpha_i^2] = 1$. Hence, the BER of PIC in Rayleigh fading channel is given by

$$P_e^{(PIC)} = \int_0^\infty Q \left(\frac{\alpha \sqrt{E_i} \left(1 - \frac{K-1}{D\rho}\right)}{\sqrt{\left(\frac{1}{D\rho}\right)^2 \sum_{\substack{k=1 \\ k \neq i}}^K \sum_{\substack{n=1 \\ n \neq i, k}}^K E_n + \frac{N_o}{2} \left(1 + \frac{K-1}{D\rho}\right)}} \right) P_{\text{Rayleigh}}(\alpha) d\alpha \quad (3.94)$$

Alternatively, the BER can be found by using (3.86). This is done by normalizing (3.93) and setting

$$b^2 = \left(1 - \frac{K-1}{D\rho}\right)^{-2} \left[\left(\frac{1}{D\rho}\right)^2 \sum_{\substack{k=1 \\ k \neq i}}^K \sum_{\substack{n=1 \\ n \neq i, k}}^K \frac{E_n}{E_i} + \frac{N_o}{2} \left(1 + \frac{K-1}{D\rho}\right) \right] \quad (3.95)$$

3.5.3 Successive interference cancellation (SIC)

In this analysis, the transmission powers of all users are assumed to be the same. In this case, the received power is affected only by the channel gain α_i . Therefore, users are ranked according to the channel each experienced. The user with the strongest gain is assigned as user 1, the one with the next strongest gain is assigned as users 2, etc. so that, $\alpha_{r,1} > \alpha_{r,2} > \alpha_{r,3} > \dots > \alpha_{r,K}$. The term $\alpha_{r,i}$ is the ranked channel gain corresponding to user i . From (3.80), the matched filter output for user 1 is

$$R_1^{(SIC)} = \alpha_{r,1} \sqrt{E_1} B_1 + \sum_{k=2}^K \alpha_{r,k} \sqrt{E_k} B_k \gamma_{k1} + \eta \quad (3.96)$$

Then, following the similar procedure as Section 3.4.3, for user 2, one obtains

$$\begin{aligned} R_2^{SIC} = & \alpha_{r,2} \sqrt{E_2} B_2 \underbrace{(1 - \gamma_{21} \gamma_{12})}_{\text{Self cancellation term}} \\ & + \sum_{k=3}^K \alpha_{r,k} \sqrt{E_k} B_k \left(\underbrace{\gamma_{k2}}_{\text{Uncancelled MAI term}} - \underbrace{\gamma_{k1} \gamma_{12}}_{\text{Cancellation noise}} \right) + \underbrace{\eta (1 - \gamma_{12})}_{\text{AWGN term}} \end{aligned} \quad (3.97)$$

Hence, generalizing, for user i the conditional mean and variance of the SIC output are

$$\begin{aligned} E[R_i^{(SIC)}] &= \alpha_{r,i} \sqrt{E_i} \left(1 - \frac{i-1}{D\rho}\right) \\ \text{Var}[R_i^{(SIC)}] &= \left(\frac{1}{D\rho}\right) \left[\left(1 + \frac{1}{D\rho}\right)^{i-1} - \left(1 + \frac{i-1}{D\rho}\right) \right] \alpha_{r,i}^2 E_i \\ &+ \left(\frac{1}{D\rho}\right) \sum_{k=2}^{i-1} \left(1 + \frac{1}{D\rho}\right)^{i-k} \left[\left(1 + \frac{1}{D\rho}\right)^{k-1} - 1 \right] E[\alpha_{r,k}^2] E_k \\ &+ \left(\frac{1}{D\rho}\right) \left(1 + \frac{1}{D\rho}\right) \sum_{k=i+1}^K E[\alpha_{r,k}^2] E_k \\ &+ \left(1 + \frac{1}{D\rho}\right)^{i-1} \frac{N_p}{2} \end{aligned} \quad (3.98)$$

Now, one needs to determine the statistics of the ranked channel gains $\alpha_{r,i}$. For the Rayleigh fading channel where the same transmitting power is assumed for all users in the system, the ranking of the users for SIC is determined based on the channel gain α_i of the received signals. In this case, the channel gain α_i is Rayleigh distributed with its cdf (with $E[\alpha_i^2] = 1$) given by

$$F_{Rayleigh}(\alpha) = 1 - e^{-\alpha^2}, \quad \alpha \geq 0 \quad (3.99)$$

and its pdf is

$$P_{Rayleigh}(\alpha) = 2\alpha e^{-\alpha^2}, \quad \alpha \geq 0 \quad (3.100)$$

After the gains of users are ranked, that is, $\alpha_{r,1} > \alpha_{r,2} > \alpha_{r,3} > \dots > \alpha_{r,K}$, it follows that the pdf of the ranked channel gain [116], $\alpha_{r,i}$, is

$$f(\alpha_{r,i}) = \frac{K!}{(i-1)!(K-i)!} F_{Rayleigh}(\alpha_{r,i})^{(K-i)} \times [1 - F_{Rayleigh}(\alpha_{r,i})]^{(i-1)} P_{Rayleigh}(\alpha_{r,i}) \quad (3.101)$$

Hence, for equal power users, and using (3.34), the bit error probability for user i is given by

$$P_e(i) = \int_{-\infty}^{\infty} Q\left(\frac{E[R_i^{(SIC)}]}{\sqrt{\text{Var}[R_i^{(SIC)}]}}\right) f(\alpha_{r,i}) d\alpha_{r,i} \quad (3.102)$$

Therefore, the average probability for the whole SIC stage would be

$$P_e^{(SIC)} = \frac{1}{K} \sum_{i=1}^K P_e(i) \quad (3.103)$$

3.5.4 Variable group hybrid interference cancellation (VGHIC)

In the Rayleigh fading channel, the term $\sqrt{E_i}$ is replaced by $\alpha_{r,i} \sqrt{E_i}$ in (3.53) to (3.60). The ranked channel gain $\alpha_{r,i}$ has been defined in Section 3.5.3. Following the similar approach as in Section 3.4.4, the mean and variance of $R_{i,j}^{(k)}$ conditioned on B_i can be found. Using the same notations and definitions

$$\begin{aligned} \mathbb{E}[R_{i,j}^{(k)} | B_i] &= \mu_i^{(k)} \\ \text{Var}[R_{i,j}^{(k)} | B_i] &= \text{Var}_i^{(k)} \end{aligned} \quad (3.104)$$

where k is a function of j and the type of receiver, and it is defined in (3.57). When $k = [(j-1) \times 2]$, it is the output of the matched filter, $R_{i,j}^{(MF)}$. If $k = (2j-1)$, then it is the output of the PIC, $R_{i,j}^{(PIC)}$. After simplifications and generalizations, one obtains the mean as

$$\mu_i^{(k)} = \begin{cases} \alpha_{r,i} \left(1 - \frac{\beta^{\left(\frac{k+1}{2}\right)^{-1}}}{D\rho} \right) & k \text{ odd} \\ \alpha_{r,i} \left(1 - \frac{\beta^{\left(\frac{k}{2}\right)}}{D\rho} \right) & k \text{ even} \end{cases} \quad (3.105)$$

where $\alpha_{r,i}$ is the ranked channel gain corresponding to user i with definitions and properties defined previously. The term r_j is the rank of the last user to be selected into group j defined in Section 3.4.4, and r_j will be determined in the following subsection. The variance is

$$\text{Var}_i^{(k)} = \left\{ \begin{aligned} & \frac{1}{D\rho} \sum_{\substack{n=g(\frac{k+1}{2})+1 \\ n \neq i}}^K E[\alpha_{r,n}^2] \\ & + \frac{1}{D\rho} \sum_{\substack{n=g(\frac{k+1}{2})+1 \\ n \neq i}}^{g(\frac{k+1}{2})} \left(V_n^{(k-1)} - \frac{E[\alpha_{r,i}^2]}{D\rho} \right) \\ & + \frac{1}{D\rho} \sum_{j=1}^{\frac{k-1}{2}} \sum_{n=g_{(j-1)}+1}^{g_{(j)}} \left(V_n^{(2j-1)} - \frac{E[\alpha_{r,i}^2]}{D\rho} \right) \\ & + \frac{1}{2} \left(\frac{E_b}{N_o} \right)^{-1} \quad ; \quad k \text{ odd} \\ \\ & \frac{1}{D\rho} \sum_{\substack{n=g(\frac{k}{2})+1 \\ n \neq i}}^K E[\alpha_{r,n}^2] \\ & + \frac{1}{D\rho} \sum_{n=g(\frac{k}{2})+1}^{g(\frac{k}{2})} \left(V_n^{(k-1)} - \frac{E[\alpha_{r,i}^2]}{D\rho} \right) \\ & + \frac{1}{D\rho} \sum_{j=1}^{\frac{k}{2}-1} \sum_{n=g_{(j-1)}+1}^{g_{(j)}} \left(V_n^{(2j-1)} - \frac{E[\alpha_{r,i}^2]}{D\rho} \right) \\ & + \frac{1}{2} \left(\frac{E_b}{N_o} \right)^{-1} \quad ; \quad k \text{ even} \end{aligned} \right. \quad (3.106)$$

where

$$V_i^{(k)} = \begin{cases} \frac{1}{D\rho} \sum_{n=g(\frac{k+1}{2})+1}^K E[\alpha_{r,n}^2] + \frac{1}{D\rho} \sum_{\substack{n=g(\frac{k-1}{2})+1 \\ n \neq i}}^{g(\frac{k+1}{2})} V_n^{(k-1)} \\ \quad + \frac{1}{D\rho} \sum_{j=1}^{\frac{k-1}{2}} \sum_{n=g_{(j-1)}+1}^{g_{(j)}} V_n^{(2j-1)} + \frac{1}{2} \left(\frac{E_b}{N_o} \right)^{-1} ; \quad k \text{ odd} \\ \\ \frac{1}{D\rho} \sum_{\substack{n=g(\frac{k}{2})+1 \\ n \neq i}}^K E[\alpha_{r,n}^2] \\ \quad + \frac{1}{D\rho} \sum_{j=1}^{\frac{k}{2}} \sum_{n=g_{(j-1)}+1}^{g_{(j)}} V_n^{(2j-1)} + \frac{1}{2} \left(\frac{E_b}{N_o} \right)^{-1} ; \quad k \text{ even} \end{cases} \quad (3.107)$$

and the initial conditions are given by

$$Var_i^{(0)} = \frac{1}{D\rho} \sum_{\substack{n=1 \\ n \neq i}}^K E[\alpha_{r,n}^2] + \frac{1}{2} \left(\frac{E_b}{N_o} \right)^{-1} \quad (3.108)$$

$$Var_i^{(1)} = \frac{1}{D\rho} \sum_{n=g_1+1}^K E[\alpha_{r,n}^2] + \frac{1}{D\rho} \sum_{\substack{n=1 \\ n \neq i}}^{g_1} \left(V_n^{(0)} - \frac{E[\alpha_{r,n}^2]}{D\rho} \right) + \frac{1}{2} \left(\frac{E_b}{N_o} \right)^{-1} \quad (3.109)$$

$$Var_i^{(2)} = \frac{1}{D\rho} \sum_{\substack{n=g_1+1 \\ n \neq i}}^K E[\alpha_{r,n}^2] + \frac{1}{D\rho} \sum_{n=1}^{g_1} \left(V_n^{(1)} - \frac{E[\alpha_{r,n}^2]}{D\rho} \right) + \frac{1}{2} \left(\frac{E_b}{N_o} \right)^{-1} \quad (3.110)$$

$$V_i^{(0)} = \frac{1}{D\rho} \sum_{\substack{n=1 \\ n \neq i}}^K E[\alpha_{r,n}^2] + \frac{1}{2} \left(\frac{E_b}{N_o} \right)^{-1} \quad (3.111)$$

$$V_i^{(1)} = \frac{1}{D\rho} \sum_{n=g_1+1}^K E[\alpha_{r,n}^2] + \frac{1}{D\rho} \sum_{\substack{n=1 \\ n \neq i}}^{g_1} V_n^{(0)} + \frac{1}{2} \left(\frac{E_b}{N_o} \right)^{-1} \quad (3.112)$$

and $E[\alpha_{r,n}^2]$ is given by

$$E[\alpha_{r,n}^2] = \int_{-\infty}^{\infty} \alpha_{r,n}^2 f(\alpha_{r,n}) d\alpha_{r,n} \quad (3.113)$$

Hence, using (3.34), the average BER of the VGHC, at the outputs of the PIC blocks for all the subtractive steps, in the Rayleigh fading channel, is given by

$$P_e^{(VGHC)} = \frac{1}{K} \sum_{j=1}^N \sum_{i=g_{(j-1)}+1}^{g_j} \int_{-\infty}^{\infty} Q \left(\frac{\mu_i^{(2j-1)}}{\sqrt{\text{Var}_i^{(2j-1)}}} \right) f(\alpha_{r,i}) d\alpha_{r,i} \quad (3.114)$$

where $r_0 = 0$, and $f(\alpha_{r,i})$ is defined in (3.101).

Determination of user groups

Similar to the AWGN case, to evaluate (3.114) one needs to find the user grouping information in the Rayleigh fading channel. The grouping of users is based on the ranked channel gain $\alpha_{r,i}$ as in the case for the analysis of SIC. The pdf of $\alpha_{r,i}$ is given by $f(\alpha_{r,i})$ in (3.101). The average channel gain corresponding to the rank i is

$$\mu_{r,i} = \int_{-\infty}^{\infty} \alpha_{r,i} f(\alpha_{r,i}) d\alpha_{r,i} \quad (3.115)$$

Since $\mu_{r,i} \geq \mu_{r,(i+1)}$ is always true and $i = 1, 2, \dots, K$, then the reference in the selection rule (3.10) for group 1 is $\mu_{r,1}$. Members of group 1 are then selected into group 1 if

$$\mu_{r,i} \geq \delta \mu_{r,1} \quad , \quad i = 2, \dots, K \quad (3.116)$$

Users are being continuously selected into the group until the following conditions are reached:

$$\begin{aligned}\mu_{r,i_1} &\geq \delta \mu_{r,1} \\ \mu_{r,i_1+1} &< \delta \mu_{r,1}\end{aligned}\tag{3.117}$$

where the index i_1 refers to the last member to be selected into group 1. The next bigger term, μ_{r,i_1+1} is set as the reference for the selection of group 2. Incidentally, i_1 is also the number of users in group 1. In general, the number of users in group j , G_j , can be determined by

$$G_j = i_j - i_{j-1}\tag{3.118}$$

When the last group of users has been determined, one can then evaluate the average BER of the VGHIC using (3.114).

3.6 Performance comparison

In this section, the analytical BER performances of the matched filter, PIC, SIC and simplified VGHIC receivers are compared and studied for AWGN and Rayleigh fading channel.

3.6.1 Additive white Gaussian noise (AWGN) channel

For this AWGN channel, it is assumed that the received signal energies or powers of users are equal and they are only corrupted by the channel noise. For the comparison, the system assumed is the asynchronous system with $D = 3$. The processing gain is set at 32.

The BER performance versus the SNR of the receivers are plotted in Figure 3.9. The conventional matched filter (MF) receiver has the worst performance. It is followed by the SIC, then the VGHIC($\delta = 0.8$), VGHIC($\delta = 0.5$) and VGHIC($\delta = 0.2$). The PIC has the best performance and it is about 3dB better than the SIC at the BER of 1×10^{-2} . However, at a low signal-to-noise ratio ($\text{SNR} = E_b/N_o$) of less than 5dB, all the interference cancellation receivers ceased to be effective. They have worse performances than the conventional MF.

The performance of the VGHIC is in between that of the PIC and SIC. When δ is closer to zero, its performance approaches that of the PIC. If δ is closer to one, its performance is similar to that of the SIC.

The BER performance of these receivers is plotted against the number of simultaneous transmitting users in the system and shown in Figure 3.10. The same observations are being noticed. At a BER of 1×10^{-2} , the PIC has a capacity of 23 users whereas that for the SIC is 17 users. The VGHIC with $\delta = 0.2, 0.5$ and 0.8 has a capacity of 22, 20 and 19, respectively. This worked out to be having 30%, 18% and 12%, respectively, more capacity than the SIC. When the number of users increases beyond 30, the PIC superior performance deteriorates and becomes worse than the VGHIC and SIC. From these observations, one can deduce that when the level of interference and/or noise is high in the system, the effectiveness of the PIC is greatly reduced rapidly and becomes worse than the conventional MF. For the VGHIC and SIC, they are still able to maintain their performance advantage over that of the MF.

Here, the BER of the VGHIC is derived for the extreme values of the design parameter, δ ($0 \leq \delta \leq 1$) so that one can see why the VGHIC performs as observed. For the VGHIC, when δ approaches zero, the VGHIC performance approaches that of the PIC. This is due to the structure of the VGHIC. From (3.68) when $\delta = 0$, all users are selected into the first group, that is,

$$G_1 = K \quad (3.119)$$

or the total number of groups, $N = 1$, where K is the total number of users in the system. Substituting G_1 and N into (3.61)

$$P_e^{(VGHIC)}(\delta = 0) = \frac{1}{K} G_1 Q \left(\frac{\mu^{(1)}}{\sqrt{V_{(0,-1)}^{(1)}}} \right) \quad (3.120)$$

Then, after using the initial conditions (3.60) and (3.119),

$$\begin{aligned}
P_e^{(VGHIC)}(\delta = 0) &= Q \left(\frac{1 - \frac{1}{D\rho}(K-1)}{\sqrt{\frac{1}{D\rho}(K-K+0) + \frac{1}{D\rho}(K-1)V_{(-1,0)}^{(0)} + \frac{1}{2(\frac{E_e}{N_e})}}} \right) \\
&= Q \left(\frac{1 - \frac{1}{D\rho}(K-1)}{\sqrt{\frac{1}{D\rho}(K-K+0) + \frac{1}{D\rho}(K-1) \left\{ \frac{1}{D\rho}[K-1+(-1)] + \frac{1}{2(\frac{E_e}{N_e})} \right\} + \frac{1}{2(\frac{E_e}{N_e})}}} \right) \quad (3.121) \\
&= Q \left(\frac{1 - \frac{1}{D\rho}(K-1)}{\sqrt{\left(\frac{1}{D\rho}\right)^2 (K-1)(K-2) + \left(1 + \frac{1}{D\rho}(K-1)\right) \frac{1}{2(\frac{E_e}{N_e})}}} \right) \\
&= P_e^{(PIC)}
\end{aligned}$$

When the value of $\delta = 1$, the structure of the VGHIC becomes that of the SIC. From the selection rule (3.68), it is obvious that there will be one member per group and a total number of K groups (that is, $G_j = 1, j = 1, 2, \dots, K$). Putting this information into (3.61), using the initial conditions (3.60) and changing the index j , one obtains

$$P_e^{(VGHIC)}(\delta = 1) = \frac{1}{K} \sum_{i=1}^K Q \left(\frac{\mu^{(i)}}{\sqrt{V_{(0,-1)}^{(i)}}} \right) \quad (3.122)$$

where

$$\begin{aligned}
\mu^{(2j-1)} &= 1 - \frac{1}{D\rho}(j-1) \\
\Rightarrow \mu^{(j)} &= 1 - \frac{1}{D\rho}(j-1)
\end{aligned} \quad (3.123)$$

and

$$V_{(x,y)}^{(2j-1)} = \frac{1}{D\rho}(K-j+x) + \frac{1}{D\rho} \sum_{i=1}^{j-1} V_{(y,0)}^{(2i-1)} + \frac{1}{2^{(E_b/N_o)}} \quad (3.124)$$

$$\Rightarrow V_{(x,y)}^{(j)} = \frac{1}{D\rho}(K-j+x) + \frac{1}{D\rho} \sum_{i=1}^{j-1} V_{(y,0)}^{(i)} + \frac{1}{2^{(E_b/N_o)}}$$

The initial condition is

$$V_{(x,y)}^{(1)} = \frac{1}{D\rho}(K-1+x) + \frac{1}{2^{(E_b/N_o)}} \quad (3.125)$$

The above expressions are actually the recursive version for calculating the BER of the SIC and they are equivalent to the iterative version from (3.47) to (3.50).

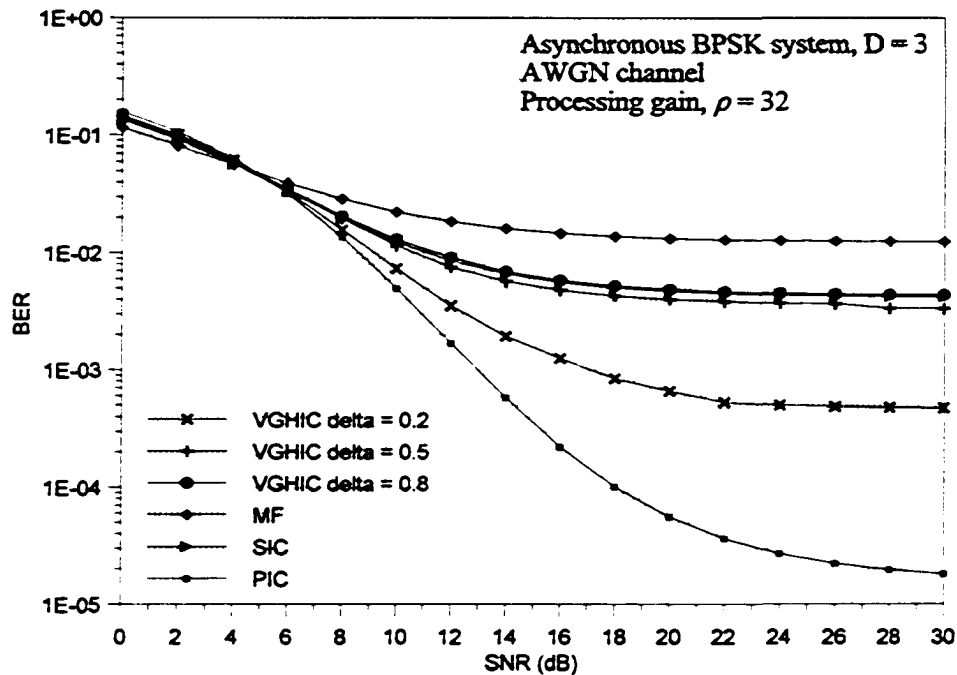


Figure 3.9: The comparison of the analytical BER performance versus the SNR in AWGN channel.

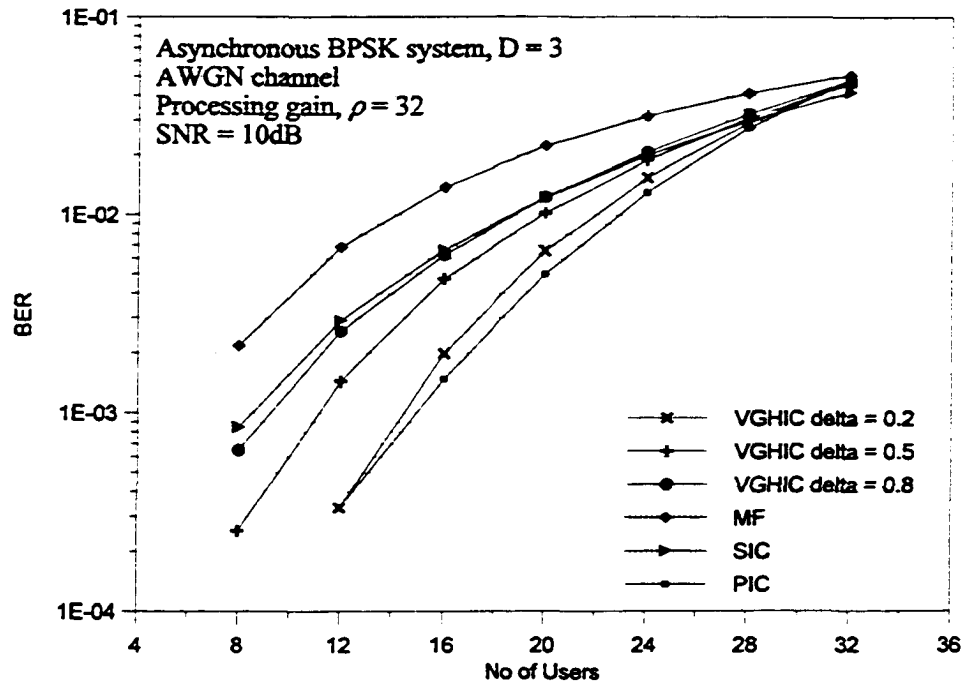


Figure 3.10: The comparison of the analytical BER performance versus the number of users in AWGN channel.

3.6.2 Rayleigh fading

For the Rayleigh fading channel it is assumed that the transmitted power of all the users are the same and the received signal powers are only affected by the corresponding channel gain of each user. The system parameters are the same as that for the AWGN case. An asynchronous system is assumed with $D = 3$, and the processing gain is 32 for all users.

Figure 3.11 shows the BER performance versus the SNR of the MF, PIC, SIC and VGHIC. In the fading channel, the situation is the reverse of that in the AWGN with the exception of the conventional MF. The MF is consistently the worst performing receiver compared with the interference cancellation receivers. From Figure 3.11, SIC and VGHIC outperforms the PIC. At the higher SNR of more than 15dB, the VGHIC ($\delta = 0.5$ and 0.8) actually outperforms the SIC by as much as 5dB and 3dB, respectively, for the BER of 1×10^{-2} . However, when the SNR is low, the SIC has an edge of about 1dB over the VGHIC.

Comparing the VGHC with different values of δ , one notices that the optimal value of δ is 0.5 in this case.

In Figure 3.12, the BER performance versus the number of simultaneous transmitting users is plotted for the receivers under investigation. The VGHC($\delta=0.5$) with 23 users is the best performing receiver with 64% and 9% more user capacity than the PIC (14 users) and SIC (21 users), respectively, at a BER of 1×10^{-2} . Here, the SIC has 50% more capacity than the PIC. Looking at the VGHC with different δ , one can arrive at the same observations as before.

With higher δ , the VGHC has more SIC component and therefore its performance approaches that of the SIC. On the other hand, with lower δ , the VGHC has more PIC component and hence its performance approaches that of the PIC. However, there is an optimal value for δ in different environment.

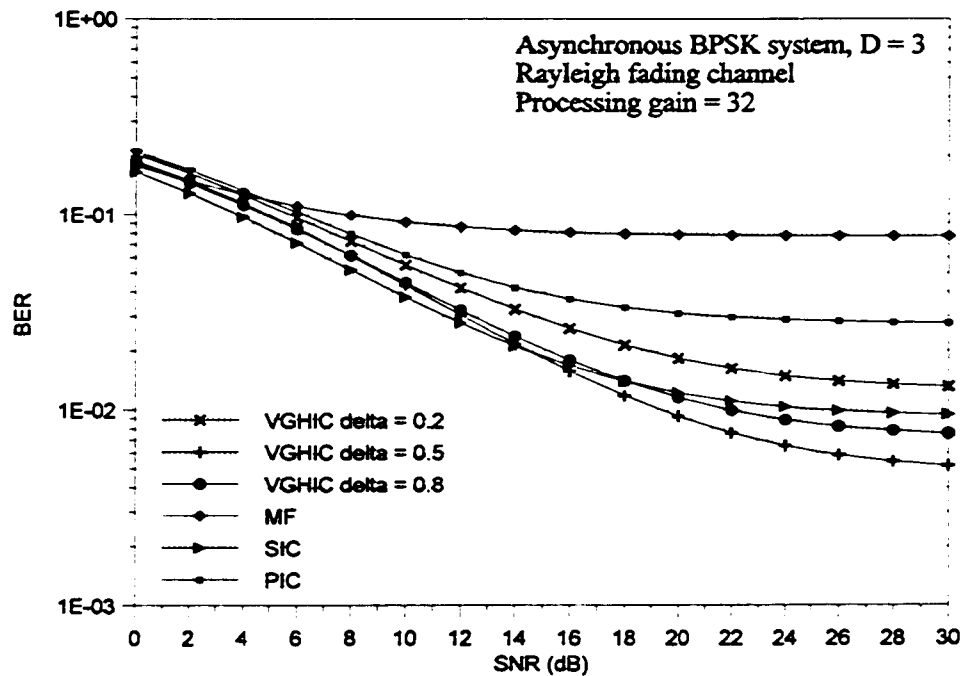


Figure 3.11: The comparison of the analytical BER performance versus the SNR in Rayleigh fading channel.

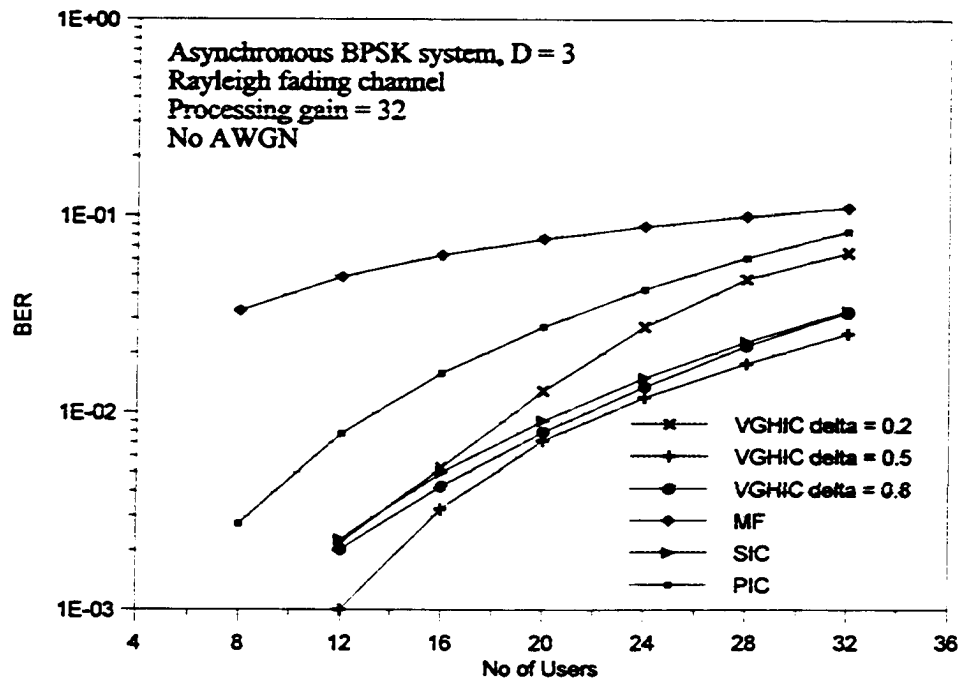


Figure 3.12: The comparison of the analytical BER performance versus the number of users in the Rayleigh fading channel.

3.7 Summary

In this chapter, the variable group hybrid interference cancellation (VGHIC) scheme has been proposed. In VGHIC, the users are grouped according to their received signal power so that those with similar received power are selected into the same group. Within each group of similar user power, parallel interference cancellation (PIC) is done. Then, successive interference cancellation (SIC) is done between the groups which have different received power. The purpose of grouping and applying different interference techniques is to create suitable conditions where appropriate techniques can be optimally applied. The PIC is effective when the received powers of users are similar. On the other hand, SIC is more effective when the received signal powers are not the same.

The bit error rate (BER) performance of the conventional matched filter (MF), PIC, SIC and simplified VGHIC receivers in both the additive white Gaussian noise (AWGN) and Rayleigh fading channel has been analyzed and compared using theoretical approaches. This

leads to the development of alternative expressions for the PIC and SIC which take into account the effect of self cancellation as a result of using the correlation sample in the signal regeneration process. In addition, the development of the original expressions for the BER performance of VGHIC in AWGN and Rayleigh fading has been achieved. It is a general expression from which one can derive the BER for the PIC and SIC by just using the appropriate parameter value. With the expressions derived, comparisons are made between the different receiver schemes in the AWGN and Rayleigh fading channel.

For the theoretical comparisons done for the AWGN channel, the VGHIC is able to achieve performance close to that of the PIC. The PIC is the best performing receiver in AWGN channel. The MF has the worst performance and it is followed by the SIC. At low SNR, the PIC becomes ineffective and performance deteriorates more rapidly than the MF.

In the Rayleigh fading channel, the situation changed with the exception of the MF, which remains as the receiver with the worst performance. The PIC only outperforms the MF and it is not as effective as the SIC in fading conditions. The SIC has a much better performance than the PIC in fading. The SIC has 50% more user capacity than the PIC. Here, the VGHIC is able to achieve the same if not better performance than the SIC. It is able to outperform SIC by a noticeable margin.

In the following chapters, the BER performance of these schemes will be simulated and compared against each other. The theoretical results and observations obtained in this chapter will then be verified by the simulation results.

Chapter 4: Improvements to the basic VGHIC structure

In this chapter, several techniques of improving the VGHIC are proposed. The processing delay of the VGHIC is looked into and a method for reducing its processing delay is proposed. The effects of these techniques on the BER performance are studied and investigated on the VGHIC along with the PIC and SIC if these techniques are applicable to them.

Section 4.1 discusses the impact of the user ordering methods on the VGHIC and SIC in the AWGN and Rayleigh fading channel. The effect of using the averaged correlation samples in the signal regeneration and cancellation component of the various receivers are studied in Section 4.2. After this, the multi-stage structure for the VGHIC is proposed in Section 4.3. This is followed by Section 4.4 which presents the idea of partial correlation combining and partial cancellation and investigates their effects on the BER performance of the VGHIC. In Section 4.5, the processing delay of the VGHIC is investigated and this leads to the proposal of a method for limiting the processing delay. Section 4.6 summarizes this chapter. The parameters and details of the simulation system can be found in Appendix D.

4.1 Methods of ordering users

Recall that in the analysis of the VGHIC in the previous chapter, it is assumed that the users are grouped after the initial detection by the matched filters (MF). This is so that the analysis is tractable and the concept can be presented clearly. However, in the original proposal, the grouping is done before the start of each cancellation step. The ordering methods considered here have been highlighted separately in [70][118][119]. However, no direct comparison has been done to investigate the relative merits of each method. This section attempts to find out how the ordering methods affect the BER performance of the successive interference cancellation portion of the VGHIC and also its effect on the SIC.

All the descriptions and discussions of the ordering methods will be done in the context of the VGHIC. However, it is also applicable to the SIC. The difference is that the SIC has only one member in each group whereas the VGHIC can have more than one member in each group.

Let the method that orders or ranks all the groups at the beginning of the cancellation be referred to as Method 1. Method 2 selects the remaining users with relatively higher powers just before each cancellation step³. This selection is based on (3.10). These two methods are shown in Figure 4.1.

For ordering Method 1, after the initial matched filter detections, the users are selected into groups of different power levels. These groups are then ordered accordingly to their average power. At every cancellation step, one group of users is detected and their regenerated signals subtracted from the composite signal. The groupings are fixed and cannot be changed during the whole cancellation process. There may be an inherent issue with this ordering method. As the grouping is done based on the correlation samples from the initial bank of matched filters, where the signals are the noisiest, and this will affect the grouping accuracy due to the high level of multi-access interference (MAI). Using the SIC as an example, the variance of the interference and noise faced by all the users before grouping is

$$\text{Var}\left[R_1^{(SIC)}\right] = \frac{1}{D\rho} \sum_{k=2}^K E_k + \frac{N_p}{2} \quad (4.1)$$

In the second method, the ordering is done before every cancellation step. With the MAI of the users in the previous cancellation steps removed, the resulting signal used for selecting the users will be cleaner and hence, there will be fewer ordering errors. Using the same

³ Note that the cancellation stage is defined such that at the end of the stage, all the users have been detected. At the end of the cancellation step, only the relevant users are been detected. For example, in the SIC, K cancellation steps form a cancellation stage if there are a total of K users to be detected in the whole system.

example, before the second cancellation step for ordering Method 2, the variance of the matched filter output is

$$\text{Var}[R_2^{(SIC)}] = \left(\frac{1}{D\rho}\right)\left(1 + \frac{1}{D\rho}\right)\sum_{k=3}^K E_k + \left(1 + \frac{1}{D\rho}\right)\frac{N_p}{2} \quad (4.2)$$

if the cancellation is done correctly, and this is smaller than (4.1). After each correct cancellation, the variance of the MAI and noise becomes smaller. However, if there are erroneous cancellations in the previous cancellation steps, the MAI will be increased as a result. The complexity of this method may be a concern as a bank of matched filter receivers must be used for the remaining users before every cancellation step.

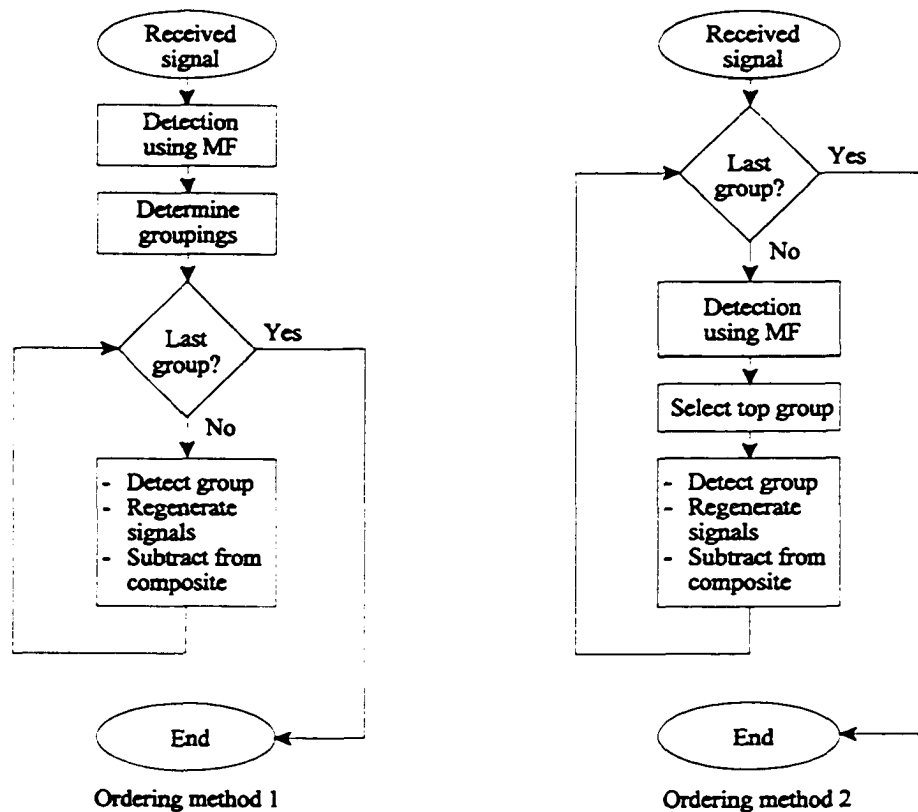


Figure 4.1: Ordering methods for the VGIC or SIC.

In the next two sections, the effect of the ordering methods will be investigated in the AWGN and Rayleigh fading channel for the VGHIC and SIC.

4.1.1 Effect in AWGN channel

The simulation is based on an asynchronous BPSK CDMA system with processing gain of 63. The time delay and phases of users are uniformly distributed on $[0, T)$ and $[0, 2\pi)$ respectively, where T is the period of the information bit.

Refer to Figure 4.2 for the comparison of ordering methods for the VGHIC($\delta = 0.8$) in the AWGN channel. In general, the use of Method 2 improves the BER performance of the VGHIC($\delta = 0.8$). However, the improvement when the number of users is 30 is not as significant. It is around 1-2dB gain. The VGHIC($\delta = 0.8$) benefits more from Method 2 when there are more users in the system. For a 30-user system with the BER of 1×10^{-2} , the gain is 3 dB. When the SNR is low (< 4 dB), there is no improvement most of the time as the interference and noise are so severe that the interference cancellation is ineffective. Thus, no benefit can be derived from Method 2.

The BER performance for VGHIC($\delta = 0.4$) with different ordering is shown in Figure 4.3. No differences can be observed in performance between the two methods. This is due to the fact that with $\delta = 0.4$, the majority of the operations are PIC instead of the SIC. Hence, the ordering method may not have a significant impact on the performance. This is coupled with the worse cancellation effectiveness when the interference level is high, that is, the number of users is large. The PIC is known to be ineffective when the level of interference is high.

As for the SIC, the different ordering methods do have an impact on the performance. The results are shown in Figure 4.4. It is similar to what has been observed for VGHIC($\delta = 0.8$).

4.1.2 Effect in fading channel

The performance of the two ordering methods in VGHC($\delta=0.8$), VGHC($\delta=0.4$) and SIC for the Rayleigh fading channel are shown in Figure 4.5, Figure 4.6 and Figure 4.7, respectively. The observations are the same as that in the AWGN channel except for the VGHC($\delta=0.4$). In the Rayleigh fading channel, Method 2 is able to provide a performance advantage over the Method 1. Due to the nature of the channel the power spread of users is larger, and this in turn would mean that there will be more SIC operations done in VGHC($\delta=0.4$). The VGHC structure can basically adapt to the power spread of the users in the system where the design parameter δ determines the degree of adaptation. In other words, δ affects the number of PIC or SIC operations to be performed given the power spread of the users. A higher δ means more SIC and lower δ means more PIC in a given situation. For this channel, the Method 2 is consistently able to provide better performance than the Method 1 for the VGHC and SIC. The VGHC with the appropriate design parameter would benefit much more than the SIC from the use of Method 2. However, this better performance requires higher receiver complexity.

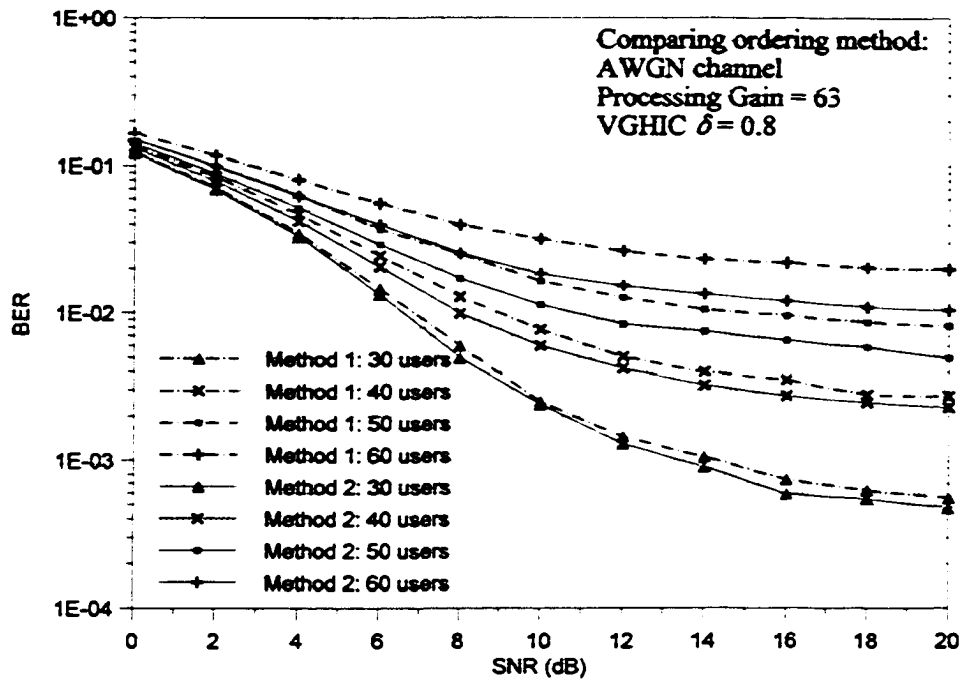


Figure 4.2: Comparison of the BER performance for the VGHIC($\delta = 0.8$) in AWGN channel between the ordering methods.

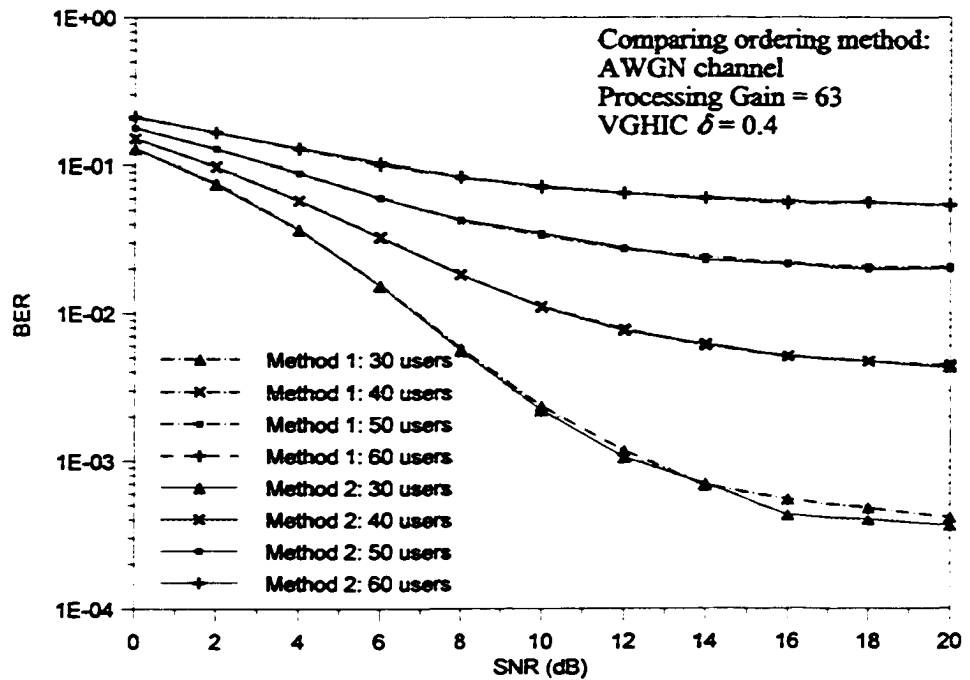


Figure 4.3: Comparison of the BER performance for the VGHIC($\delta = 0.4$) in the AWGN channel between the ordering methods.

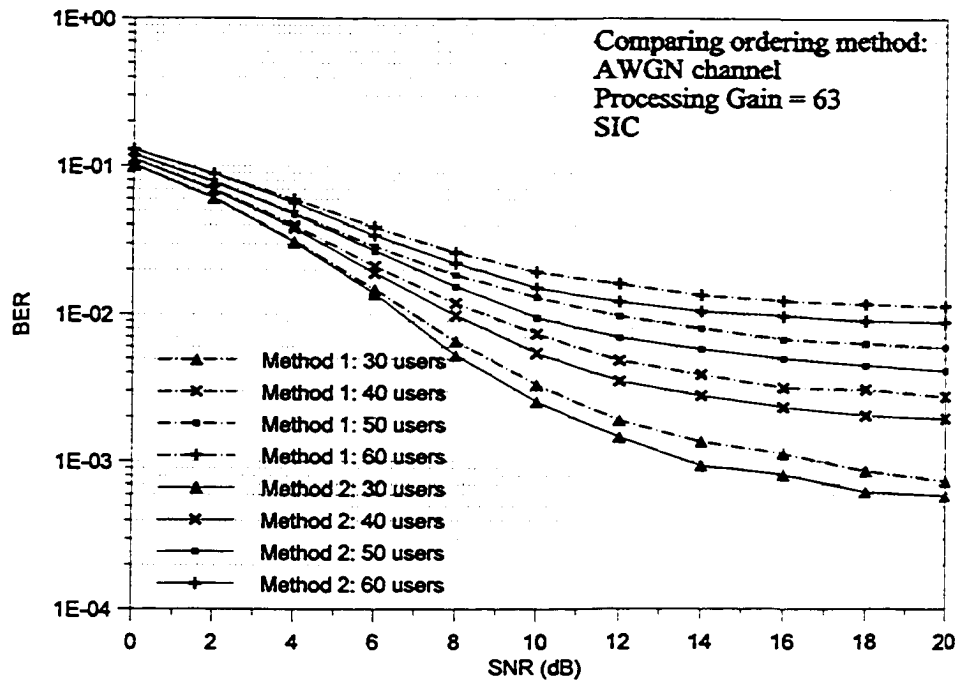


Figure 4.4: Comparison of the BER performance for the SIC in the AWGN channel between the ordering methods

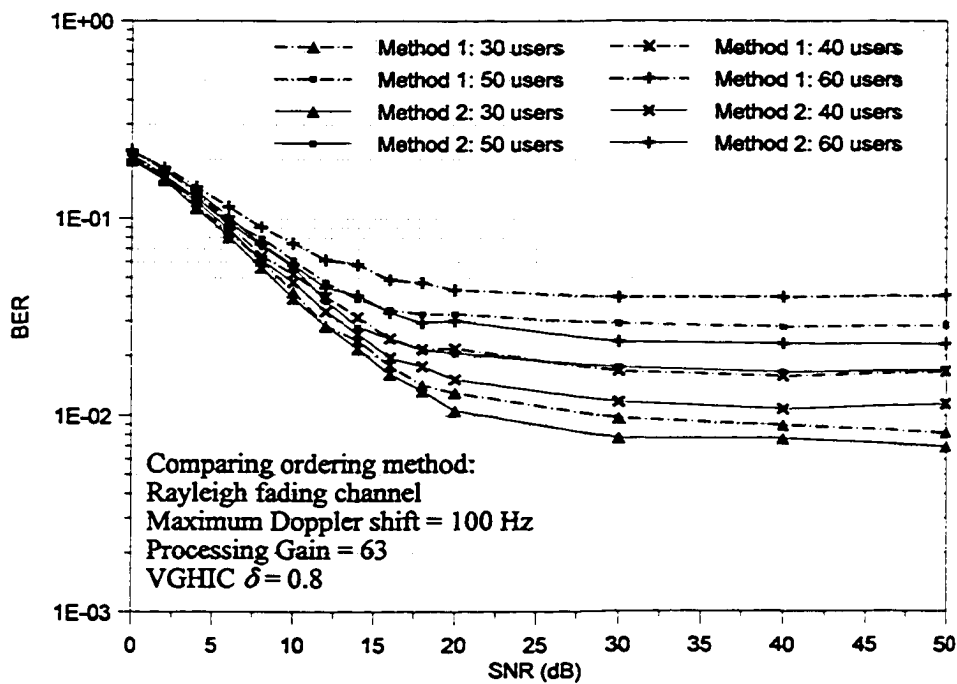


Figure 4.5: Comparison of the BER performance for the VGHIC($\delta = 0.8$) in the Rayleigh fading channel between the ordering methods.

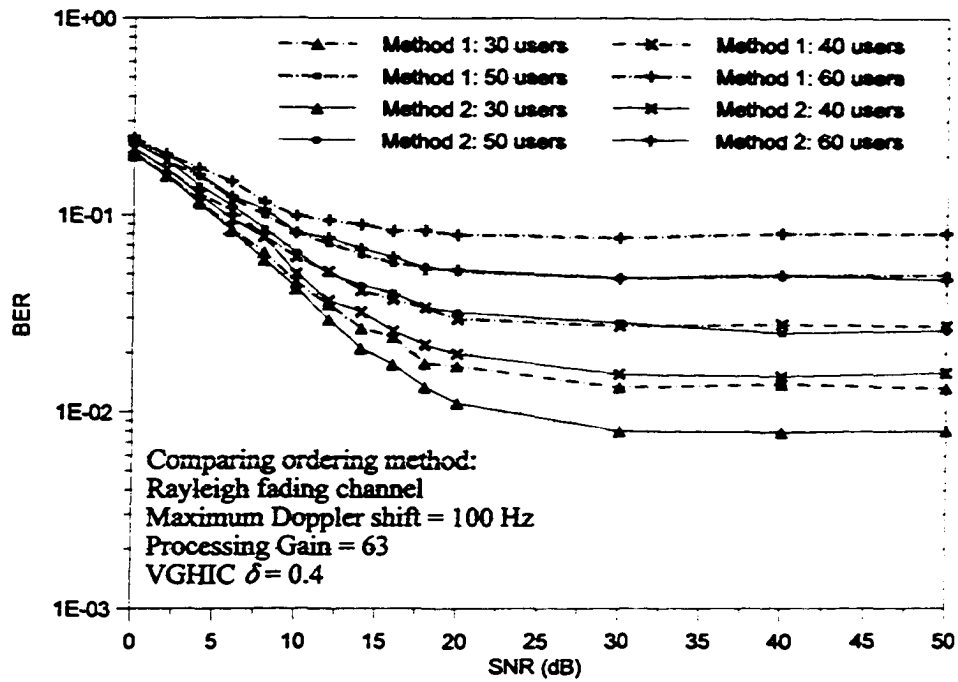


Figure 4.6: Comparison of the BER performance for the VGHIC($\delta = 0.4$) in the Rayleigh fading channel between the ordering methods.

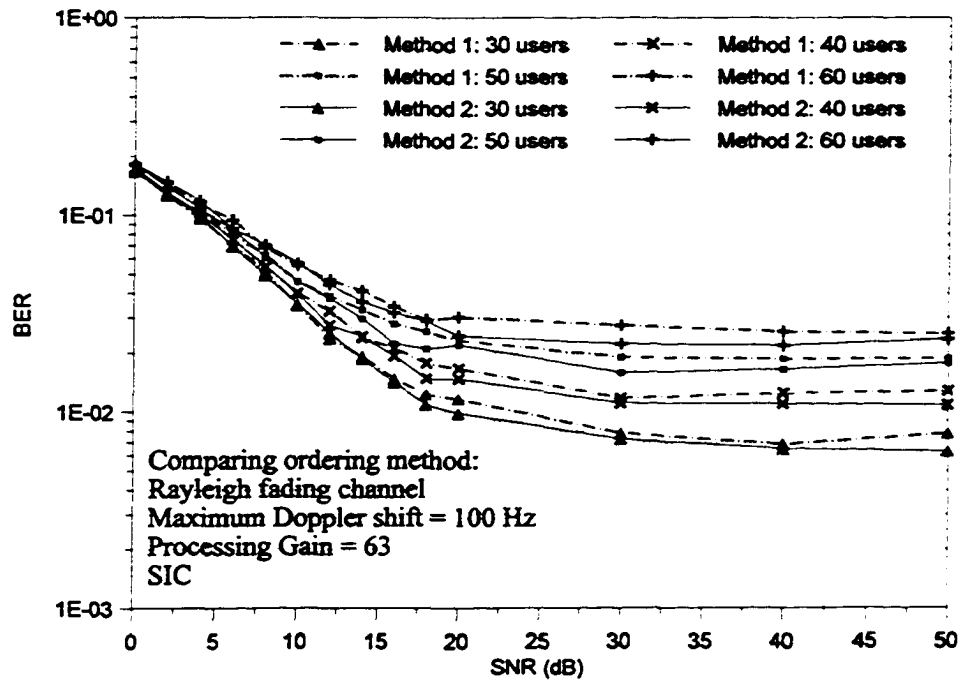


Figure 4.7: Comparison of the BER performance for the SIC in the Rayleigh fading channel between the ordering methods.

4.2 Averaging correlation samples

Recall that in the previous analysis, the correlation samples at the output of the matched filter (MF) are used as estimates of the signal amplitudes in the signal regeneration and cancellation processes. They are corrupted by the multi-access interference (MAI) and noise. This can be seen from (3.16)

$$R_i^{(MF)}(m) = A_i(m) + \sum_{k=1, k \neq i}^K A_k(m) \gamma_{ki}(m) + \eta \quad (4.3)$$

where $A_i(m)$ and $\gamma_{ki}(m)$ are defined in (3.17) and (3.19). The term $R_i^{(MF)}(m)$ is the correlation sample at the output of the matched filter for bit m of user i . Therefore, in order to increase the accuracy of the amplitude estimates, one can average (4.3) over N_{ave} information bits. This will effectively reduce the MAI and noise power by a factor of N_{ave} as follows (conditioning on user i):

$$\begin{aligned} \text{Var} \left[\frac{1}{N_{ave}} \sum_{m=1}^{N_{ave}} R_i^{(MF)}(m) \right] &= \frac{1}{N_{ave}^2} \sum_{m=1}^{N_{ave}} \text{Var} \left[\left\{ A_i(m) + \underbrace{\sum_{k=1, k \neq i}^K A_k(m) \gamma_{ki}(m)}_{\text{MAI term}} + \underbrace{\eta}_{\text{noise term}} \right\} \right] \quad (4.4) \\ &= \frac{1}{N_{ave}^2} \sum_{m=1}^{N_{ave}} [\sigma^2(\zeta) + \sigma^2(\eta)] \\ &= \frac{1}{N_{ave}} [\sigma^2(\zeta) + \sigma^2(\eta)] \end{aligned}$$

where

$$\sigma^2(\zeta) = \text{Var} \left[\sum_{k=1, k \neq i}^K A_k(m) \gamma_{ki}(m) \right] \quad (4.5)$$

$$\sigma^2(\eta) = \text{Var}[\eta]$$

$$\text{Var}[x] = \text{E}[x^2] - \text{E}[x]^2$$

Here, the MAI and noise term are assumed to be Gaussian and independent of each other.

Using the averaging may help one to improve the accuracy of the estimates, but it cannot be done without limits. This is because in practice, the transmission channel is time-varying in nature. If excessive averaging is done, the accuracy will decrease. Hence, one needs to find a good compromise where the averaging helps to improve the performance of the receivers.

In this section, the effect of averaging length on the various receivers will be investigated in the AWGN and Rayleigh fading channel. The AWGN channel represents the ideal case when the time-varying nature of the wireless transmission can be controlled perfectly (for example, perfect power control). The Rayleigh fading channel is used to simulate the time varying nature of the channel.

4.2.1 Effect in AWGN channel

In the AWGN channel, the results are obtained for the various receivers with signal-to-noise ratios (SNR) of 5, 10 and 15 dB, and in a system with 30 and 60 users. The effects of the averaging length for the PIC, SIC, VGHIC($\delta = 0.4$) and VGHIC($\delta = 0.8$) are presented in Figure 4.8, Figure 4.9, Figure 4.10 and Figure 4.11, respectively.

For the PIC, increasing the averaging length beyond 30 bits does not improve the performance. At low SNR of 5 dB, averaging is still effective, but the degree of improvement is not as significant.

Looking at the results for SIC, averaging actually decreases its performance in the AWGN channel. This can be explained by how the SIC works. The SIC works best when the received signal powers of users are unequal [115]. If one considers the information bits of the user individually, different bits of the same user will experience a different amount of MAI. The MAI will either enhance or reduce the power of that particular bit. With the power of individual bits differentiated, the SIC will be much more effective. When averaging is used, the power differentiation between users is reduced and the effectiveness of the SIC will be reduced. This interesting observation on the SIC leads to the proposal of the partial

combining of correlation samples (PCC) which will be discussed in one of the following sections.

For the VGHIC, averaging does improve the performance in general. This is due to the hybrid nature of the VGHIC. With averaging, the power differentiation between users is reduced. This would only mean that there will be more PIC operations within the VGHIC. The VGHIC($\delta = 0.4$) has very similar behaviour as that of the PIC.

The VGHIC($\delta = 0.8$) needs longer averaging length for its performance to improve. This is because its structure has more SIC operations. As δ approaches the value of one, the VGHIC will have more and more SIC operations until it eventually reduces to SIC. With long averaging length, the variance will be reduced significantly. Eventually there will be less SIC operations as larger number of users will be grouped together (ie. fewer groups) due to their very close correlation sample values as a result of averaging. This would mean that there will be more PIC operations, thus, the performance increases.

4.2.2 Effect in fading channel

In the Rayleigh fading channel investigations, in addition to the conditions mentioned in the previous subsection, the effects of the different ordering methods and Doppler frequencies on the receivers are also studied.

For the channel with the maximum Doppler frequency of 100Hz, the BER performance corresponding to different averaging lengths for various receivers are shown in Figure 4.12, Figure 4.13 and Figure 4.14.

For best performance for the Doppler shift of 100Hz, the averaging length for the PIC is 30 bits. However, there is no observable penalty or benefit if one extends the averaging to 70 bits. The situation is different for the SIC, the optimal averaging length is 15 bits for best performance with ordering Method 2. Whereas for ordering Method 1, the optimal length is

about 30 bits. Beyond the optimal point, its performance will degrade. For both the VGHC($\delta=0.4$) and VGHC($\delta=0.8$), the optimal averaging length is 30 bits, beyond which the performance degrades.

The performance with the Doppler shift of 300Hz is presented in Figure 4.15, Figure 4.16 and Figure 4.17. In this case, the optimal averaging length for all the receivers is shortened by about 30%. Beyond the optimal point the BER performance degrades more rapidly than for the case when the Doppler shift is 100Hz. This observation is expected as the coherence time of the fading channel is directly related to the maximum Doppler shift. The coherence time indicates how long the channel will remain invariant and it is given by [120]

$$Coherence\ time \approx \frac{9}{16\pi f_m} \quad (4.6)$$

where f_m is the maximum Doppler shift. With longer coherence time, one can expect the use of longer averaging length to be beneficial. These results are tabulated in Table 4.1.

Comparing the performance of the ordering methods in the SIC, VGHC($\delta = 0.4$) and VGHC($\delta = 0.8$) structures, one can safely conclude that Method 2 is better. The deficiency of using Method 2 would be the increased complexity.

Table 4.1: Optimal averaging length

Receiver	Maximum Doppler shift = 100Hz Coherence time = 1.79 ms	Maximum Doppler shift = 300Hz Coherence time = 0.597 ms
	Optimal length / bits (equivalent time)	Optimal length / bits (equivalent time)
PIC	30 (0.461 ms)	20 (0.308 ms)
SIC	15 (0.231 ms)	10 (0.154 ms)
VGHC($\delta = 0.4$)	30 (0.461 ms)	20 (0.308 ms)
VGHC($\delta = 0.4$)	30 (0.461 ms)	20 (0.308 ms)

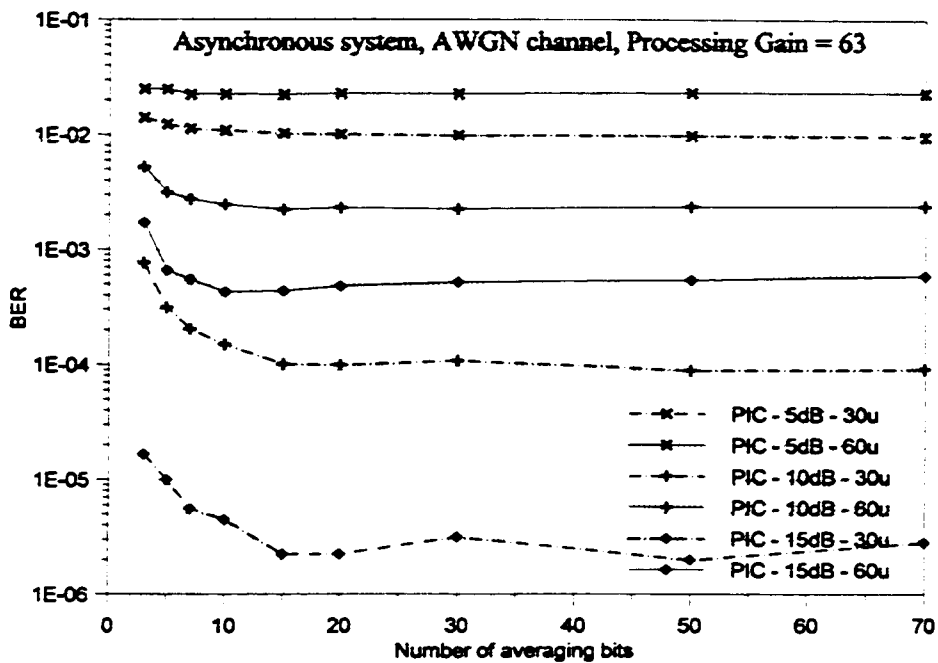


Figure 4.8: Effect of the number of averaging bits on the BER performance of the PIC in AWGN channel.

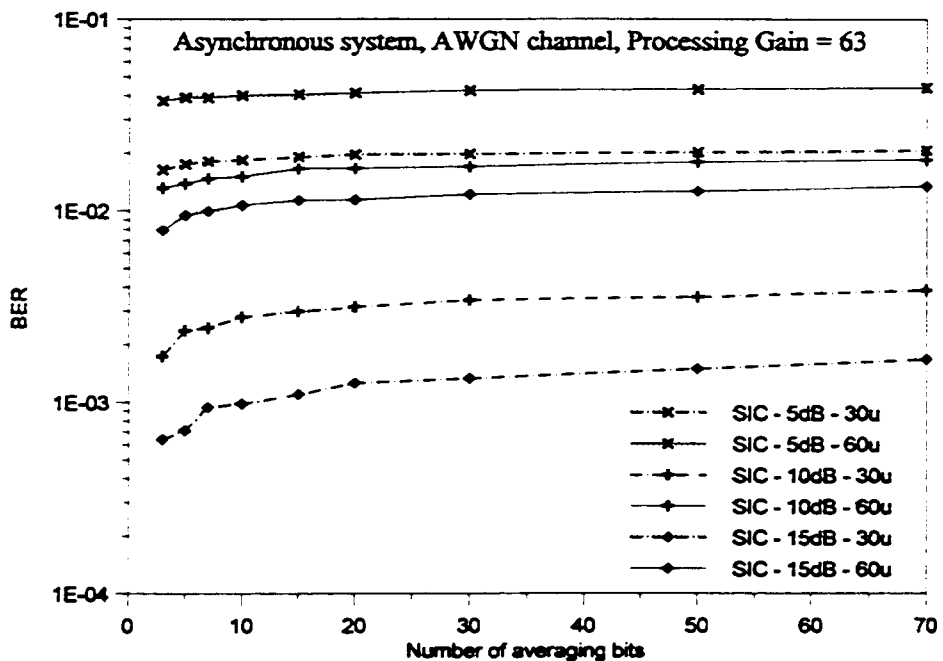


Figure 4.9: Effect of the number of averaging bits on the BER performance of the SIC in AWGN channel.

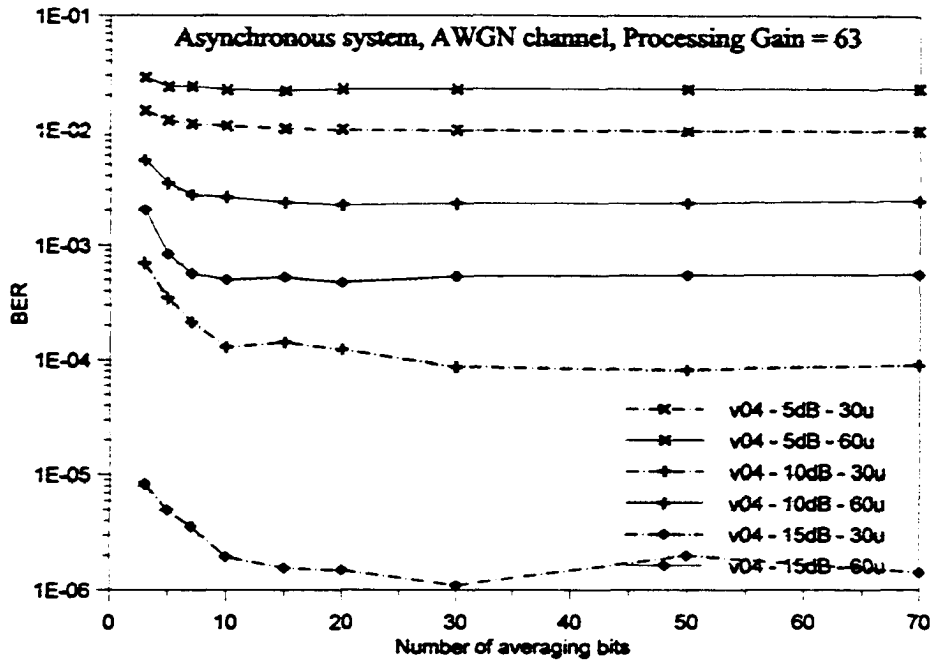


Figure 4.10: Effect of the number of averaging bits on the BER performance of the VGIC($\delta=0.4$) in AWGN channel.

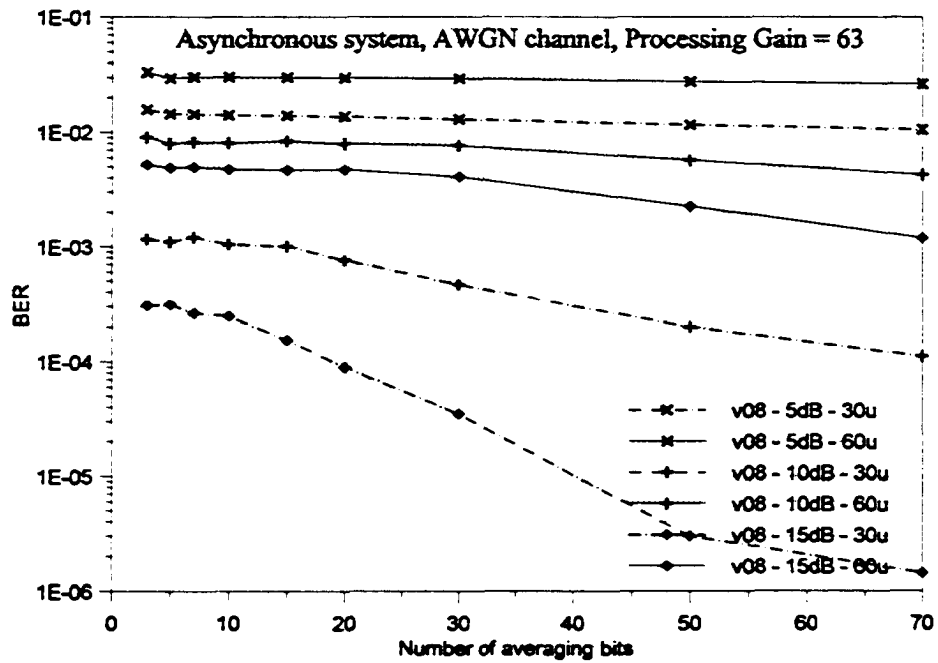


Figure 4.11: Effect of the number of averaging bits on the BER performance of the VGIC($\delta=0.8$) in AWGN channel.

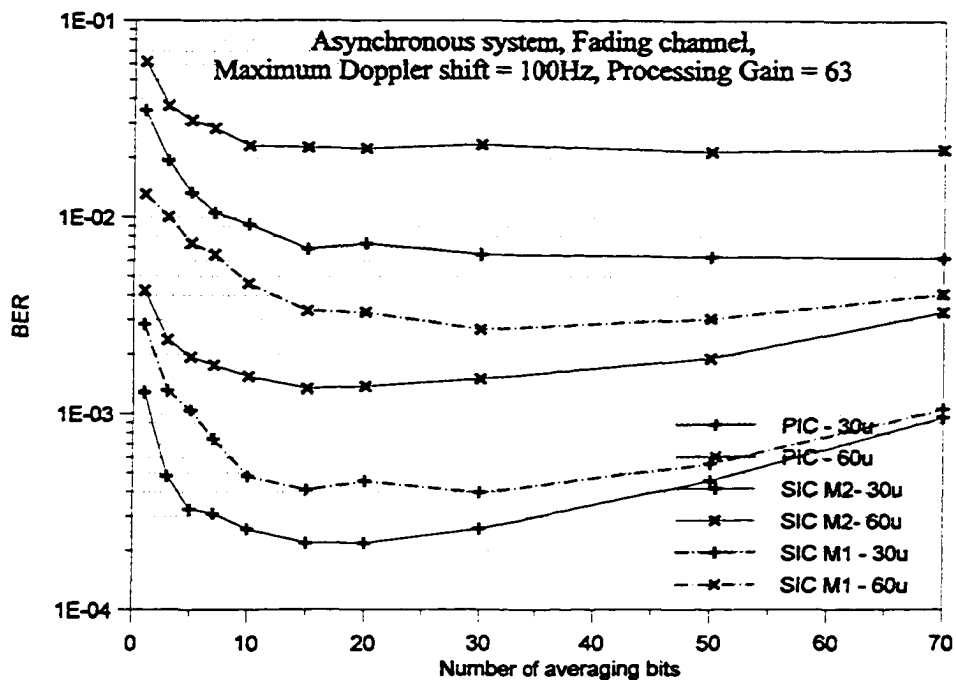


Figure 4.12: Effect of the number of averaging bits on the BER performance of the PIC and SIC (with ordering method M1 and M2) in Rayleigh fading channel with maximum Doppler shift of 100 Hz.

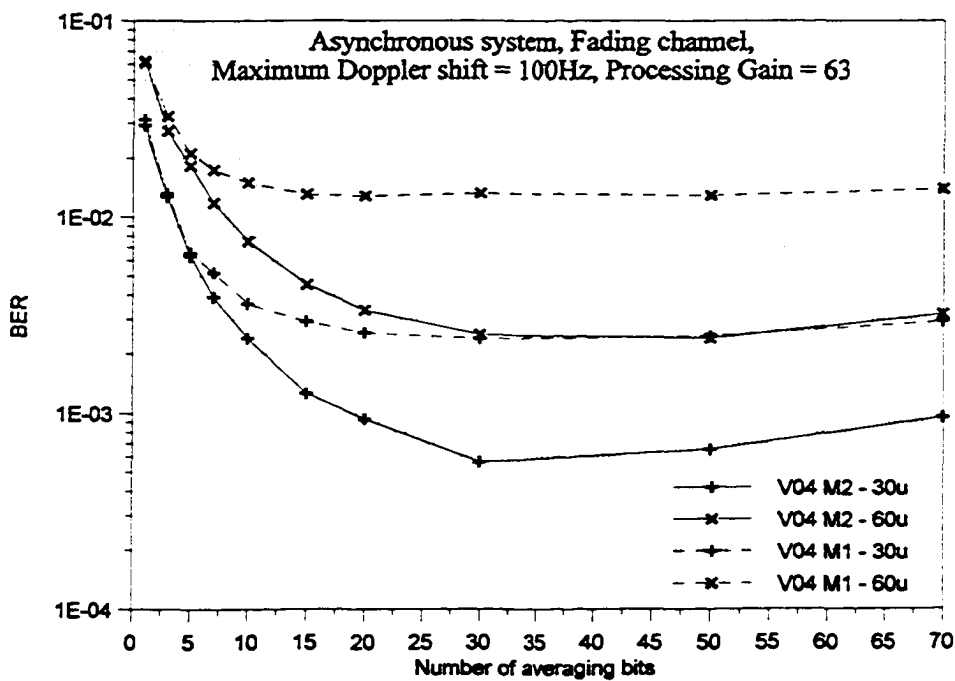


Figure 4.13: Effect of the number of averaging bits on the BER performance of the VGHC ($\delta = 0.4$) (with ordering method M1 and M2) in Rayleigh fading channel with maximum Doppler shift of 100 Hz.

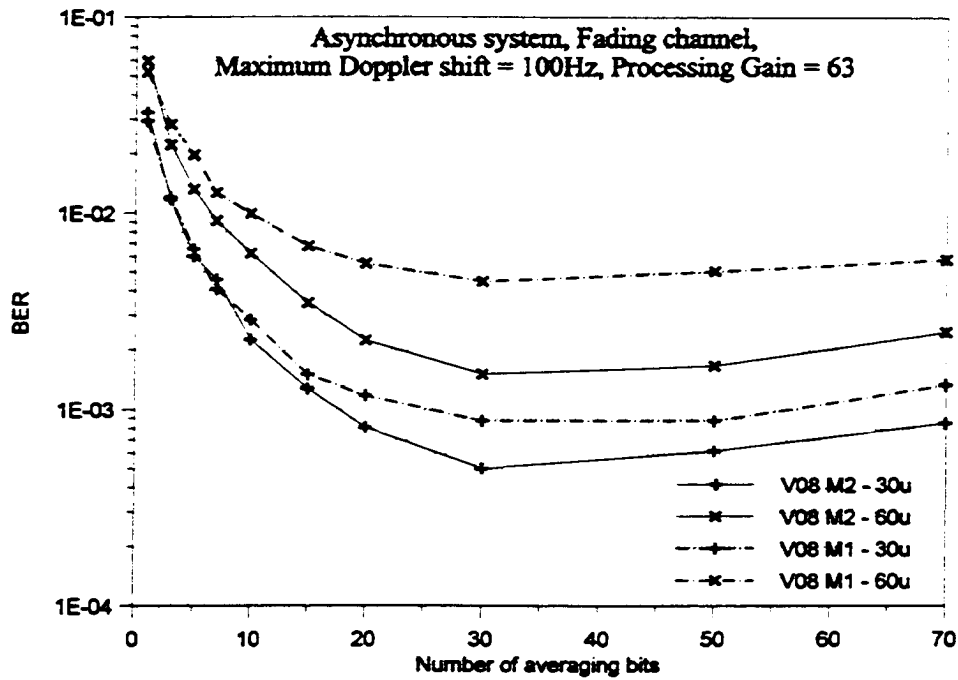


Figure 4.14: Effect of the number of averaging bits on the BER performance of the VGHC ($\delta = 0.8$) (with ordering method M1 and M2) in Rayleigh fading channel with maximum Doppler shift of 100 Hz.

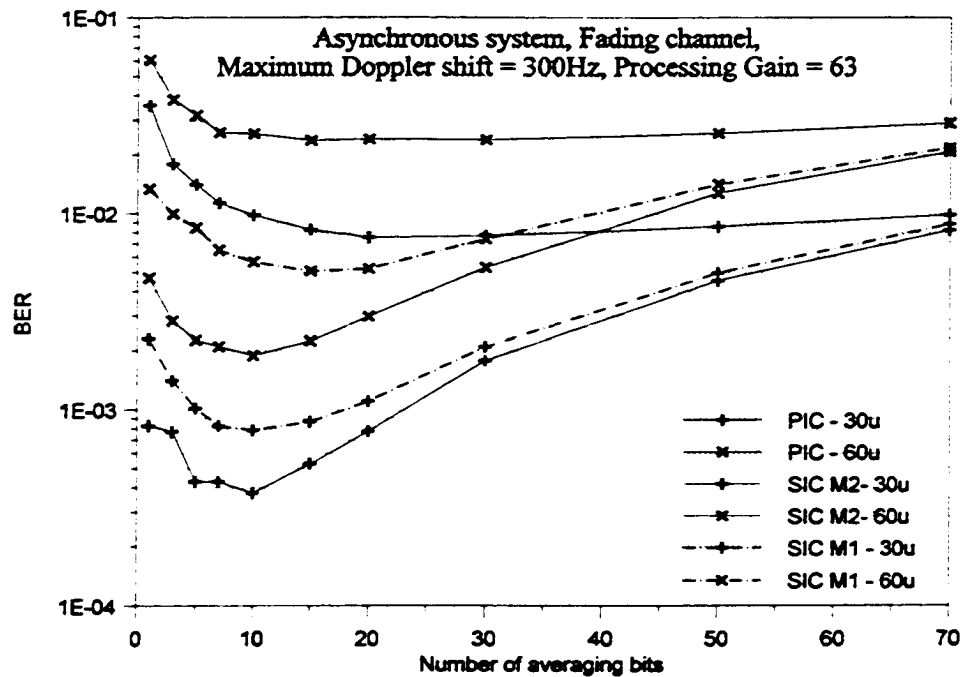


Figure 4.15: Effect of the number of averaging bits on the BER performance of the PIC and SIC (with ordering method M1 and M2) in Rayleigh fading channel with maximum Doppler shift of 300 Hz.

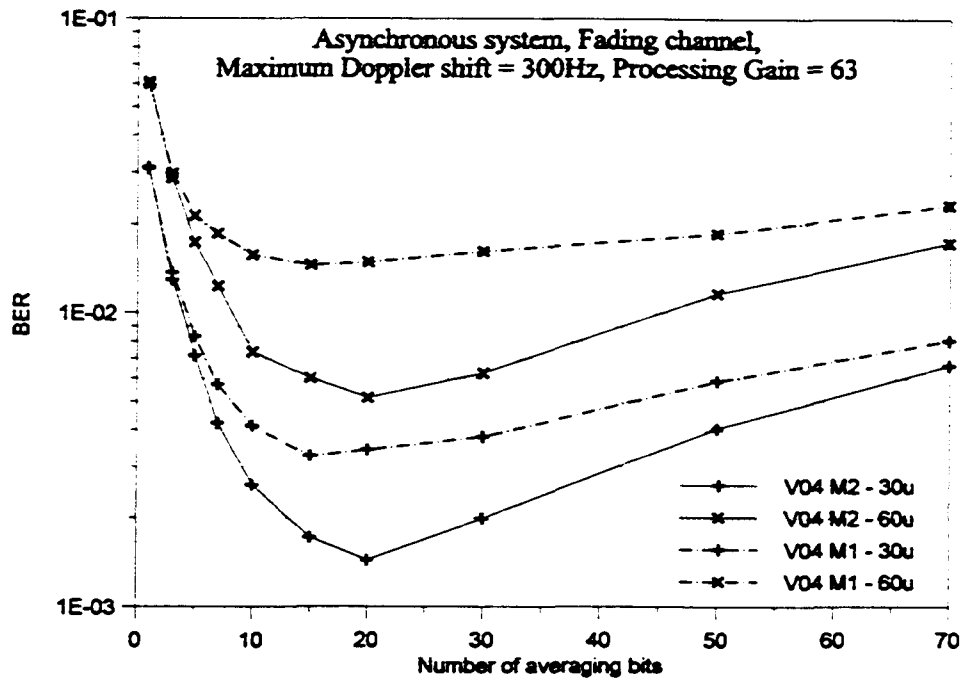


Figure 4.16: Effect of the number of averaging bits on the BER performance of the VGHC ($\delta = 0.4$) (with ordering method M1 and M2) in Rayleigh fading channel with maximum Doppler shift of 300 Hz.

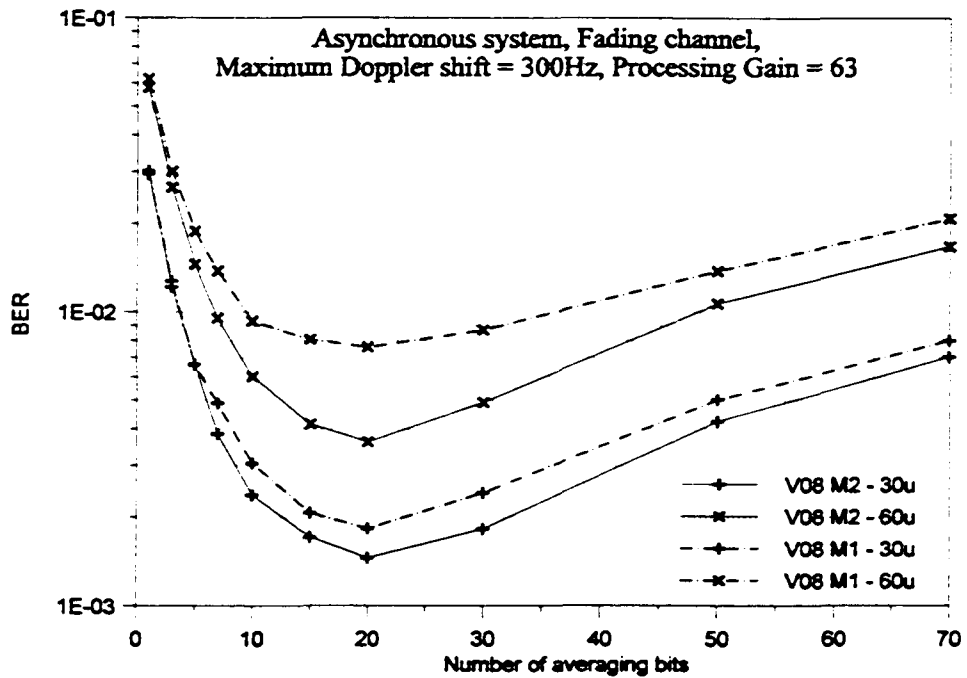


Figure 4.17: Effect of the number of averaging bits on the BER performance of the VGHC ($\delta = 0.8$) (with ordering method M1 and M2) in Rayleigh fading channel with maximum Doppler shift of 300 Hz.

4.3 The multi-stage structure

In this section, the structure of the multi-stage VGHIC is proposed. The overall structure is similar to that of the single stage VGHIC but there are minor structural differences. The group cancellation unit (GCU) for the j^{th} subtractive step of the s^{th} cancellation stage for a M -stage VGHIC scheme is illustrated in Figure 4.18. The index j also represents the group number. At the first stage of cancellation, all users are split into a total of N groups and, hence, $j = 1, \dots, N$. The grouping of the users occurs only in stage 1 and for the subsequent stages, the "User Selection Block" marked in Figure 4.18 is replaced by a bank of matched filters that correspond to the number of users in that particular group. In addition, the "User Detection Block" exists only at the final cancellation stage (Stage M). After the determination of the users in each group, the correlation samples of the group member are then passed into the PIC structure (Figure 3.3) for processing. The improved correlation samples at outputs of the PIC structure are then used for detection and signal regeneration. Following that, the regenerated signals are then subtracted from the delayed composite signal. The resulting composite signal is then passed forward to the next subtractive step for the detection of the next group of users. This carries on until all the users are processed. Note that for the multi-stage VGHIC scheme presented here, correlation sample values are used as measures of all the user signal power levels as well as for all the regenerations of user signals for cancellation.

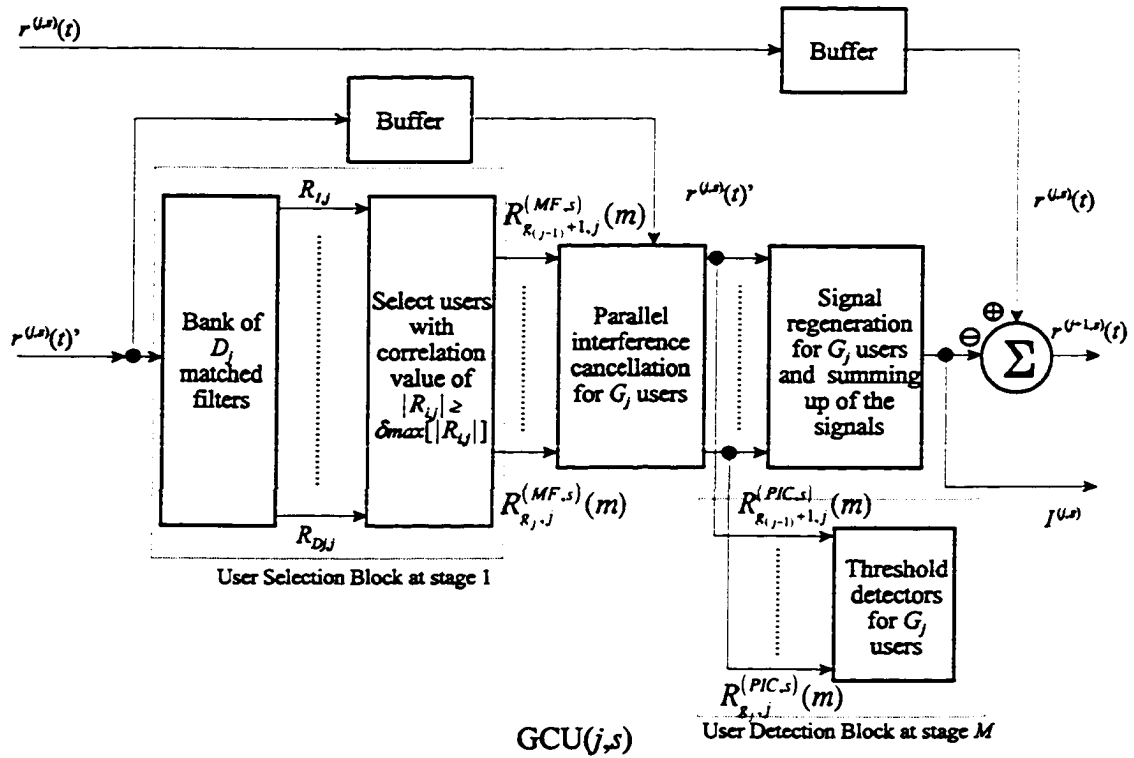


Figure 4.18: Structure of the group cancellation unit (GCU) for the j^{th} subtractive step of the s^{th} cancellation stage for a M -stage VGHC scheme

The term $R_{i,j}^{(MF,s)}(m)$ refers to the correlation sample of bit m of the i^{th} user at the output of the matched filter for the j^{th} subtractive step in stage s , for $(m-1)T + \tau_i \leq t < mT + \tau_i$. Similarly, $R_{i,j}^{(PIC,s)}(m)$ is the correlation sample of bit m of the i^{th} user at the output of the PIC block within $\text{GCU}(j,s)$ for the j^{th} subtractive step in stage s . The multistage structure of the VGHC is shown in Figure 4.19. For stage 1, $r^{(j,1)}(t) = r^{(j,1)}(t)$, and the j^{th} subtractive step of stage 1, we have for $(m-1)T + \tau_i \leq t < mT + \tau_i$,

$$r^{(j,1)}(t) = r^{(j-1,1)}(t) - \sum_{k=g_{(j-2)}+1}^{g_{(j-1)}} \left[R_{k,(j-1)}^{(PIC,1)}(m) S_k(t) \right] \quad (4.7)$$

$$R_{i,j}^{(MF,1)}(m) = A_i(m) + \sum_{\substack{k=g_{(j-1)}+1 \\ k \neq i}}^K A_k(m) \gamma_{ki}(m) + \sum_{k=g_{(j-2)}+1}^{g_{(j-1)}} \Delta_k^{(j-1,1)} \gamma_{ki}(m) + \eta \quad (4.8)$$

$$r_{PIC,j}^{(j,1)}(t) = r^{(j-1,1)}(t) - \sum_{\substack{k=g_{(j-1)+1} \\ k \neq i}}^{g_j} R_{k,j}^{(MF,1)}(m) S_k(t) \quad (4.9)$$

$$R_{i,j}^{(PIC,1)}(m) = A_i(m) + \sum_{k=g_j+1}^K A_k(m) \gamma_{ki}(m) + \sum_{\substack{k=g_{(j-1)+1} \\ k \neq i}}^{g_j} \Lambda_k^{(j,1)} \gamma_{ki}(m) + \sum_{k=g_{(j-2)+1}}^{g_{(j-1)}} \Delta_k^{(j-1,1)} \gamma_{ki}(m) + \eta \quad (4.10)$$

where

$$\Delta_k^{(j,s)} = A_k(m) - R_{k,j}^{(PIC,s)}(m) \quad (4.11)$$

$$\Lambda_k^{(j,s)} = A_k(m) - R_{k,j}^{(MF,s)}(m) \quad (4.12)$$

and the cross-correlation factor for bit m between user k and i is defined in (3.19) and $\gamma_{ii}(m) = 1$. The term $S_k(t)$ is defined in (3.3), and, $A_i(m) = (\sqrt{E_i})B_i^{(m)}$ for the period $(m-1)T + \tau_i \leq t < mT + \tau_i$. However, from stage 2 onwards, $r^{(j,s)}(t)$ is the result of canceling the interferences of those users that are not in the immediate group from the composite signal $r^{(j,s)}(t)$ as shown in Figure 4.19. By making use of the information gained from the previous stage, one can achieve better detection of the desired group of users by canceling the interferences from other groups before the detection process. For stage 2 onwards, we have for the j^{th} subtractive step and $(m-1)T + \tau_i \leq t < mT + \tau_i$,

$$r^{(j,s)}(t) = r^{(j-1,s)}(t) - \sum_{k=g_{(j-2)+1}}^{g_{(j-1)}} \left[R_{k,(j-1)}^{(PIC,s)}(m) S_k(t) \right] \quad (4.13)$$

$$r^{(j,s)}(t)' = r^{(j,s)}(t) - \sum_{k=j+1}^N I^{(k,s-1)}(m) \quad (4.14)$$

$$R_{i,j}^{(MF,s)}(m) = A_i(m) + \sum_{\substack{k=g_{(j-1)}+1 \\ k \neq i}}^{g_j} A_k(m) \gamma_{ki}(m) \quad (4.15)$$

$$+ \sum_{n=j+1}^N \sum_{k=g_{(n-1)}+1}^{g_n} \Delta_k^{(n,s-1)} \gamma_{ki}(m) + \sum_{k=g_{(j-2)}+1}^{g_{(j-1)}} \Delta_k^{(j-1,s)} \gamma_{ki}(m)$$

$$r_{PIC,j}^{(j,1)}(t) = r^{(j-1,s)}(t)' - \sum_{\substack{k=g_{(j-1)}+1 \\ k \neq i}}^{g_j} R_{k,j}^{(MF,s)}(m) S_k(t) \quad (4.16)$$

$$R_{i,j}^{(PIC,s)}(m) = A_i(m) + \sum_{n=j+1}^N \sum_{k=g_{(n-1)}+1}^{g_n} \Delta_k^{(n,s-1)} \gamma_{ki}(m) \quad (4.17)$$

$$+ \sum_{k=g_{(j-2)}+1}^{g_{(j-1)}} \Delta_k^{(j-1,s)} \gamma_{ki}(m) + \sum_{\substack{k=g_{(j-1)}+1 \\ k \neq i}}^{g_j} \Lambda_k^{(j,s)} \gamma_{ki}(m)$$

where $S_k(t)$, $\Delta_k^{(j,s)}$, $\Lambda_k^{(j,s)}$, $\gamma_{ki}(m)$ are defined in (3.3), (4.11), (4.12), (3.19), respectively, and

$$I^{(j,s)}(m) = \sum_{k=g_{(j-1)}+1}^{g_j} R_{k,j}^{(PIC,s)}(m) S_k(t) \quad (4.18)$$

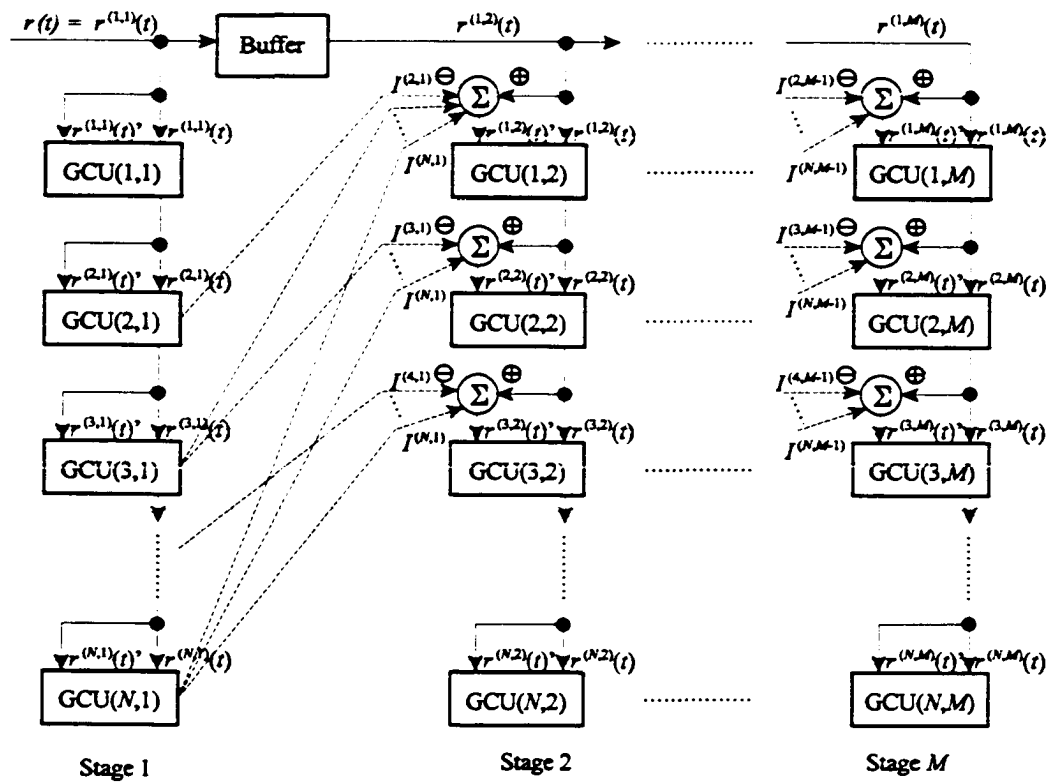


Figure 4.19: Structure of the M -stage VGHC scheme

The performance of the multi-stage VGHC will be investigated and compare against the multi-stage PIC and SIC in the next section.

4.4 Partial combination of correlations samples and partial cancellation

In this section, the partial combination of correlation samples (PCC) and partial cancellation (PC) is proposed and investigated. Then, their effect on the multi-stage VGHC is investigated. The VGHC with PCC and PC is termed the improved VGHC or I-VGHC.

4.4.1 Partial combination of correlation samples

In the simulations of asynchronous systems, interference cancellation was implemented on blocks of symbols (cancellation block) utilizing the average correlation sample values of that block as the estimates of each user's signal amplitude. The number of symbols in a cancellation block was predetermined. It was shown in the previous section that significant performance gain could be achieved by canceling blocks of data symbols using the averaged correlation sample values for that block as the estimates of the user signal amplitudes.

However, this section will demonstrate that further performance gain can be achieved by making use of the correlation sample values of individual data bits or symbols together with the average correlation sample value of that block as the estimates of the amplitude of each user's signal. Due to the non-orthogonality of the pseudo-random codes assigned to different users, and the randomness of the data generated by different users, the desired user signal will experience different amounts of MAI at different times. When the MAI is large, the probability of a detection error will be increased. If the wrongly detected bit used for cancellation is regenerated using the average correlation sample value, its interference on other users will be enhanced instead of being canceled. This section presents a simple partial combining of correlation samples (PCC) method which deals with this issue and at the same time takes full advantage of the use of average correlation sample values.

Let the individual correlation sample value of bit m be represented by $R_{i,j}^{(*,s)}(m)$ where $*$ refers to either MF or PIC, and is consistent with the notation in the previous sections. Thus, the average correlation sample value over n bits is

$$\bar{R}_{i,j}^{(*,s)}(n) = \frac{1}{n} \sum_{m=1}^n \left| R_{i,j}^{(*,s)}(m) \right| \quad (4.19)$$

where $|x|$ is the magnitude of x . Let the correlation sample value, after partial combining of the individual correlation sample value of bit m and the average correlation sample value, be

$$R_{i,j}^{P(*,s)}(m) = (1 - p_f(s)) R_{i,j}^{(*,s)}(m) + p_f(s) \operatorname{sgn}\left[R_{i,j}^{(*,s)}(m) \right] \bar{R}_{i,j}^{(*,s)}(n) \quad (4.20)$$

where $\text{sgn}[x]$ is the sign of x , and, $p_f(s)$ is the partial combining factor to be set for stage s ($0 \leq p_f(s) \leq 1$). The first term on the right-hand side of (4.20) is the amount of the individual correlation sample value to be used in $R_{ij}^{p_f(s)}(m)$; when $p_f(s) = 0$, $R_{ij}^{p_f(s)}(m) = R_{ij}^{(s)}(m)$, the individual correlation sample of bit m is used. The second term represents the amount of the average correlation sample value to be used in $R_{ij}^{p_f(s)}(m)$; when $p_f(s) = 1$, only the average correlation sample value will be used to determine $R_{ij}^{p_f(s)}(m)$. The term $R_{ij}^{(s)}(m)$ in (4.8) can be replaced directly by (4.20) for the implementation of the partial combining of correlation samples.

In general, one can determine the relative probability of detection error of bit m by examining the magnitude of the corresponding correlation sample value. If the magnitude is high (MAI interferes in a positive way), one will expect that the detection process will have a high probability of yielding a correct output. Hence, if we use the average correlation sample value in the IC process, we can achieve a better cancellation of MAI. This is so as the average correlation sample value has a lower variance than the individual correlation sample value. If the individual correlation sample value (with high magnitude) is used, the interference can be excessively canceled, and this effectively results in poorer performance.

If the magnitude of the correlation sample value is small, and close to the threshold level of the detector, the probability of a detection error will be higher. In this case, if we use the individual correlation sample value (which is now small) in the IC process, the impact of the wrong decision on the performance of the IC scheme can be alleviated. If the average correlation sample value (of larger magnitude) is used in place of the individual correlation sample value, the MAI will be enhanced instead of being cancelled.

4.4.2 Partial cancellation

In addition to the partial combining of correlation sample values, the performance of the VGHIC scheme can be improved using the idea of partial cancellation for the PIC [56].

Using similar reasoning, a simpler partial cancellation scheme can be incorporated into the PIC section of the VGHIC scheme. (4.12) can then be modified to

$$\Lambda_k^{p(j,s)} = A_k(m) - p_c(s) R_{k,j}^{(MF,s)}(m) \quad (4.21)$$

where $p_c(s)$ is the partial cancellation factor for stage s and $0 \leq p_c(s) \leq 1$. The term $p_c(s)$ determines the amount of the regenerated signal to be canceled from the composite received signal $r^{(j,1)}(t)$ (Figure 3.3).

4.4.3 Effects in AWGN channel

This subsection comprises two parts. The first part is the comparison of the BER performance in the AWGN channel with different signal-to-noise ratios (SNRs) between the multistage VGHIC and the improved multistage VGHIC (I-VGHIC) scheme. The I-VGHIC scheme is the VGHIC scheme with PCC and PC. Following that, the performance of the multistage I-VGHIC scheme is compared with the multistage PIC and SIC schemes in the AWGN channel.

The bit error rate (BER) of the 1-stage VGHIC scheme with and without partial combining of correlation sample values (PCC) and partial cancellation (PC) is presented in Figure 4.20. For the 1-stage VGHIC-PCC scheme, $p_c(1) = 0.5$, while for the VGHIC-PC scheme, $p_c(1) = 0.8$. These values are found through simulations to provide the best overall performance for stage 1 of the VGHIC scheme when the average correlation sample value has been obtained over 30 bits. It can be seen that the PCC and the PC methods applied separately result in a 13% increase in user capacity each at a BER of 1×10^{-3} . Using PCC and PC together increases the user capacity by 25% at a BER of 1×10^{-3} . We shall refer to the VGHIC scheme with both PCC and PC as the improved VGHIC (I-VGHIC) scheme. For the PCC method, it was found by simulations that there was no performance increase beyond two stages. For the PC method, there was no performance gain beyond the first stage. This is quite plausible intuitively, because in the first stage, the correlation samples are very noisy, and the PCC and PC methods are effective in reducing the amount of MAI. As the VGHIC scheme proceeds

to further stages, the correlation samples improve during the process, and, hence, the estimations of user signal levels become better. As a result, the PCC and PC techniques become less effective.

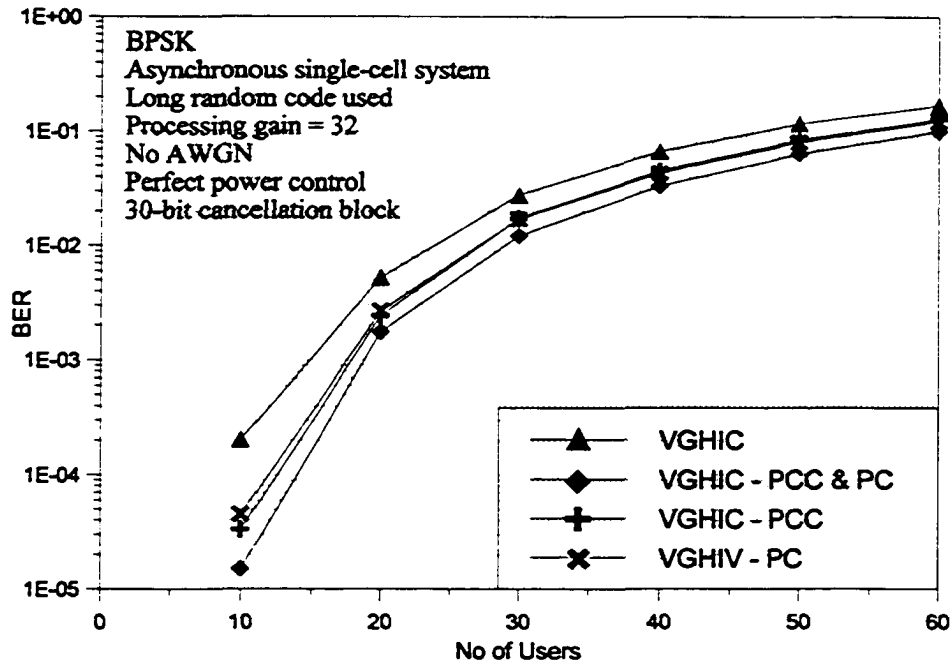


Figure 4.20: BER of the one-stage VGHC scheme with the partial combining of correlation samples (PCC) and partial cancellation (PC) in a single-cell asynchronous system with perfect fast and slow power control. Cancellations were done for 30-bit blocks and the average correlation sample value over 30 bits was used.

The performance comparison of the multistage VGHC and I-VGHC schemes in the AWGN channel for a 30-user asynchronous single-cell system is shown in Figure 4.21. For both schemes, δ was set to 0.8. As seen from Figure 4.21, the multistage structure performs significantly better than the single stage structure. The 2-stage VGHC scheme outperforms the 1-stage VGHC scheme by a margin of 5.5dB at a BER of 4×10^{-2} , while the 3-stage VGHC outperforms the 2-stage VGHC by 0.75 dB at the same BER. The 2-stage I-VGHC is 4.5 dB better than the 1-stage I-VGHC and the 3-stage I-VGHC is 1 dB better than the 2-stage I-VGHC at a BER of 2×10^{-2} . One can see that significant performance gain can be achieved by using the multistage structure, but as the number of cancellation stages goes

beyond 2 or 3, the increase in performance is smaller. Also, from Figure 4.21, the I-VGHIC scheme significantly outperforms the VGHIC scheme. The 1-stage I-VGHIC is 3.75 dB better than the 1-stage VGHIC at a BER of 4×10^{-2} . The 2-stage I-VGHIC performs slightly better than the 3-stage VGHIC scheme.

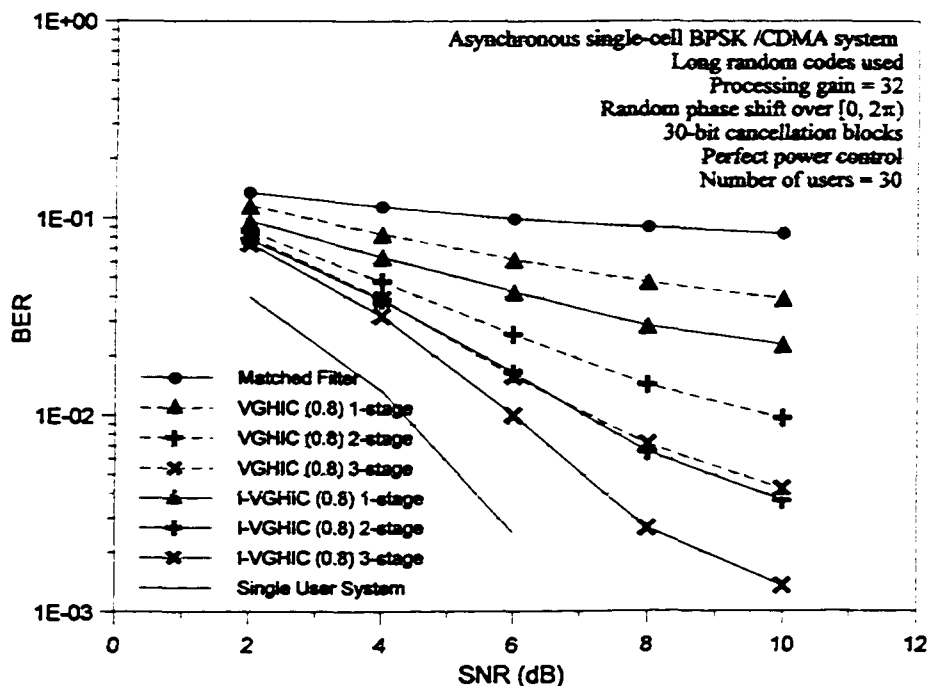


Figure 4.21: Performance comparison between the multistage VGHIC and I-VGHIC schemes in AWGN channel with different SNRs (a single-cell asynchronous system)

The performance of the one, two and three-stage I-VGHIC schemes with $\delta = 0.7$ and $\delta = 0.8$ is compared with the SIC, 1-stage PIC and 6-stage PIC in Figure 4.23. It is found that the performance gain is insignificant when the number of PIC stages is increased beyond six. Interestingly, when the number of users increases beyond 25, the performance of the PIC scheme deteriorates significantly and when that number increases beyond 40, the PIC scheme performs worse than the conventional matched filter receiver. Furthermore, when the number of users increases beyond 40, the 6-stage PIC actually performs worse than the 1-stage PIC. Thus, one can conclude for the PIC that, once the amount of interference exceeds a certain threshold level, the PIC scheme breaks down and additional cancellation stages reduce

performance. This was also observed in [121][122]. On the other hand, the SIC and the I-VGHIC schemes are still effective and perform better than the conventional matched filter receiver even when interference is high.

4.4.4 Effects in Rayleigh fading channel

We also note that the 1-stage I-VGHIC with $\delta = 0.7$ outperforms the 1-stage I-VGHIC with $\delta = 0.8$ (Figure 4.23). This is because a smaller value of δ implies more PIC than SIC operations (see (3.10)), and when the powers of the users are equal (AWGN channel), the PIC is more effective than the SIC [82]. However, the performance of the 2-stage and 3-stage I-VGHIC ($\delta = 0.7$) scheme is worse than that of the corresponding I-VGHIC ($\delta = 0.8$) scheme. This is due to the inherent deficiency of the multistage PIC scheme mentioned in the previous paragraph. Notice that when the number of users increases over 50, the 3-stage I-VGHIC ($\delta = 0.7$) actually performs worse than the 2-stage I-VGHIC ($\delta = 0.7$). For a multistage structure, the I-VGHIC ($\delta = 0.8$) scheme is clearly superior to the I-VGHIC ($\delta = 0.7$). The advantage of this I-VGHIC scheme is that one can adjust the parameter δ to match different channel conditions.

For a BER of 1×10^{-2} , the conventional system capacity is 9 users. The use of SIC increases capacity by 1.9 times, while the 6-stage PIC scheme has 3.1 times the capacity of the matched filter receiver. The 1-stage I-VGHIC ($\delta = 0.7$) has 3.1 times the capacity of the matched filter receiver and is on par with the 6-stage PIC scheme, but the 1-stage I-VGHIC ($\delta = 0.7$) is still effective when the interference is high; it is not so with the 6-stage PIC scheme. The 3-stage I-VGHIC ($\delta = 0.8$) has the best performance. Its capacity is 5.1 times that of the matched filter receiver, and 1.6 times that of the 6-stage PIC. Clearly, the I-VGHIC scheme is superior in the AWGN channel with equal power users.

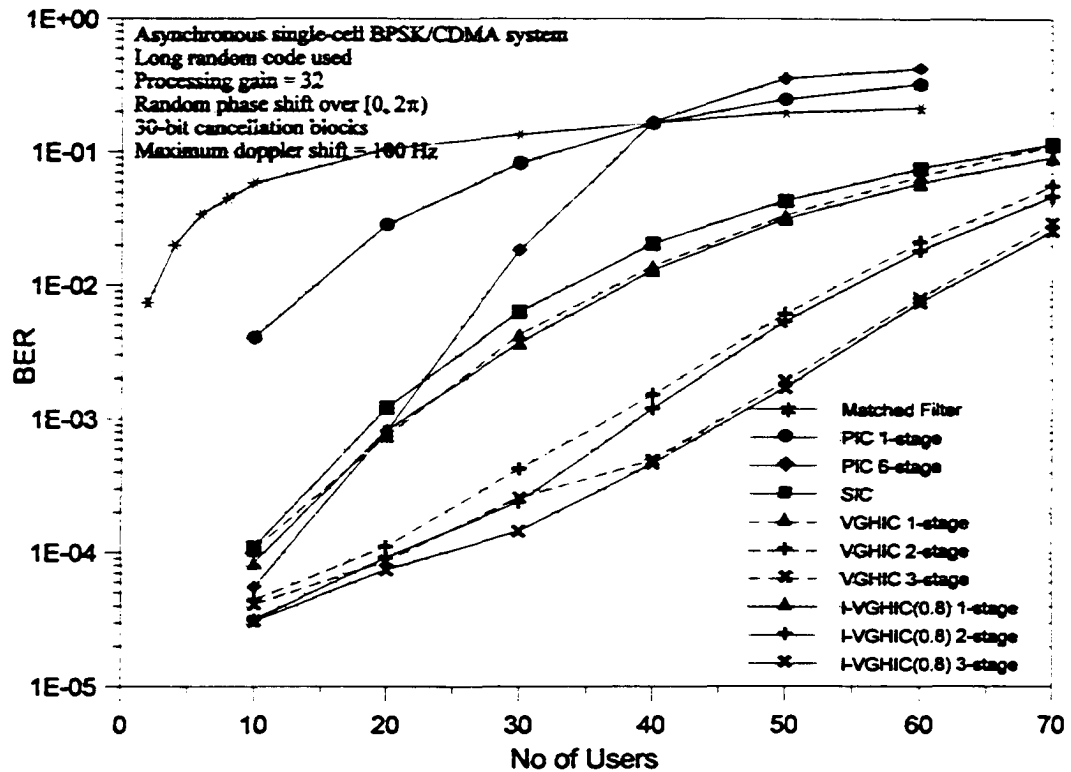


Figure 4.22: BER comparison between the I-VGHIC scheme and other subtractive cancellation schemes in flat Rayleigh fading channel with no AWGN (an asynchronous single-cell system)

Figure 4.22 shows the simulation results on the flat Rayleigh fading channel for the conventional matched filter, SIC, single and multistage PIC, VGHIC and I-VGHIC receivers. It is noted that in the flat Rayleigh fading channel, the improvement in the performance of the I-VGHIC over the VGHIC is not as significant as in the AWGN channel. However, the performance increase is still noticeable, especially when the number of users is less than 40. The 6-stage PIC only performs better than the single stage SIC when the number of users is less than 20. As already explained, both the single and multistage PIC schemes become ineffective when the number of users increases beyond 40. As can be observed from Figure 4.22, the capacity of the 3-stage I-VGHIC at a BER of 1×10^{-2} is 21 times better than that of the matched filter receiver, 2.25 times better than that of the 6-stage PIC scheme and 1.85 times better than that of the SIC. Note that multistage SIC may not be practical due to its very long processing delay. From the previous simulation results, it can be shown that the 3-stage I-VGHIC has about the same, if not shorter, processing delay as the single stage SIC.

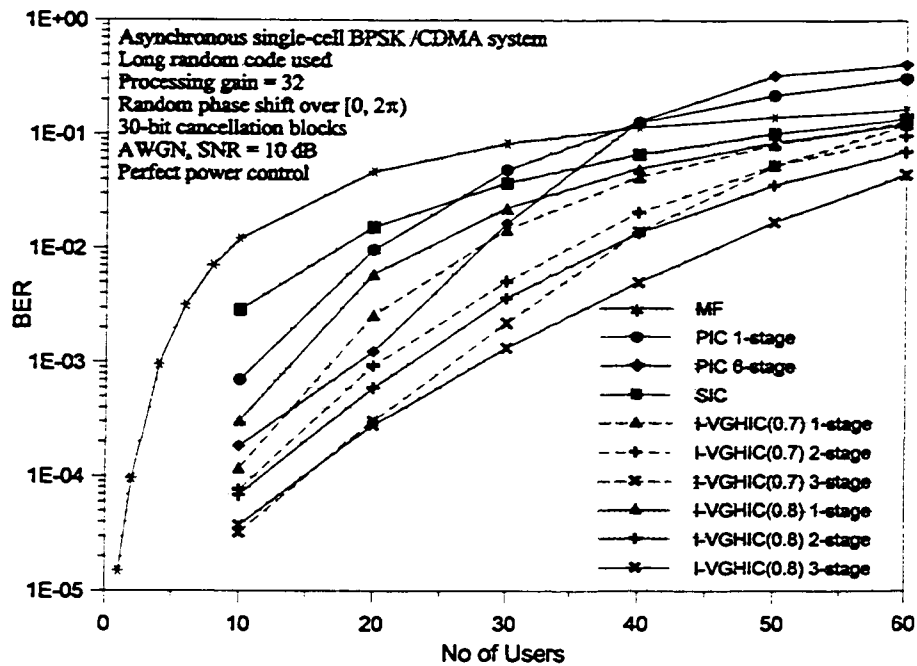


Figure 4.23: Performance comparison between the I-VGHIC scheme and other subtractive cancellation schemes in AWGN channel at SNR = 10 dB (asynchronous single-cell system)

4.5 Processing delay

Due to the adaptive nature of the VGHIC or the I-VGHIC, the determination of its processing delay is not a straightforward task. The statistics of the processing delay are obtained from simulations. This section presents the processing delay of the I-VGHIC in the AWGN and flat Rayleigh fading channels. Although this section refers to the I-VGHIC, similar observations applies to VGHIC as there is no difference in the structure between the VGHIC and I-VGHIC.

4.5.1 Statistics of the delay

The total number of subtractive steps for the I-VGHIC with $\delta = 0.6, 0.7$ and 0.8 , in the AWGN (SNR = 10 dB) and flat Rayleigh fading channels are shown in Figure 4.24. When δ is smaller, the number of subtractive steps is also smaller. This is because a smaller δ means that more users are being selected into each cancellation group (see (3.10)) and as a result, the total number of subtractive steps decreases. Furthermore, the number of subtractive steps in the AWGN channel is lower than that in the Rayleigh fading channel regardless of the value of δ . This is a clear example of the adaptive nature of the I-VGHIC in which its structure changes to suit different signal power profiles. However, for the AWGN channel where all users have the same power at the base station, the I-VGHIC does not become a pure PIC. This is because magnitudes of correlation samples are used as the basis for grouping of users and even if the powers of all users are the same, the cross-correlations between users will be different. Hence, different users will not experience the same amount of MAI, and that results in dissimilar correlation sample values between users. This, in turn means that the correlation sample value spread can be large enough to cause the users to be split into more than one group.

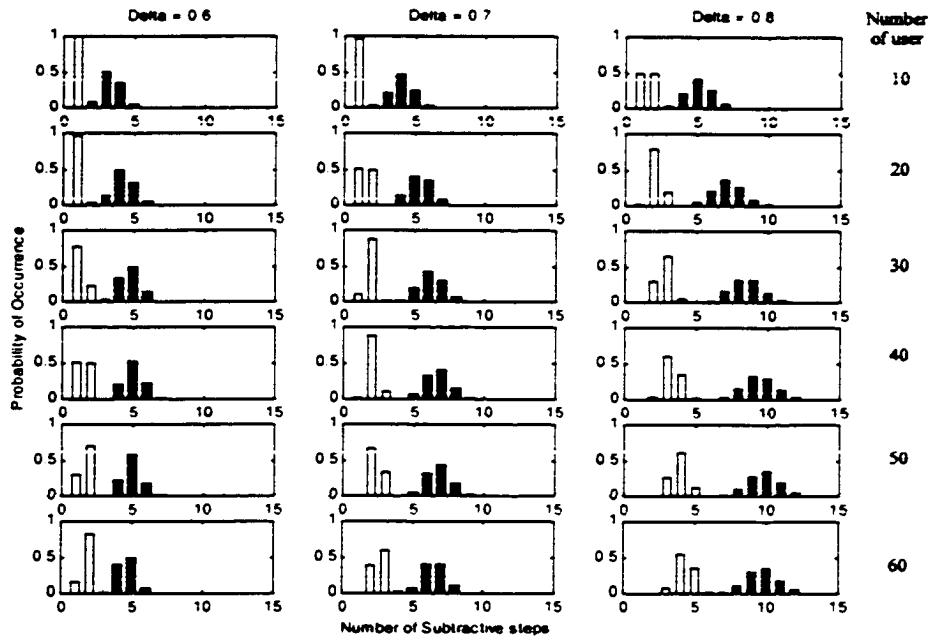


Figure 4.24: The number of subtractive steps for one stage of the I-VGHIC with $\delta = 0.6, 0.7$ and 0.8 , in the AWGN (SNR = 10 dB) and flat Rayleigh fading channels with different numbers of users (asynchronous single-cell system). \square : AWGN channel; \blacksquare : Flat Rayleigh fading channel.

It can be observed that there is a limit on the number of subtractive steps for different values of δ regardless of the number of users. The processing delay is bounded for the I-VGHIC, and it does not depend on the number of users once the number of users increases beyond a certain value. This is an advantage over the SIC where the number of subtractive steps is proportional to the number of users. The cumulative distribution of the number of subtractive steps is shown in Figure 4.25. However, the processing delay of the I-VGHIC is still longer than that of the PIC. Thus, it is desirable to further reduce the number of subtractive steps and hence, processing delay of the I-VGHIC.

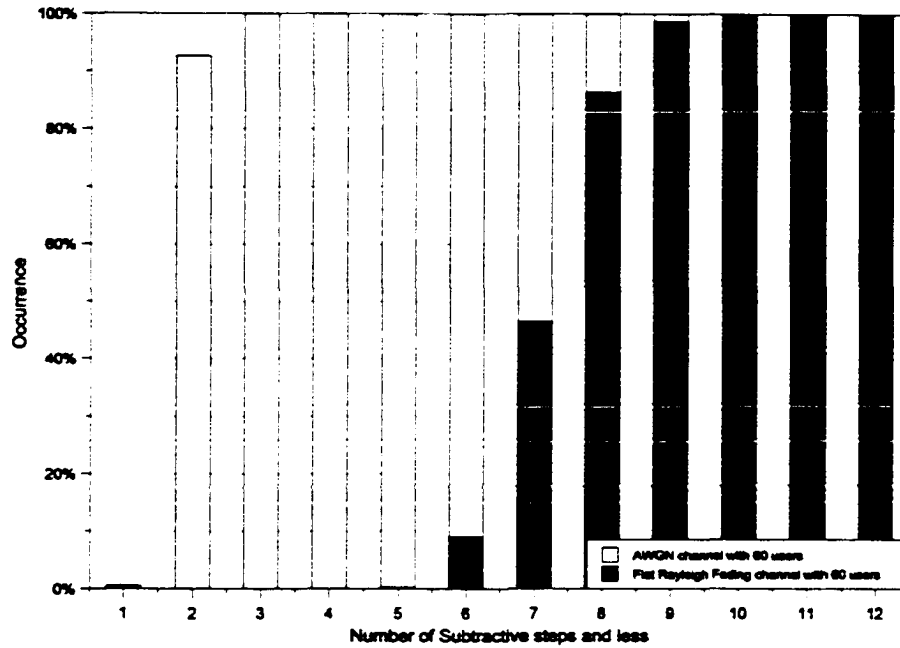


Figure 4.25: Cumulative distribution of the number of subtractive step for each full I-VGHIC interference cancellation stage of an asynchronous single-cell system. Processing gain = 63.

4.5.2 A method of limiting the delay

In this section, a simple method of limiting the number of subtractive steps of the I-VGHIC is proposed and investigated. Its effect on the BER is also investigated. Let the I-VGHIC with limited number of steps be denoted by I-VGHIC(m, n) with $m \geq n$. The parameter m specifies the maximum number of subtractive steps that the VGHC(m, n) can encompass. For the first $m - n$ groups, the grouping procedure is based on the original selection rule (3.3), but for the remaining n groups, the alternative selection rule (4.22) is used, namely

$$|R_{i,j}| \geq (m - j) \left(\frac{\Delta R}{m - j + 1} \right) + |R_{\min,j}| \quad (4.22)$$

where j is the subtractive step number such that

$$m - n < j \leq m \quad (4.23)$$

and

$$\Delta R = \left| R_{\max,j} \right| - \left| R_{\min,j} \right| \quad (4.24)$$

where $R_{\max,j}$ and $R_{\min,j}$ is the maximum and minimum correlation sample value, respectively, at subtractive step j . The aim of the alternative selection rule (4.22) is to split the remaining users into exactly n groups according to the magnitude of their correlation samples. First, the maximum and minimum correlation magnitudes are obtained, then the range of correlation sample magnitudes corresponding to the n groups is obtained. Let us say for VGHC($m = 5$, $n = 2$), the scheme is limited to a maximum of $m = 5$ subtractive steps for all users. For the first ($5 - 2 = 3$) subtractive steps, users will be selected using (3.3) and the remaining users will be split into $n = 2$ groups using (4.22). At the 4th subtractive step, users with correlation sample magnitudes between $R_{\max,4}$ and $(\Delta R/2 + R_{\min,4})$ are selected into the 4th group. All the remaining users are included in the 5th, or the last group. Next, the effect of this limiting method on the performance is investigated.

4.5.3 Effect on performance

Figure 4.26 compares the uncoded BER performance for the one, two and three-stage I-VGHC and I-VGHC(m,n) with $\delta=0.7$ in the Rayleigh fading channel. The Rayleigh fading channel is used to evaluate the performance of the I-VGHC(m,n) because the standard I-VGHC only exhibits longer processing delay when the signal powers of the users are unequal.

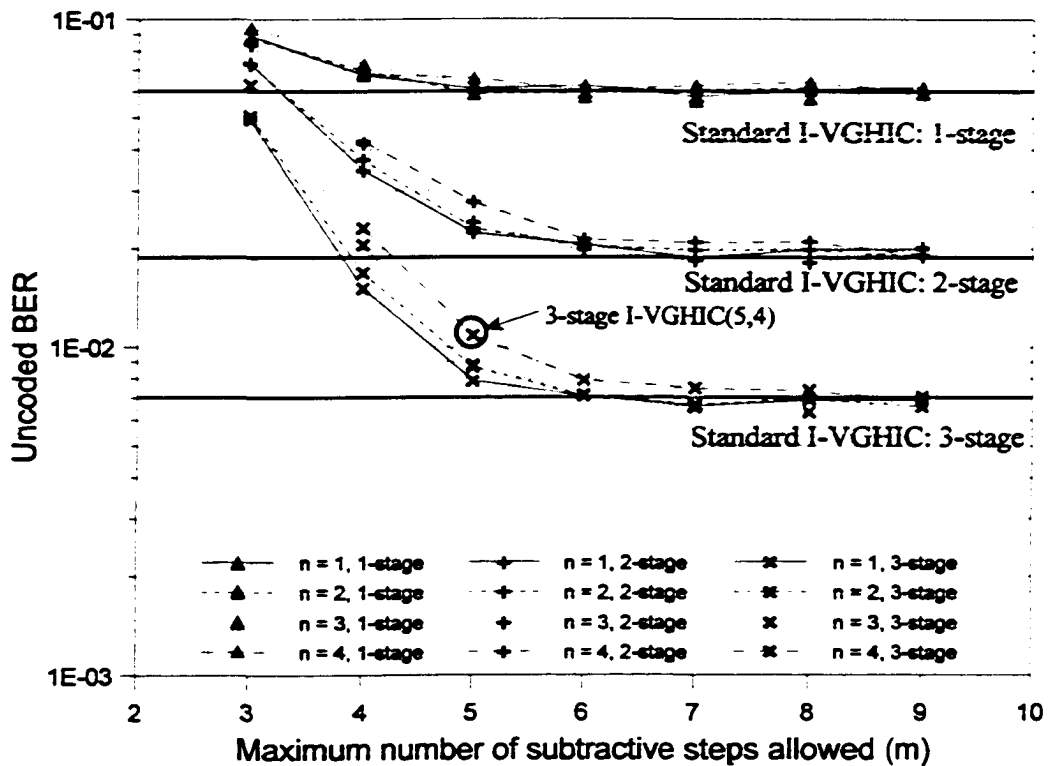


Figure 4.26: Performance comparison between the standard I-VGHIC and the I-VGHIC(m,n) (both with $\delta = 0.7$) for different values of m and n in flat Rayleigh fading channel with 60 simultaneously transmitting users. (Asynchronous single-cell BPSK/CDMA system with maximum Doppler shift = 100 Hz and processing gain = 32).

Consider the point marked with a circle in Figure 4.26. It lies on the line corresponding to ($n = 4, 3$ -stage) and its x-axis value is 5. This point reflects the BER of the 3-stage I-VGHIC(5,4). The next point to the right along the line of ($n = 4, 3$ -stage) shows the corresponding BER of the 3-stage I-VGHIC(6,4). One can notice that as the maximum number of subtractive steps allowed is increased, the performance of the I-VGHIC(m,n) approaches that of the standard I-VGHIC. When $m \geq 7$, the I-VGHIC(m,n) performs just as well as the standard I-VGHIC. This is because for the I-VGHIC with $\delta = 0.7$, the maximum number of subtractive steps is 8 regardless of the number of users (Figure 4.24). With $m < 7$ and increasing n , the performance of the I-VGHIC(m,n) degrades because its basic structure deviates from that of the standard I-VGHIC. The good performance of the standard I-VGHIC is due to the fact that it uses PIC within each group of users with similar power levels and SIC between groups of users that have different power levels. In this sense, the I-

VGHIC combines the advantages of both the PIC and SIC. When this structure is changed, the performance will naturally degrade as shown in Figure 4.26.

One advantage of the I-VGHIC over the PIC and SIC is that its structure can be changed to suit different applications with a simple change of the parameter values. One can use Figure 4.24 and Figure 4.26 (or similar for other values of δ) for the determination of the values of m and n , and the number of cancellation stages to satisfy delay constraints and BER requirements.

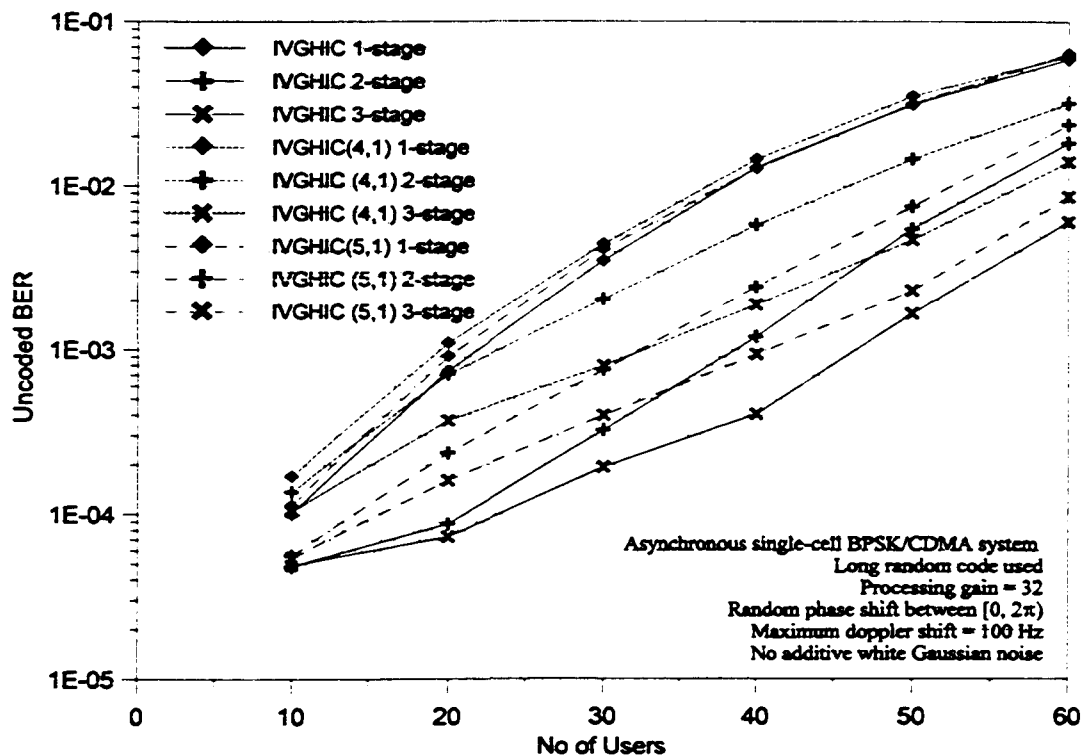


Figure 4.27: Comparison of the BER performance of the multi-stage I-VGHIC and I-VGHIC(m,n) with $\delta = 0.7$ in flat Rayleigh fading channel.

The simulated BER performance of the one, two and three-stage I-VGHIC(4,1) and I-VGHIC(5,1) is shown against that of the standard I-VGHIC in Figure 4.27. The value of δ is 0.7 in all cases. As we limit the number of subtractive steps, the BER performance of the multi-stage I-VGHIC(m,n) becomes worse than the I-VGHIC. When the number of subtractive steps is limited to 5, the user capacity drops by 4.5%, 18% and 13% for the one,

two and three-stage I-VGHIC(5,1), respectively, at a BER of 10^{-3} . At the same BER, the user capacity of the one, two and three-stage I-VGHIC(4,1) decreases by 9%, 41% and 30% respectively. This observation clearly shows that the I-VGHIC requires certain minimum number of subtractive steps to function properly. Once that limit is exceeded, the performance will degrade significantly as in the case of the I-VGHIC(4,1). However, the single-stage I-VGHIC is found to be more tolerant of the imposed limit on the number of subtractive steps than the multi-stage I-VGHIC .

The processing delay of the I-VGHIC and I-VGHIC(m,n) is shown in Figure 4.28 together with that of the SIC. When referring to the processing delay of the I-VGHIC, the maximum or worst case processing delay is plotted. The processing delay is defined as the multiples of the time that a 1-stage PIC requires to complete the detection process. The 1-stage PIC will have a processing delay of 1. The processing delay of the SIC is directly related to the number of users to be detected as it only detects and cancels one user at a time. Note that one subtractive step in the I-VGHIC has a processing delay of 2 because it comprises a PIC and SIC operation (Figure 3.2). The relation between the number of users and the processing delay associated with the I-VGHIC is not as straight forward as for the PIC or SIC, because it varies with the power spread of the received signals. When the signal powers of all users are about the same, there is less delay because there will be more PIC than SIC operations (see (3.10)). This is evident in Figure 4.28 from the curves corresponding to I-VGHIC in Rayleigh fading and AWGN channels. This observation applies to different values of δ . Hence, the processing delay is longer in Rayleigh fading channels.

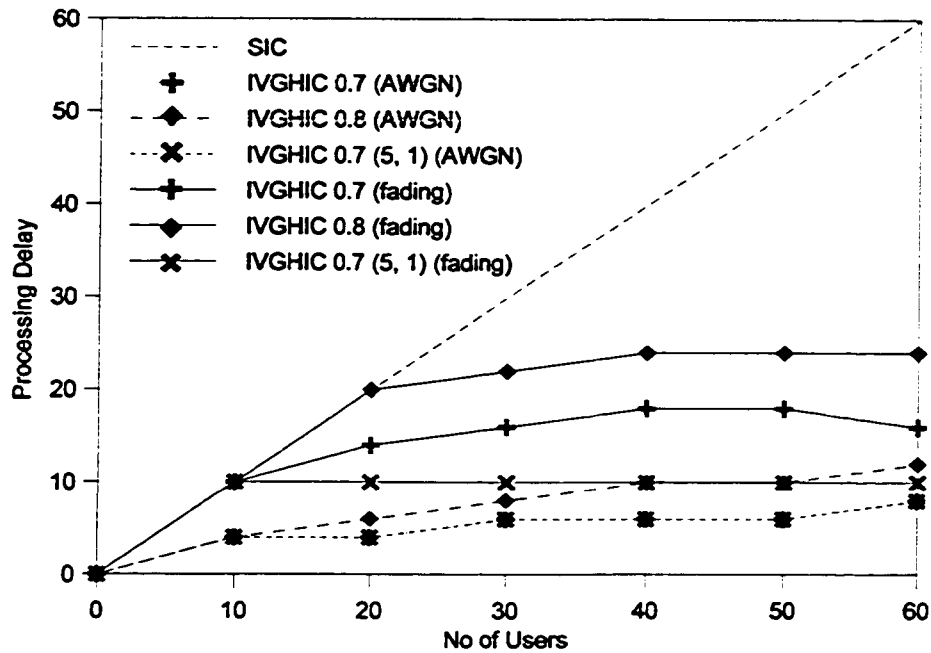


Figure 4.28: Delay profile showing the processing delays of one stage of the SIC, I-VGHIC and I-VGHIC(m,n) (with $\delta = 0.7$ and 0.8) in AWGN and flat Rayleigh fading channels.

One can also notice that for fading channels the I-VGHIC processing delay is the same as that of the SIC when the number of users to be detected is low. The I-VGHIC with $\delta = 0.8$ has the same processing delay as the SIC when the number of users is less than 20. However, when the number of users increases, the processing delay associated with I-VGHIC (with $\delta = 0.8$) reaches a maximum of 24 and remains there regardless of the number of users. For the I-VGHIC with $\delta = 0.7$, the processing delay is shorter as more PIC operations are performed instead of SIC operations (see (3.10)). The processing delay reaches a maximum of only 16. For the I-VGHIC(5,1) with $\delta = 0.7$ the processing delay is limited to a maximum of 10 as expected, since a maximum of five hybrid subtractive steps are allowed. This is a 40% reduction of the processing delay over the standard I-VGHIC with $\delta = 0.7$. The penalty is a drop in user capacity which has been discussed earlier.

For the AWGN channel, the processing delay is much shorter for all cases corresponding to the I-VGHIC with different parameters. The processing delay associated with the I-VGHIC (with $\delta = 0.8$) is at most 12, while for the I-VGHIC (with $\delta = 0.7$) the delay reaches a maximum of only 8. It can be observed that the processing delay of the I-VGHIC(5,1) with

$\delta = 0.7$ and the standard I-VGHIC with $\delta = 0.7$ are exactly the same in the AWGN channel. This is because the number of subtractive steps needed by the standard I-VGHIC in the AWGN channel is smaller than the set limit, and hence, there is no difference between the two versions of the I-VGHIC. Thus, also the BER performance in the AWGN channel will not be affected. Note that the processing delays of both the SIC and the PIC are the same for both AWGN and Rayleigh fading channels.

4.6 Summary

Two methods of ordering the users have been investigated, and it is found that ordering Method 2 is superior to ordering Method 1. However, the computational complexity of Method 2 is higher than that of Method 1. For Method 1, users are ordered after the initial bank of matched filters. Then, the users are directly processed in the order determined. In Method 2, users are ordered at every cancellation step based on the most up-to-date composite signal.

For the receivers using the correlation samples as estimates of signal powers in the signal regeneration and cancellation process, the use of the averaged correlation samples helps to improve the accuracy of the estimates. The effect of averaging length on the various receivers is investigated in the AWGN and Rayleigh fading channel. It has been found that in an AWGN channel, the VGHIC and PIC benefits from this, while the SIC suffers performance loss. For the fading channel, averaging helps to improve the performance of the VGHIC, PIC and SIC. However, there is an optimal averaging length for each receiver. This averaging length is also directly affected by the maximum Doppler shift of the channel.

The multi-stage structure of the VGHIC has also been presented and it is evident from the simulations that the multistage VGHIC provides an overall superior performance over multistage PIC and SIC. In both channels, the VGHIC outperforms the conventional matched filter receiver by a large margin.

An improved version of the variable group hybrid interference cancellation scheme (I-VGHIC) using partial combining of correlation samples and partial cancellation has been proposed. Simulations show that the I-VGHIC outperforms the original VGHIC by a significant margin in the AWGN channel with equal power users. However, the performance increase due to the use of the I-VGHIC in flat Rayleigh fading channel with ineffective power control is not as significant as that in the AWGN channel.

It has been shown that the VGHIC/I-VGHIC exhibits different processing delay profiles depending on the power spread of received signals. The processing delay is shorter when the powers of the user signals are equal as in the AWGN channel. On the other hand, when the powers of the user signals are unequal, the processing delay of the I-VGHIC is longer. This is due to the adaptive nature of the I-VGHIC which adjusts its structure for better detection according to the received signal power spread.

A simple method of limiting the number of subtractive steps of the I-VGHIC has been proposed. It is found that the BER performance of the I-VGHIC degrades significantly when the limit on the number of subtractive steps is too low. Multi-stage I-VGHIC is found to be more sensitive to the imposed limit than the single stage I-VGHIC. However, for a one-stage I-VGHIC, one can reduce the processing delay by 40% sacrificing only 4.5% in user capacity at an uncoded BER of 1×10^{-3} .

From the investigation in this chapter, it has been found and verified that a major advantage of the VGHIC over the other subtractive interference cancellation schemes is that its structure can be changed to suit different performance criteria with a simple change of parameters. This flexibility allows it to outperform other receivers.

Chapter 5: Performance of the VGHIC with non-ideal channel conditions

The variable group hybrid interference cancellation (VGHIC) scheme proposed outperformed both the successive (SIC) and parallel (PIC) interference cancellation in the system with perfect fast power control and the system without fast power control. However, the timing and phase information were assumed to be known. In practical systems, these parameters are estimated and they contain errors. Here, the robustness of the multi-stage VGHIC with that of the matched filter, SIC and PIC in both the AWGN and flat Rayleigh fading channel is compared. The effect of estimation errors on the effectiveness of the multi-stage structure is also studied.

Simulations done in the previous chapters investigate the performance in the flat Rayleigh fading channel. In practical CDMA systems, one usually experience multipath frequency selective fading, and RAKE receivers are usually used to combat or at least mitigate its effect. Therefore, the effect of integrating the I-VGHIC with the RAKE receiver needs to be looked into. This chapter investigates the different ways which the RAKE receiver can be incorporated into the I-VGHIC structure. The effects of different RAKE implementations on the bit error rate (BER) performance in multipath frequency selective fading channels are evaluated.

In Section 5.1, the impacts of the timing and phase estimation errors on the BER performance of different schemes are compared with that of the single stage VGHIC in the AWGN and flat Rayleigh fading channels. Their effects on the multistage structures of the VGHIC, PIC and SIC are studied and the user capacities have also been compared. The RAKE receiver implementations are investigated in Section 5.2 where 3 methods of incorporating the RAKE receiver into the I-VGHIC structure are proposed and studied. Then, the BER performance of the I-VGHIC with different RAKE implementations in four different frequency selective fading channels is presented and discussed.

5.1 Robustness against imperfect channel parameter estimates

To investigate the robustness of the receivers against imperfect channel estimates, an asynchronous single-cell BPSK/CDMA system is considered. The details can be found in Appendix D. However, the processing gain is 32 and there are 10 samples collected per chip, that is, the sampling rate is $4.096 \times 10 \times 10^6$ samples per second. Data bits are not encoded. When estimation errors are introduced into the system, all users will experience the same error.

For the AWGN channel, received signals from all users are equal (perfect fast power control is assumed), while for the flat Rayleigh fading channel, there is no fast power control (or fast power control is assumed to be totally ineffective). The maximum Doppler shift is 100 Hz. Additionally, the effects of path loss and shadowing were assumed to be effectively removed in all cases, and all users had random phase shifts distributed uniformly over $[0, 2\pi)$. For the VGHIC, the design parameter δ is set to 0.8.

5.1.1 BER improvement over the single stage VGHIC with errors

The bit error rate (BER) versus phase estimation error for the conventional matched filter receiver (MF), multi-stage SIC, multi-stage PIC and multi-stage VGHIC are compared with that of the one-stage VGHIC in Figure 5.1. The channel used is AWGN with equal received signal power for all users. The BER improvement over the one-stage VGHIC is defined as

$$BER \text{ improvement (receiver)} = 10 \cdot \log \left(\frac{BER_{VGHIC}}{BER_{receiver}} \right) \text{ dB} \quad (5.1)$$

where BER_{VGHIC} is the BER of the reference one-stage VGHIC. If the BER improvement factor for a certain receiver is positive, it means that its BER performance is better (lower BER) than that of the one-stage VGHIC.

As shown in Figure 5.1, only the MF and one-stage SIC perform worse than the one-stage VGHIC. It is interesting to note that while the single stage VGHIC outperforms the single stage SIC, the multi-stage VGHIC has slightly worse performance than the multi-stage SIC. The BER performance versus phase estimation error in the flat Rayleigh fading channel is presented in Figure 5.3. The situation in this case is quite different from the AWGN case, only the multi-stage VGHIC and SIC are able to outperform the one-stage VGHIC. Even the three-stage PIC is not as effective as the single stage VGHIC, although the PIC still outperforms the conventional MF. Furthermore, for the multi-stage VGHIC and SIC, there is insignificant BER improvement beyond the 2 stages. It should be noted that the BER versus timing errors has similar behaviour for the AWGN and fading channel because we are comparing relative performance between different receiver structures.

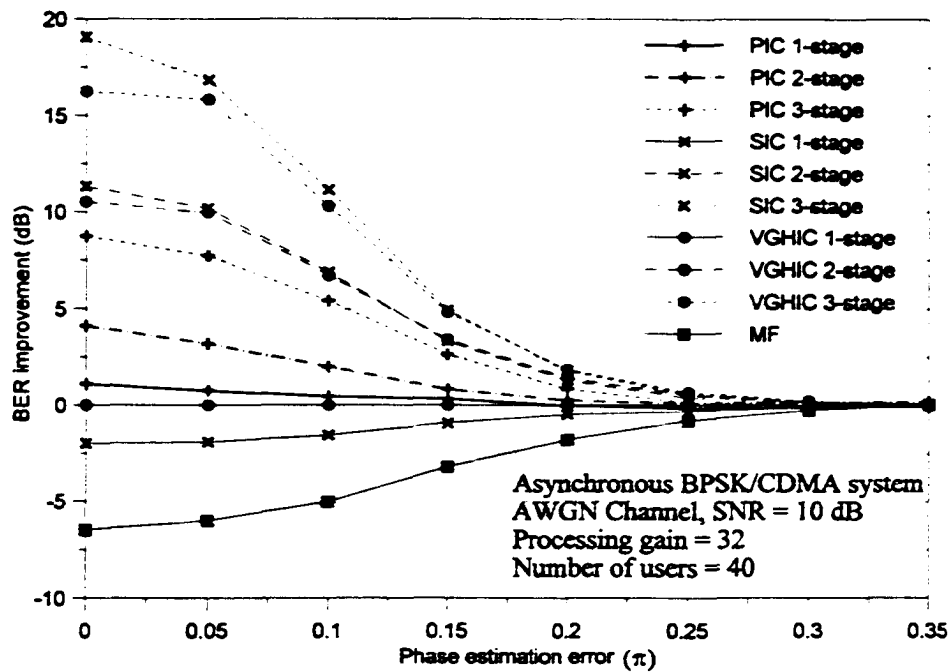


Figure 5.1: BER improvement versus phase estimation error for various receivers in an AWGN channel.

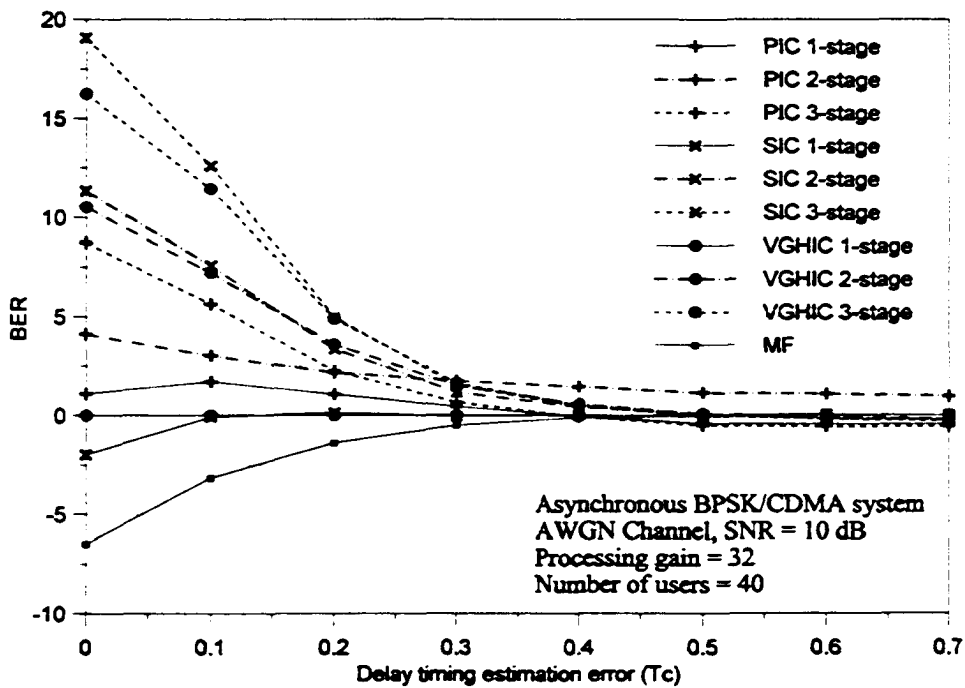


Figure 5.2: BER improvement versus delay timing estimation error for various receivers in AWGN channel.

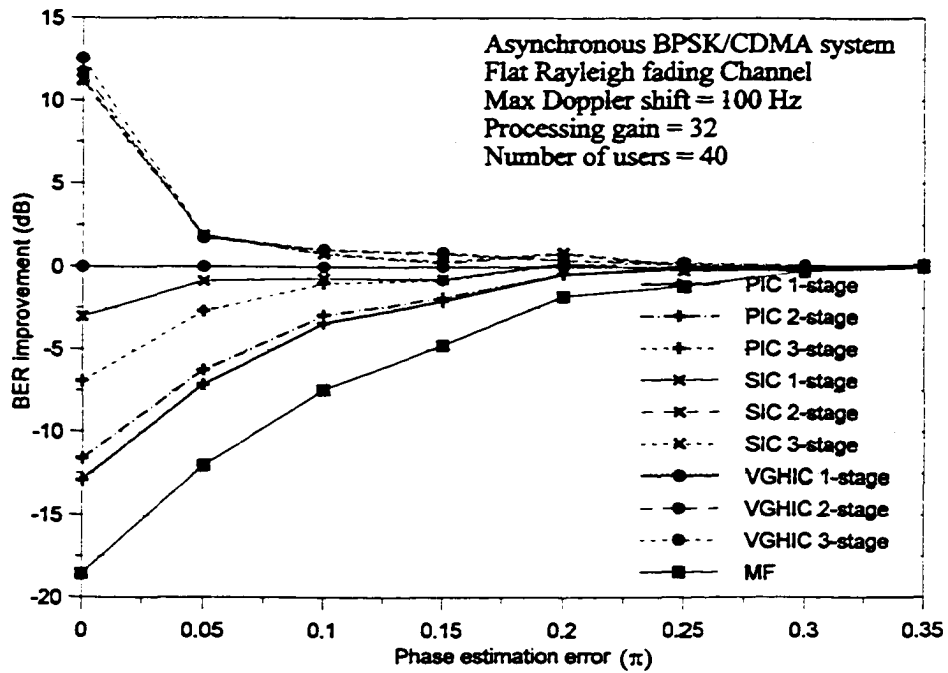


Figure 5.3: BER improvement versus phase estimation error for various receivers in a flat Rayleigh fading channel.

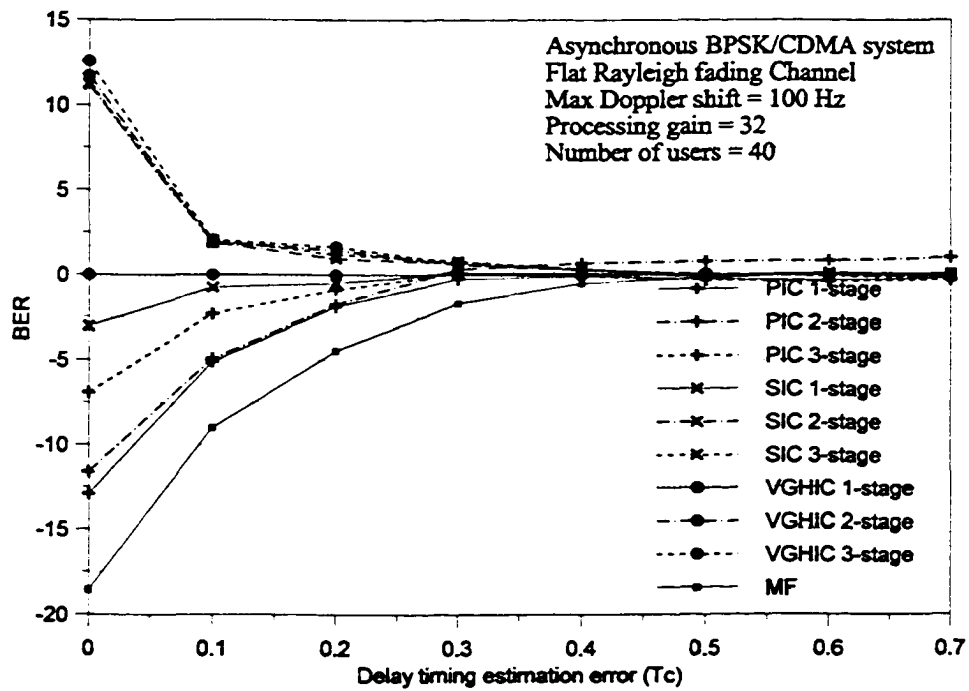


Figure 5.4: BER improvement versus delay timing estimation error for various receivers in flat Rayleigh fading channel.

5.1.2 BER degradation on the multi-stage structures

To investigate the effect of the phase and timing errors on the BER of the single and multi-stage VGHIC, we modify (5.1) to

$$BER \text{ degradation (with estimation error)} = 10 \cdot \log \left(\frac{BER_{no \text{ errors}}}{BER_{with \text{ estimation error}}} \right) \text{ dB} \quad (5.2)$$

A negative value for (5.2) indicates that the BER is higher than the reference BER when there are no estimation errors.

Figure 5.5 shows the BER degradation versus the percentage estimation errors for the multi-stage VGHIC in the AWGN channel. The curves corresponding to the 2-stage and 3-stage VGHIC drop off much faster than that of the 1-stage VGHIC. This indicates that the multi-stage structure is more sensitive to estimation errors than the single stage one. However, this does not mean that the multi-stage structure has worse BER performance. Even though the multi-stage VGHIC is more sensitive to estimation errors it still outperforms the single stage VGHIC as shown in Figure 5.1. Another observation is that the VGHIC is more tolerant to phase errors than to timing errors. For a 30% error in the phase estimation, the BER degradation is 4 dB, while the same error in timing estimation results in a BER degradation of 9 dB for the 1-stage VGHIC. For the flat Rayleigh fading channel, the BER degradation versus the percentage estimation errors for the multi-stage VGHIC is presented in Figure 5.6. In this case, the observations are similar. The main difference is that the BER degradation for the 2-stage and 3-stage VGHIC is almost the same in a fading channel, whereas in the AWGN channel the BER degradation is greater for the 3-stage VGHIC when compared with the 2-stage VGHIC. Looking at Figure 5.7 and Figure 5.8 for the SIC, one notices similar behaviours.

For the PIC, it experiences more severe degradation for the first stage than the VGHIC and SIC in the AWGN channel in Figure 5.9. The degradation for the second stage is not as large as that of the VGHIC and SIC. However, there is a large reduction of performance for the third stage and this is different from that of the VGHIC and SIC. The situation in the

Rayleigh fading channel is also similar for the PIC in Figure 5.10 and the degradation looks almost linearly proportional to the error. This is different from that of the VGHIC and SIC where the performance drop is quite rapid at first and the rate of degradation slows down as the error increases further.

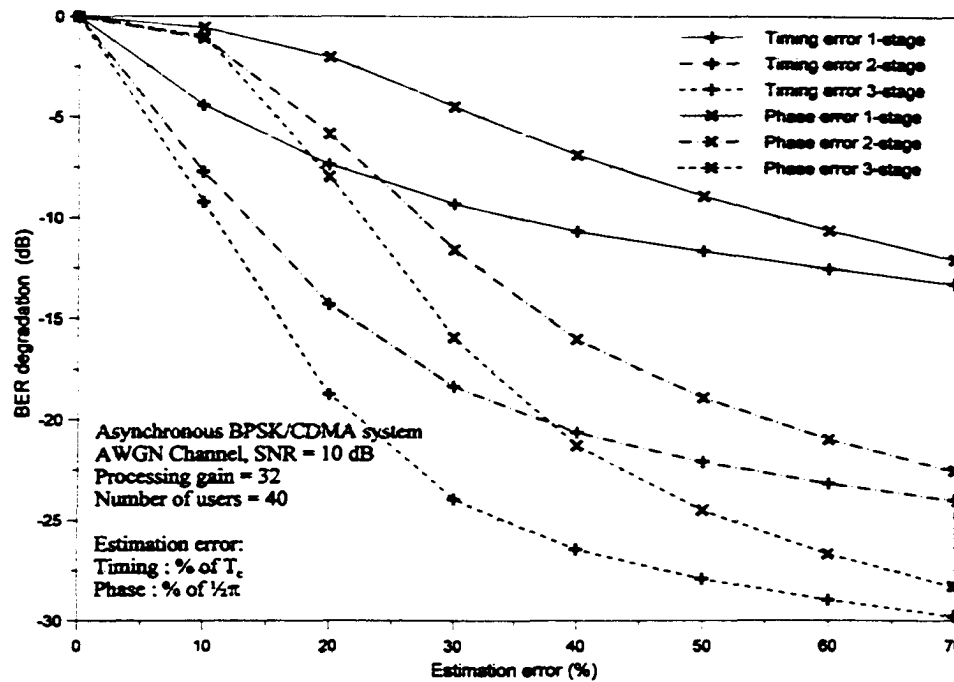


Figure 5.5: BER degradation versus phase and timing estimation errors for the multi-stage VGHIC in AWGN channel.

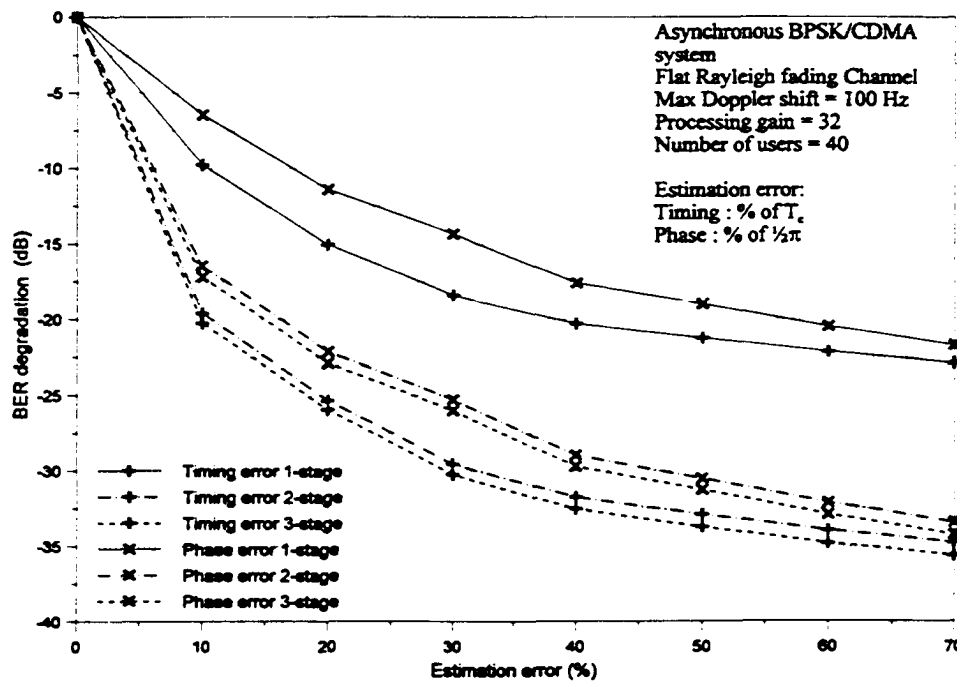


Figure 5.6: BER degradation versus phase and timing estimation errors for the multi-stage VGHIC in flat Rayleigh fading channel.

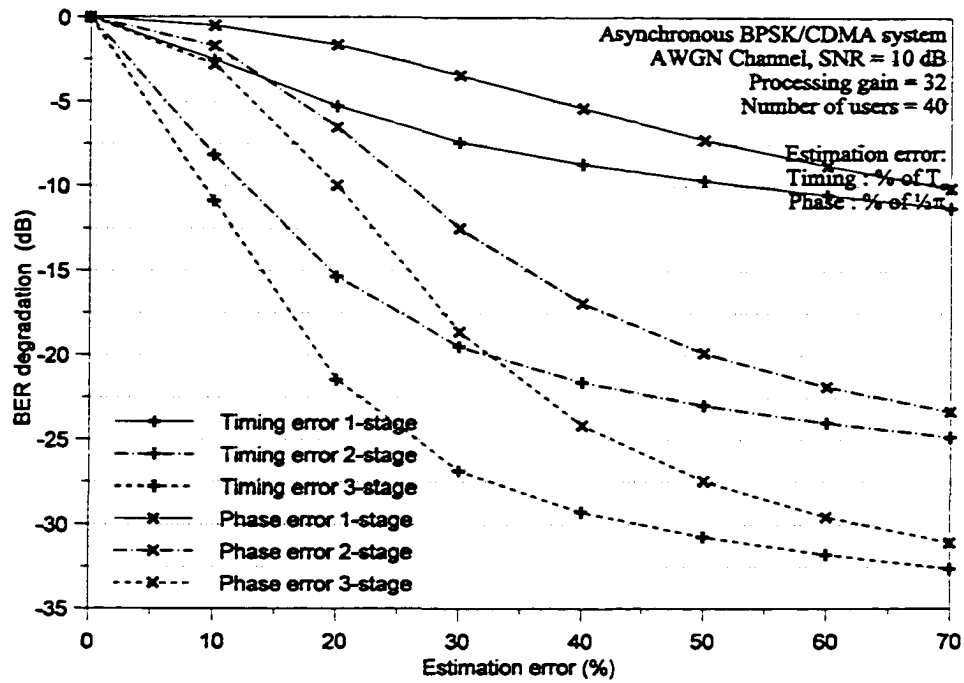


Figure 5.7: BER degradation versus phase and timing estimation errors for the multi-stage SIC in AWGN channel.

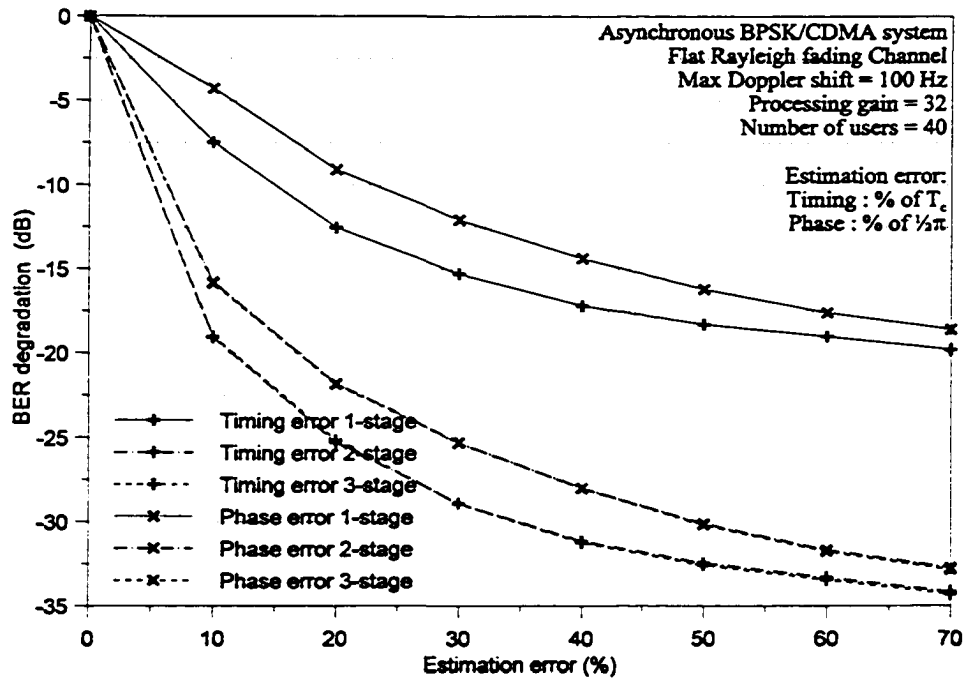


Figure 5.8: BER degradation versus phase and timing estimation errors for the multi-stage SIC in flat Rayleigh fading channel.

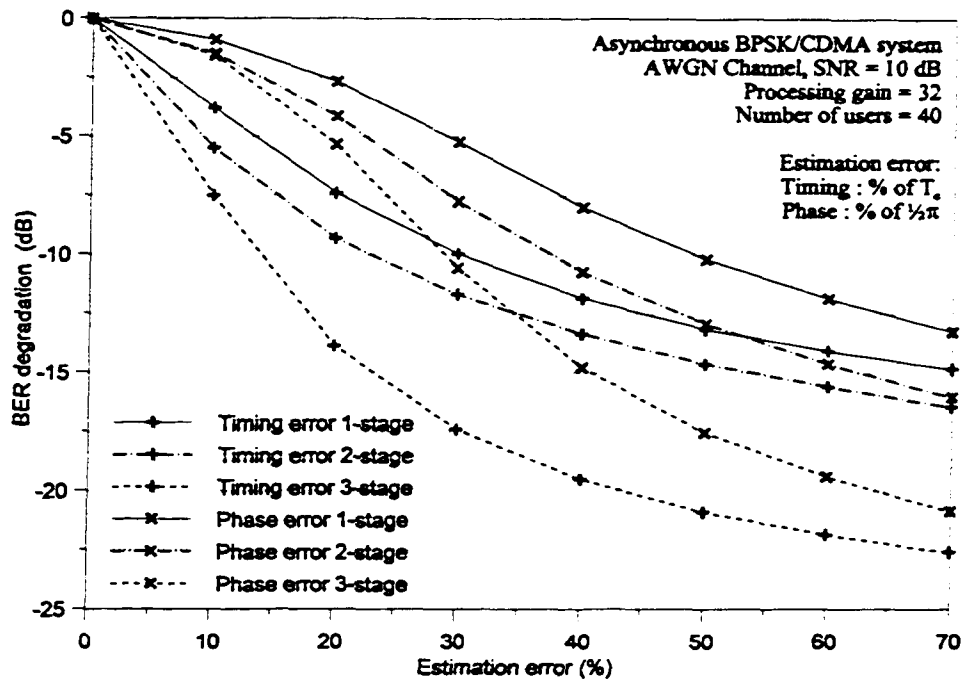


Figure 5.9: BER degradation versus phase and timing estimation errors for the multi-stage PIC in AWGN channel.

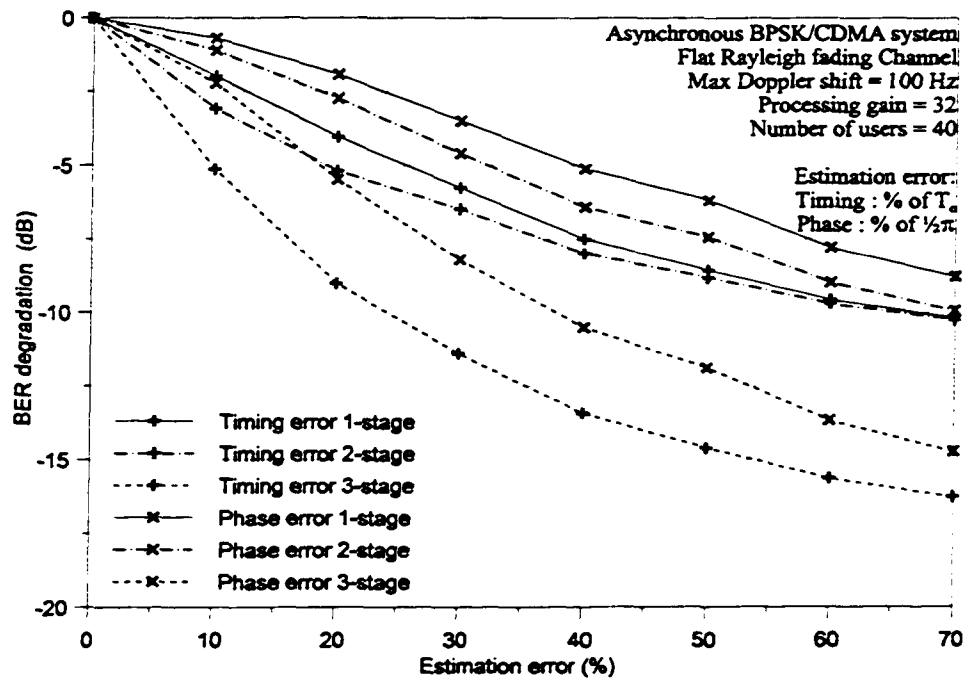


Figure 5.10: BER degradation versus phase and timing estimation errors for the multi-stage PIC in flat Rayleigh fading channel.

5.1.3 Capacity comparison

For the AWGN channel, at a BER of 1×10^{-2} , there is a significant jump in the user capacity (100%) when going from a single stage VGHIC to the 2-stage VGHIC in Figure 5.11 and Figure 5.12. The capacity increases by another 40% with the use of the 3-stage structure. When estimation error increases, the 2-stage VGHIC is still able to provide the same amount of relative gain over that of the single stage VGHIC. However, this is not the case with the 3-stage VGHIC as its capacity decreases much more rapidly. The same can be observed for the SIC. The capacity increase by using a 2-stage SIC is close 200% more than that of a single stage SIC. However, as shown in the previous sections, the SIC has much longer processing delay than the VGHIC or PIC. As for the PIC the multi-stage PIC is able to maintain a constant relative capacity gain between each cancellation stage as the error increases.

Referring to Figure 5.13 and Figure 5.14 in the fading channel, one can notice that when the level of error is high, there is no gain in the capacity by the use the multi-stage VGHIC. This point corresponds to a timing and phase error of $0.1T_c$ and 0.08π , respectively. This is also true for the SIC. Comparing between the VGHIC and SIC, the VGHIC has about 10% more user capacity when the error is low. With increasing error, this capacity advantage is eroded away. When the timing and phase error reach $0.1T_c$ and 0.08π respectively, both the VGHIC and SIC have the same user capacity. Beyond this point, the SIC has a slight capacity advantage over the VGHIC. The multi-stage PIC has the lowest user capacity among the receivers. The 3-stage PIC has been outperformed by the single stage VGHIC by as much as 50% in user capacity for a BER of 1×10^{-2} .

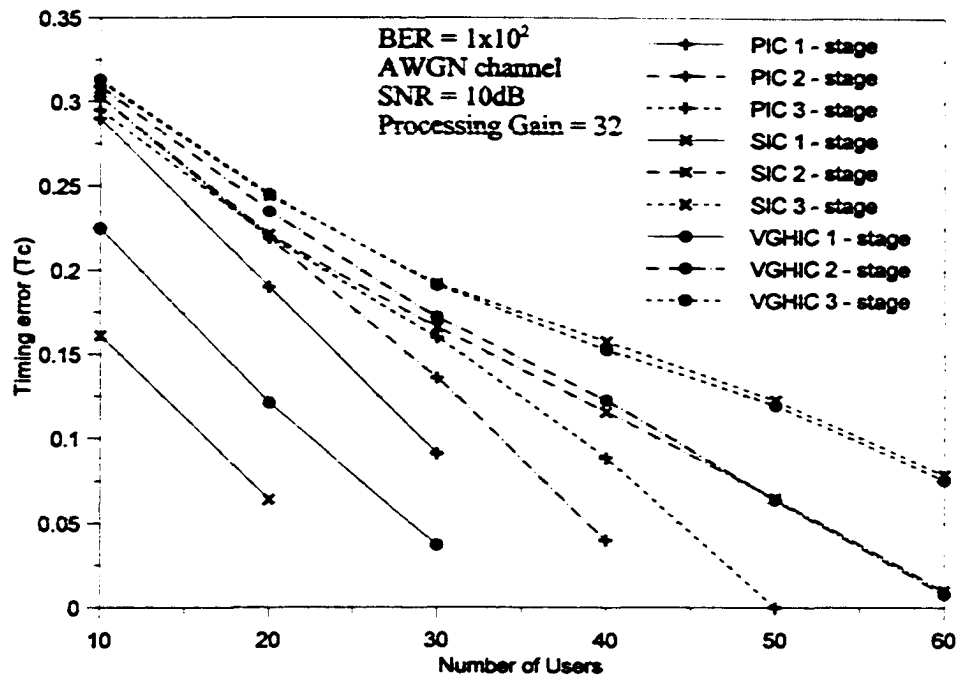


Figure 5.11: User capacity of the multi-stage PIC, SIC and VGHIC with the timing error in AWGN channel.

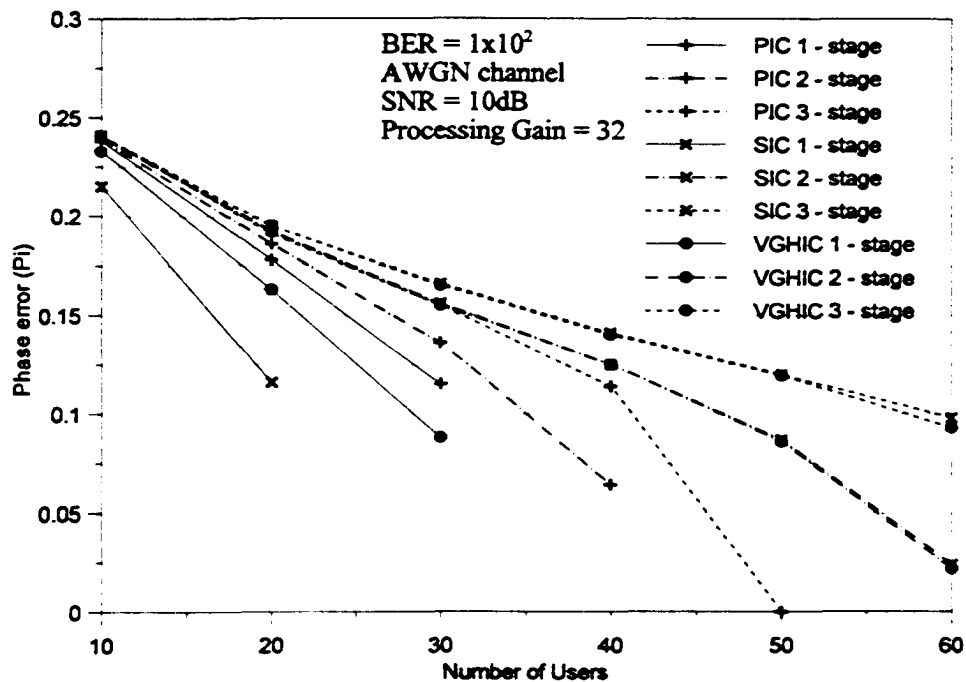


Figure 5.12: User capacity of the multi-stage PIC, SIC and VGHIC with the phase error in AWGN channel.

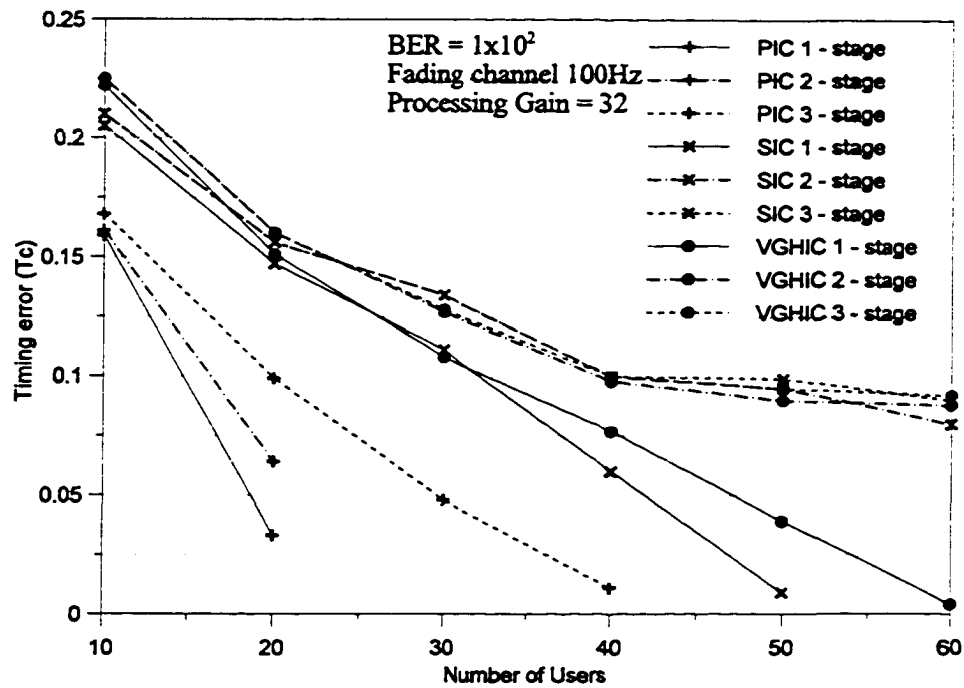


Figure 5.13: User capacity of the multi-stage PIC, SIC and VGHIC with the timing error in Rayleigh fading channel.

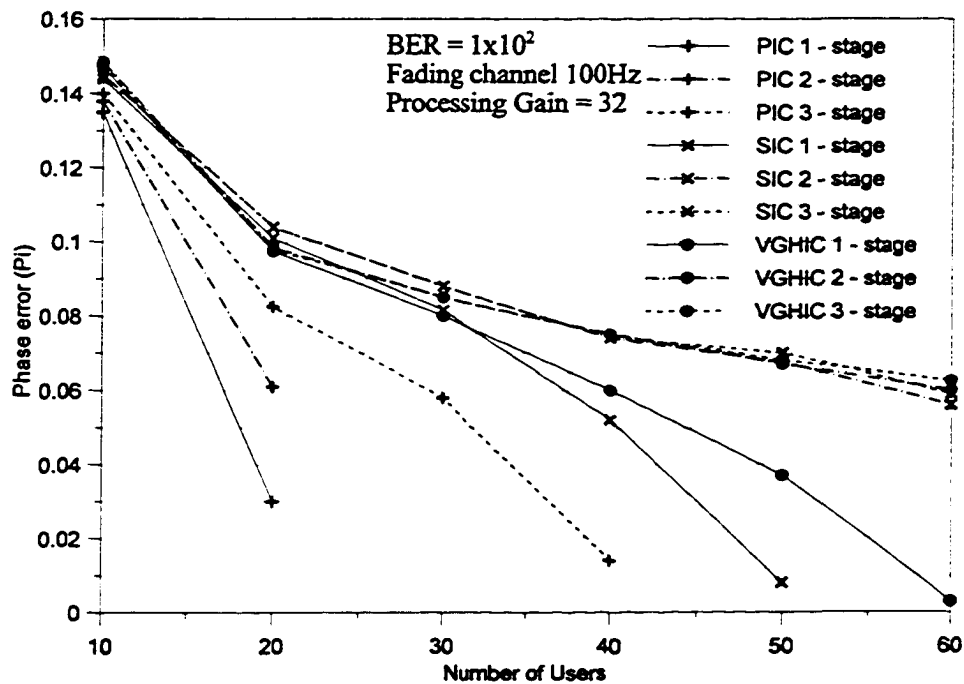


Figure 5.14: User capacity of the multi-stage PIC, SIC and VGHIC with the phase error in Rayleigh fading channel.

5.2 RAKE receiver implementations

In this section, the basic RAKE receiver is presented first. Then, the three methods through which RAKE receivers can be integrated into the multistage I-VGHIC are described. Structurally the I-VGHIC is the same as the VGHIC, hence, what applies to the I-VGHIC is also applicable to the VGHIC.

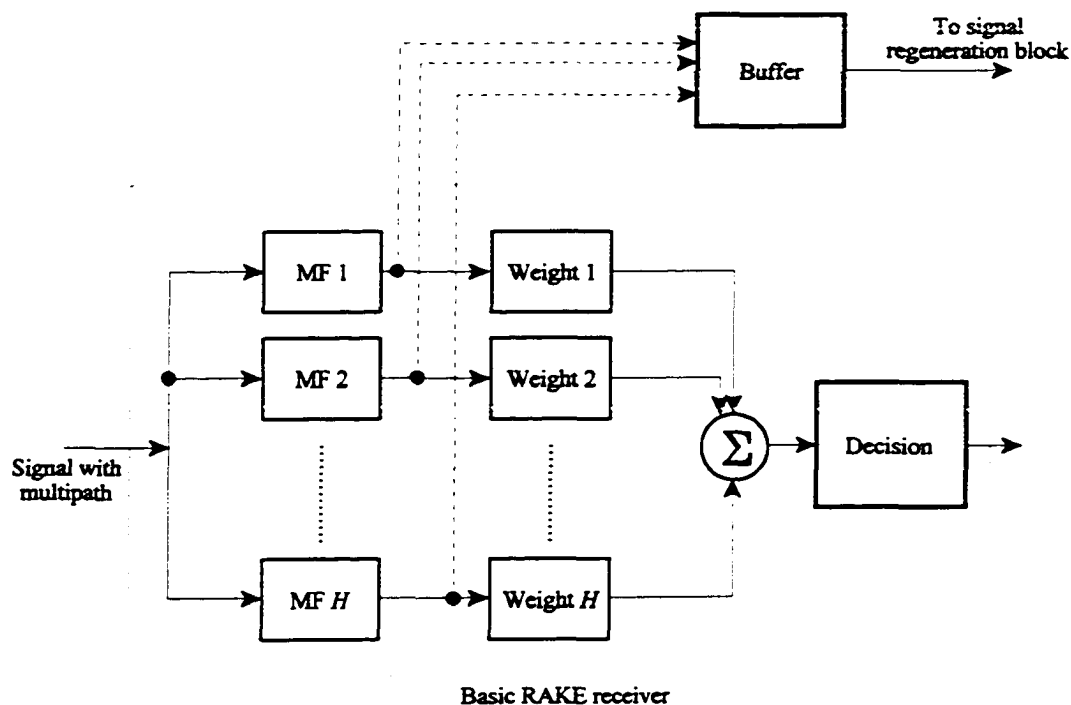


Figure 5.15: A H -finger RAKE receiver

The basic RAKE receiver is shown in Figure 5.15. Each resolvable multipath component of the signal is detected by a different RAKE finger⁴. The outputs of the matched filters (MFs) are weighted and combined, so that a better estimate of the signal can be achieved. Since the receiver employs coherent detection, maximum ratio combining is used. Hence,

⁴ For the brevity of presentation, the number of RAKE fingers is assumed to be the same as the number of resolvable paths. Very often these two are not the same.

the weights are proportional to the signal strength at the output of the RAKE fingers [123]. Note that the outputs of the fingers are stored in a buffer so that they can be used as estimates of signal amplitudes on different paths in the signal regeneration blocks of the I-VGHIC during the cancellation process in Method 1 and 3.

5.2.1 Various configurations

Method 1

This is a straightforward implementation of the RAKE receiver in the I-VGHIC structure where one hopes to improve the performance of the RAKE receiver by reducing the interference from other users. The RAKE receiver shown in Figure 5.15 replaces all the matched filters in the I-VGHIC. However, the structure of the parallel interference cancellation block needs to be modified slightly to accommodate the RAKE receivers. The modified structure is shown in Figure 5.16. In the signal regeneration block of Figure 3.2 and Figure 5.16, the multipath signals are regenerated based on matched filter outputs of each of the RAKE fingers. These RAKE finger outputs are stored in buffers (Figure 5.15) when the multipath signals are detected in the previous cancellation stage. If this is the first cancellation stage, the outputs are simply those of a conventional RAKE receiver. In this method, the regenerated signals corresponding to individual paths captured by the RAKE fingers are added (with their original phases and time delays preserved) before the actual subtraction. Hence, self-interference among different path signals of the same user is not cancelled. Let the I-VGHIC with this implementation of RAKE receiver be I-VGHIC-M1 so that reference to this method can be made easily when comparing the performance in the following sections.

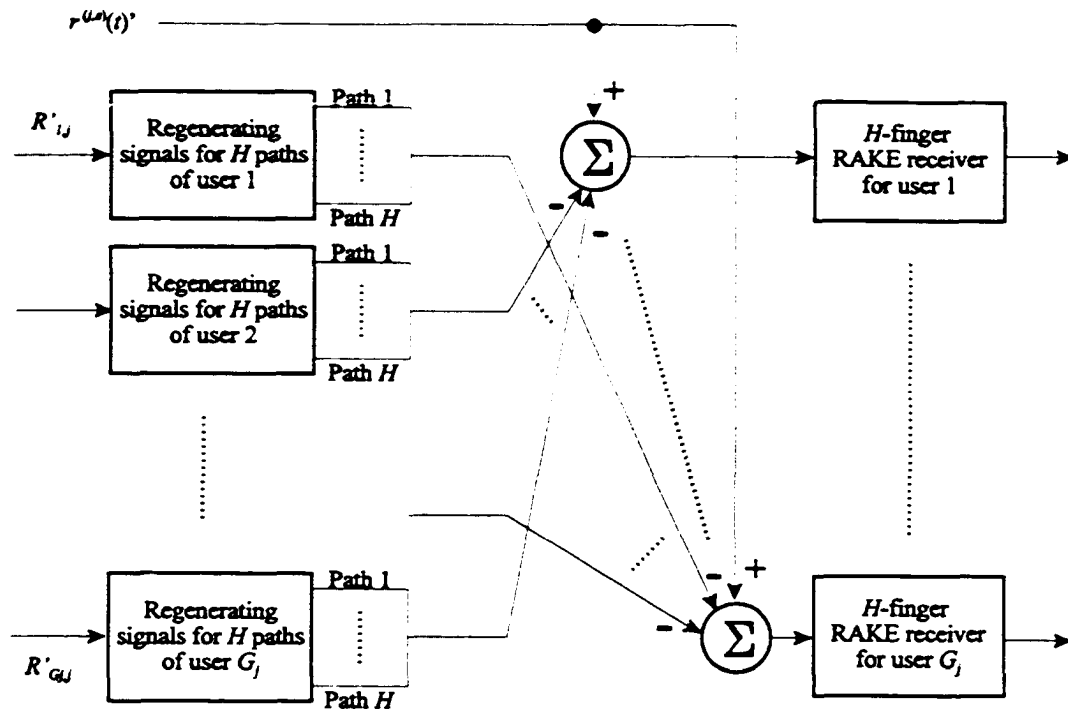


Figure 5.16: Modified parallel interference cancellation (PIC) with RAKE receivers

Method 2

Alternatively, one can treat every resolvable multipath component (intended to be captured by a RAKE finger) of each user signal as an individual and independent signal belonging to a distinct “transmitter” in the interference cancellation process. In this way, the self- and multiuser- interference on individual multipath components of the same user will be reduced. With a cleaner signal for each finger of the RAKE receiver, its overall performance could be improved. The structure of the I-VGHIC remains the same, although in this case, the resolvable multipath signals are despread, regenerated and subtracted separately. In this case, the number of “transmitters” is equal to number of RAKE fingers multiplied by the number of actual users. After the last stage of interference cancellation, the multipath components of each user are then combined and detected as in a conventional RAKE receiver (Figure 5.15). The I-VGHIC with this structure is denoted as I-VGHIC-M2.

Method 3

This method is a combination of the previous two approaches. The idea is to use Method 2 for the first stage of interference cancellation, and then Method 1 for the subsequent stages. The reason for the proposal of this structure will become clear when the simulation results are discussed later. To avoid confusion, the group cancellation units corresponding to Method 1 and Method 2 are denoted by $GCU_1(j_1, s)$ and $GCU_2(j_2, s)$, respectively. The indices j_1 and j_2 denote the cancellation group number for each respective method, and they are different. The multistage structure of the I-VGHIC for Method 3 or I-VGHIC-M3 is illustrated in Figure 5.17.

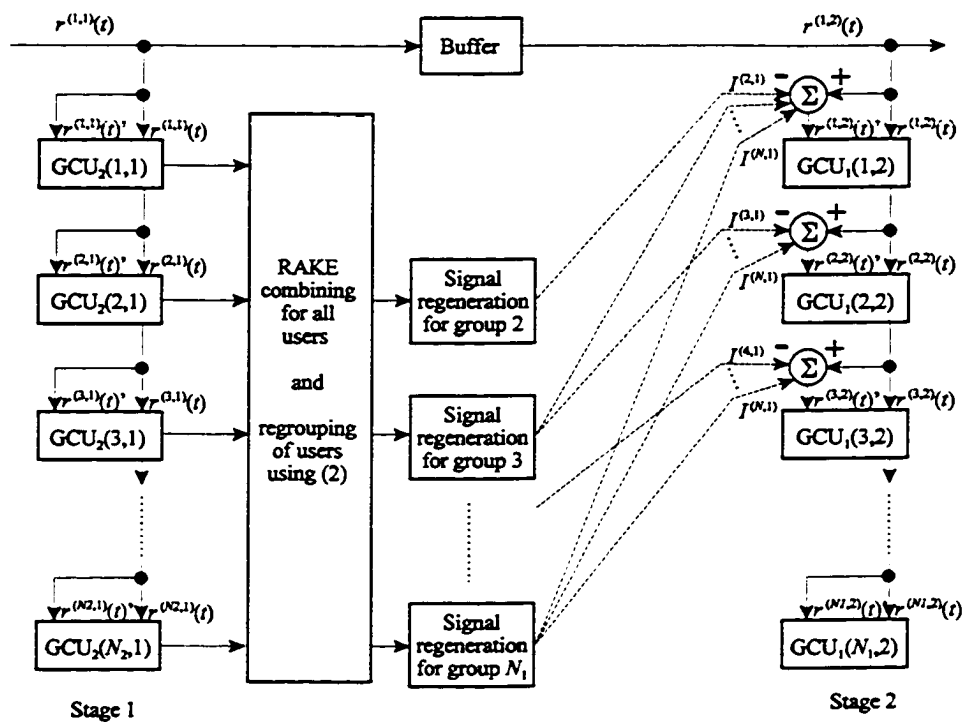


Figure 5.17: Structure of the multistage I-VGHIC-M3

After the multipath components of all users are detected individually in stage 1 (using Method 2), the corresponding multipath components of each user are combined to produce an overall correlation sample for each user. Following that, the users are grouped using

selection rule (3.10) based on the overall correlation sample. Then, signals of different groups of users are generated to be used in the next cancellation stage (using Method 1). Note that the number of user groups in stage 1 (N_1) is different from that in stage 2 (N_2). However, from stage 2 onwards the number of user groups is the same as they use the same cancellation scheme.

5.2.2 The simulation system

The simulation system considered was an asynchronous single-cell BPSK/CDMA system. The processing gain was 32, and all the users were transmitting simultaneously. All interference cancellation was done on 30-bit blocks, and the average correlation sample values over 30 bits were used for the estimation of the signal power of each multipath component. Furthermore, the chip rate was set at 4.096 Mcps (megachips per second) and the data were sent in continuous blocks of 10 ms. There were 5 samples collected per chip, that is, the sampling rate was $4.096 \times 5 \times 10^6$ samples per second.

The BER performance is investigated for 4 different multipath frequency selective fading channels [124]. These channel impulse response models are reproduced in Table 5.1. Channel A is the low delay spread case that occurs 40% of the time while Channel B is the medium delay spread case which occurs 55% of the time. With a chip rate of 4.096 Mcps, not all multipath components can be resolved and captured by the RAKE fingers. The unresolvable paths are shaded and will not be captured by the RAKE receivers in all simulations. However, their self-interference effect is accounted for. The carrier frequency is 2 GHz. Furthermore, the relative delays used in simulations are integer multiples of the sampling period and they are not exactly equal to the values shown. Except for path 2 of the pedestrian channel A (for which the difference is about 11%), the delays used in simulations are within 5% of Table 5.1.

Table 5.1: Channel impulse response parameters

Path	Pedestrian (3 km/h)				Vehicular (120 km/h)			
	Channel A		Channel B		Channel A		Channel B	
	Relative delay (ns)	Average power (dB)	Relative delay (ns)	Average power (dB)	Relative delay (ns)	Average power (dB)	Relative delay (ns)	Average power (dB)
1	0	0	0	0	0	0	0	-2.5
2	110	-9.7	200	-9	310	-1	300	0
3	190	-19.2	800	-4.9	710	-9	8 900	-12.8
4	410	-22.8	1 200	-8	1 090	-10	12 900	-10
5	-	-	2 300	-7.8	1 730	-15	17 100	-25.2
6	-	-	3 700	-23.9	2 510	-20	20 000	-16

Data bits are not encoded. Long random spreading sequences are used in all simulations. Additionally, the effects of path loss and shadowing are assumed to be effectively removed in all cases, and all users have random phase shifts distributed uniformly over $[0, 2\pi)$. Lastly, no white Gaussian noise is added to the system.

5.2.3 Performance comparison

This section presents and discusses the simulation results obtained for the multipath frequency selective fading channels described in Table 5.1. First, the performance of the conventional matched filter (MF) RAKE receiver without interference cancellation is discussed. Then, the performance of the multistage I-VGHIC-M1 and I-VGHIC-M2 are compared. At this point, the reason for the proposal of I-VGHIC-M3 is highlighted, and its performance is compared with the other 2 schemes. Finally, some general observations about the I-VGHIC with RAKE receivers are presented.

Referring to Figure 5.18 for the case of a pedestrian moving at 3km/h in a low delay spread environment, the conventional MF RAKE receiver with 2 fingers actually performs worse

than a single matched filter (MF). This is because the signal strength of the resolvable second path is much lower (-22.8 dB; see Table 5.1), and hence its detection is very unreliable. As a result, when this path is used, the performance of the MF RAKE receiver degrades. With interference cancellation, there is almost no degradation in performance. For the medium delay spread case with slow moving mobile (Figure 5.19), the RAKE receiver performance improves accordingly when the number of fingers increases from 1 to 4. However, the performance gain from increasing the fingers diminishes especially when the number of users is high. In this case, I-VGHIC-M1 and I-VGHIC-M2 behave similarly to the MF RAKE receiver. The only difference between them is that interference cancellation RAKEs are consistently outperforming the MF RAKE receiver. Looking at the case where the mobile speed is high (Figure 5.20 and Figure 5.21), the 4-finger MF RAKE receiver is not any better than the 2-finger MF RAKE receiver. In fact, when the number of users is high, it actually performs worse. On the other hand, the performance of the 1-stage I-VGHIC-M1 and I-VGHIC-M2 is significantly better, although the 1-stage I-VGHIC-M1 with 4 RAKE fingers is worse than the 2-finger I-VGHIC-M1. From the above observations, we can safely conclude that RAKE receiver with interference cancellation is much more robust than the conventional RAKE receiver in most situations.

Comparing the 1-stage I-VGHIC-M1 and I-VGHIC-M2 in Figure 5.18 to Figure 5.21, the 1-stage I-VGHIC-M2 has better performance. This is because the weaker paths now produce more reliable despread samples due to the interference cancellation process of the I-VGHIC structure. However, looking at the performance of the 2-stage I-VGHIC-M1 and I-VGHIC-M2 in Figure 5.22 to Figure 5.25, the opposite is true. The 2-stage I-VGHIC-M1 actually outperforms the I-VGHIC-M2 especially for the case with 4 RAKE fingers (Figure 5.24 and Figure 5.25). This means that the performance gain from increasing the number of cancellation stages is higher in I-VGHIC-M1 than I-VGHIC-M2. This brings us to the idea behind the proposal of the I-VGHIC-M3. As the first stage of the I-VGHIC-M2 is more effective than that of the I-VGHIC-M1, it's used as the first stage in the I-VGHIC-M3. Then, the structure of the I-VGHIC-M1 is used in the second and subsequent cancellation stages of the I-VGHIC-M3. The performance of the resulting I-VGHIC-M3 can be seen in Figure

5.22 to Figure 5.25. Its performance is the best of the 3 schemes although for the case with 1 and 2 RAKE fingers, there is only a marginal improvement.

There are a few interesting observations one can make from the simulation results. Firstly, for a 1-finger I-VGHIC, regardless of how many cancellation stages, the BER performance stays the same. Then, for the rapidly fading case (Vehicular channel A and B), the 2- and 4-finger I-VGHIC actually performs better than in the relatively slow fading case (Pedestrian channel A and B). To provide a raw BER of 1×10^{-2} (which corresponds to a BER of lower than 1×10^{-6} if coding is used [125]), the 2-stage 2-finger I-VGHIC-M3 can only support up to 5 users in the Pedestrian Channel B environment, but in Vehicular Channel A (with similar delay spread) it is able to support up to 35 users. However, the fast power control present in commercial CDMA systems should be effective in compensating for the relatively slow fading rate of the Pedestrian A and B channels. This would increase the performance of the receiver and hence, the user capacity. Apart from pedestrian A channel, the use of more RAKE fingers in the I-VGHIC will lead to a better BER performance. This is not the case with the conventional RAKE receiver. For the four simulated conditions, the optimum number of fingers for the conventional RAKE receiver for investigated channels is 2. There is no performance gain when the number is increased to 4.

It is evident from the simulation results that the use of the RAKE receiver with interference cancellation can increase the user capacity of the CDMA system considerably. However, the actual degree of increase will depend on the number of RAKE fingers used, the nature of the channel and the number of cancellation stages.

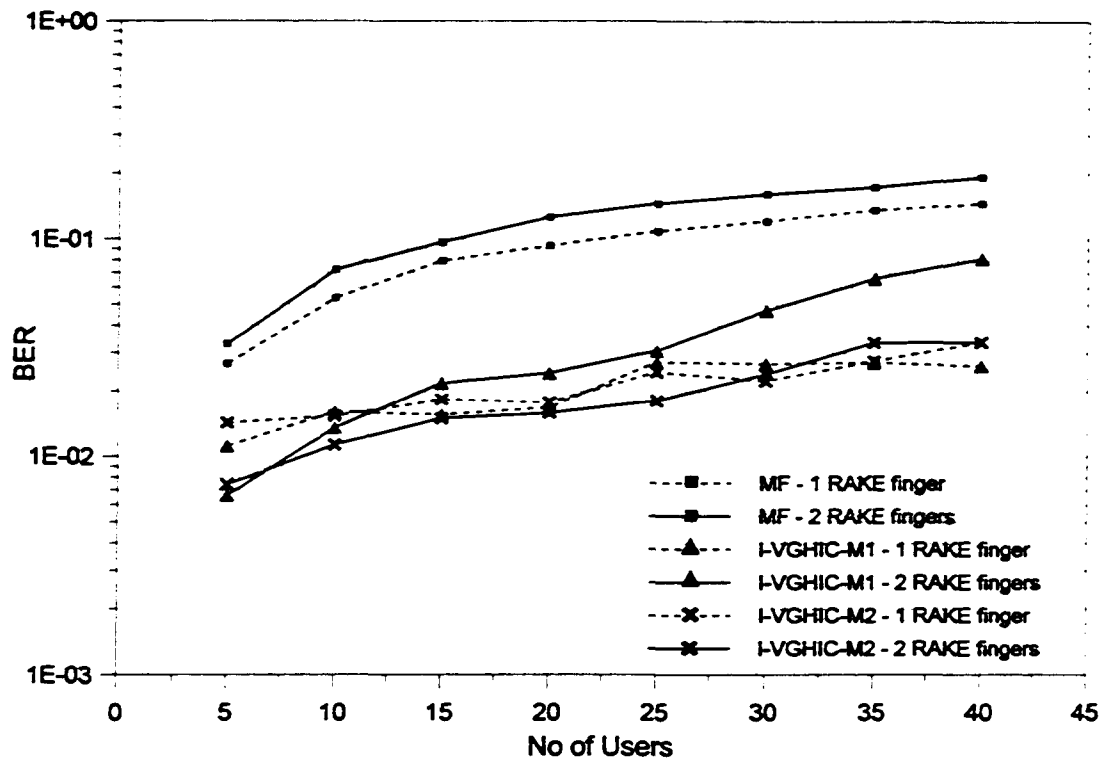


Figure 5.18: Pedestrian (3 km/h) - Channel A: 1-stage I-VGHIC

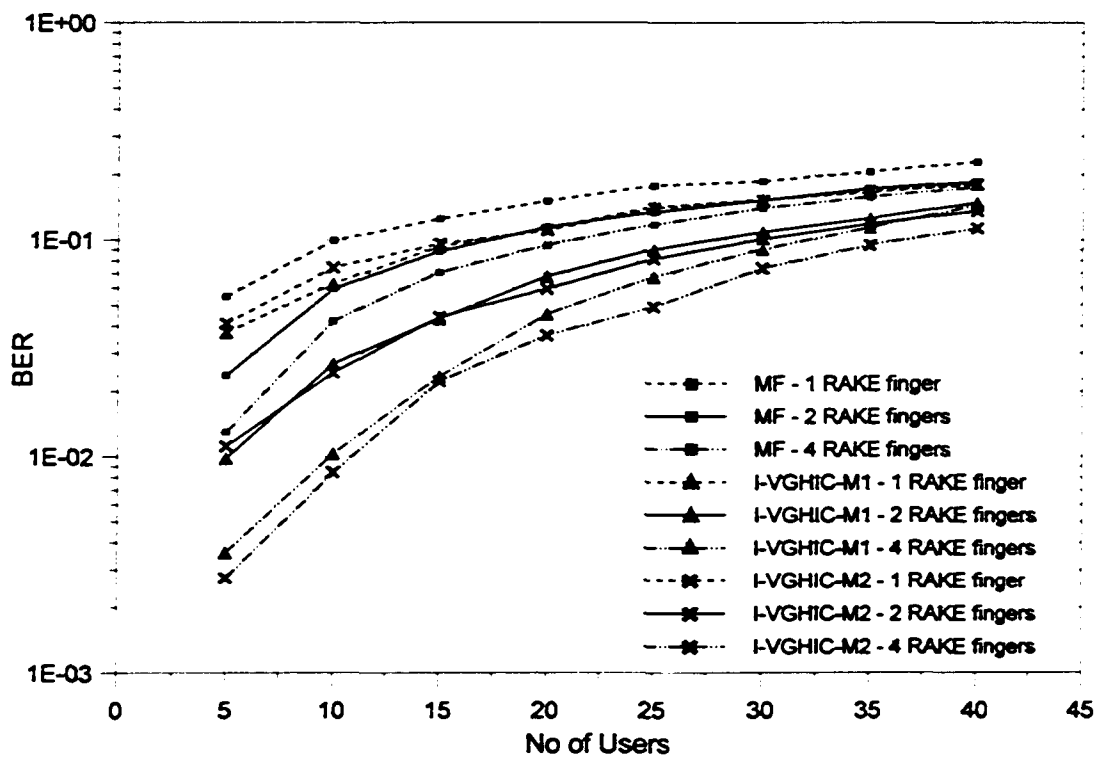


Figure 5.19: Pedestrian (3 km/h) - Channel B: 1-stage I-VGHIC

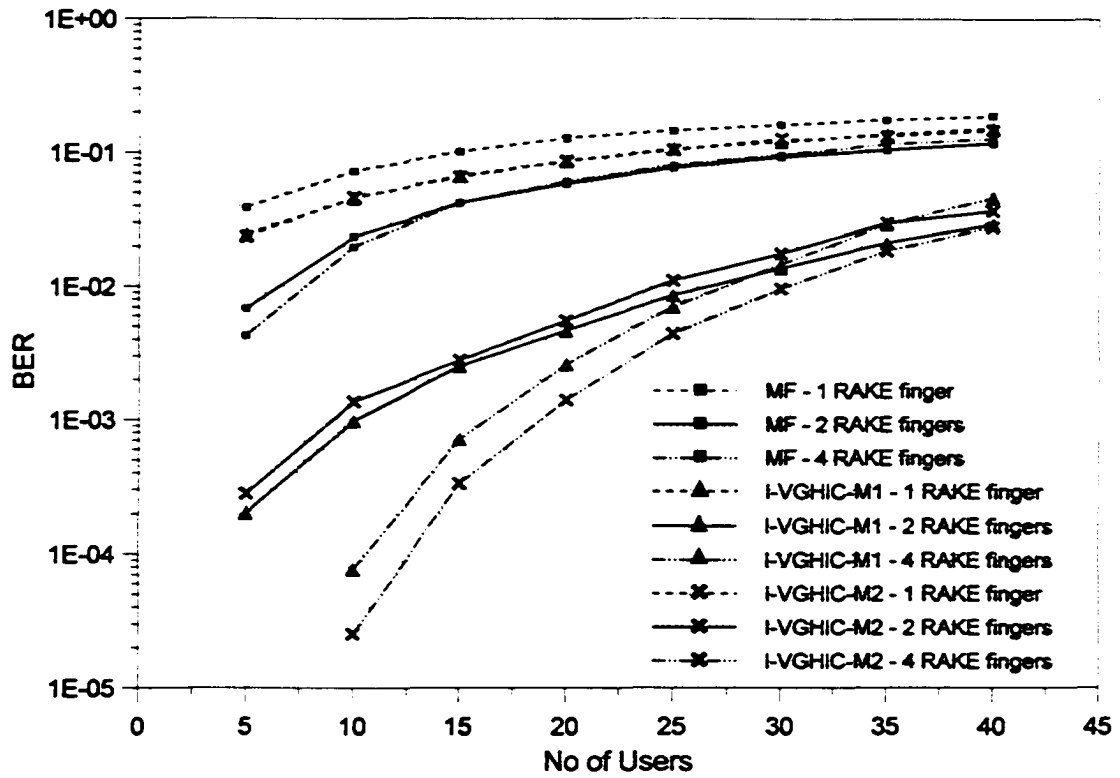


Figure 5.20: Vehicular (120 km/h) - Channel A: 1-stage I-VGHIC

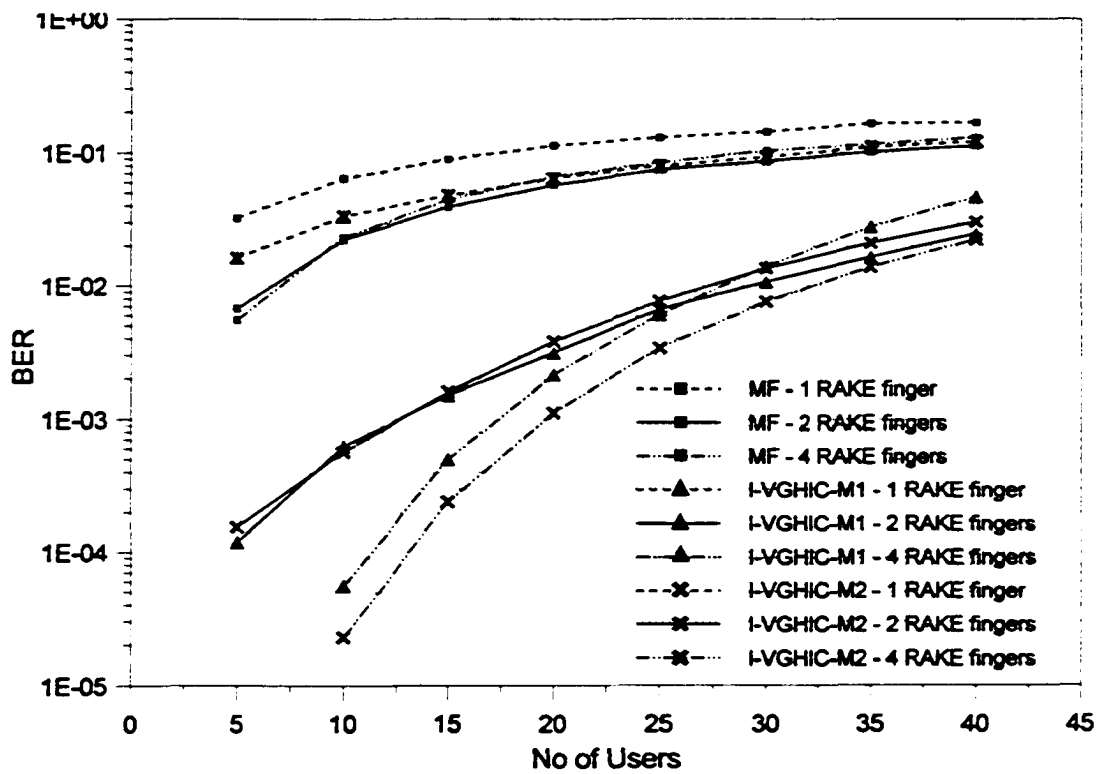


Figure 5.21: Vehicular (120 km/h) - Channel B: 1-stage I-VGHIC

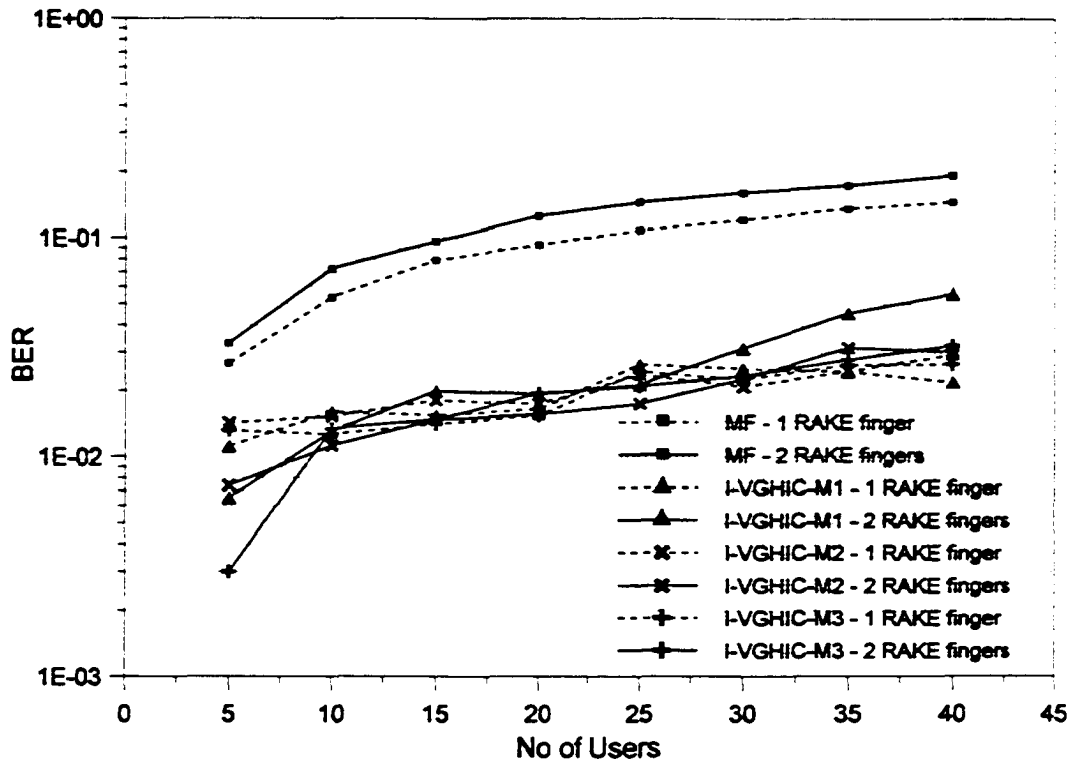


Figure 5.22: Pedestrian (3 km/h) - Channel A: 2-stage I-VGHIC

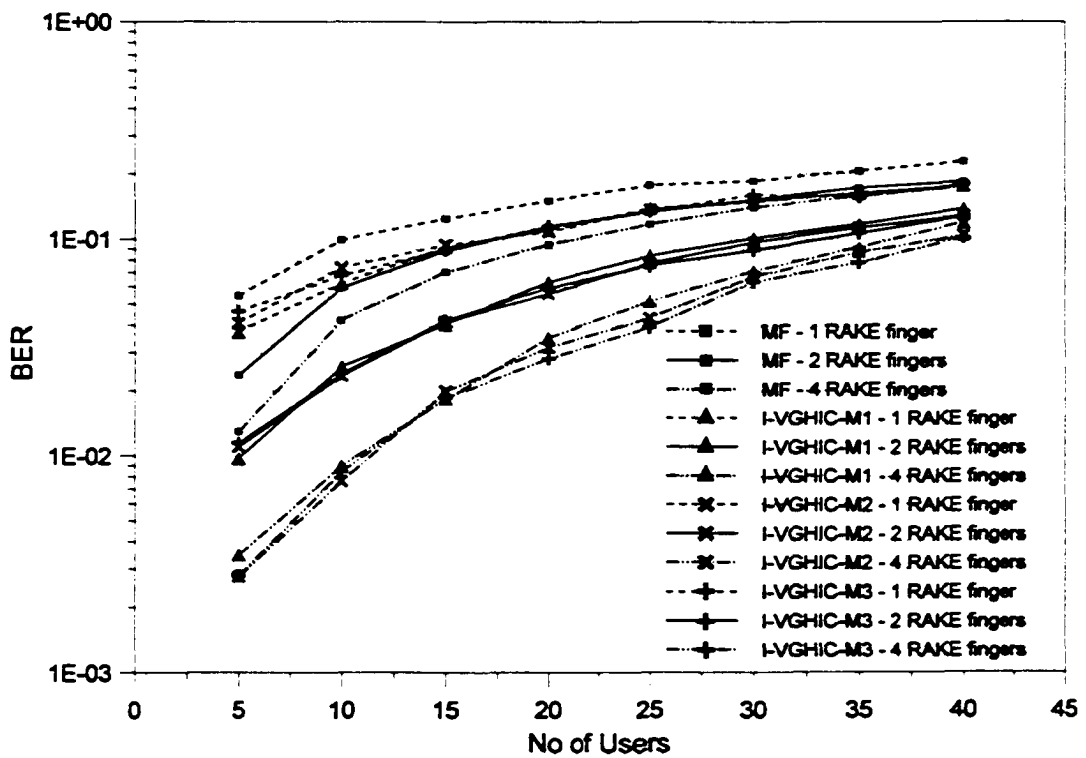


Figure 5.23: Pedestrian (3 km/h) - Channel B: 2-stage I-VGHIC

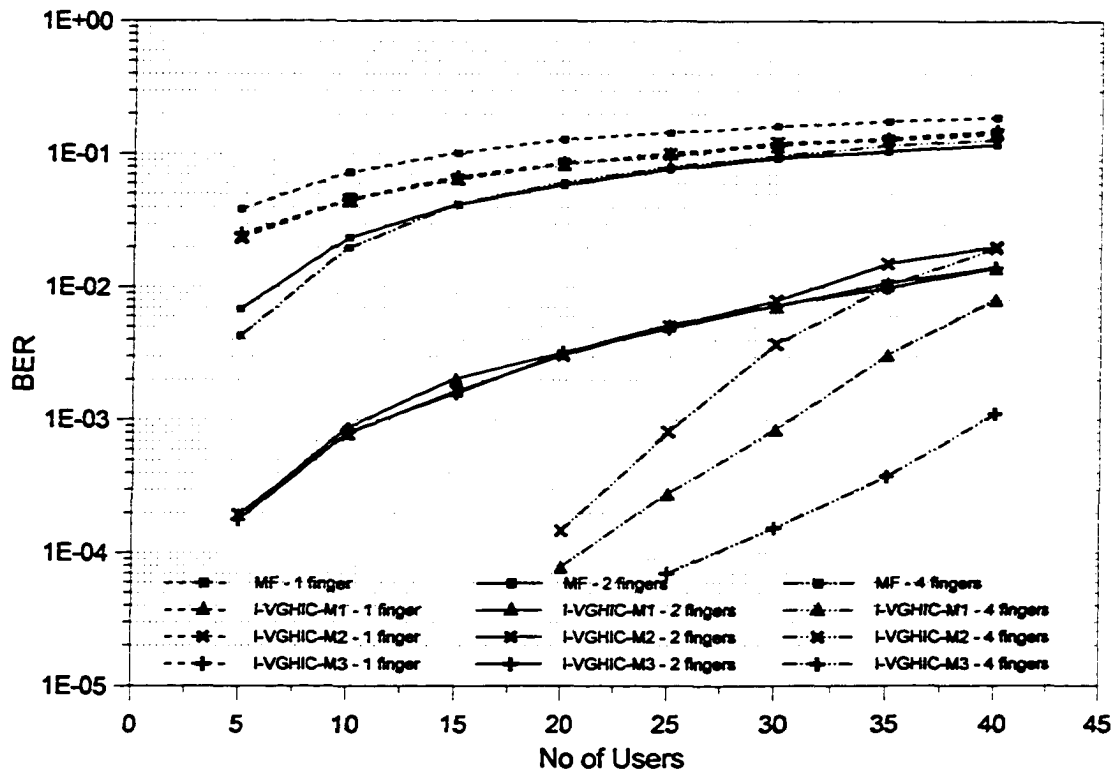


Figure 5.24: Vehicular (120 km/h) - Channel A: 2-stage I-VGHIC

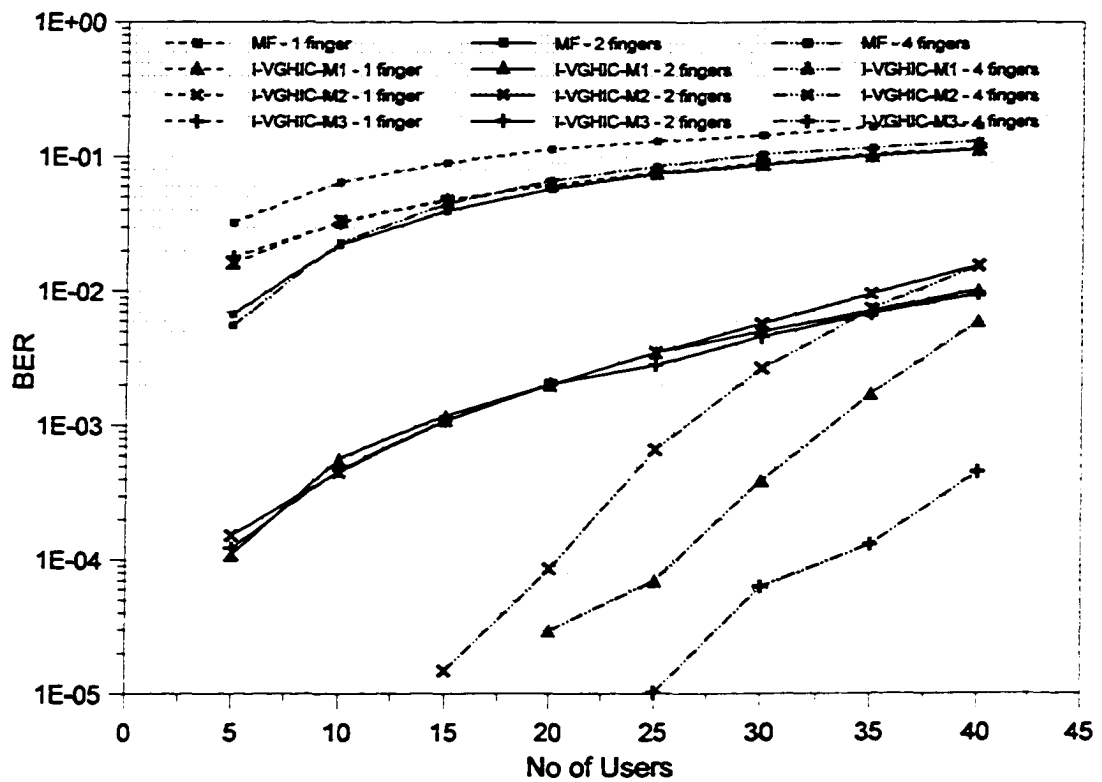


Figure 5.25: Vehicular (120 km/h) - Channel B: 2-stage I-VGHIC

5.3 Summary

The BER performance of the multi-stage VGHIC receiver is studied in an AWGN channel and a flat Rayleigh fading channel. The VGHIC performance is then compared with that of the SIC, PIC and the conventional matched filter receivers. The single stage VGHIC exhibits less sensitivity to phase and timing estimation errors than the multi-stage VGHIC. However, the multi-stage VGHIC still outperforms the single stage VGHIC. It is also observed that the VGHIC is more tolerant of the phase estimation errors than the timing estimation errors. This is also true for the SIC and PIC.

Simulations show that the VGHIC maintains an overall performance lead over the SIC and PIC even with high estimation errors. However, the performance gain from using the multi-stage structure diminishes rapidly as the estimation errors are increased.

Three methods of incorporating the RAKE structure in the I-VGHIC receiver have been presented and their performance investigated using realistic channel conditions. The simulation results verify that the RAKE receiver with interference cancellation outperforms the conventional RAKE receiver. This is because the RAKE receiver with interference cancellation is able to effectively combine more paths of a decaying multipath delay profile than without cancellation. However, the degree of improvement depends on the channel characteristics, number of RAKE fingers and the ways in which the RAKE structure is incorporated into the I-VGHIC receivers. It is observed that the RAKE receiver with interference cancellation performs better in rapidly fading vehicular environment than in the relatively slow fading pedestrian environment.

Chapter 6: Conclusions

This dissertation has proposed and investigated a novel variable group hybrid interference cancellation (VGHIC) scheme for code division multiple access (CDMA) systems. In Section 6.1, a summary of the work done is presented together with conclusions derived from the detailed study. The future research directions that can be extended from this thesis are outlined in Section 6.2.

6.1 Summary and concluding remarks

The capacity of the CDMA system is interference limited. This is due to the signal of every user interfering with each other and this is known as the multiple access interference (MAI). The matched filter (MF) receiver used in CDMA is not optimal as MAI is treated as useless and unwanted noise. This leads to the proposal of the multiuser receivers that take into account the MAI during the detection process. The optimal multiuser receiver based on the maximum likelihood detection has very good performance in comparison to that of the conventional MF. However, its computational complexity is very high. Sub-optimal receivers with much less computational requirements have been proposed as a result. Among these receivers, interference cancellation (IC) receivers are practically viable because of their structural simplicity and good performance. There are three main types, namely, the parallel (PIC), successive (SIC) and hybrid (HIC) interference cancellation receivers. The PIC has good performance when the received signal powers of users are uniform, while the SIC exhibits good performance when the received power profile is spread over a larger range. However, the PIC suffers from the near-far effect and the SIC has high processing delay. Hence, the HIC structures are proposed to mitigate the shortcomings of the PIC and SIC with minimum performance loss. For the previously proposed HICs, the design parameters are the number of groups and the number of users in each group.

The variable group HIC (VGHIC) proposed in this thesis is different from others. The focus is to combine the advantages of the PIC and SIC instead of mitigating their limitations as

what it has been for previously proposed HIC. In the VGHIC, users are grouped such that those with similar powers are selected into the same group. The PIC is used for the members of each group while the SIC is applied to groups with different powers. This is because the PIC is effective when the powers of users are similar and the SIC is more suited for the case when the signal powers are dissimilar. The bit error rate (BER) performance of the MF, PIC, SIC and simplified VGHIC receivers in the additive white Gaussian noise (AWGN) and Rayleigh fading channels has been analyzed and compared theoretically. The theoretical approaches here take into account the effect of self-cancellation that is due to the use of correlation samples in cancellations. The BER expression derived for the VGHIC is a general expression from which one can find the BER for the PIC and SIC by just using the appropriate parameter values. From theoretical studies, the VGHIC performs as well as the PIC in the AWGN channel and it also has the same performance as the SIC in fading channel.

Different improvements have been proposed to enhance the performance of the VGHIC. Two methods of ordering the users have been investigated and it is found that when the ordering is done before every cancellation step, the performance is better but at the expense of higher computational complexity. For the receivers using the correlation samples as estimates, the use of the averaged correlation samples helps to improve the accuracy of the estimates. It has been found that there is an optimal averaging length for each receiver in different channels. The multi-stage structure of the VGHIC has also been presented, and it is evident from the simulations that the multistage VGHIC provides an overall superior performance over multistage PIC and SIC. In both channels, the VGHIC outperforms the conventional matched filter receiver by a large margin. An improved version of the VGHIC (I-VGHIC) using partial combining of correlation samples and partial cancellation has been proposed, and simulations show that the I-VGHIC outperforms the original VGHIC.

Due to the adaptive nature of the VGHIC structure, it exhibits different processing delay profiles depending on the power spread of received signals. A simple method of limiting the number of subtractive steps of the I-VGHIC has been proposed. It is found that the BER performance of the I-VGHIC degrades significantly when the limit on the number of

subtractive steps is too low. Multi-stage I-VGHIC is found to be more sensitive to the imposed limit than the single stage I-VGHIC. However, for a one-stage I-VGHIC, one can reduce the processing delay by 40% sacrificing only 4.5% in user capacity at an uncoded BER of 1×10^{-3} .

When phase and timing estimation errors are introduced, the single stage VGHIC exhibits less sensitivity to errors than the multi-stage VGHIC. Moreover, the VGHIC is more tolerant to phase estimation errors than delay timing estimation errors. Simulations show that the VGHIC maintains an overall performance gain over the SIC and PIC even with high estimation errors. However, the performance gain from using the multi-stage structure deteriorates with increasing estimation errors.

The RAKE structure has been integrated into the I-VGHIC receiver in three different ways. Their performances are investigated using realistic channel conditions. The results verify that the RAKE receiver with IC outperforms the conventional RAKE receiver. However, the degree of improvement depends on the channel characteristics, number of RAKE fingers, and the ways in which the RAKE structure is incorporated.

As follows from the investigations, a major advantage of the VGHIC over the other IC schemes is its ability to adapt its structure to changing power profile of the user received signals. Hence, the VGHIC is able to perform consistently under extreme situations. Moreover, if desired, its structure can be easily changed to suit specific operating conditions with a simple change of the values of the design parameter. This flexibility coupled with good performance, relatively low complexity, and acceptable processing delay makes the VGHIC a viable option for increasing the capacity of CDMA systems.

6.2 Future work

The main feature of the VGHIC is the ability to adapt to different received power profiles. Due to the simple structure of the IC type of receivers, the VGHIC can be used in conjunction with other techniques to derive the maximum gain out of most CDMA systems.

One potential area of application is the multi-carrier CDMA (MC-CDMA) which can be considered as a hybrid of the orthogonal frequency division multiplexing (OFDM) and CDMA. This means the MC-CDMA also possesses desirable qualities such as high bandwidth efficiency and robustness against the frequency selective fading channels. There are three basic versions of the MC-CDMA [126][127][128] each having its own advantages and disadvantages. Despite their differences, all of them have the common use of multiple carriers for transmission. For multiple carriers with each of them experiencing different channels, it is clear that the power profile of the received signals for each carrier will be different. Therefore, the adaptive structure of the VGHIC when used in MC-CDMA systems may be able to work in synergy with the system to provide excellent performance. This is especially important for the MC-CDMA systems as they are potential candidates for 4G systems.

Another interesting application is in the area of multiple antennas. Once again, the adaptive ability of the VGHIC can be integrated with the processing algorithm of the antennas systems to increase performance. Existing interference cancellation schemes have already been investigated with antenna arrays to provide good performance [129][130][131][132]. It is felt that these antenna systems can potentially benefit a lot more with the integration of the VGHIC. Hence, it would be of interest to know whether the VGHIC structure has any added advantages in these systems.

Appendix A: Property of the Cross-Correlation and Time Delay

A.1 The Cross-Correlation between users

The timing diagram between user i and j is shown in Figure A.1. The delay time difference, τ , between i and j is given by

$$\tau = \Delta\tau + nT_c \quad (\text{A.1})$$

where

$$\Delta\tau = \text{remainder} \left[\frac{\tau}{T_c} \right] \quad (\text{A.2})$$

is the remainder of the division of τ/T_c . The term n is the largest integer that is less than τ/T_c and it is given by

$$n = \left\lfloor \frac{\tau}{T_c} \right\rfloor \quad (\text{A.3})$$

where T_c is the chip period. The processing gain is ρ . For the brevity of presentation the subscript ij is dropped from the above equations.

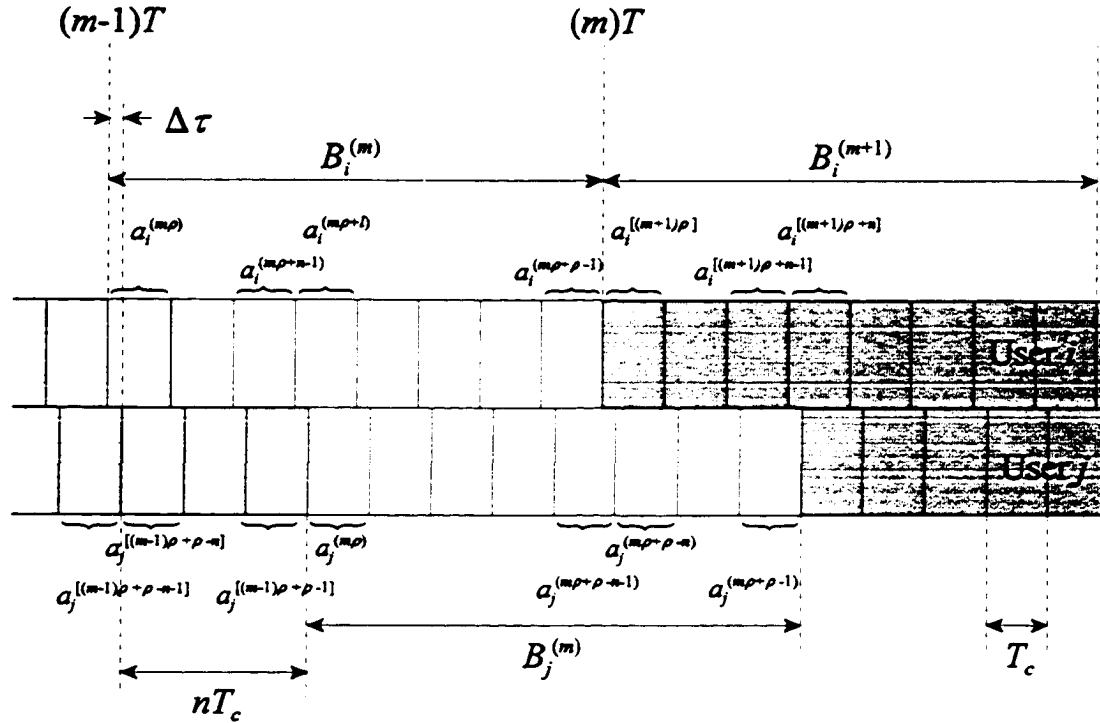


Figure A.1: Delay between user i and j

The information bit, $b_i(t)$ and spreading, $c_i(t)$ waveforms of user i are

$$b_i(t) = \sum_{m=-\infty}^{\infty} B_i^{(m)} p_T(t - mT) \quad (\text{A.4})$$

and

$$c_i(t) = \sum_{n=-\infty}^{\infty} a_i^{(n)} p_{T_c}(t - nT_c) \quad (\text{A.5})$$

where the terms $B_i^{(m)}$ and $a_i^{(n)}$ are the information bit sequence and the spreading chip sequence respectively. They are binary i.i.d random variables assuming value of 1 and -1 with equal probability. The functions $p_T(t)$ and $p_{T_c}(t)$ are assumed to be rectangular pulse with period T and T_c , respectively, that is, $b_i(t) = B_i^{(m)}$ for $(m-1)T \leq t < mT$ and $c_i(t) = a_i^{(n)}$ for $(n-1)T_c \leq t < nT_c$.

Consider a two user system, where the received signal is

$$\begin{aligned} r(t) &= S_i(t) + S_j(t) \\ &= b_i(t)c_i(t) + b_j(t)c_j(t) \end{aligned} \quad (\text{A.6})$$

In the interval $[(m-1)T, mT)$, the desired signal for user i is

$$\begin{aligned} \tilde{B}_i^{(m)} &= \int_{(m-1)T}^{mT} b_i(t)c_i(t)c_i(t) dt + \int_{(m-1)T}^{mT} b_j(t)c_j(t)c_i(t) dt \\ &= B_i^{(m)} + \gamma_{ji}^{(m)} \end{aligned} \quad (\text{A.7})$$

where the cross correlation with respect to user i is

$$\gamma_{ji}^{(m)} = \int_{(m-1)T}^{mT} b_j(t)c_j(t)c_i(t) dt \quad (\text{A.8})$$

When user j lags user i , then

$$\begin{aligned} \gamma_{ji}^{(m)} &= \frac{1}{T} B_j^{(m-1)} \left[\Delta\tau \sum_{x=0}^n a_j^{[(m-1)\rho + \rho - n - 1 + x]} a_i^{(m\rho + x)} \right. \\ &\quad \left. + (T - \Delta\tau) \sum_{x=0}^{n-1} a_j^{[(m-1)\rho + \rho - n + x]} a_i^{(m\rho + x)} \right] \\ &\quad + \frac{1}{T} B_j^{(m)} \left[\Delta\tau \sum_{x=0}^{\rho - n - 2} a_j^{(m\rho + x)} a_i^{(m\rho + n + 1 + x)} \right. \\ &\quad \left. + (T - \Delta\tau) \sum_{x=0}^{\rho - n - 1} a_j^{(m\rho + x)} a_i^{(m\rho + n + x)} \right] \end{aligned} \quad (\text{A.9})$$

Hence, evaluating the first and second moments one obtains,

$$\begin{aligned}
E[\gamma_{ji}^{(m)}] &= 0 \\
E[(\gamma_{ji}^{(m)})^2] &= \frac{1}{T^2} \{ E[\Delta\tau^2](n+1) + E[(T-\Delta\tau)^2](n) \} \\
&\quad + \frac{1}{T^2} \{ E[\Delta\tau^2](\rho-n-1) + E[(T-\Delta\tau)^2](\rho-n) \} \\
&= \frac{1}{\rho} \left\{ 1 - \frac{2}{T} E[\Delta\tau] + \frac{2}{T^2} E[\Delta\tau^2] \right\}
\end{aligned} \tag{A.10}$$

since the processing gain is

$$\rho = \frac{T}{T_c} \tag{A.11}$$

and $E[B_i^{(m)}] = 0$, $E[(B_i^{(m)})^2] = 1$, $E[a_i^{(n)}] = 0$ and $E[(a_i^{(n)})^2] = 1$.

Referring to (A.10), one notices that the expression is independent of the term n in (A.1) but depends on the processing gain and $\Delta\tau$. In the next section, the probability density function (pdf) of $\Delta\tau$ will be derived so that its first and second moment can be found

A.2 Probability density function (pdf) of $\Delta\tau_{ij}$

In the previous section the delay time difference between two users has been defined briefly. Here, it will be defined in details so that the probability density function (pdf) of $\Delta\tau_{ij}$ can be determined.

First, the absolute time delay of user i (with reference from $t = 0$) can be given by

$$A_i = \varepsilon\tau_i + n_i T_c \tag{A.12}$$

where

$$\varepsilon\tau_i = \text{remainder} \left[\frac{A_i}{T_c} \right] \tag{A.13}$$

is the remainder of the division of (A_i/T_c) . The term n_i is the largest integer that is less than (A_i/T_c) and it is given by

$$n_i = \left\lfloor \frac{A_i}{T_c} \right\rfloor \quad (\text{A.14})$$

where T_c is the chip duration. The time delay experienced by user i is assumed to be independent and uniformly distributed in $[0, T)$, then the pdf of $\varepsilon\tau_i$ and n_i can be expressed as

$$f_{\varepsilon\tau_i}(z) = \frac{1}{T_c} \quad , \quad 0 \leq z < T_c \quad (\text{A.15})$$

and

$$f_{n_i}(z) = \frac{1}{\rho} \quad , \quad \begin{array}{l} 0 \leq z < \rho \\ z \in \text{Integer} \end{array} \quad (\text{A.16})$$

or, alternatively represented as (for the term $n_i T_c$)

$$f_{n_i T_c}(z) = \frac{1}{\rho} \sum_{x=0}^{\rho-1} \delta_d(z - x T_c) \quad , \quad 0 \leq z < T \quad (\text{A.17})$$

with the term ρ being the processing gain and $\delta_d(t)$ is the dirac delta function. Note that the pdf of A_i can be obtained from the convolution of (A.15) and (A.17) since A_i can be considered as the summation of two independent variables. Hence, the pdf of A_i is

$$\begin{aligned} f_{A_i}(z) &= \int_{-\infty}^{\infty} f_{n_i}(z-y) f_{n_i T_c}(y) dy \\ &= \frac{1}{\rho T_c} = \frac{1}{T} \quad , \quad 0 \leq z < T \end{aligned} \quad (\text{A.18})$$

The delay time difference is defined as

$$\begin{aligned}\tau_{ij} &= |A_i - A_j| \\ &= |(\varepsilon\tau_i - \varepsilon\tau_j) + (n_i - n_j)T_c|\end{aligned}\quad (\text{A.19})$$

Let

$$\tau_{ij} = \Delta\tau_{ij} + n_{ij}T_c \quad (\text{A.20})$$

where

$$\begin{aligned}\Delta\tau_{ij} &= \text{remainder} \left[\frac{\tau_{ij}}{T_c} \right], \quad 0 \leq \Delta\tau_{ij} < T_c \\ n_{ij} &= \left\lfloor \frac{\tau_{ij}}{T_c} \right\rfloor, \quad n_{ij} \geq 0\end{aligned}\quad (\text{A.21})$$

As A_i and A_j are i.i.d. random variables that have the uniform distribution, it is equally probable that one is greater than the other. Hence, we shall only consider the case that $A_i \geq A_j$. With this assumption in mind, the possible events are as follows:

$$\Delta\tau_{ij} = \begin{cases} \varepsilon\tau_i - \varepsilon\tau_j & , \quad \varepsilon\tau_i \geq \varepsilon\tau_j; n_i \geq n_j \\ \varepsilon\tau_i - \varepsilon\tau_j + T_c & , \quad \varepsilon\tau_i < \varepsilon\tau_j; (n_i - 1) \geq n_j \end{cases} \quad (\text{A.22})$$

From here, before the probability density function (pdf) of $\Delta\tau_{ij}$ can be determined, one need to find the pdf of $(\varepsilon\tau_i - \varepsilon\tau_j)$ and $(\varepsilon\tau_i - \varepsilon\tau_j + T_c)$. Letting $\varepsilon\tau_{ij} = (\varepsilon\tau_i - \varepsilon\tau_j)$ and using (A.15), one can obtain the pdf of $\varepsilon\tau_{ij}$ as

$$f_{\varepsilon\tau_{ij}}(\varepsilon\tau_{ij}) = \begin{cases} \frac{1}{T_c} \left(-\frac{1}{T_c} \varepsilon\tau_{ij} + 1 \right) & , \quad 0 \leq \varepsilon\tau_{ij} < T_c \\ 0 & , \quad \text{elsewhere} \\ \frac{1}{T_c} \left(\frac{1}{T_c} \varepsilon\tau_{ij} + 1 \right) & , \quad -T_c \leq \varepsilon\tau_{ij} < 0 \end{cases} \quad (\text{A.23})$$

Thus, letting $\varepsilon\tau_{ij}' = (\varepsilon\tau_i - \varepsilon\tau_j + T_c)$ and using (A.22) and (A.23) with the condition $\varepsilon\tau_i < \varepsilon\tau_j$, the pdf of $\varepsilon\tau_{ij}'$ is

$$\begin{aligned}
f_{\varepsilon\tau_y}(\varepsilon\tau_{ij}') &= \int_{-\infty}^{\infty} f_{\varepsilon\tau_y}(\varepsilon\tau_{ij}'-y)f_{T_c}(y) dy \\
&= \int_{-\infty}^{\infty} f_{\varepsilon\tau_y}(\varepsilon\tau_{ij}'-y) \delta_d(y-T_c) dy \\
&= f_{\delta\tau_y}(\varepsilon\tau_{ij}'-T_c) \\
&= \frac{1}{T_c} \left(\frac{1}{T_c} (\varepsilon\tau_{ij}'-T_c) + 1 \right) \\
&= \frac{1}{T_c} \left(\frac{1}{T_c} \varepsilon\tau_{ij}' \right)
\end{aligned} \tag{A.24}$$

Since the probability of $\varepsilon\tau_i < \varepsilon\tau_j$ and $\varepsilon\tau_i > \varepsilon\tau_j$ are the same, the pdf of $\Delta\tau_{ij}$ is therefore,

$$\begin{aligned}
f_{\Delta\tau_{ij}}(z) &= f_{\varepsilon\tau_y}(z|_{0 \leq \varepsilon\tau_y < T_c}) + f_{\varepsilon\tau_y}(z|_{-T_c \leq \varepsilon\tau_y < 0}) \\
&= \frac{1}{T_c} \left(-\frac{1}{T_c} z + 1 \right) + \frac{1}{T_c} \left(\frac{1}{T_c} z \right) \\
&= \frac{1}{T_c} \quad , \quad 0 \leq \Delta\tau_{ij} < T_c
\end{aligned} \tag{A.25}$$

Thus, the mean and second moment can be obtained as

$$\begin{aligned}
E[\Delta\tau_{ij}] &= \frac{T_c}{2} \\
E[(\Delta\tau_{ij})^2] &= \frac{T_c^2}{3}
\end{aligned} \tag{A.26}$$

Appendix B: Mean and variance of the correlation sample for SIC

Here, we would like to find the mean and variance of the correlation sample value for user 3 and user 4 of the SIC scheme. After despreading, demodulation and LPF, for user 1, we have

$$R_1^{(SIC)} = \sqrt{E_1} B_1 + \sum_{k=2}^K \sqrt{E_k} B_k \gamma_{k1} + \eta \quad (\text{B.1})$$

As we use the correlation sample value as the estimate of the user signal power, the regenerated signal of user 1 is subtracted from the delayed version of the original received signal $r(t)$ resulting in the composite signal

$$r_2(t) = r(t) - \sqrt{\frac{2}{T}} R_1^{(SIC)} c_1(t) \cos(\omega_c t) \quad (\text{B.2})$$

For user 2, after despreading, demodulation and LPF, we have

$$\begin{aligned} R_2^{(SIC)} &= \sqrt{E_2} B_2 + \sum_{k=3}^K \sqrt{E_k} B_k \gamma_{k2} + \left(\sqrt{E_1} B_1 - R_1^{(SIC)} \right) \gamma_{12} + \eta \\ &= \sqrt{E_2} B_2 (1 - \gamma_{21} \gamma_{12}) \\ &\quad + \sum_{k=3}^K \sqrt{E_k} B_k (\gamma_{k2} - \gamma_{k1} \gamma_{12}) + \eta (1 - \gamma_{12}) \end{aligned} \quad (\text{B.3})$$

The composite signal present before the matched filter of the user 3 is

$$r_3(t) = r(t) - \sum_{i=1}^2 \sqrt{\frac{2}{T}} R_i^{(SIC)} c_i(t) \cos(\omega_c t) \quad (\text{B.4})$$

After matched-filtering, the correlation sample for user 3 is

$$\begin{aligned}
R_3^{(SIC)} &= \sqrt{E_3} B_3 + \sum_{k=4}^K \sqrt{E_k} B_k \gamma_{k3} + \sum_{k=1}^2 \left(\sqrt{E_k} B_k - R_k^{(SIC)} \right) \gamma_{k3} + \eta \\
&= \sqrt{E_3} B_3 (1 - \gamma_{31} \gamma_{13} - \gamma_{32} \gamma_{23} + \gamma_{31} \gamma_{12} \gamma_{23}) \\
&\quad + \sqrt{E_2} B_2 (-\gamma_{21} \gamma_{13} + \gamma_{21} \gamma_{12} \gamma_{23}) \\
&\quad + \sum_{k=4}^K \sqrt{E_k} B_k (\gamma_{k3} - \gamma_{k1} \gamma_{13} - \gamma_{k2} \gamma_{23} + \gamma_{k1} \gamma_{23} \gamma_{23}) \\
&\quad + \eta (1 - \gamma_{13} - \gamma_{23} + \gamma_{23} \gamma_{23})
\end{aligned} \tag{B.5}$$

Taking the expectation and variance of (B.5), using (3.32), and simplifying, one obtains

$$\begin{aligned}
\mathbb{E}[R_3^{(SIC)}] &= \sqrt{E_3} \left(1 - 2 \left(\frac{1}{D\rho} \right) \right) \\
\text{Var}[R_3^{(SIC)}] &= \mathbb{E}[(R_3^{(SIC)})^2] - \mathbb{E}[R_3^{(SIC)}]^2 \\
&= \left[1 - 4 \left(\frac{1}{D\rho} \right) + 4 \left(\frac{1}{D\rho} \right)^2 + \left(\frac{1}{D\rho} \right)^3 \right] E_3 + \left[\left(\frac{1}{D\rho} \right)^2 + \left(\frac{1}{D\rho} \right)^3 \right] E_2 \\
&\quad + \left[\left(\frac{1}{D\rho} \right) + 2 \left(\frac{1}{D\rho} \right)^2 + \left(\frac{1}{D\rho} \right)^3 \right] \sum_{k=4}^K E_k \\
&\quad + \left(1 + \frac{1}{D\rho} + \left(\frac{1}{D\rho} \right)^2 \right) \frac{N_e}{2} - \left[1 - 2 \left(\frac{1}{D\rho} \right) \right]^2 E_3 \\
&= \left(\frac{1}{D\rho} \right)^3 E_3 + \left(\frac{1}{D\rho} \right)^2 \left(1 + \frac{1}{D\rho} \right) E_2 \\
&\quad + \left(\frac{1}{D\rho} \right) \left(1 + \frac{1}{D\rho} \right)^2 \sum_{k=4}^K E_k + \left(1 + \frac{1}{D\rho} \right)^2 \frac{N_e}{2}
\end{aligned} \tag{B.6}$$

Similarly for user 4, the correlation sample is

$$\begin{aligned}
R_4^{(SIC)} &= \sqrt{E_4} B_4 + \sum_{k=5}^K \sqrt{E_k} B_k \gamma_{k4} + \sum_{k=1}^3 \left(\sqrt{E_k} B_k - R_k^{(SIC)} \right) \gamma_{k4} + \eta \\
&= \sqrt{E_4} B_4 \left(1 - \gamma_{41} \gamma_{14} - \gamma_{42} \gamma_{24} - \gamma_{43} \gamma_{34} + \gamma_{41} \gamma_{12} \gamma_{24} \right. \\
&\quad \left. + \gamma_{41} \gamma_{13} \gamma_{34} + \gamma_{42} \gamma_{23} \gamma_{34} + \gamma_{41} \gamma_{12} \gamma_{23} \gamma_{34} \right) \\
&\quad + \sqrt{E_3} B_3 \left(-\gamma_{31} \gamma_{14} - \gamma_{32} \gamma_{24} + \gamma_{31} \gamma_{12} \gamma_{24} \right. \\
&\quad \left. + \gamma_{31} \gamma_{13} \gamma_{34} + \gamma_{32} \gamma_{23} \gamma_{34} - \gamma_{31} \gamma_{12} \gamma_{23} \gamma_{34} \right) \\
&\quad + \sqrt{E_2} B_2 \left(-\gamma_{21} \gamma_{14} + \gamma_{21} \gamma_{12} \gamma_{24} + \gamma_{21} \gamma_{13} \gamma_{34} - \gamma_{21} \gamma_{12} \gamma_{23} \gamma_{34} \right) \\
&\quad + \sum_{k=4}^K \sqrt{E_k} B_k \left(\gamma_{k4} - \gamma_{k1} \gamma_{14} - \gamma_{k2} \gamma_{24} - \gamma_{k3} \gamma_{34} + \gamma_{k1} \gamma_{12} \gamma_{24} \right. \\
&\quad \left. + \gamma_{k1} \gamma_{13} \gamma_{34} + \gamma_{k2} \gamma_{23} \gamma_{34} + \gamma_{k1} \gamma_{12} \gamma_{23} \gamma_{34} \right) \\
&\quad + \eta \left(1 - \gamma_{14} - \gamma_{24} - \gamma_{34} + \gamma_{12} \gamma_{24} \right. \\
&\quad \left. + \gamma_{13} \gamma_{34} + \gamma_{23} \gamma_{34} - \gamma_{12} \gamma_{23} \gamma_{34} \right)
\end{aligned} \tag{B.7}$$

Taking the expectation and variance of (B.7), using (3.32), and simplifying,

$$\begin{aligned}
E[R_4^{(SIC)}] &= \sqrt{E_4} \left(1 - 3 \left(\frac{1}{D\rho} \right) \right) \\
\text{Var}[R_4^{(SIC)}] &= E[(R_4^{(SIC)})^2] - E[R_4^{(SIC)}]^2 \\
&= \left[1 - 6 \left(\frac{1}{D\rho} \right) + 9 \left(\frac{1}{D\rho} \right)^2 + 3 \left(\frac{1}{D\rho} \right)^3 + \left(\frac{1}{D\rho} \right)^4 \right] E_4 \\
&\quad + \left[2 \left(\frac{1}{D\rho} \right)^2 + 3 \left(\frac{1}{D\rho} \right)^3 + \left(\frac{1}{D\rho} \right)^4 \right] E_3 + \left[\left(\frac{1}{D\rho} \right)^2 + 2 \left(\frac{1}{D\rho} \right)^3 + \left(\frac{1}{D\rho} \right)^4 \right] E_2 \\
&\quad + \left[\left(\frac{1}{D\rho} \right) + 3 \left(\frac{1}{D\rho} \right)^2 + 3 \left(\frac{1}{D\rho} \right)^3 + \left(\frac{1}{D\rho} \right)^4 \right] \sum_{k=5}^K E_k \\
&\quad + \left[1 - 3 \left(\frac{1}{D\rho} \right) + 3 \left(\frac{1}{D\rho} \right)^2 + \left(\frac{1}{D\rho} \right)^3 \right] \frac{N_0}{2} - \left[1 - 3 \left(\frac{1}{D\rho} \right) \right]^2 E_4 \\
&= \left(\frac{1}{D\rho} \right)^3 \left(1 + \frac{1}{D\rho} \right) E_4 + \left(\frac{1}{D\rho} \right)^2 \left(1 + \frac{1}{D\rho} \right) \left(2 + \frac{1}{D\rho} \right) E_3 + \left(\frac{1}{D\rho} \right)^2 \left(1 + \frac{1}{D\rho} \right)^2 E_2 \\
&\quad + \left(\frac{1}{D\rho} \right) \left(1 + \frac{1}{D\rho} \right)^3 \sum_{k=5}^K E_k + \left(1 + \frac{1}{D\rho} \right)^3 \frac{N_0}{2}
\end{aligned} \tag{B.8}$$

Appendix C: The CDF and PDF of the sum of Rayleigh and Gaussian random variables.

Here, the cumulative distribution function (cdf) and the probability density function (pdf) of the sum of a Rayleigh and a Gaussian random variable is derived. The results obtained will be used in the analysis of the BER performance of the various interference schemes in Rayleigh fading channel.

Let the Rayleigh-distributed random variable (r.v.) be X with the pdf of

$$p(x) = \frac{x}{a^2} e^{-\frac{x^2}{2a^2}}, \quad x \geq 0 \quad (\text{C.1})$$

where a^2 is the variance of the 2 zero-mean statistically independent Gaussian r.v.s that make up X .

Let the zero-mean Gaussian-distributed random variable (r.v.) be Y with the pdf of

$$p(y) = \frac{1}{\sqrt{2\pi b^2}} e^{-\frac{y^2}{2b^2}} \quad (\text{C.2})$$

where b^2 is the variance of Y .

We want to find the pdf of the r.v., Z [133] such that

$$Z = X + Y \quad (\text{C.3})$$

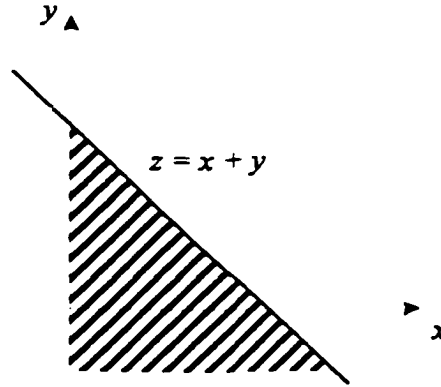


Figure C.1: Graphical representation of the region of Z.

The cdf of Z (shaded area in Figure C.1) is, therefore,

$$F(z) = \int_{-\infty}^z \int_0^{z-y} p(x) p(y) dx dy \quad (C.4)$$

Substituting (C.1) and (C.2) into (C.4), we have

$$\begin{aligned} F(z) &= \int_{-\infty}^z \left(\int_0^{z-y} \frac{x}{a^2} e^{-\frac{x^2}{2a^2}} dx \right) \frac{1}{\sqrt{2\pi b^2}} e^{-\frac{y^2}{2b^2}} dy \\ &= \int_{-\infty}^z \left(1 - e^{-\frac{(z-y)^2}{2a^2}} \right) \frac{1}{\sqrt{2\pi b^2}} e^{-\frac{y^2}{2b^2}} dy \\ &= \int_{-\infty}^z \left(\frac{1}{\sqrt{2\pi b^2}} e^{-\frac{y^2}{2b^2}} - \frac{1}{\sqrt{2\pi b^2}} e^{-\frac{1}{2} \left(\frac{b^2(z-y)^2 + a^2 y^2}{a^2 b^2} \right)} \right) dy \\ &= \frac{1}{2} + \frac{1}{2} \operatorname{erf} \left(\frac{z}{\sqrt{2b^2}} \right) - \frac{1}{\sqrt{2\pi b^2}} e^{-\frac{1}{2} \left(\frac{a^2 b^2}{a^2 + b^2} \right) z^2} \int_{-\infty}^z e^{-\frac{1}{2} \left(\frac{y - \frac{a^2 b^2}{a^2 + b^2} z}{\frac{a^2 b^2}{a^2 + b^2}} \right)^2} dy \\ &= \frac{1}{2} + \frac{1}{2} \operatorname{erf} \left(\frac{z}{\sqrt{2b^2}} \right) - \frac{1}{\sqrt{2\pi b^2}} e^{-\frac{1}{2} \left(\frac{a^2}{a^2 + b^2} \right) z^2} \cdot \sqrt{2\pi \frac{a^2 b^2}{a^2 + b^2}} \left[\frac{1}{2} + \frac{1}{2} \operatorname{erf} \left(\frac{z - \frac{b^2}{a^2 + b^2} z}{\sqrt{2 \frac{a^2 b^2}{a^2 + b^2}}} \right) \right] \\ &= \frac{1}{2} + \frac{1}{2} \operatorname{erf} \left(\frac{z}{\sqrt{2b^2}} \right) - \sqrt{\frac{a^2}{a^2 + b^2}} e^{-\frac{1}{2} \left(\frac{a^2}{a^2 + b^2} \right) z^2} \left[\frac{1}{2} + \frac{1}{2} \operatorname{erf} \left(\frac{az}{\sqrt{2b^2(a^2 + b^2)}} \right) \right] \end{aligned} \quad (C.5)$$

Differentiating the cdf (C.5) with respect to z results in the pdf of Z ,

$$\begin{aligned}
 p(x) &= F'(z) \\
 &= \frac{1}{\sqrt{2\pi b^2}} e^{-\frac{z^2}{2b^2}} \\
 &\quad - \sqrt{\frac{a^2}{a^2+b^2}} \left(-\frac{z^2}{a^2+b^2}\right) e^{-\frac{1}{2}\left(\frac{z^2}{a^2+b^2}\right)} \left[\frac{1}{2} + \frac{1}{2} \operatorname{erf}\left(\frac{az}{\sqrt{2b^2(a^2+b^2)}}\right)\right] \\
 &\quad - \sqrt{\frac{a^2}{a^2+b^2}} \left(\frac{2}{\sqrt{\pi}} \frac{1}{2} \frac{a}{\sqrt{2b^2(a^2+b^2)}}\right) e^{-\left(\frac{a^2 z^2}{2b^2(a^2+b^2)}\right)} e^{-\frac{1}{2}\left(\frac{z^2}{a^2+b^2}\right)} \\
 &= \frac{1}{\sqrt{2\pi b^2}} e^{-\frac{z^2}{2b^2}} \\
 &\quad + \frac{az}{2(a^2+b^2)\sqrt{a^2+b^2}} e^{-\frac{1}{2}\left(\frac{z^2}{a^2+b^2}\right)} \left[1 + \operatorname{erf}\left(\frac{az}{\sqrt{2b^2(a^2+b^2)}}\right)\right] \\
 &\quad - \frac{a^2}{\sqrt{2\pi b^2(a^2+b^2)}} e^{-\frac{z^2}{2b^2}} \\
 &= \frac{b}{\sqrt{2\pi(a^2+b^2)}} e^{-\frac{z^2}{2b^2}} + \frac{az}{2(a^2+b^2)\sqrt{a^2+b^2}} e^{-\frac{1}{2}\left(\frac{z^2}{a^2+b^2}\right)} \left[1 + \operatorname{erf}\left(\frac{az}{\sqrt{2b^2(a^2+b^2)}}\right)\right] \quad (C.6)
 \end{aligned}$$

Appendix D: The Simulation System

In all simulations, unless otherwise mentioned, the parameter receiver structures used will be what is presented below.

D.1 Parameters used

An asynchronous single-cell BPSK/CDMA system was considered. The processing gain was set at 32 and all the users were transmitting simultaneously. All interference cancellation was done on 30-bit blocks, and the average correlation sample values over 30 bits were used for the estimation of the user signal powers. Furthermore, the chip rate was set at 4.096 Mcps (megachips per second) and the data were sent in continuous blocks of 10 ms.

For the flat Rayleigh fading channel, the maximum Doppler shift was 100 Hz. The Rayleigh simulator is the one in [134]. Data bits were not encoded. Long random spreading sequences were used. Additionally, the effects of path loss and shadowing were assumed to be effectively removed in all cases, and all users had random phase shifts distributed uniformly over $[0, 2\pi)$. For all the I-VGHIC scheme, $p_f(1) = 0.5$, $p_f(2) = 0.5$, $p_f(3) = 1.0$, and, $p_c(1) = 0.8$, $p_c(2) = 1.0$, $p_c(3) = 1.0$. These parameter values for the I-VGHIC scheme were found using simulations to provide the best overall performance. Note that for the AWGN channel, the signal levels of all users were assumed to be equal which may also imply perfect power control case.

D.2 Receiver structures used

All the receivers implemented in the simulation have been presented in Chapter 3. For the VGHIC, the version used is the one in Section 3.2 and not the simplified VGHIC used in the analysis. The ordering strategy used in the SIC is the ordering method 2 in Figure 4.1.

REFERENCES

- [1] S. Verdú, "Minimum probability of error for asynchronous Gaussian multiple-access channels", *IEEE Trans. on Info. Theory*, vol. 32, pp. 85-96, January 1986.
- [2] P. Orten and T. Ottosson, "Robustness of DS-CDMA multiuser detectors", *Proc. IEEE Globecom Theory Mini Conf.*, pp. 144-148, November 1997.
- [3] R. M. Buehrer, N. S. Correal and B. D. Woerner, "A comparison of multiuser receivers for cellular CDMA", *Proc. IEEE Globecom*, pp. 1571-1577, Westminster, UK, November 1996.
- [4] A. J. Voorman, D. Koulakiotis, A. H. Aghvami and R. Prasad, "Performance evaluation of the decorrelating detector for DS-CDMA systems over multi-path Rayleigh fading channels with AWGN", *Proc. IEEE Int. Symp. on Personal, Indoor and Mobile Radio Comms.*, pp. 228-232, September 1998.
- [5] N. S. Correal, R. M. Buehrer and B. D. Woerner, "Real-time DSP implementation of a coherent partial interference cancellation multiuser receiver for DS-CDMA", *Proc. IEEE Int. Conf. on Comms.*, pp. 1536-1540, June 1998.
- [6] N. S. Correal and B. D. Woerner, "Non-Coherent Real-time DSP Implementation of a Parallel Partial Interference Cancellation Multiuser Receiver for DS-CDMA", *Proc. IEEE Veh. Tech. Conf.*, pp. 2172-2176, May 1998.
- [7] K. I. Pedesen, T. E. Kolding, I. Seskar and J. M. Holtzman, "Practical implementation of successive interference cancellation in DS/CDMA systems", *Proc. IEEE Int. Conf. on Universal Personal Comms.*, pp. 321-325, Massachusetts, September 1996.
- [8] M. Sawahashi, H. Andoh, K. Higuchi and F. Adachi, "Experiments on coherent multistage interference canceller for DS-CDMA mobile radio", *Proc. IEEE Int. Symp. on Personal, Indoor and Mobile Radio Comms.*, pp. 491-495, September 1998.
- [9] G. Q. Xue, J. F. Weng, T. Le-Ngoc and S. Tahar, "Impact of imperfect power control and channel estimation on the performance of multiuser detectors", *Proc. IEEE Globecom*, pp. 138-142, November 1999.
- [10] K. W. Ang and W. A. Krzymień, "A novel variable group hybrid interference cancellation scheme for CDMA systems", *Proc. IEEE & IEE Int. Conf. on Telecomms.*, Cheju, Korea, session 3A.1, June 1999

- [11] K. W. Ang and W. A. Krzymieñ, "An improved multi-stage variable group hybrid multi-user interference cancellation scheme for CDMA systems", *Proc. IEEE Int. Symp. on Personal, Indoor and Mobile Radio Comms.*, session B3-3, Osaka, Japan, September 1999.
- [12] K. W. Ang and W. A. Krzymieñ, "A Method of Limiting the Processing Delay of the Improved Multi-Stage Variable Group Hybrid Interference Cancellation Scheme for CDMA Systems", *Proc. IEEE Veh. Tech. Conf. - Fall*, pp. 1648-1652, Amsterdam, The Netherlands, September 1999.
- [13] K. W. Ang and W. A. Krzymieñ, "Effects of the different configurations of RAKE receivers on the performance of interference cancellation scheme in frequency selective fading channel", *Proc. International Conf. on Comms. System*, session W2-2.2, Singapore, November 2000.
- [14] K. W. Ang and W. A. Krzymieñ, "Performance of the multi-stage variable group hybrid interference cancellation scheme with timing and phase errors", *Proc. IEEE Veh. Tech. Conf. - Spring*, pp. 1905-1909, Jeju, Korea, April 2003.
- [15] A. C. McCormik and P. M. Grant, "A novel interference cancellation receiver for uplink multi-carrier CDMA", *Proc. IEEE Int. Symp. on Spread Spectrum Techniques and Applications*, pp. 155-158, Parsippany, New Jersey, September 2000.
- [16] S. Jung and H. Kim, "An improved hybrid multiuser interference cancellation scheme based on the clustering algorithm", *Proc. IEEE Veh. Tech. Conf.*, pp. 683-687, Atlantic City, New Jersey, October 2001.
- [17] M. K. Simon, J. K. Omura, R. A. Scholtz and B. K. Levitt, *Spread Spectrum Communications Handbook*, Revised edition, McGraw-Hill Inc., 1994.
- [18] C. E. Shannon, "A Mathematical Theory of Communications", *Bell Syst. Tech. J.*, vol. 27, (Part I), pp. 379-423, (Part II), pp. 623-656, 1948.
- [19] R. C. Dixon, *Spread Spectrum Systems: With Commercial Applications*, 3rd edition, John Wiley & Sons Inc., 1994.
- [20] J. S. Lee and L. E. Miller, *CDMA Engineering Handbook*, Artech House, 1998.
- [21] W. W. Peterson and E. J. Weldon, *Error-correcting Codes*, Cambridge, Massachusetts, MIT press, 1972.
- [22] W. Stahnke, "Primitive binary polynomials", *Math. Comp.*, vol. 27, pp. 977-980, October 1973.
- [23] R. Lidl and H. Niederreiter, *Finite Fields*, Readings, Massachusetts, Addison-Wesley, 1983.

- [24] S. Ariyavisitakul and L. F. Chang, "Signal and Interference Statistics of a CDMA System with Feedback Power Control", *IEEE Trans. on Comms.*, vol. 41, no. 11, pp. 1626-1634, November 1993.
- [25] S. Ariyavisitakul, "Signal and Interference Statistics of a CDMA System with Feedback Power Control - Part II", *IEEE Trans. on Comms.*, vol. 42, pp. 597-605, February 1994.
- [26] S. Seo, T. Dohi and F. Adachi, "SIR-Based Transmit Power Control of Reverse Link for Coherent DS-CDMA Mobile Radio", *IEICE Trans. Comms.*, vol. E81-B, no. 7, pp. 1508-1516, July 1998.
- [27] G. E. Corazza, G. D. Maio and F. Vatalaro, "CDMA Cellular Systems Performance with Fading, Shadowing, and Imperfect Power Control", *IEEE Trans. on Veh. Tech.*, vol. 47, no. 2, pp. 450-459, May 1998.
- [28] W. M. Tam and F. C. M. Lau, "Analysis of Power Control and Its Imperfections in CDMA Cellular Systems", *IEEE Trans. on Veh. Tech.*, vol. 48, no. 5, pp. 1706-1717, September 1999.
- [29] J. G. Proakis, *Digital Communications*, 3rd edition, McGraw-Hill, Inc., 1995.
- [30] P. Wei, J. R. Zeidler and W. H. Ku, "Adaptive Interference suppression for CDMA Overlay Systems", *IEEE Journal Selected Areas in Comm.*, vol. 12, no. 9, pp. 1510-1523, December 1994.
- [31] Y. Wang and S. Cheng, "An Multiple Access Interference (MAI) Cancellation Detector at the Mobile Terminal in CDMA Systems", *Proc. IEEE Int. Symp. on Spread Spectrum Techniques and Applications*, pp. 922-926, Sun City, South Africa, September 1998.
- [32] N. R. Patel and T. O'Farrel, "Optimal Single-User Detection For DS/CDMA Systems Achieving Complete MAI Cancellation", *Proc. IEEE Int. Symp. on Spread Spectrum Techniques and Applications*, pp. 941-945, Sun City, South Africa, September 1998.
- [33] U. Madhow, "Blind Adaptive Interference Suppression for Direct-Sequence CDMA", *IEEE Proc.*, vol. 86, no. 10, pp. 2049-2069, October 1998.
- [34] S. Verdú, *Multiuser Detection*, Cambridge University Press, 1998.
- [35] S. D. Gray, M. Kocic and D. Brady, "Multiuser Detection in Mismatched Multiple-Access Channels", *IEEE Trans. Comms*, vol. 43, pp. 3080 - 3089, December 1995.
- [36] R. Lupas and S. Verdu, "Linear multiuser detectors for synchronous code-division multiple-access channels", *IEEE Trans. on Information Theory*, vol. 35, pp. 123-136, January 1989.

- [37] R. Lupas and S. Verdú, "Near-Far Resistance of Multiuser Detectors in Asynchronous Channels", *IEEE Trans. Comms.*, vol. 38, pp. 496 - 508, April 1990.
- [38] A. Klein and P. W. Baier, "Linear Unbiased Data Estimation in Mobile Radio Systems Applying CDMA", *IEEE Journal Selected Areas in Comm.*, vol. 11, pp. 1058-1066, September 1993.
- [39] Z. Xie, R. T. Short, and C. K. Rushforth, "A Family of Suboptimum Detectors for Coherent Multiuser Communications", *IEEE Journal Selected Areas in Comm.*, vol. 8, pp. 683 - 690, May 1990.
- [40] K. I. Pedersen, T. E. Kolding, I. Seskar and J. M. Holtzman, "Practical Implementation of Successive Interference Cancellation in DS/CDMA Systems", *Proc. IEEE Int. Conf. on Universal Personal Comms.*, pp. 321-325, September 1996.
- [41] N. S. Correal, R. M. Buehrer and B. D. Woerner, "Improved CDMA Performance through Bias Reduction for Parallel Interference Cancellation", *Proc. IEEE Int. Symp. on Personal, Indoor and Mobile Radio Comms.*, pp. 565-569, September 1997.
- [42] N. S. Correal and B. D. Woerner, "Non-Coherent Real-time DSP Implementation of a Parallel Partial Interference Cancellation Multiuser Receiver for DS-CDMA", *Proc. IEEE Veh. Tech. Conf.*, pp. 2172-2176, May 1998.
- [43] M. Sawahashi, H. Andoh, K. Higuchi and F. Adachi, "Experiments on Coherent Multistage Interference Canceller for DS-CDMA Mobile Radio", *Proc. IEEE Int. Symp. on Personal, Indoor and Mobile Radio Comms.*, pp. 491-495, September 1998.
- [44] J. R. Lequepeys, N. Daniele, D. Lattard, B. Piaget, D. Varreau, L. Ouvry and C. Boulanger, "CESSIUM: a single component for implementing high data rates DSSS/CDMA interference cancellation receivers", *Proc. IEEE Int. Symp. on Spread Spectrum Techniques and Applications*, pp. 888-892, Sun City, South Africa, September 1998.
- [45] M. K. Varanasi, "Group Sequence Detection for the Asynchronous Gaussian Code-Division Multiple-Access Channel", *Proc. IEEE Globecom Comms. Theory Mini Conf.*, pp. 136-140, November 1994.
- [46] M. K. Varanasi and B. Aazhang, "Multistage detection in asynchronous code-division multiple-access communications", *IEEE Trans. Comms.*, vol. 38, pp. 509-519, April 1990.
- [47] K. Kansanen, M. Latva-aho and M. Juntti, "Performance of Parallel Interference Cancellation in UTRA FDD Uplink", *Proc. ACTS Mobile Comms. Summit*, pp. 643-647, Sorrento, Italy, June 1999.

- [48] M. J. Juntti, M. Latva-aho, K. Kansanen and O. Kaurahalmel, "Performance of Parallel Interference Cancellation for CDMA in Estimated Fading Channels with Delay Mismatch", *Proc. IEEE Int. Symp. on Spread Spectrum Techniques and Applications*, pp. 936-940, Sun City, South Africa, September 1998.
- [49] M. K. Varanasi, "Group Detection for Synchronous Gaussian Code-Division Multiple-Access Channels", *IEEE Trans. Comms*, vol. 41, pp. 1083 - 1096, July 1995.
- [50] H. Sugimoto, L. K. Rasmussen, T. J. Lim and T. Oyama, "Mapping functions for successive interference cancellation in CDMA", *Proc. IEEE Veh. Tech. Conf.*, pp. 2301-2305, Ottawa, Canada, May 1998.
- [51] R. M. Buehrer and B. D. Woerner, "The Asymptotic Multiuser Efficiency of M-stage Interference Cancellation Receivers", *Proc. IEEE Int. Symp. on Personal, Indoor and Mobile Radio Comms.*, pp. 570-574, September 1997.
- [52] C. Boulanger, L. Ouvry and M. Bouvier des Noës, "Multistage Linear DS-CDMA Receivers", *Proc. IEEE Int. Symp. on Spread Spectrum Techniques and Applications*, pp. 663-667, Sun City, South Africa, September 1998.
- [53] M. Alam, T. Ojanperä and R. Prasad, "Near-Far Resistance of Parallel Interference Cancellation Detector in a Multirate DS-CDMA Systems", *Proc. IEEE Veh. Tech. Conf.*, pp. 1830-1834, Amsterdam, The Netherlands, September 1999.
- [54] Lars K. Rasmussen, "On Ping -Pong Effects in Linear Interference Cancellation for CDMA", *Proc. IEEE Int. Symp. on Spread Spectrum Techniques and Applications*, pp. 348-352, Parsippany, New Jersey, September 2000.
- [55] D. Guo, L. K. Rasmussen and T. J. Lim, "Linear Parallel Interference Cancellation in Long-code CDMA Multiuser Detection", *IEEE Journal Selected Areas in Comm.*, vol. 17, no. 12 , pp. 2074-2081, December 1999.
- [56] D. Divsalar, M. K. Simon and D. Raphaeli, "Improved Parallel Interference Cancellation for CDMA", *IEEE Trans. on Comms.*, vol. 46, no. 2, pp. 258-268, February 1998.
- [57] B. Y. Cho, D. Choi, S. Lee and Y. Oh, "Performance of the Improved PIC Receiver for DS-CDMA over Rayleigh Fading Channels", *Proc. IEEE Int. Symp. on Spread Spectrum Techniques and Applications*, pp. 45-49, Parsippany, New Jersey, September 2000.
- [58] Z. Pu, H. Wang, X. You and S. Cheng, "Improved partial parallel interference cancellation for direct sequence CDMA communications", *Proc. IEEE Int. Symp. on Personal, Indoor and Mobile Radio Comms.*, session 7-2, Osaka, Japan, September 1999.

- [59] A. F. Meeteren, T. Ojanperä, H. Nikookar and R. Prasad, "Groupwise weighted parallel interference cancellation for asynchronous multirate DS-CDMA", *Proc. IEEE Veh. Tech. Conf. - fall*, pp. 1820-1824, Amsterdam, The Netherlands, September 1999.
- [60] R. Fantacci, "Proposal of an Interference Cancellation Receiver with Low Complexity for DS/CDMA Mobile Communication Systems", *IEEE Trans. on Veh. Tech.*, vol. 48, no. 4, pp. 1039-1046, July 1999.
- [61] W. Hou and B. Chen, "Adaptive Detection in Asynchronous Code-Division Multiple-Access System in Multipath Fading Channels", *IEEE Trans. on Comms.*, vol. 48, no. 5, pp. 863-874, May 2000.
- [62] M. Abdulrahman and A. U. H. Sheikh, "Decision Feedback equalization for CDMA in indoor wireless communications", *IEEE Journal Selected Areas in Comm.*, vol. 12, pp. 698-706, May 1994.
- [63] G. Xue, J. Weng, T. Le-Ngoc, and S. Tahar, "Adaptive Multistage Parallel Interference Cancellation for CDMA", *IEEE Journal Selected Areas in Comm.*, vol. 17, pp. 1815 - 1827, October 1999.
- [64] C. Wang, K. Wu and M. Lai, "On weight initialization for adaptive multistage parallel interference cancellation in CDMA systems", *Proc. IEEE Signal Processing Advances in wireless Comms.*, pp. 194-197, Taoyuan, Taiwan, March 2001.
- [65] A. Høst-Madsen and K. Cho, "MMSE/PIC multiuser detection for DS/CDMA systems with inter- and intra-cell interference", *IEEE Trans. on Comms.*, vol. 47, no. 2, pp. 291-299, February 1999.
- [66] N. A. Mohamed and J. G. Dunham, "A simple combined conjugate gradient beamforming and interference cancellation scheme for DS-CDMA in a multipath fading channel", *Proc. IEEE Wireless Comms and Networking Conf.*, pp. 859 -863, New Orleans, Los Angeles, September 1999.
- [67] J. Weng, G. Xue, T. Le-Ngoc and S. Tahar, "Multistage interference cancellation with diversity reception for asynchronous QPSK DS/CDMA systems over multipath fading channels", *IEEE Journal Selected Areas in Comm.*, vol. 17, pp. 2162-2180, December 1999.
- [68] A. J. Viterbi, "Very Low Rate Convolutional Codes for Maximum Theoretical Performance of Spread-Spectrum Multiple-Access Channels", *IEEE Journal Selected Areas in Comm.*, vol. 8, pp. 641-649, May 1990.
- [69] R. Kohno, H. Imai, M. Hatori, and S. Pasupathy, "Combinations of an adaptive array antenna and a canceller of interference for direct-sequence spread-spectrum multiple-access system", *IEEE Journal Selected Areas in Comm.*, vol. 8, pp. 675 - 682, May 1990.

- [70] P. Patel and J. Holtzman, "Analysis of a Simple Successive Interference Cancellation Scheme in a DS/CDMA System", *IEEE Journal Selected Areas in Comm.*, vol. 12, no. 5, pp. 768-807, June 1994.
- [71] P. Patel and J. Holtzman, "Analysis of a DS/CDMA successive interference cancellation scheme using correlations", *Proc. IEEE Globecom*, pp. 76-80, Houston, Texas, November 1993.
- [72] A. Johansson, L. K. Rasmussen and T. J. Lim, "One-shot filtering equivalence for linear successive interference cancellation in CDMA", *Proc. IEEE Veh. Tech. Conf.*, pp. 2163-2167, May 1997.
- [73] K. S. Kim and C. S. Kang, "A simple and accurate analysis method of SIC performance using spatial cell modeling in DS/CDMA system", *Proc. IEEE Int. Symp. on Personal, Indoor and Mobile Radio Comms.*, pp. 1290-1293, September 1998.
- [74] K. Jamal and E. Dahlman, "Multi-Stage Serial Interference Cancellation for DS-CDMA", *Proc. IEEE Veh. Tech. Conf.*, vol. 2, pp. 671-675, Atlanta, USA, April 1996.
- [75] T. Oyama, S. Sun, H. Sugimoto, T. J. Lim, L. K. Rasmussen and Y. Matsumoto, "Performance comparison of multi-stage SIC and limited tree-search detection in CDMA", *Proc. IEEE Veh. Tech. Conf.*, pp. 1854-1858, Ottawa, Canada, May 1998.
- [76] L. K. Rasmussen, T. J. Lim, and T. M. Aulin, "Breadth-first maximum likelihood detection in multiuser CDMA", *IEEE Trans. Comms.*, vol. 45, pp. 1176-1178, October 1997.
- [77] L. K. Rasmussen, S. Sun, T. J. Lim, and H. Sugimoto, "Impact of estimation errors on multiuser detection in CDMA", *Proc. IEEE Veh. Tech. Conf.*, pp. 1844-1848, Ottawa, Canada, May 1998.
- [78] A. L. C. Hui and K. B. Letaief, "Successive interference cancellation for multiuser asynchronous DS/CDMA detectors in multipath fading links", *IEEE Trans. Comms.*, vol. 46, pp. 384-391, March 1998.
- [79] Y. C. Yoon, R. Kohno, and H. Imai, "A spread-spectrum multiaccess system with cochannel interference cancellation for multipath fading channels", *IEEE Journal Selected Areas in Comm.*, vol. 11, pp. 1067 - 1075, September 1993.
- [80] M. Yao and T. J. Lim, "Successive interference cancellation in multipath fading CDMA channels with differential PSK", *Proc. IEEE Int. Symp. on Personal, Indoor and Mobile Radio Comms.*, session 7-4, Osaka, Japan, September 1999.
- [81] R. M. Buehrer, "Equal BER performance in linear successive interference cancellation for CDMA systems", *IEEE Trans. Comms.*, vol. 49, pp. 1250-1258, July 2001.

- [82] P. Patel and J. Holtzman, "Performance comparison of a DS/CDMA system using a successive interference cancellation (IC) scheme and a parallel IC scheme under fading", *Proc. IEEE Int. Conf. on Comms.*, pp. 510-514, May 1994.
- [83] H. Arslan, S. C. Gupta, G. E. Bottomley and S. Chennakeshu, "Combined successive cancellation and joint demodulation for the suppression of adjacent channel interference", *Proc. IEEE Wireless Comms and Networking Conf.*, pp. 1114-1118, New Orleans, Los Angeles, September 1999.
- [84] A. Lampe, "An analytic solution to the performance of iterated soft decision interference cancellation for coded CDMA transmission over frequency selective fading channels", *Proc. IEEE Int. Symp. on Spread Spectrum Techniques and Applications*, pp. 368-372, Parsippany, New Jersey, September 2000.
- [85] O. Nesper and P. Ho, "A reference symbol assisted interference cancelling hybrid receiver for an asynchronous DS/CDMA system", *Proc. IEEE Int. Symp. on Personal, Indoor and Mobile Radio Comms.*, pp. 108-112, Taipei, Taiwan, October 1996.
- [86] D. Hong, Y. You, S. Jeong and C. Kang, "Pipelined successive interference cancellation scheme for DS/CDMA system", *Proc. IEEE Wireless Comms and Networking Conf.*, pp. 1489 -1492, New Orleans, LA, September 1999.
- [87] T. Kim, D. Hong, C. Kang and D. Hong, "Adaptive pipelined successive interference cancellation for a DS/CDMA system", *Proc. IEEE Int. Conf. on Comms.*, pp. 740-743, June 2000.
- [88] G. E. Bottomley, "Improved successive cancellation of DS-CDMA signals using signal orthogonalization", *Proc. IEEE Int. Conf. on Universal Personal Comms.*, pp. 141-144, Massachusetts, September 1996.
- [89] D. Raphael, "Suboptimal maximum-likelihood multiuser detection of synchronous CDMA on frequency-selective multipath channels", *IEEE Trans. on Comms.*, vol. 48, pp. 875-885, May 2000.
- [90] N. S. Correal and B. D. Woerner, "Evaluation of dual spatial and polarization diversity reception for DS-CDMA multiuser detection", *Proc. IEEE Int. Conf. on Universal Personal Comms.*, pp. 789-793, October 1998.
- [91] L. Mailaender and H. Huang, "Analysis of a successive interference canceller with multiple antennas for DS/CDMA on multipath fading channels", *Proc. UCSD Conf. On Wireless Comms.*, pp. 47-53, March 1999.
- [92] L. Mailaender, "A multiple antenna successive interference canceller for mixed voice/data systems", *Proc. IEEE Wireless Comms and Networking Conf.*, pp. 66-70, New Orleans, LA, September 1999.

- [93] H. H. Chen and Z. Q. Liu, "A novel CDMA multiuser detector with immunity against decision error propagation", *Proc. IEEE Veh. Tech. Conf.*, pp. 567-571, May 1997.
- [94] W. T. Sang, K. B. Letaief and R. S. Cheng, "Combined coding and successive interference cancellation with random interleaving for DS/CDMA communications", *Proc. IEEE Veh. Tech. Conf. - fall*, pp. 1825-1829, Amsterdam, The Netherlands, September 1999.
- [95] M. Brandt-Pearce, "Soft-decision multiuser detector for coded CDMA systems", *Proc. IEEE Int. Conf. on Comms.*, pp. 365-369, June 1998.
- [96] E. Leung and P. Ho, "A successive interference cancellation scheme for an OFDM system", *Proc. IEEE Int. Conf. on Comms.*, pp. 375-379, June 1998.
- [97] F. Kleer, S. Hara and R. Prasad, "Performance evaluation of a successive interference cancellation scheme in a quasi-synchronous MC-CDMA system", *Proc. IEEE Int. Conf. on Comms.*, pp. 370-374, June 1998.
- [98] F. Wijk, G. M. J. Janssen and R. Prasad, "Groupwise successive interference cancellation in a DS/CDMA system", *Proc. IEEE Int. Symp. on Personal, Indoor and Mobile Radio Comms.*, pp. 742-746, Toronto, Canada, September 1995.
- [99] S. H. Hwang, C. G. Kang and S. W. Kim, "Performance analysis of interference cancellation schemes for a DS/CDMA system under delay constraint", *Proc. IEEE Int. Symp. on Personal, Indoor and Mobile Radio Comms.*, pp. 569-573, Taipei, Taiwan, October 1996.
- [100] S. Sun, L. K. Rasmussen, H. Sugimoto and T.J. Lim, "A hybrid interference canceller in CDMA", *Proc. IEEE Int. Symp. on Spread Spectrum Techniques and Applications*, pp. 150-154, Sun City, South Africa, September 1998.
- [101] S. Sun, L. K. Rasmussen, T.J. Lim and H. Sugimoto, "A matrix-algebraic approach to linear hybrid interference cancellation in CDMA", *Proc. IEEE Int. Conf. on Universal Personal Comms.*, pp. 1319-1323, Florence, Italy, October 1998.
- [102] A. Johansson and L. K. Rasmussen, "Linear group-wise successive interference cancellation in CDMA", *Proc. IEEE Int. Symp. on Spread Spectrum Techniques and Applications*, pp. 121-126, Sun City, South Africa, September 1998.
- [103] S. R. Kim, J. G. Lee and H. Lee, "Adaptive hybrid serial/parallel interference cancellation in CDMA systems", *Proc. IEEE Int. Conf. on Universal Personal Comms.*, pp. 341-344, Massachusetts, USA, September 1996.
- [104] D. Kim, S. Kang, S. Kwon and C. Kang, "Multiuser detection using blockwise successive interference cancellation in DS/CDMA systems", *Proc. IEEE Veh. Tech. Conf.*, pp. 1835-1838, May 1998.

- [105] D. Koulakiotis and A. H. Aghvami, "Evaluation of a DS/CDMA multiuser receiver employing a hybrid form of interference cancellation in Rayleigh-fading channels", *IEEE Comms. Letters*, vol. 2, pp. 61-63, March 1998.
- [106] J. Kim, J. Jeong, S. Yeom, B. Choi and Y. Park, "Performance analysis of the hybrid interference canceller for multiple access interference cancellation", *Proc. TENCON*, pp. 1236 -1239, September 1999.
- [107] T. Oon, R. Steele and Y. Li, "Performance of an adaptive successive serial-parallel CDMA cancellation scheme in flat Rayleigh fading channels", *Proc. IEEE Veh. Tech. Conf.*, pp. 193-197, May 1997.
- [108] A. Johansson and L. K. Rasmussen, "Linear group-wise successive interference cancellation in CDMA", *Proc. IEEE Int. Symp. on Spread Spectrum Techniques and Applications*, pp. 121-126, Sun City, South Africa, September 1998.
- [109] M. B. Pursley, D.V. Sarwate and W.E. Stark, "Error Probability for Direct-Sequence Spread-Spectrum Multiple-Access Communications - Part I: Upper and Lower Bounds", *IEEE Trans. on Comms.*, vol.com 30, no. 5, pp. 975-984, May 1982.
- [110] M. B. Pursley, "Performance evaluation for phase-coded spread-spectrum multi-access communication - Part I: System analysis", *IEEE Trans. on Comms.*, vol.com 25, pp. 795-799, August 1977.
- [111] R. K. Morrow, "Accurate CDMA BER calculations with low computational complexity", *IEEE Trans. on Comms.*, vol. 46, pp. 1413-1417, November 1998.
- [112] T. S. Rappaport, *Wireless Communications: Principles and Practice*, Prentice-Hall Inc., 1996, Appendix C.1, pp.577-582.
- [113] K. Jamal and E. Dahlman, "Multi-Stage Serial Interference Cancellation for DS-CDMA", *Proc. IEEE Veh. Tech. Conf.*, vol. 2, pp. 671-675, Atlanta, USA, April 1996.
- [114] A. L. C. Hui and K. B. Letaief, "Successive Interference Cancellation for Multiuser Asynchronous DS/CDMA Detectors in Multipath Fading Links", *IEEE Trans. on Comms.*, vol. 46, no. 3, pp. 384-390, March 1998.
- [115] R. M. Buehrer, "Equal BER performance in linear successive interference cancellation for CDMA systems", *IEEE Trans. on Comms.*, vol. 49, no. 7, pp. 1250-1258, July 2001.
- [116] H. A. David, *Order Statistics*, 2nd edition, John Wiley & Sons Inc., 1981.
- [117] J. G. Proakis, *Digital Communications*, McGraw-Hill, Inc., 1995, Section 14-3, pp. 772-777.

- [118] D. Hong, Y. You, S. Jeong and C. Kang, "Pipelined successive interference cancellation scheme for DS/CDMA system", *Proc. IEEE Wireless Comms and Networking Conf.*, pp. 1489 -1492, New Orleans, LA, September 1999.
- [119] T. Oyama, S. Sun, H. Sugimoyo, T. J. Lim, L. K. Rasmussen and Y. Matsumoto, "Performance comparison of multi-stage SIC and limited tress-search detection in CDMA", *Proc. IEEE Veh. Tech. Conf.*, pp. 1854-1858, Ottawa, Canada, May 1998.
- [120] R. Steele, *Mobile Radio Communications*, IEEE Press, 1994.
- [121] S. Moshavi, "Survey of Multiuser detection for DS-CDMA Communications", *Bellcore Publication*, IM-555, August 1996
- [122] D. Divsalar and M. Simon, "Improved CDMA performance using parallel interference cancellation", *JPL Publication*, 95-21, October 1995
- [123] T.S. Rappaport, *Wireless Communications: Principles and Practice*, Prentice-Hall Inc., New Jersey, 1996, pp.329-338.
- [124] ITU-R M.1225, Guidelines for evaluation of radio transmission technologies for IMT-2000, 1997.
- [125] C. Antón-Haro, X. Mestre and J.R. Fonollosa, "Array-based and joint detection methods for the TDD mode of UTRA", *Proc. IEEE Int. Symp. on Personal, Indoor and Mobile Radio Comms.*, Osaka, Japan, September 1999, session B3-2.
- [126] S. Hara and R. Prasad, "Overview of multicarrier CDMA", *IEEE Comms. Mag.*, vol. 35, pp. 126-133, December 1997.
- [127] N. Yee, J-P. Linnartz and G. Fettweis, "Multicarrier CDMA in indoor wireless radio networks," *Proc. Int. Symp. on Personal, Indoor and Mobile Radio Comms.*, Yokohama, Japan, pp. 109-113, September 1993.
- [128] V. M. DaSilva and E. S. Sousa, "Performance of Orthogonal CDMA Codes for Quasi-Synchronous Communication Systems", *Proc. IEEE Int. Conf. on Universal Personal Comms.*, Ottawa, Canada, pp. 995-999, October 1993.
- [129] L. L. W. Leung, R. Cheng, K. B. Letaief and R. D. Murch, "Combined multiuser interference cancellation and antenna array processing for DS/CDMA systems," *Proc. IEEE Int. Symp. on Personal, Indoor and Mobile Radio Comms.*, vol. 2, pp. 1096 -1100, September 2000.
- [130] T. Moon, S. Kang, Y. Lee and C. Kang, "A combining technique of array antenna and interference cancellation for wideband CDMA systems", *Proc. IEEE Veh. Tech. Conf.*, pp. 736-740, Ottawa, Canada, May 1998.

- [131] D. Dahlhaus and Z. Cheng, "Smart antenna concepts with interference cancellation for joint demodulation in the WCDMA UTRA uplink", *Proc. IEEE Int. Symp. on Spread Spectrum Techniques and Applications*, pp. 244-248, Parsippany, New Jersey, September 2000.
- [132] Ning Kong, "Space-time diversity multistage parallel interference cancellation (MPIC) for CDMA", *Proc. IEEE Veh. Tech. Conf - Fall.*, pp. 2826-2833, September 2000.
- [133] A. Papoulis, *Probability, Random Variables, and Stochastic Processes*, 3rd edition, McGraw-Hill Inc., 1991.
- [134] W. C. Jakes ed., *Microwave Mobile Communications*, IEEE Press, New Jersey, 1974.